

Oxidative stress and nitrosative stress, their interaction and implications for bioprocessing

Ivo Kretzers

A thesis submitted to the University of Strathclyde in accordance with the regulations governing the award of the degree of

Doctor of Philosophy

Strathclyde Fermentation Centre

Strathclyde Institute of Pharmacy and Biomedical Sciences

University of Strathclyde

Glasgow, The UK

January 2014

Copyright declaration

This thesis is the result of the author's original research. It has been composed by the author and has not been previously submitted for examination which has led to the award of a degree.

The copyright of this thesis belongs to the author under the terms of the United Kingdom Copyright Acts as qualified by University of Strathclyde Regulation 3.50. Due acknowledgement must always be made of the use of any material contained in, or derived from, this thesis.

Signed:



Date:

12/01/2014.

Acknowledgment

First of all I would like to thank my supervisors, Professor Brian McNeil and Dr. Linda Harvey for giving me the opportunity to do my PhD at the fermentation centre at the Strathclyde Institute of Pharmacy and Bioscience.

I am also thankful to my colleagues and friends for their support; Dr. Mariana Fazenda, Dr. Manal Eshelli, Dr. Ebtihaj Jambi, Dr. Tantina Kumlung, Dr. Pete Gardner, Brian Griffin, Laura Jeffrey and last but not least Walter McEwan, for his technical support and knowledge and experience on fermentation science.

I would also like to thank; Dr. Tamara Martin, Dr. Ng Pei Yuen, Dr. Gillian Stenson, Martin Wernowski, Emma Torrence, Tansi Kodai, Leon Williamson and Mark MacAskill for the pleasant working environment on the 4th floor of the SIPBS building especially when we had to come in during the weekends.

I am especially thankful towards my family; my parents and my loving wife Debbie in particular for their support and encouragement.

Abstract

The present study focuses on a series of physiological studies to study oxidative and nitrosative stress and online monitoring of fungal biomass growth in submerged batch cultures of the filamentous fungus *Aspergillus niger B1-D*, modified to secrete lysozyme.

The results of the undertaken studies described here show that increasing concentrations of polymyxin B, added to a bioreactor, increase oxidative stress during cultivation of *Aspergillus niger B1-D* in a bioreactor. This was shown by the increased superoxide dismutase (SOD) and catalase (CAT) activities after addition of polymyxin B. This increased oxidative stress also results in a decrease in production of lysozyme, which is at least 75% lower in all polymyxin B processes.

Varying oxygen transfer rate (OTR), by changing the stirring rate, in the lag phase of a batch fermentation, *utilising the Aspergillus niger B1-D* strain, results in increased oxidative stress with increased stirring rates. The resulting lysozyme production was at least 75% lower compared to the optimum agitation setting. This optimum setting was 200-400 rpm, which was controlled by the dissolved oxygen tension.

Adding increasing amounts of sodium nitroprusside (SNP) reduces oxidative stress resulting in an increased production of lysozyme. The use of SNP also showed increased CAT activities, which points towards an interaction between oxidative and nitrosative stress due to the release of nitric oxide from SNP.

Applying an online biomass sensor (Buglab) during batch cultivation of *Aspergillus niger B1-D* showed that this sensor can accurately monitor fungal biomass growth from 7 g/l onwards.

Contents

1	Introduction	2
1.1	Oxidative stress	3
1.2	Reactive oxygen species (ROS)	4
1.2.1	Superoxide anion radical ($\cdot\text{O}_2^-$)	4
1.2.2	Hydrogen peroxide (H_2O_2).....	4
1.2.3	Hydroxyl radical ($\cdot\text{OH}$)	5
1.3	ROS sites.....	5
1.4	ROS kinetics	6
1.5	ROS effects on cells and cellular components.....	7
1.5.1	DNA.....	7
1.5.2	Lipid peroxidation	7
1.5.3	Proteins	10
1.6	Anti-oxidant enzymes.....	11
1.6.1	Superoxide dismutase (SOD).....	11
1.6.2	Catalase (CAT).....	13
1.6.3	Peroxidases	14
1.7	Other anti-oxidant compounds.....	15
1.7.1	Glutathione (GSH).....	15
1.7.2	NADPH.....	16
1.7.3	Trehalose	16
1.8	Alternative respiratory pathways.....	17
1.8.1	Oxidative stress and respiration	19
1.9	Morphology	20
1.10	Nitrosative stress.....	21
1.10.1	Introduction	21
1.10.2	Nitric oxide (NO) generation.....	22
1.10.3	RNS chemistry	25
1.10.4	RNS defences.....	26

1.10.5	RNS damage	27
1.11	Interaction between ROS, RNS generation and oxidative stress defences	29
1.11.1	Denitrification	29
1.11.2	Combining aerobic and anaerobic respiration	32
1.12	Process parameters affecting ROS formation	34
1.12.1	Introduction	34
1.12.2	Inoculum	34
1.12.3	Reactor modes	35
1.12.4	Process control	36
1.13	Summary and aims	38
1.13.1	Summary	38
1.13.2	Aims	39
2	Materials and methods	42
2.1	Stirred tank reactor (STR), control system and associated analytical reactor equipment	42
2.2	Culture conditions	45
2.2.1	Strain	45
2.2.2	Medium	45
2.2.3	Inoculum preparation for batch fermentations	46
2.2.4	Shake flask cultivation	46
2.2.5	Stirred tank reactor	46
2.3	Analyses	47
2.3.1	Biomass	47
2.3.2	Glucose and ammonium	47
2.3.3	Adenosine triphosphate (ATP)	48
2.3.4	Culture viability	48
2.3.5	Lysozyme	49
2.3.6	Nitrite assay	50
2.3.7	Superoxide dismutase (SOD)	53

2.3.8	Catalase (CAT).....	56
2.3.9	Intracellular protein content	58
2.4	Data treatment.....	60
2.4.1	Statistics.....	60
2.4.2	Data representation.....	61
2.4.3	Experimental data modifications	62
2.5	Experimental variations and assays used in each chapter	64
2.5.1	The effect of polymyxin B on oxidative stress defence mechanisms during cultivation of <i>Aspergillus niger B1-D</i>	64
2.5.2	Oxygen transfer at the start of a fermentation can lead to oxidative stress in <i>Aspergillus niger B1-D</i>	64
2.5.3	Nitric oxide and its interaction with oxidative stress defences in submerged cultures of <i>Aspergillus niger</i>	65
2.5.4	Infrared monitoring of hyphal growth during submerged culture of <i>Aspergillus niger</i>	66
3	The effect of polymyxin B on oxidative stress defence mechanisms during cultivation of <i>Aspergillus niger B1-D</i>.....	68
3.1	Introduction and aims.....	68
3.1.1	Aims	70
3.2	Results.....	71
3.2.1	Polymyxin B and its effect on biomass formation, carbon consumption and nitrogen consumption.....	71
3.2.2	Polymyxin B and its effect on respiration.....	80
3.2.3	Polymyxin B and its effect on oxidative stress related biomarkers	85
3.2.4	Polymyxin B and its effect on intracellular protein content, lysozyme production and viability	90
3.2.5	Overview of statistics.....	95
3.3	Discussion	97
3.3.1	Polymyxin B and its effect on biomass formation, carbon consumption and nitrogen consumption.....	97

3.3.2	Polymyxin B and its effect on respiration.....	98
3.3.3	Polymyxin B and its effect on oxidative stress related biomarkers 100	
3.3.4	Polymyxin B and its effect on intracellular protein content, lysozyme production and viability	102
3.4	Conclusions	103
4	Does oxidative stress in the lag phase of a fermentation cause adverse effects?.....	105
4.1	Introduction and aims.....	105
4.1.1	Aims	107
4.2	Results.....	108
4.2.1	Agitation and its effect on biomass formation, carbon consumption and nitrogen consumption	111
4.2.2	Agitation and its effect on dissolved oxygen tension (DOT) and respiration.....	120
4.2.3	Agitation and its effect on oxidative stress related biomarkers	126
4.2.4	Agitation and its effect on intracellular protein content and viability	129
4.2.5	Overview of statistics.....	133
4.3	Discussion	135
4.3.1	Agitation and its effect on biomass formation, carbon consumption and nitrogen consumption	135
4.3.2	Agitation and its effect on dissolved oxygen tension (DOT) and respiration.....	136
4.3.3	Agitation and its effect on oxidative stress related biomarkers	138
4.3.4	Agitation and its effect on intracellular protein content, lysozyme production and viability	139
4.4	Conclusions	140
5	Nitric oxide and its interaction with oxidative stress defences in submerged cultures of <i>Aspergillus niger</i>.....	143

5.1	Introduction and aims.....	143
5.1.1	Aims	146
5.2	Results.....	147
5.2.1	Growth experiments using sodium nitrite, hydroxy urea and SNP 147	
5.2.2	Reactor experiments for studying the effect of SNP on cultivation of <i>A. niger</i> B1-D.....	152
5.3	Discussion	183
5.3.1	Growth experiments using sodium nitrite, hydroxy urea and SNP 183	
5.3.2	Reactor experiments for studying the effect of SNP on cultivation of <i>A. niger</i> B1-D.....	184
5.4	Conclusions	196
6	Infrared monitoring of hyphal growth during submerged culture of <i>Aspergillus niger</i>.....	198
6.1	Introduction and aim	198
6.1.1	Aim	199
6.2	Results.....	200
6.2.1	Biomass growth during stirred tank reactor experiments.....	200
6.2.2	Model based on raw data	201
6.3	Discussion	204
6.4	Conclusions	205
7	Discussion, Conclusions and Future Work	207
7.1	Discussion	207
7.2	Conclusions	208
7.3	Future Work.....	209
8	References	212
I	Graphs repeat experiments for Chapter 3.....	235

I.1	Graphs of repeat experiments	235
II	Graphs repeat experiments for Chapter 4.....	244
II.1	Graphs of repeat experiments	244
III	Graphs repeat experiments for Chapter 5.....	253
III.1	Graphs of repeat experiments	253

List of figures

1. Introduction

- Figure 1-1:** Various reactions and products of lipid peroxidation; CD is conjugated diene. 9
- Figure 1-2:** Composite scheme of fungal mitochondrial electron transport. 18
- Figure 1-3:** Conversion of L-arginine into L-citrulline. 23
- Figure 1-4:** Nitrate metabolism of filamentous fungi. 31
- Figure 1-5:** Pathway for fungal ammonium fermentation. 31
- Figure 1-6:** Schematic drawing of anaerobic and aerobic respiration and the interactions that are possible between ROS and RNS. 33

2. Materials and methods

- Figure 2-1:** Operational setup of Bioflo3000 with reactor during *A. niger* B1-D fermentation. 43
- Figure 2-2:** Calibration curve used for the estimation of lysozyme. 50
- Figure 2-3:** Griess reaction resulting in the azo chromophore. 51
- Figure 2-4:** Calibration curve used for the estimation of nitrite. 52
- Figure 2-5:** Reaction mechanism monitored during analyses of SOD. 53
- Figure 2-6:** Optical density (OD) plotted against time for one of the standards that were used during this project. 55
- Figure 2-7:** Calibration curve used for the estimation of SOD. 56
- Figure 2-8:** Optical density (OD) plotted against time for one of the standards that were used during this project. 57
- Figure 2-9:** Calibration curve used for the estimation of CAT. 58
- Figure 2-10:** Calibration curve used for the estimation of intracellular protein content. 59

3. The effect of polymyxin B on oxidative stress defence mechanisms during cultivation of *Aspergillus niger* B1-D.

Figure 3-1: DCW (g/l) during batch cultivation in a STR of <i>A. niger</i> B1-D.	72
Figure 3-2: Residual glucose (g/l) during batch cultivation in a STR of <i>A. niger</i> B1-D.	75
Figure 3-3: Residual Ammonium (g/l) during batch cultivation in a STR of <i>A. niger</i> B1-D.	78
Figure 3-4: OUR (mM/g DCW/h) and (B) CER (mM/g DCW/h) during batch cultivation in a STR of <i>A. niger</i> B1-D.	82
Figure 3-5: R.Q. during batch cultivation in a STR of <i>A. niger</i> B1-D.	83
Figure 3-6: SOD (U/g DCW) during batch cultivation in a STR of <i>A. niger</i> B1-D.	87
Figure 3-7: CAT (U/g DCW) during batch cultivation in a STR of <i>A. niger</i> B1-D.	88
Figure 3-8: Intracellular protein content (mg/g DCW) during batch cultivation in a STR of <i>A. niger</i> B1-D.	91
Figure 3-9: Lysozyme concentration (mg/l) during batch cultivation in a STR of <i>A. niger</i> B1-D.	92
Figure 3-10: Viability (A570nm/g DCW) values during batch cultivation in a STR of <i>A. niger</i> B1-D.	94

4. Does oxidative stress in the lag phase of a fermentation cause adverse effects?

Figure 4-1: Lysozyme concentration (mg/l) during batch cultivation in a STR of <i>A. niger</i> B1-D.	109
Figure 4-2: DCW (g/l) during batch cultivation in a STR of <i>A. niger</i> B1-D.	112
Figure 4-3: Residual glucose (g/l) during batch cultivation in a STR of <i>A. niger</i> B1-D.	115
Figure 4-4: Residual ammonium (g/l) during batch cultivation in a STR of <i>A. niger</i> B1-D.	118

Figure 4-5: (A) DOT (%) and (B) OUR (mM/g DCW/h) during batch cultivation in a STR of <i>A. niger B1-D</i> .	121
Figure 4-6: (A) CER (mM/g DCW/h) and (B) R.Q. during batch cultivation in a STR of <i>A. niger B1-D</i> .	124
Figure 4-7: (A) SOD (U/g DCW) and (B) CAT (U/g DCW) during batch cultivation in a STR of <i>A. niger B1-D</i> .	127
Figure 4-8: Intracellular protein content (mg/g DCW) during batch cultivation in a STR of <i>A. niger B1-D</i> .	130
Figure 4-9: Viability (A_{570nm} /g DCW) during batch cultivation in a STR of <i>A. niger B1-D</i> .	132
5. Nitric oxide and its interaction with oxidative stress defences in submerged cultures of <i>Aspergillus niger</i>	
Figure 5-1: DCW (g/l) during shake flask cultivation of <i>A. niger B1-D</i> .	149
Figure 5-2: DCW (g/l) during shake flask cultivation of <i>A. niger B1-D</i> .	150
Figure 5-3: DCW (g/l) during shake flask cultivation of <i>A. niger B1-D</i> .	151
Figure 5-4: Nitrite concentration during batch cultivation in a stirred tank reactor of <i>A. niger B1-D</i> .	153
Figure 5-5: DCW (g/l) during batch cultivation in a STR of <i>A. niger B1-D</i> .	155
Figure 5-6: Residual glucose (g/l) during batch cultivation in a STR of <i>A. niger B1-D</i> .	158
Figure 5-7: Residual Ammonium (g/l) during batch cultivation in a STR of <i>A. niger B1-D</i> .	161
Figure 5-8: (A) OUR (mM/g DCW/h) and (B) CER (mM/g DCW/h) during batch cultivation in a STR of <i>A. niger B1-D</i> .	164
Figure 5-9: R.Q. during batch cultivation in a STR of <i>A. niger B1-D</i> .	167
Figure 5-10: Intracellular ATP concentrations (μ g/g DCW) during batch cultivation in a STR of <i>A. niger B1-D</i> .	169

Figure 5-11: (A) SOD (U/g DCW) and (B) CAT (U/g DCW) during batch cultivation in a STR of <i>A. niger B1-D</i> .	173
Figure 5-12: Intracellular protein content (mg/g DCW) during batch cultivation in a STR of <i>A. niger B1-D</i> .	176
Figure 5-13: Lysozyme concentration (mg/l) during batch cultivation in a STR of <i>A. niger B1-D</i> .	178
Figure 5-14: Viability (A_{570nm} /g DCW) during batch cultivation in a STR of <i>A. niger B1-D</i> .	180
Figure 5-15: Intracellular protein, SOD and ATP concentrations during batch cultivation in a STR of <i>A. niger B1-D</i> .	193
Figure 5-16: CAT and nitrite concentrations during batch cultivation in a STR of <i>A. niger B1-D</i> .	194
Figure 5-17: Viability and RQ during batch cultivation in a STR of <i>A. niger B1-D</i> .	195
6. Infrared monitoring of hyphal growth during submerged culture of <i>Aspergillus niger</i>	
Figure 6-1: DCW values during batch cultivation in a STR of <i>A. niger B1-D</i> .	200
Figure 6-2: Spectral values against time (A) and DCW plotted against corresponding spectral values (B) during batch cultivation of <i>A. niger B1-D</i> in an STR.	202
Figure 6-3: Measured DCW and predicted model values against time (A) and measured DCW values plotted against calculated DCW values (B) during batch cultivation <i>A. niger B1-D</i> in a STR.	203
I. Graphs repeat experiments for Chapter 3	
Figure I-1: DCW (g/l) during batch cultivation in a STR of <i>A. niger B1-D</i> .	235
Figure I-2: Residual glucose (g/l) during batch cultivation in a STR of <i>A. niger B1-D</i> .	236
Figure I-3: Residual Ammonium (g/l) during batch cultivation in a STR of <i>A. niger B1-D</i> .	237

Figure I-4: (A) OUR (mM/g/h) and (B) CER (mM/g/h) during batch cultivation in a STR of <i>A. niger B1-D</i> .	238
Figure I-5: R.Q. during batch cultivation in a STR of <i>A. niger B1-D</i> .	239
Figure I-6: (A) SOD (U/g) and (B) CAT (U/g) during batch cultivation in a STR of <i>A. niger B1-D</i> .	240
Figure I-7: (A) Intracellular protein content (mg/g) and (B) Lysozyme concentration (mg/l) during batch cultivation in a STR of <i>A. niger B1-D</i> .	241
Figure I-8: Viability (A_{570nm} /g DCW) during batch cultivation in a stirred tank reactor of <i>A. niger B1-D</i> .	242
II. Graphs repeat experiments for Chapter 4	
Figure II-1: DCW (g/l) during batch cultivation in a STR of <i>A. niger B1-D</i> .	244
Figure II-2: Residual glucose (g/l) during batch cultivation in a STR of <i>A. niger B1-D</i> .	245
Figure II-3: Residual ammonium (g/l) during batch cultivation in a STR of <i>A. niger B1-D</i> .	246
Figure II-4: (A) DOT (%) and (B) OUR (mM/g/h) during batch cultivation in a STR of <i>A. niger B1-D</i> .	247
Figure II-5: (A) CER (mM/g/h) and (B) R.Q. during batch cultivation in a STR of <i>A. niger B1-D</i> .	248
Figure II-6: (A) SOD (U/g) and (B) CAT (U/g) during batch cultivation in a STR of <i>A. niger B1-D</i> .	249
Figure II-7: (A) Intracellular protein content (mg/g) and (B) Lysozyme concentration (mg/l) during batch cultivation in a STR of <i>A. niger B1-D</i> .	250
Figure II-8: Viability (A_{570nm} /g DCW) during batch cultivation in a stirred tank reactor of <i>A. niger B1-D</i> .	251
III. Graphs repeat experiments for Chapter 5	
Figure III-1: Nitrite concentration during batch cultivation in a stirred tank reactor of <i>A. niger B1-D</i> .	253

Figure III-2: DCW (g/l) during batch cultivation in a STR of <i>A. niger B1-D</i> .	254
Figure III-3: Residual glucose (g/l) during batch cultivation in a STR of <i>A. niger B1-D</i> .	255
Figure III-4: Residual Ammonium (g/l) during batch cultivation in a STR of <i>A. niger B1-D</i> .	256
Figure III-5: (A) OUR (mM/g/h) and (B) CER (mM/g/h) during batch cultivation in a STR of <i>A. niger B1-D</i> .	257
Figure III-6: R.Q. (A) and ATP ($\mu\text{g/g DCW}$); (B) during batch cultivation in a STR of <i>A. niger B1-D</i> .	258
Figure III-7: (A) SOD (U/g) and (B) CAT (U/g) during batch cultivation in a STR of <i>A. niger B1-D</i> .	259
Figure III-8: (A) Intracellular protein content (mg/g) and (B) Lysozyme concentration (mg/l) during batch cultivation in a STR of <i>A. niger B1-D</i> .	260
Figure III-9: Effect of various concentrations of SNP on viability ($A_{570\text{nm}}/\text{g DCW}$) during batch cultivation in a stirred tank reactor of <i>A. niger B1-D</i> .	261

List of tables

3. The effect of polymyxin B on oxidative stress defence mechanisms during cultivation of *Aspergillus niger B1-D*.

Table 3-1: Effect of polymyxin B on specific growth rate during batch fermentations of <i>A. niger B1-D</i> .	72
Table 3-2: Statistical analyses of DCW using the Bonferoni post-hoc test, with significant differences between treatment. In which; SEM is standard error of means, LCL is lower confidence limit and UCL is upper confidence limit.	73
Table 3-3: Statistical analyses of specific growth rate using the Tukey post-hoc test. In which; SEM is standard error of means, LCL is lower confidence limit and UCL is upper confidence limit.	73
Table 3-4: Effect of polymyxin B on GCR during batch fermentations of <i>A. niger B1-D</i> .	75

Table 3-5: Statistical analyses of residual glucose using the Bonferoni post-hoc test, with significant differences between treatment. In which; SEM is standard error of means, LCL is lower confidence limit and UCL is upper confidence limit.	76
Table 3-6: Statistical analyses of GCR using the Tukey post-hoc test. In which; SEM is standard error of means, LCL is lower confidence limit and UCL is upper confidence limit.	76
Table 3-7: Effect of polymyxin B on ACR during batch fermentations of <i>A. niger B1-D</i> .	78
Table 3-8: Statistical analyses of residual ammonium using the Bonferoni post-hoc test, with significant differences between treatment. In which; SEM is standard error of means, LCL is lower confidence limit and UCL is upper confidence limit.	79
Table 3-9: Statistical analyses of ACR using the Tukey post-hoc test. In which; SEM is standard error of means, LCL is lower confidence limit and UCL is upper confidence limit.	79
Table 3-10: Statistical analyses of OUR using the Bonferoni post-hoc test, with significant differences between treatment. In which; SEM is standard error of means, LCL is lower confidence limit and UCL is upper confidence limit.	83
Table 3-11: Statistical analyses of CER using the Bonferoni post-hoc test, with significant differences between treatment. In which; SEM is standard error of means, LCL is lower confidence limit and UCL is upper confidence limit.	84
Table 3-12: Statistical analyses of R.Q. using the Bonferoni post-hoc test, with significant differences between treatment. In which; SEM is standard error of means, LCL is lower confidence limit and UCL is upper confidence limit.	84
Table 3-13: Statistical analyses of SOD using the Bonferoni post-hoc test, with significant differences between treatment. In which; SEM is standard error of means, LCL is lower confidence limit and UCL is upper confidence limit.	89

Table 3-14: Statistical analyses of CAT using the Bonferoni post-hoc test, with significant differences between treatment. In which; SEM is standard error of means, LCL is lower confidence limit and UCL is upper confidence limit. 89

Table 3-15: Statistical analyses of intracellular protein using the Bonferoni post-hoc test, with significant differences between treatment. In which; SEM is standard error of means, LCL is lower confidence limit and UCL is upper confidence limit. 91

Table 3-16: Statistical analyses of lysozyme using the Bonferoni post-hoc test, with significant differences between treatment. In which; SEM is standard error of means, LCL is lower confidence limit and UCL is upper confidence limit. 93

Table 3-17: Statistical analyses of Viability using the Bonferoni post-hoc test, with significant differences between treatment. In which; SEM is standard error of means, LCL is lower confidence limit and UCL is upper confidence limit. 94

Table 4 18: Statistical overview of all the tests done in this chapter. 96

4. Does oxidative stress in the lag phase of a fermentation cause adverse effects?

Table 4-1: Effect of various agitation settings on Yps during batch fermentations of *A. niger B1-D*. 109

Table 4-2: Statistical analyses of Lysozyme using the Bonferoni post-hoc test. In which; SEM is standard error of means, LCL is lower confidence limit and UCL is upper confidence limit. 110

Table 4-3: Effect of various agitation settings on specific growth rate during batch fermentations of *A. niger B1-D*. 112

Table 4-4: Statistical analyses of DCW using the Bonferoni post-hoc test. In which; SEM is standard error of means, LCL is lower confidence limit and UCL is upper confidence limit. 113

Table 4-5: Statistical analyses of specific growth rate using the Tukey post-hoc test. In which; SEM is standard error of means, LCL is lower confidence limit and UCL is upper confidence limit. 113

Table 4-6: Effect of various agitation settings on GCR rate during batch fermentations of <i>A. niger</i> B1-D.	115
Table 4-7: Statistical analyses of residual glucose using the Bonferoni post-hoc test. In which; SEM is standard error of means, LCL is lower confidence limit and UCL is upper confidence limit.	116
Table 4-8: Statistical analyses of GCR using the Tukey post-hoc test. In which; SEM is standard error of means, LCL is lower confidence limit and UCL is upper confidence limit.	116
Table 4-9: Effect of various agitation settings on ACR rate during batch fermentations of <i>A. niger</i> B1-D.	118
Table 4-10: Statistical analyses of residual ammonium using the Bonferoni post-hoc test. In which; SEM is standard error of means, LCL is lower confidence limit and UCL is upper confidence limit.	119
Table 4-11: Statistical analyses of ACR using the Tukey post-hoc test. In which; SEM is standard error of means, LCL is lower confidence limit and UCL is upper confidence limit.	119
Table 4-12: Statistical analyses of OUR using the Bonferoni post-hoc test. In which; SEM is standard error of means, LCL is lower confidence limit and UCL is upper confidence limit.	122
Table 4-13: Statistical analyses of CER using the Bonferoni post-hoc test. In which; SEM is standard error of means, LCL is lower confidence limit and UCL is upper confidence limit.	125
Table 4-14: Statistical analyses of R.Q. using the Bonferoni post-hoc test. In which; SEM is standard error of means, LCL is lower confidence limit and UCL is upper confidence limit.	125
Table 4-15: Statistical analyses of SOD using the Bonferoni post-hoc test. In which; SEM is standard error of means, LCL is lower confidence limit and UCL is upper confidence limit.	128
Table 4-16: Statistical analyses of CAT using the Bonferoni post-hoc test. In which; SEM is standard error of means, LCL is lower confidence limit and UCL is upper confidence limit.	128

Table 4-17: Statistical analyses of intracellular protein content using the Bonferoni post-hoc test. In which; SEM is standard error of means, LCL is lower confidence limit and UCL is upper confidence limit. 130

Table 4-18: Statistical analyses of Viability using the Bonferoni post-hoc test. In which; SEM is standard error of means, LCL is lower confidence limit and UCL is upper confidence limit. 132

Table 4-19: Statistical overview of all the tests done in this work. 134

5. Nitric oxide and its interaction with oxidative stress defences in submerged cultures of *Aspergillus niger*

Table 5-1: Statistical analyses of DCW of the sodium nitrite series using the Bonferoni post-hoc test. In which; SEM is standard error of means, LCL is lower confidence limit and UCL is upper confidence limit. 149

Table 5-2: Statistical analyses of DCW of the hydroxy urea series using the Bonferoni post-hoc test. In which; SEM is standard error of means, LCL is lower confidence limit and UCL is upper confidence limit. 150

Table 5-3: Statistical analyses of DCW of the SNP series using the Bonferoni post-hoc test. In which; SEM is standard error of means, LCL is lower confidence limit and UCL is upper confidence limit. 151

Table 5-4: Statistical analyses of nitrite using the Bonferoni post-hoc test. In which; SEM is standard error of means, LCL is lower confidence limit and UCL is upper confidence limit. 153

Table 5-5: Effect of SNP on specific growth rate during batch fermentations of *A. niger* B1-D. 155

Table 5-6: Statistical analyses of DCW using the Bonferoni post-hoc test. In which; SEM is standard error of means, LCL is lower confidence limit and UCL is upper confidence limit. 156

Table 5-7: Statistical analyses of specific growth rate using the Tukey post-hoc test. In which; SEM is standard error of means, LCL is lower confidence limit and UCL is upper confidence limit. 156

Table 5-8: Effect of SNP on GCR during batch fermentations of *A. niger* B1-D. 158

Table 5-9: Statistical analyses of residual glucose using the Bonferoni post-hoc test. In which; SEM is standard error of means, LCL is lower confidence limit and UCL is upper confidence limit.	159
Table 5-10: Statistical analyses of GCR using the Bonferoni post-hoc test. In which; SEM is standard error of means, LCL is lower confidence limit and UCL is upper confidence limit.	159
Table 5-11: Effect of SNP on ACR during batch fermentations of <i>A. niger B1-D</i> .	161
Table 5-12: Statistical analyses of residual ammonium using the Bonferoni post-hoc test. In which; SEM is standard error of means, LCL is lower confidence limit and UCL is upper confidence limit.	162
Table 5-13: Statistical analyses of ACR using the Bonferoni post-hoc test. In which; SEM is standard error of means, LCL is lower confidence limit and UCL is upper confidence limit.	162
Table 5-14: Statistical analyses of OUR using the Bonferoni post-hoc test. In which; SEM is standard error of means, LCL is lower confidence limit and UCL is upper confidence limit.	165
Table 5-15: Statistical analyses of CER using the Bonferoni post-hoc test. In which; SEM is standard error of means, LCL is lower confidence limit and UCL is upper confidence limit.	165
Table 5-16: Statistical analyses of R.Q. using the Bonferoni post-hoc test. In which; SEM is standard error of means, LCL is lower confidence limit and UCL is upper confidence limit.	167
Table 5-17: Statistical analyses of ATP using the Bonferoni post-hoc test. In which; SEM is standard error of means, LCL is lower confidence limit and UCL is upper confidence limit.	170
Table 5-18: Statistical analyses of SOD using the Bonferoni post-hoc test. In which; SEM is standard error of means, LCL is lower confidence limit and UCL is upper confidence limit.	174
Table 5-19: Statistical analyses of CAT using the Bonferoni post-hoc test. In which; SEM is standard error of means, LCL is lower confidence limit and UCL is upper confidence limit.	174

Table 5-20: Statistical analyses of intracellular protein using the Bonferoni post-hoc test. In which; SEM is standard error of means, LCL is lower confidence limit and UCL is upper confidence limit. 176

Table 5-21: Statistical analyses of lysozyme using the Bonferoni post-hoc test. In which; SEM is standard error of means, LCL is lower confidence limit and UCL is upper confidence limit. 178

Table 5-22: Statistical analyses of Viability using the Bonferoni post-hoc test. In which; SEM is standard error of means, LCL is lower confidence limit and UCL is upper confidence limit. 180

Table 5-23: Statistical overview of all the tests carried out above. 182

I. Graphs repeat experiments for Chapter 3

Table I-1: Effect of polymyxin B on specific growth rate during batch fermentations of *A. niger B1-D*. 235

Table I-2: Effect of polymyxin B on GCR during batch fermentations of *A. niger B1-D*. 236

Table I-3: Effect of polymyxin B on ACR during batch fermentations of *A. niger B1-D*. 237

II. Graphs repeat experiments for Chapter 4

Table II-1: Effect of various agitation settings on specific growth rate during batch fermentations of *A. niger B1-D*. 244

Table II-2: Effect of various agitation settings on GCR rate during batch fermentations of *A. niger B1-D*. 245

Table II-3: Effect of various agitation settings on ACR rate during batch fermentations of *A. niger B1-D*. 246

III. Graphs repeat experiments for Chapter 5

Table III-1: Effect of SNP on specific growth rate of batch fermentations of *A. niger B1-D*. 254

Table III-2: Effect of SNP on GCR during batch fermentations of *A. niger B1-D*. 255

Table III-3: Effect of SNP on ACR batch fermentations of *A. niger B1-D*. 256

Abbreviations

Ammonium consumption rate = ACR

Carbon evolution rate = CER

Catalase = CAT

Dissolved oxygen tension = DOT

Glucose consumption rate = GCR

Nitric oxide synthase = NOS

Oxygen transfer rate = OTR

Oxygen uptake rate = OUR

Reactive oxygen species = ROS

Resistance temperature detector = RTD

Respiration coefficient = R.Q.

Sodium nitroprusside = SNP

Standard deviation = stdev

Stirred tank reactor = STR

Superoxide dismutase = SOD

Chapter 1

Introduction

1 Introduction

Filamentous fungi have been utilised in many industrial processes (Alvarez-Vasquez *et al.*, 2000). One of the reasons for using fungal strains for these processes is that a number of filamentous fungi have GRAS status, due to their utilisation in foods and food processing (Archer *et al.*, 1994). Filamentous fungi are also capable of secreting large quantities of proteins, up to 20 g/l, and are capable of post-translational modifications to proteins such as glycosylation (Finkelstein, 1987, Amanullah *et al.*, 2002, El-Enshasy *et al.*, 2006).

An example of an industrial process that uses a fungal strain is citric acid production utilising *Aspergillus niger* (Alvarez-Vasquez *et al.*, 2000) Currently methods are being used to genetically modify fungi and produce compounds by secretion into the medium such as; glucoamylase, bovine chymosin, human lactoferrin, human interleukin-6, thaumatin and hen egg-white lysozyme (Archer *et al.*, 1990, Wang *et al.*, 2005).

Industrial production of these compounds is performed by utilising reactors of various scales, the major drawback of fungal fermentations is the high viscosity of the fermentation broth once hyphal growth starts (Kreiner *et al.*, 2000, Wang *et al.*, 2005). This high viscosity creates mixing problems inside the reactor which causes an unequal distribution of oxygen inside the reactor (Wang *et al.*, 2005). Industry usually solves this by increasing aeration and agitation, thereby maintaining appropriate dissolved oxygen levels. A drawback of this method is that potentially parts of the reactor are over or under oxygenated thereby causing oxidative stress via oxygen shocks when biomass moves from parts of the reactor with low oxygen levels to high oxygen levels.

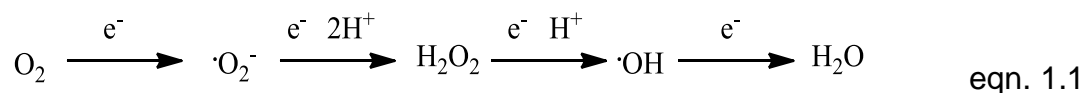
Oxidative stress has been shown to damage enzymes and proteins, resulting in a decrease in product yield (Li *et al.*, 2008d). Previous research has also shown that inoculating a reactor leads to oxidative stress, which is likely to be

one of the causes for the lag phases usually present in fermentations (O'Donnell *et al.*, 2007).

The industrial relevance described previously makes research into oxidative stress potentially lucrative. The authors intend is to give an overview of what oxidative stress is and defence mechanisms against it. The emphasis of the research will lie on studying physiological responses, when varying various parameters during fermentations, in relation to oxidative stress defence mechanisms. As the filamentous nature during fermentations often results in an unequal distribution of oxygen inside the bioreactor it should be useful to monitor biomass growth online and results on this subject were part of the research presented here as well.

1.1 Oxidative stress

The reduction of O_2 can be toxic to all organisms. O_2 is progressively reduced into water during respiration processes inside the cell. This sequential univalent process requires four electrons; incomplete reduction, however gives rise to three different molecules that are very harmful to the cell. See eqn. 2.1 for the reaction (Wojtaszek, 1997).



Reactive oxygen species (ROS) is a term used to describe the toxic oxidants that are produced when oxygen is degraded. Cells utilise a range of defence mechanisms to prevent the damaging effects of the intermediates produced during oxygen reduction. The term that is generally used to describe the damaging effects to the cell is “oxidative stress”.

Because aerobic organisms have many defensive capabilities at their disposal to protect themselves against oxygen radicals, oxidative stress usually occurs when there is an imbalance between the two.

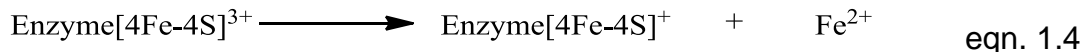
1.2 Reactive oxygen species (ROS)

1.2.1 Superoxide anion radical ($\cdot\text{O}_2^-$)

The formation of $\cdot\text{O}_2^-$ has been shown in eqn. 2.1 and requires the input of a small amount of energy (Wojtaszek, 1997, Radi et al., 2002, Silverman and Epstein, 1975). The reactivity of $\cdot\text{O}_2^-$ with non-radical species is far less compared to $\cdot\text{OH}$. It does have the capability of reacting very quickly with some other radicals, such as nitric oxide (NO) according to (Eiserich et al., 1998, Brown et al., 2009).



The superoxide anion radical can also react with iron-sulphur ($[\text{4Fe-4S}]^{2+}$) clusters in enzymes/proteins (Wojtaszek, 1997).

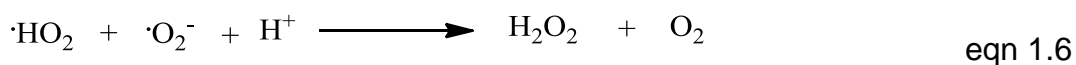


1.2.2 Hydrogen peroxide (H_2O_2)

$\cdot\text{O}_2^-$ is just the first step in the degradation of O_2 . Subsequently it can be dismutated into H_2O_2 (Martinezcayuela, 1995).



This reaction mechanism is however not likely to occur as these molecules would have to be present simultaneously in a solution. Therefore a more likely reaction is described here:



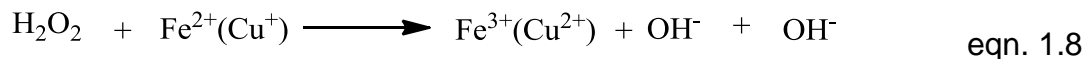


H₂O₂ is the most stable oxygen radical, however this radical is still capable of directly oxidizing proteins by converting thiol (-OH) groups to sulphenic acids (-SOH) and deactivating iron-sulphur groups (Mhamdi *et al.*, 2012).

There are two causes of H₂O₂ occurrence inside a cell. The first is normal aerobic respiration of cells in which glucose and oxygen are degraded through the normal respiratory pathways. In the second enzymes can also generate H₂O₂, enzymes worth mentioning here are xanthine, urate, D-amino acid oxidases, monoamine oxidase and superoxide dismutase (SOD); (Halliwell and Gutteridge, 1985, Hauptmann *et al.*, 1996).

1.2.3 Hydroxyl radical ($\cdot\text{OH}$)

The hydroxyl ion can be generated through the Fenton reaction from H₂O₂ in the presence of transition metals (Wojtaszek, 1997).



The hydroxyl radical is a highly reactive ion that will react almost instantly with almost every biological molecule: e.g. sugars, amino acids, phospholipids, DNA bases and organic acids (Cadenas and Davies, 2000). The *in vivo* concentration of OH⁻ is very small, because of the high reactivity of this molecule.

1.3 ROS sites

The main formation site of ROS are the mitochondria (Turrens, 2003). ROS are generated by the respiratory pathway by electron leakage and are therefore abundantly present inside cells that have aerobic respiration (Perrone *et al.*, 2008). For example, in the electron chain at the

ubiquinone/ubiquinol pool, a single electron is transferred from ubiquinone (oxidized form) to semi-ubiquinone (free radical form) and then to ubiquinol. One single electron can therefore pass to oxygen directly and not to the next carrier in this electron transport chain resulting in oxygen radicals (Cadenas and Davies, 2000).

The enzyme monoamine oxidase in the outer mitochondrial membrane also reduces O_2 to H_2O_2 within the mitochondrial matrix and cytosol (Hauptmann *et al.*, 1996).

1.4 ROS kinetics

Section 2.3 explains that the major formation site of ROS is the mitochondria. Since most ROS formation is a result from electron leakage in the mitochondria the rate of ROS is logically linked to the mitochondrial metabolic state. The rate of $^{\cdot}O_2^-$ formation is controlled by a mass rate equation (Turrens, 2003).

$$\frac{d[O_2^-]}{dt} = k[O_2] \times [R] \quad \text{eqn. 1.9}$$

In which:

$$\frac{d[O_2^-]}{dt} = \text{the rate of superoxide anion formation in M/s}$$

k = formation rate constant in M/s

$[O_2]$ = concentration of oxygen available in M

$[R]$ = concentration of electron donors in M

According to eqn. 2.9, a decrease in electron donors will result in a decrease in the formation rate of $^{\cdot}O_2^-$. A decrease in R can be the result of an increased electron flow across the alternative respiratory pathways.

Mitochondrial production of ROS is also mediated by NO through a mechanism that involves reversible binding to cytochrome oxidase (Complex IV, see Figure 1-2, see paragraph 1.8). It has been postulated that the inhibitory effect of NO is the reason for the increase in oxidative stress under moderately hypoxic conditions in mammalian cells (Turrens, 2003).

1.5 ROS effects on cells and cellular components

1.5.1 DNA

Previous sections have identified three molecules that can mediate damage to healthy cells, which have an aerobic respiration system. These molecules are $\cdot\text{O}_2^-$, H_2O_2 and $\cdot\text{HO}$. The specific identity of which radical is responsible of DNA damage is still a focus of study however $\cdot\text{HO}$ seems to be an obvious candidate (Marnett, 2000). $\cdot\text{HO}$ attacks the sugar residues of DNA readily and this will result in sugar fragmentation, base loss and the production of single strand breaks (Marnett, 2000, Imlay and Linn, 1988). Specifically $\cdot\text{OH}$ adds itself onto the desoxyguanosine base yielding 8-hydroxydesoxyguanosine (Giulivi *et al.*, 1995). Accumulation of 8-hydroxydesoxyguanosine inside the cell is widely used as an indicator for DNA-oxidation. This damage mechanism could lead to loss of integrity and function, which then could lead to cell death by necrosis or apoptosis (Morel and Barouki, 1999).

1.5.2 Lipid peroxidation

There are two types of lipids that can be damaged by ROS. The first one is membrane lipids (phospholipids) and the second one is lipoproteins (Sigler *et al.*, 1999). The damage is caused by the hydroxyl radical, which removes a hydrogen atom from the side chain of lipids, thereby forming a carbon radical.

The carbon radical can react with O₂, forming peroxy (ROO), which is able to extract another hydrogen atom. This chain reaction can continue until non-radical species are formed (Sigler *et al.*, 1999). When lipid peroxidation occurs the membrane bilayers loses their integrity and molecules that normally do not pass will reach parts of the cell where they are normally excluded from (Sigler *et al.*, 1999).

This chain reaction, lipid peroxidation, can eventually generate alkanes, ketones, oxiranes and aldehydes. A schematic diagram is given in Figure 1-1 to show this generation of secondary molecules.

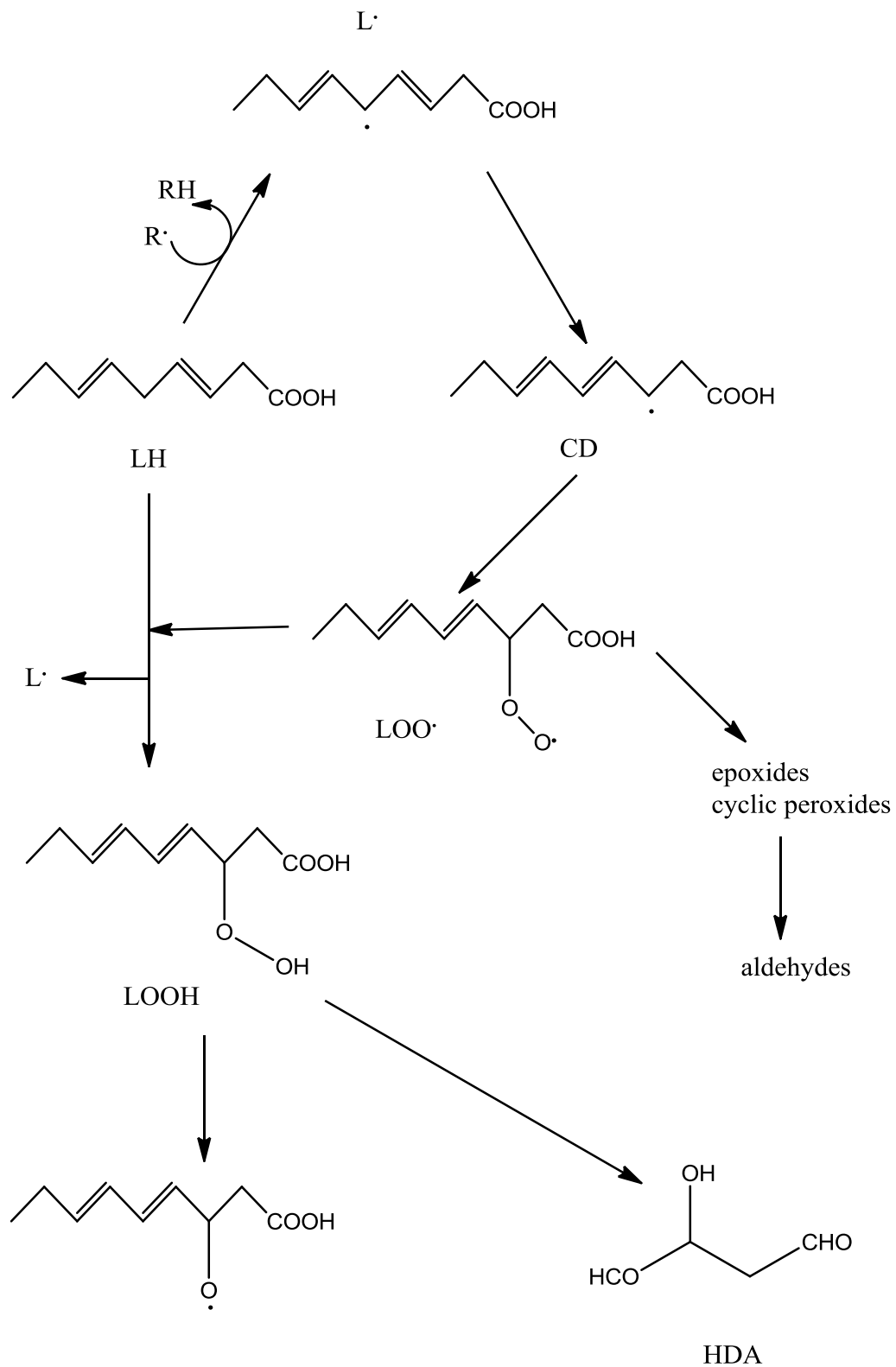


Figure 1-1: Various reactions and products of lipid peroxidation; CD is conjugated diene; adapted from (Sigler et al., 1999)

Kayali has studied lipid peroxidation in *Fusarium equiseti* and *Fusarium acuminatum* and found that metals could result in lipid peroxidation as well (Kayali and Tarhan, 2005). The same author also studied the effect of variations in nitrogen and carbon source on the SOD, CAT GPx and lipidperoxidation levels in *F. Acuminatum* and found that the higher concentrations of carbon source, in the case of this study, resulted in less lipid peroxidation than the lower concentrations. The activity of SOD, CAT and GPx and lipid peroxidation were negatively correlated with each other (Ayar-Kayali and Tarhan, 2004).

1.5.3 Proteins

Oxidative stress can result in protein modifications, literature so far showed three mechanisms of oxygen radicals modifying proteins which are; S-thiolation, carbonylation and oxidation of [4Fe-4S] groups.

1) S-thiolation

S-thiolation is a response to irreversible oxidation of cysteine groups. Cysteine thiol (SH) groups can oxidize, which can subsequently result in intermolecular cross linking of protein or enzymes. This intermolecular cross linking can lead to enzyme inactivation (Shenton and Grant, 2003). This irreversible damage can be prevented by S-thiolation in which protein/enzyme SH groups form mixed disulphides with low molecular mass thiols such as glutathione (GSH) (Shenton and Grant, 2003). Shenton showed that H₂O₂ treatment of the yeast *S. Cereviseae* resulted in S-thiolation of glyceraldehydes-3-phosphate dehydrogenase (Shenton and Grant, 2003).

2) Carbonylation

Carbonyl (CO) groups are produced on protein side chains when they are oxidized. The groups that are most vulnerable to this are proline, arginine, lysine and threonine (Dalle-Donne *et al.*, 2003). Previous research done in

this lab has shown an increase in intracellular protein carbonyl content during oxygen enrichment experiments utilising the *A. niger B1-D* strain (Li *et al.*, 2008d). This study showed that oxygen enrichment in itself could damage proteins, thereby potentially decreasing product yield.

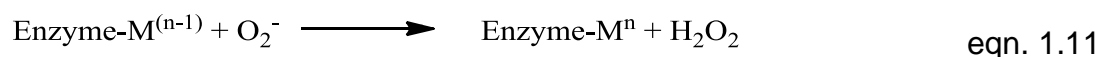
3) Oxidation of [4Fe-4S]²⁺

As explained previously (eqn 2.3 and eqn. 2.4) enzymes and proteins can be damaged by oxidation of [4Fe-4S]²⁺. The released iron will accumulate inside the cells and this can cause vacuole fragmentation, which in turn has been shown to increase sensitivity to stresses such as nutrient limitation or pH changes in *S. cerevisiae* (Costa and Moradas-Ferreira, 2001). Some identified targets of the superoxide anion radical in *E. coli* are (Imlay, 1995); aconitase, dihydroxyacid dehydratase, fumarases A and B and 6-phosphogluconate dehydratase. These enzymes belong to a class of dehydratases and the damage can go at a rate exceeding 10⁶ M⁻¹ s⁻¹ (Imlay, 1995).

1.6 Anti-oxidant enzymes

1.6.1 Superoxide dismutase (SOD)

Superoxide dismutase catalyzes the reaction that converts $\cdot\text{O}_2^-$ into H₂O₂ and oxygen. There are four types of this enzyme; iron SOD (Fe-SOD), manganese SOD (Mn-SOD), copper-zinc SOD (Cu,Zn-SOD) and Nickel SOD (Ni-SOD) (Blokhina *et al.*, 2003, Angelova *et al.*, 2005). The metals seem to serve as an oxidation and reducing agent thereby catalyzing the dismutation reaction (Halliwell and Gutteridge, 1985):



The net reaction is:



The two types that are present in filamentous fungi are Mn-SOD, which is present in the mitochondria and Cu,Zn-SOD which is in the cytosol (Blokchina *et al.*, 2003). The SOD enzyme has been studied extensively over the years. Previous research has shown various ways to study oxidative stress inside cells. A very common method has been to add various chemicals such as; menadione, H₂O₂, cumene hydroperoxide and 1-chloro-2,4-dinitrobenzene (Mutoh *et al.*, 2005). Menadione and H₂O₂ both resulted in increased SOD activity in filamentous fungi during batch fermentations (Kreiner *et al.*, 2002), however as this method is far away from real practice oxygen enrichment experiments were found to be a more suitable method to study oxidative stress inside reactors and as such SOD activity in *Aspergillus niger* has been characterized inside reactors during fermentations. Some of the outcomes from research done in this lab were that increasing oxidative stress inside reactors had as effect an increase in SOD activity. Gassing a reactor with 25% of oxygen enriched air led to an increase in the concentration of both 'O₂' and SOD (Kreiner *et al.*, 2002, Bai *et al.*, 2003), but at a higher oxygen level (50%), the activity of SOD and concentration of 'O₂' decreased. This event has been linked to the alternative respiratory pathway of *Aspergillus niger* becoming much more active at high oxygen levels, which will reduce the generation of ROS in the form of heat generation (Bai *et al.*, 2003).

A wide range of therapeutic applications for SOD have been described such as; prevention of tumor promotion (Nishikawa *et al.*, 2001) and protection of tissues after infections or traumatic injuries such as burns (Vorauer-Uhl *et al.*, 2001, Yabe *et al.*, 2001), therefore production of SOD is an important process. Dellomonaco has investigated SOD trends inside reactors utilising *Kluyveromyces marxianus* (Dellomonaco *et al.*, 2007). Their approach was to vary oxidative stress conditions via oxygen transfer rate to improve SOD production (Dellomonaco *et al.*, 2007) resulting in higher SOD yields. Nanou

tried to optimize carotene production by using *Blakeslea trispora* (Nanou *et al.*, 2011). His approach was to enhance aeration, an additional result was also an increase in SOD activity whenever the aeration was increased (Nanou *et al.*, 2011). Both papers by Dellomonaco and Nanou showed peak SOD activities in the lag phase and stationary phase of the fermentations.

1.6.2 Catalase (CAT)

Catalase is an enzyme that directly decomposes H₂O₂ into water, thereby protecting cells against oxidative stress. The overall reaction of this conversion is given in eqn. 2.13. CAT forms an intermediate complex with H₂O₂ after which water and oxygen are produced (Blokhina *et al.*, 2003).



In filamentous fungi two catalase genes exist and they are differentially regulated. In *A. nidulans* research *catA* and *catB* have been characterized (Kawasaki *et al.*, 1997). *CatA* seems to be active during the spore phase and *catB* is active in growing mycelia. Literature has identified two more genes for CAT, *catC* and *catD* which are active in *Aspergillus nidulans* (Kawasaki and Aguirre, 2001) and in *Neurospora crassa* this third and fourth gene (Peraza and Hansberg, 2002, Schliebs *et al.*, 2006) were also reported.

Previous research suggests that catalase enzymes are not freely distributed inside cells, but are located in specific intracellular organelles, such as peroxisomes and the cytosol, in the case of *S. cerevisiae* (Izawa *et al.*, 1996).

Recent publications have also shown that catalase (one of the main anti-oxidative enzymes) is also capable of scavenging peroxynitrite (ONOO⁻) in a chemically defined system, as well as in a biological system using *S. cerevisiae* (Sahoo *et al.*, 2009, Gebicka and Didik, 2009).

Nanou has investigated the effect of increased oxidative stress levels on the production of carotene as described previously (Nanou *et al.*, 2011). The enhanced aeration resulted in an increase of CAT activity during the entire fermentation with two distinctive peaks in the trend, one during the exponential phase and another one after the carbon source was depleted during the stationary phase (Nanou *et al.*, 2011).

1.6.3 Peroxidases

Peroxidases are secreted, microsomal, cytosolic or organelle localized enzymes that are present in all domains of life (Hofrichter *et al.*, 2010). The review by Hofrichter explains that there are currently two superfamilies of peroxidases; (a) the so-called heme-thiolate peroxidases, comprising the *Caldariomyces fumago* chloroperoxidase and aromatic peroxygenases from agaric basidiomycetes and (b) the dye-decolorizing peroxidases from fungi and eubacteria (Hofrichter *et al.*, 2010).

Peroxidases in general have the potential to be industrially relevant, as their substrates can consist of; phenols and halogenated phenols, polycyclic aromatic hydrocarbons, endocrine disruptive chemicals, pesticides, dioxins, polychlorinated biphenyls, industrial dyes and other xenobiotics in which, these compounds are oxidized or polymerized by peroxidases, thereby decreasing their toxicity to the environment (le Roes-Hill *et al.*, 2010).

As with CAT, peroxidases are present to regulate intracellular levels of H₂O₂. The presence of the intermediate compound between CAT and H₂O₂ (described previously) seems to drive this peroxidatic reaction (Blokhina *et al.*, 2003).

Glutathione peroxidase

GPx is a type of peroxidase which has glutathione (see 2.7.1) (GSH) as an electron donor. It can get rid of H₂O₂ from the cell, which is a similar function as CAT (see eqn. 2.14).



GPx is also able to reduce organic peroxides such as lipid hydroperoxide and tert-butyl hydroperoxide (Inoue *et al.*, 1999).

GPx is probably one of the better characterized enzymes in eukaryotes, including fungi. Most yeasts however seem to lack GPx as do bacteria. However *S. cerevisiae* has been found to have three homologues for GPx, which were found in a genome database and were characterized in this organism. The three homologues were named GPX 1, 2 and 3 in which deletion of GPX3 seemed to give the strain hypersensitivity to H₂O₂ (Inoue *et al.*, 1999).

A. niger also has been shown to have GPx activity as was shown by previous research done in this lab. The results showed a clear increase in GPx activity while increasing the oxidative stress levels by either enriched oxygen or menadione treatment (Bai *et al.*, 2003).

1.7 Other anti-oxidant compounds

1.7.1 Glutathione (GSH)

GSH is a tripeptide (γ -L-glutamyl-L-cystinylglycine), which is thought to have an important role in buffering the cell against ROS (Li *et al.*, 2008e). GSH might reduce a number of oxidants via GPx or non-enzymatically which will result in its oxidized form glutathiol (GSSG). GSSG is then recycled and

reduced to GSH by a NADPH-dependent reaction that is catalysed by glutathione reductase (GR) (Li *et al.*, 2008e).

In *S. cerevisiae* glutathione has been shown to be essential for the reduction of H₂O₂ by the increased expression of GSH1 (encoding for γ -glutamylcysteine) and GLR1 (encoding for glutathione reductase) (Izawa *et al.*, 1998). A study done by Li showed that the addition of H₂O₂ resulted in increases GPx, GSH and GSSG values in the *A. niger B1-D* strain (utilised in the studies presented here as well) (Li *et al.*, 2008e). The study pointed towards mechanisms in place that are similar to *S. cerevisiae*.

1.7.2 NADPH

In cell life NADPH is an important reducing agent, which has also been shown to function as an antioxidant (Minard and McAlister-Henn, 2001). The enzyme sources for NADPH are glucose-6-phosphate dehydrogenase (G6PDH) and isocitrate dehydrogenase. Deletion of these two enzymes has been shown to be detrimental to cells viability. Deletion of G6DPH in yeast showed increased sensitivity to oxidative stress and an inability to develop any adaptive responses (Minard and McAlister-Henn, 2001).

1.7.3 Trehalose

Trehalose can be found in many organisms, including bacteria, fungi, plants, invertebrates and mammals. Due to its distinct physical features, trehalose is able to protect cells against a variety of environmental stressors (Arguelles, 2000). In fungi trehalose is either used as reserve compound or as a stress metabolite. Research found has shown that trehalose amounts increase when oxidative stress is applied (Fillinger *et al.*, 2001).

Fillinger showed that in *Aspergillus nidulans* trehalose can be found at high concentrations as well (Fillinger *et al.*, 2001). As with *S. cerevisiae* the same

gene encoding for the expression of trehalose-6-phosphate synthase was removed from *A. nidulans* and was found to be sensitive to moderate amounts of stress (temperature increase to 45°C and 2 mM of H₂O₂). This sensitivity was measured by monitoring trehalose content, germination and conidiation (Fillinger *et al.*, 2001).

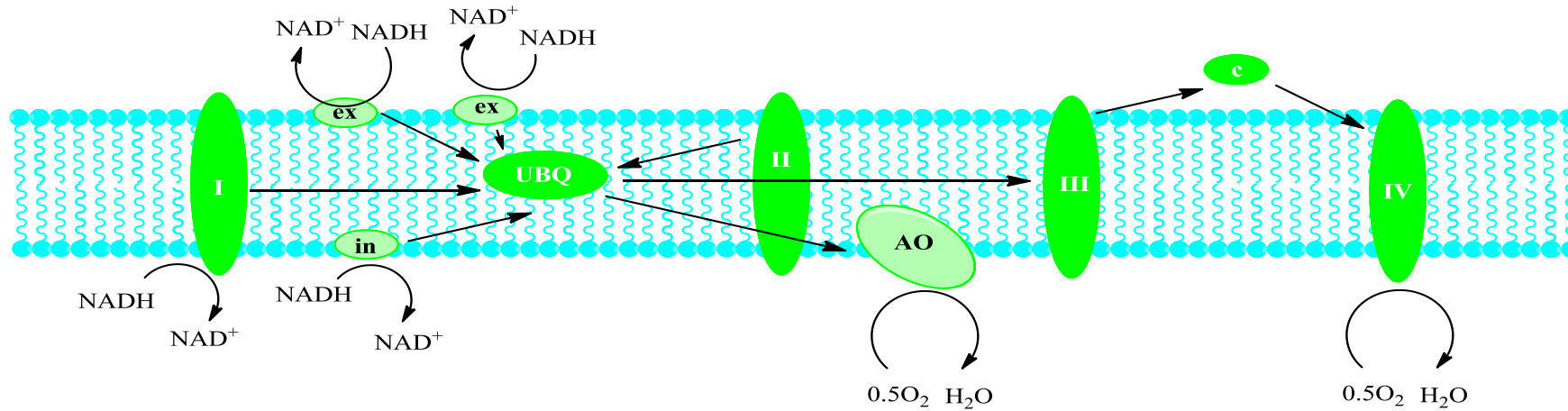
1.8 Alternative respiratory pathways

All aerobic organisms use oxidative phosphorylation to produce ATP. This process takes place via the oxidation of NADH and FADH₂. The respiratory chain accepts electrons from these reduces coenzymes and transfers them to oxygen forming water. The free energy that arises from this oxidation drives the translocation of protons across the inner membrane of the mitochondria. This proton motive force consists of a pH gradient and a transmembrane electric potential. This drives ATP synthesis by the enzyme F₀F₁-ATP synthase (Stryer, 1995).

The respiratory chain consists of four protein complexes: Complex I (NADH:ubiquinone oxidoreductase), Complex II (succinate:ubiquinone oxidoreductase), Complex III (ubiquinone:cytochrome *c* oxidoreductase), Complex IV(cytochrome *c* oxidase) (Joseph-Horne *et al.*, 2001).

During electron transfer, energy is conserved at three sites by pumping out protons across the inner membrane, which are Complex I, III, IV. Each complex has specific inhibitors, such as rotenone and piericidin for complex I, antimycin for complex III and cyanide for complex IV (Joseph-Horne *et al.*, 2001). Complex II does not pump protons due to low free energy change during respiration. See Figure 1-2 for the fungal respiratory and electron transfer chain.

Intermembrane Space



Matrix

Figure 1-2: Composite scheme of fungal mitochondrial electron transport.

I, II, III, IV, core electron transport complexes; ex, external NADH:ubiquinone oxidoreductase; in, internal NADH:ubiquinone oxidoreductase; UBQ, ubiquinone:ubiquinol pool; c, peripheral cytochrome c. Arrows indicate direction of electron flow adapted from (Joseph-Horne et al., 2001)

Most plants and fungi have an alternative to complex I in the form of NADH dehydrogenase. These enzymes accept electrons and transfer them to the ubiquinone directly. The alternative oxidase bypasses complex III and IV. Both of these enzymes do not pump out protons and therefore the energy is lost as heat (73kJ/2e) (Siedow and Umbach, 1995).

NADH dehydrogenase

A review by Videira details the role of NADH dehydrogenases (Videira and Duarte, 2001). The review found that in plants four alternative NADH dehydrogenases have been described. NADH dehydrogenases have been best described in yeasts, yeasts have similar enzymes but lack complex I. In the mitochondria of *Neurospora crassa* multiple NADH dehydrogenases have been described as well of which the internal enzyme was particularly active during the exponential phase. However research by Duarte showed that this internal NADH dehydrogenase is especially needed during the spore germination (Duarte *et al.*, 2003). Both papers state that complex I and NADH dehydrogenase are functionally complementary, which suggests that NADH dehydrogenase is not solely used as a way to alleviate oxidative stress.

1.8.1 Oxidative stress and respiration

As mentioned before respiration is needed to produce ATP, however this ATP production is in fungi dependent on mitochondrial activity and the activity of ATP synthase (Stryer, 1995). Zuin analyzed the effect of H₂O₂ on the respiration of *Schizosaccharomyces pombe* and found that, by growing this organism on respiratory-sufficient and H₂O₂ medium, oxidative stress had a severe negative effect on respiration and viability of cells (Zuin *et al.*, 2008). Zuin however didn't investigate how ATP production was affected. Qin studied the effect of oxidative stress on the respiration of *Penicillium expansum* and how it responded to H₂O₂ and found evidence that mitochondrial proteins were disproportionately affected under imposed

oxidative stress resulting in a lower ATP content (Qin *et al.*, 2011). This paper also looked at ATP production and how this was affected by the addition of H₂O₂, the lower ATP content of cells suggest either the complexes of the mitochondria are inhibited or ATP synthase. The effect of inhibiting ATP synthase in combination with H₂O₂ was even more severe on the survival of cells, suggesting that the mitochondrial proteins are mostly affected instead of ATP synthase by imposed oxidative stress (Qin *et al.*, 2011).

1.9 Morphology

In liquid, filamentous fungi exhibit two types of morphology. The first one is pellets, which are compressed hyphae, and the second one is hyphea. During fermentations these two morphological types are usually mixed with each other, where hyphal growth can consist of freely dispersed hyphea or clumped hyphae (Wang *et al.*, 2005).

A lot of research has been done to identify which morphological shape is optimal for production of heterologues or homologues proteins. Wang's review goes into this by mentioning that different types of products have different optimum morphologies (Wang *et al.*, 2005). An example that was mentioned was that for optimum penicillin production, from *Penicillium chrysogenum*, free mycelia are needed, while for citric acid production in *A.niger* pellets are needed.

The different morphologies that filamentous fungi have can pose problems in reactors. As biomass increases the rheological properties of the fermentation broth start to change unfavourably. This usually results in a high apparent viscosity, which leads to non-Newtonian behaviour of the fermentation broth. Shear thinning and pseudoplasticity are two characteristics of this. The high viscosity leads to poor mass transfer (mostly oxygen) and this will decrease overall productivity (Kreiner *et al.*, 2003, Wang *et al.*, 2005). This problem

usually doesn't occur in cultures that are in pellet form, however here the diameter of the pellets can become a problem. When pellet sizes increase so does diameter and when that happens the mass transfer rate (oxygen) might not be enough to let oxygen reach the inside of the pellet, which will result in oxygen starvation inside the pellets (Kreiner *et al.*, 2003).

The previous described morphology is known as macromorphology. Another term that has been introduced to describe the microscopic morphology of hyphae is micromorphology, however so far no uniform method has been developed to describe these properly. Because no standard methods exist to study morphology changes during fermentation, the effect of oxidative stress on morphology becomes a difficult subject (Wang *et al.*, 2005). A general consensus in literature seems that fungal cell surrounded by high concentrations of oxygen generally adopt a morphology that reduces the surface area exposed to that environment (Wang *et al.*, 2005).

Morphology can be influenced by pH where high pH produces pellets and low pH produces mycelia (Wang *et al.*, 2005) the same review also says that high stirring rates yield small pellets or free filaments depending on process conditions while low stirring rates yield big pellets.

1.10 Nitrosative stress

1.10.1 Introduction

Many organisms are capable of generating nitric oxide (NO). This nitric oxide can in sufficient amounts cause damage either by itself or by reacting with oxygen radicals. A substantial amount of research has been spent on this molecule in relation to immune responses and plant physiology, however to this author's knowledge no relevance of this molecule has been shown yet

inside bioreactors.(Li et al., 2010a, Vieira et al., 2009, Silverman and Epstein, 1975)

NO is considered to be an important signalling molecule inside plants and animals. It can function in relation to disease resistance, abiotic stress, cell death, respiration, senescence, root development, germination and hormone responses (Wendehenne et al., 2001, Crawford and Guo, 2005).

1.10.2 Nitric oxide (NO) generation

Intracellular nitric oxide (NO) is synthesized in a two-step process which involves the oxidation of the terminal guanidine nitrogen of L-arginine resulting in the formation of L-citrulline and NO (Zaki *et al.*, 2005). See Figure 1-3 for a schematic representation.

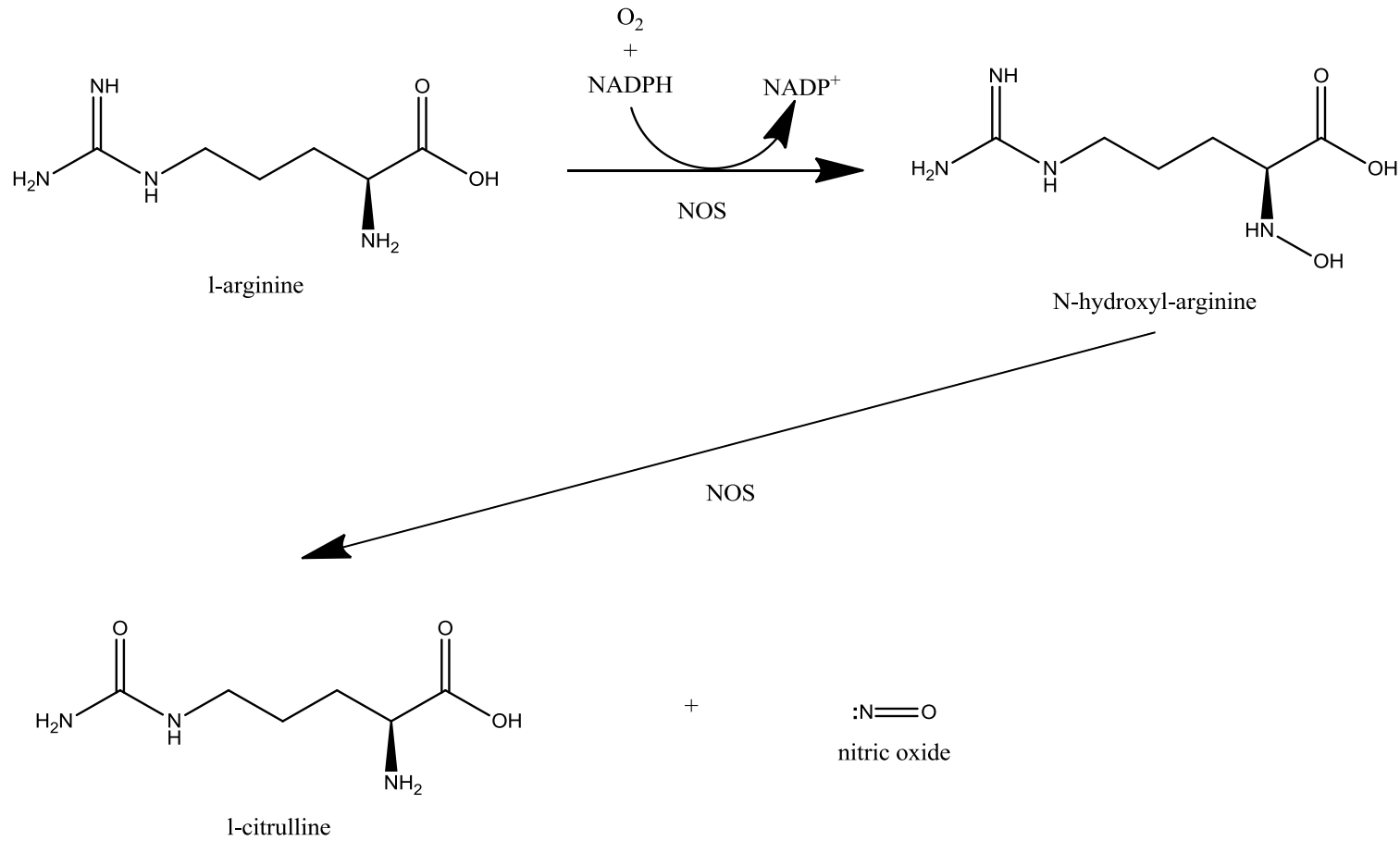


Figure 1-3: Conversion of L-arginine into L-citrulline (adapted from (Stryer, 1995)).

The lifetime of NO is about 30 minutes at a concentration of about 10^{-7} M, in its various oxidative states the lifetime might only be a few seconds (Poole, 2005). The enzyme responsible for the conversion is nitric oxide synthase (NOS). In mammalian cells there are three more enzymes that can catabolise arginine. These are; arginase, glycine amidinotransferase, arginine decarboxylase and arginine deiminase (Morris, 2004).

By using biochemical approaches Almeida has identified NOS activity in *S. cerevisiae* (Almeida *et al.*, 2007). Two basic methods were used for this; an NOS assay kit and NO-selective electrode. The organism was treated with H_2O_2 and showed increased NOS activity, with increased arginine content and NO content as well. An interesting result of this study was also an increase in nitrate content of the organism after cells were treated with H_2O_2 .

In *Coniothyrium minutans* NO and L-arginine have been linked to the conidiation of this filamentous fungus (Gong *et al.*, 2007). The research showed however only provided evidence to this via L-arginine experiments. A gene named CMCP1, which was previously identified to encode for L-arginine-specific carbamoyl-phosphate synthase, was disrupted thereby resulting in a conidiation deficiency. This deficiency could be restored by adding L-arginine, however no direct link in this paper was presented between NO and conidiation. Their literature study however did indicate this and therefore it was hypothesized that NO might be involved in conidiation of filamentous fungi as well. This was proven more convincingly by Li, as he used sodium nitroprusside (SNP) to study the effect of NO on conidiation of this organism. Proof was provided using a similar approach by Almeida (disrupting the gene for L-arginine) with the only difference that NO was also tested and showed that conidiation could be restored by it.

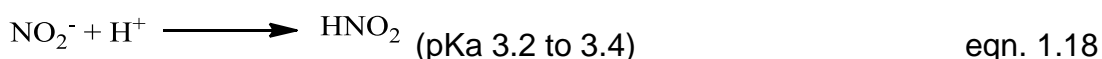
1.10.3 RNS chemistry

Parallel to ROS reactive nitrogen species (RNS) can be formed. RNS usually indicates nitric oxide (NO) and NO-derived molecules such as; peroxyxynitrite (ONOO⁻), dinitrogen trioxide (N₂O₃), S-nitrosoglutathione (GSNO), nitrogen dioxide (NO₂), nitrosyl cation (NO⁺) and S-nitrosothiols (Valderrama *et al.*, 2007, Poole, 2005, Gaston, 1999).

ONOO⁻ is formed by a reaction that has been described previously (eqn 1.2), however literature showed that more reactions exist that can yield nitrogen derived molecules that can damage cells. The first reaction is what happens when NO reacts with oxygen. This is a three-step reaction which will eventually yield NO₂⁻ (Bryan and Grisham, 2007):



Nitrite itself can under acidic conditions form NO as well. This is outlined in the following reactions (Weitzberg and Lundberg, 1998, Lundberg and Weitzberg, 2005):



The reactions that have been described in this paragraph have been investigated in blood (Bryan and Grisham, 2007, Lundberg and Weitzberg, 2005) and in the stomach (Weitzberg and Lundberg, 1998). In cells from

plants, animals, microorganisms most of these reactions haven't been described.

The predominant reaction that comes forward in literature inside plant or animal cells is the reaction between O_2^- and NO to form ONOO^- (Radi *et al.*, 2002, Blokhina and Fagerstedt, 2010).

1.10.4 RNS defences

The immune cell armoury consists of potent reactive oxygen and nitrogen species, which can damage DNA, proteins and lipids. In phagocytic cells NOS is induced via cytokine stimulation (Brown *et al.*, 2009). Some pathogens have developed RNS defence mechanisms thereby increasing their resistance against these chemical insults.

Research in *E. coli* has shown that it possesses flavohaemoglobin denitrosylase (HMP) that is induced by NO. The proposed detoxification mechanisms for a number of RNS using HMP are (Hausladen *et al.*, 1998):



Previously glutathione (section 1.7.1) has been described however literature points towards another function of this compound in which glutathione can become nitrated, by NO exposure, to form S-nitroglutathione (GSNO). The compound in itself can also react with ONOO^- , which yields the oxidated form of glutathione (Radi *et al.*, 2002). Glutathione is a second indication of the interactive nature between oxidative and nitrosative stress. The first indication was the formation of ONOO^- described in section 1.2.1 and CAT described in section 1.6.2. Oxidated glutathione has GPx to convert it back to

glutathione. In *E. coli* S-nitrosoglutathione (GSNO) reductase was found, which can convert GSNO back to glutathione (de Jesus-Berrios *et al.*, 2003).

Most of the described radical formation seems to take place in the mitochondria (Radi *et al.*, 2002). The review by Radi states that mitochondria may partially detoxify ONOO^- , by cytochrome c oxidase, ubiquinol and glutathione, however the relative contribution of these weren't found in the literature. Schopfer showed that isolated ubiquinol interacted directly with ONOO^- , which resulted in the formation of ubisemiquinone (Schopfer *et al.*, 2000). A remark that should be made here is that the article shows quite clearly an oxidation of ubiquinol by ONOO^- in a chemically defined system, however as Schopfer confirmed it would be difficult to prove this in live cells.

Recently CAT has been shown to scavenge for ONOO^- this has been shown in a chemically defined system as well as in *S. cerevisiae* (Gebicka and Didik, 2009, Sahoo *et al.*, 2009). Gebicka observed a difference between ONOO^- decay rates with and without CAT, in a spectrometer. Sahoo deleted the genes encoding for flavohemoglobin (YHB1) and formaldehyde dehydrogenase (Δsfa1), an enzyme that can metabolize GSNO, in *S. cerevisiae* and subjected the organism to sublethal doses of ONOO^- , which resulted in higher CAT activities.

1.10.5 RNS damage

DNA

Modification of DNA has mostly been shown to happen when ONOO^- is formed (Zaki *et al.*, 2005). Yermilov *et al.*, (1995) showed that treating DNA with peroxynitrite resulted in the formation of 8-nitroguanine, which resulted in the removal of this base from DNA. The same paper also showed that nitrite wasn't able to form 8-nitroguanine, which points towards peroxynitrite being the most dangerous nitrogen radical for DNA (Yermilov *et al.*, 1995). Douki and Cadet (1996) did similar research but mostly found an enhancement of

oxidation when exposing DNA to ONOO⁻. Douki and Cadet (1996) also showed that adenine became more sensitive to oxidation after treatment with ONOO⁻. Both of these papers however studied these effects in vitro and not on live cells.

Zaki *et al.*, (2005) also mentions that RNA seems to be more sensitive to mutations caused by ONOO⁻ than normal DNA. As most viral DNA is RNA this could partially explain why the mutation rate of viruses is higher than normal double strands DNA (Zaki *et al.*, 2005). No studies on DNA damage by ONOO⁻ were found relating to filamentous fungi.

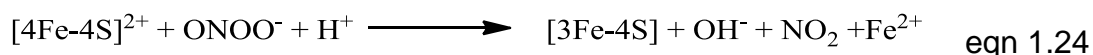
Mitochondria

Cytochrome c oxidase reacts very quickly with NO in its reduced state ($k=10^8 \text{ M}^{-1} \text{ s}^{-1}$). This leads to the formation of the nitrosyl-cytochrome a_3 complex (Brown, 2001). The heme iron of cytochrome c normally binds oxygen and after the reaction with oxygen is finished the heme iron returns to its non oxidized form (Radi *et al.*, 2002). NO and oxygen compete for this heme iron making the NO binding a reversible process, however when NO binds to cytochrome c it does severely inhibit respiration (Radi *et al.*, 2002). Pearce showed that NO in itself doesn't inhibit complex I directly, however ONOO⁻ and S-nitrosothiols can do this by transnitrosation or oxidation of critical thiols in complex I (Pearce *et al.*, 2001). Complex II might be inhibited by NO binding to iron sulphur clusters however this has only been shown to happen in significant quantities at high NO concentrations (Radi *et al.*, 2002). The review by Radi does point out that Fe-S clusters in complex II are very stable and do not readily oxidize, however secondary nitrogen intermediates, such as ONOO⁻ might more easily bind to these Fe-S clusters.

Proteins

The damage mechanisms described for protein or enzyme damage is protein nitration which is a reaction of the iron sulphur groups with ONOO⁻ (Brandes

et al., 2007, Hausladen *et al.*, 1998, Kuo *et al.*, 2000, Radi *et al.*, 2002). The next equation describes this in more detail:



Kuo further investigated the nitration of tyrosine into 3-nitrotyrosine and found post-translational nitration of tyrosine after treatment of ONOO⁻ in vitro, which could potentially happen in vivo as well (Kuo *et al.*, 2000). An example mentioned by Radi is the inactivation of aconitase (Radi *et al.*, 2002). This enzyme can be inactivated by NO and ONOO⁻ in which the inactivation by NO is reversible and ONOO⁻ is permanent.

1.11 Interaction between ROS, RNS generation and oxidative stress defences

1.11.1 Denitrification

When trying to explain the interaction between ROS, RNS generation and oxidative stress defences first of all a short overview of nitrate respiration has to be given. Nitrate respiration is a widespread phenomenon in fungi and bacteria (Morozkina and Kurakov, 2007, Thomson *et al.*, 2012). Under low oxygen conditions denitrifying bacteria can derive energy via electron transport coupled to the reduction of nitrogen oxides (NO₃⁻, NO₂⁻, NO and N₂O) (Morozkina and Kurakov, 2007, Thomson *et al.*, 2012). Most soil fungi denitrify nitrates (NO₃⁻) into nitrous oxide (N₂O). The amount of nitrous oxide released into the environment of which fungi are the source is under optimum conditions in the range of 1-8%. This means that fungal denitrification has important implications for ecology (Morozkina and Kurakov, 2007, Thomson *et al.*, 2012).

The process starts out with nitrate, which is converted into nitrite and then ammonium or NO. The enzymes responsible for this conversion are nitrate reductase, nitrite reductase and NO reductase (Morozkina and Kurakov,

2007). Nitrite reductase can also convert nitrite into ammonium, however this is an anaerobic process (Morozkina and Kurakov, 2007). Figure 1-4 shows schematically what has just been described. If ammonium is formed then this can coincide with ATP formation when catabolic oxidation of electron donors (ethanol) to acetate and substrate level phosphorylation takes place (Takaya, 2002), Figure 1-5 shows schematically the pathway for fungal ammonium fermentation.

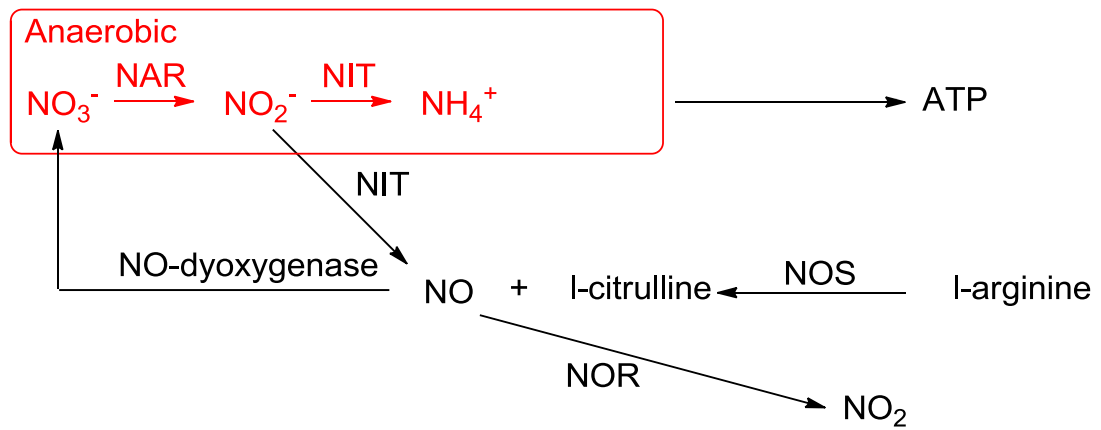


Figure 1-4: Nitrate metabolism of filamentous fungi.

NAR is nitrate reductase, NIT is nitrite reductase, NOS is nitric oxide synthase and NOR is nitric oxide reductase, adapted from (Morozkina and Kurakov, 2007, Thomson et al., 2012).

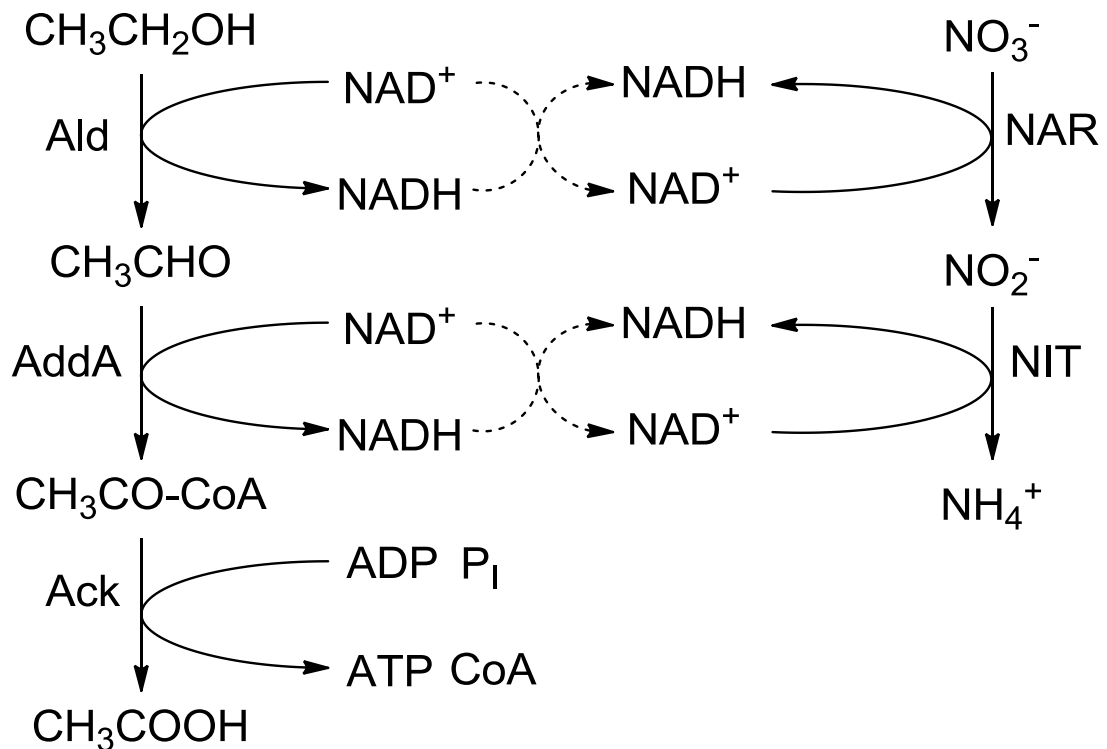


Figure 1-5: Pathway for fungal ammonium fermentation.

Alcohol dehydrogenase (Ald), acetaldehyde dehydrogenase (Add), acetate kinase (Ack), nitrate reductase (NAR), nitrite reductase (NIR) and inorganic phosphate (P_i) adapted from (Morozkina and Kurakov, 2007)

1.11.2 Combining aerobic and anaerobic respiration

The literature studied here hasn't directly established a link between ROS and RNS generation, however it very clearly points towards this. CAT for instance is also capable of converting ONOO^- (Sahoo *et al.*, 2009). This points towards an interaction between oxidative and nitrosative stress that is highlighted in Figure 1-6. Figure 1-6 combines anaerobic respiration (Figure 1-4) with aerobic respiration (eqn. 1.1). Where NO is clearly shown as a molecule that is involved in both aerobic respiration and anaerobic respiration.

When NO reacts with $^{\cdot}\text{O}_2^-$ to form ONOO^- it could influence CAT activity, with respect to hydrogen peroxide resulting in a potential decrease of the microorganisms ability to cope with oxidative stress. Literature evidence is very scarce on the interaction between aerobic and anaerobic respiration and its influence on oxidative stress defence mechanisms. It is not even sure if this interaction is either positive or negative. Another question that can be asked is; can this mechanism be exploited in a bioreactor?

The reasons for leaving out other oxidative stress defence mechanisms and nitrosative stress defence mechanisms is that the work presented in this thesis has been focused on the oxidative stress defences depicted in Figure 1-6.

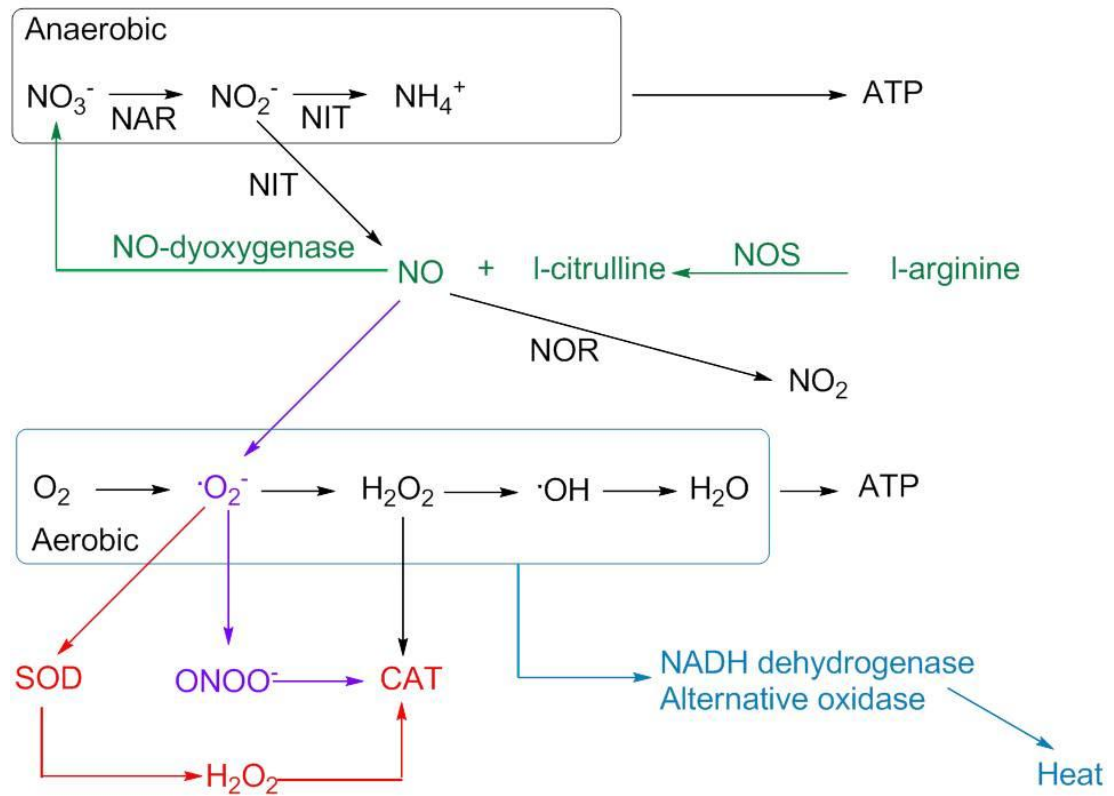


Figure 1-6: Schematic drawing of anaerobic and aerobic respiration and the interactions that are possible between ROS and RNS, adapted from (Wojtaszek, 1997, Morozkina and Kurakov, 2007, Thomson et al., 2012). Nitrate reductase (NAR), nitrite reductase (NIT), Nitric oxide reductase (NOR) and nitric oxide synthase (NOS). The purple highlighted mechanism represents a potential interaction, the green highlighted mechanism depicts the source of NO, the blue highlighted mechanism represents the alternative pathway and the red highlighted mechanism represents.

1.12 Process parameters affecting ROS formation

1.12.1 Introduction

The industrial relevance of filamentous fungi has been pointed out in the general introduction. Unsatisfactory yield levels of protein during fermentation are often the result of various process parameters. Specifically during fermentations filamentous fungi are exposed to a number of conditions that can initiate stress such as; concentration gradients due to viscosity and insufficient mixing, pH, temperature, shear stress, oxygen limitation and carbon limitation.

1.12.2 Inoculum

From this chapter it is clear that cells which have an aerobic respiration system produce ROS. Aerobic cells are also able to cope with a relative high concentration of ROS due to various enzymatic and biochemical defence mechanisms (SOD, glutathione etc.).

Inoculation of a cultured organism into a reactor results in a lag period (Li *et al.*, 2008e) which is caused by the adaptation of the culture to the new environment. Recent research showed that the inoculation of shake flasks into a bioreactor leads to oxidative stress (O'Donnell *et al.*, 2007). These oxidative stress events can be monitored by measuring the activity levels of catalase and superoxide dismutase and the levels of O_2^- or H_2O_2 . From previous research it was shown that oxygenated inocula seemed to be able to deal more effectively with oxidative stress. This was attributed to the increase in CAT and SOD activity levels (O'Donnell *et al.*, 2007).

1.12.3 Reactor modes

Fermentations can be done utilising different reactor modes such as; batch, fed-batch, solid state and continuous fermentation. These various options to perform a fermentation can have different effects on oxidative stress and its associated defence mechanisms.

Continuous fermentation

Various fungal products/processes require one kind of fungal morphology (Kreiner *et al.*, 2003, Wang *et al.*, 2005). Research on oxidative stress in chemostat cultures offer the advantage of the variation of just one variable of interest and this is compared to batch cultures an advantage. In batch cultures most parameters of interest change in time (biomass, carbon source etc.). Continuous fermentation was performed previously in the Fermentation Centre at Strathclyde to investigate the influence of oxidative stress on morphology an enzymatic response while exposing *A. niger* to increased levels of oxidative stress (Bai *et al.*, 2003, Bai *et al.*, 2004, Kreiner *et al.*, 2003). Results from these studies indicated that continuous fermentations are able to cope better with increased levels of oxidative stress, once the continuous phase was reached, as was shown by the non-significant effect on morphology and non-significant effects on heterologous protein expression on this organism, however batch fermentations showed decreased yields of heterologous proteins when exposing *A. niger* to increasing levels of oxidative stress (Bai *et al.*, 2004).

Cheng *et. at.*, (2008) showed by comparing batch/fed-batch fermentation to continuous fermentation of *S. cerevisiae* that stress responses (also associated to oxidative stress) were higher during batch/fed-batch fermentation. An example of a continuous fermentation process is the production of mycoprotein by Quorn (Wiebe, 2002).

Solid state fermentation

The immobilization of microbial cells on different carriers leads to changes in their microenvironment, because of these changes, immobilized cells show various modifications in physiology and biochemical composition when compared to suspended cells (Angelova *et al.*, 2000). Literature has shown that during the stationary growth phase, immobilized cells showed a prolonged period of growth and decreased protein content (Angelova *et al.*, 2000). When looking at SOD and CAT in terms of differences between the two operational modes it was found that especially SOD activity was significantly higher in immobilized fungal cells. SOD activity in free cells was at its peak 60 U mg^{-1} and in immobilized cells SOD activity was 100 U mg^{-1} . Catalase activity was higher too in immobilized cells but not as pronounced when comparing to SOD (Angelova *et al.*, 2000).

1.12.4 Process control

Morphology of fungal fermentations can increase the viscosity of the fermentation broth, as described before this can decrease the mass transfer of oxygen. Some counteractive measures to this problem are increasing the stirring rate and airflow, which are usually controlled in fermentations, by setting the dissolved oxygen tension (DOT) inside the reactor before inoculation. There are however some limitations to this as the increase of stirring rate can only be limited to the amount of shear stress hyphae can take (Wang *et al.*, 2005).

Literature clearly shows that process control, focused on DOT, can have large effects on protein content, morphology and biomass growth (Wang *et al.*, 2005). Previous research done in this lab has shown that applying enriched oxygen at the start of the fermentation resulted in increased levels of oxidative stress in *A. niger* (O'Donnell *et al.*, 2011), however no definitive link between stirring rate and oxidative stress levels has been found in literature.

Another aspect of process control is the application of new online sensors to monitor various process parameters such as; biomass, metabolites and product concentrations. Advantages of such sensors include: real time monitoring of bioprocesses, which allows for rapid responses when processes are not going as expected (Cervera *et al.*, 2009). Most of these sensors work on the principle of light absorbance, which is also often utilised offline to analyze samples, for example optical density (OD) is often used to monitor biomass growth. Optical sensors usually work in the region of 800 to 2500 nm and measure changes in the absorbance of light over this range when the process is running. Lambert-Beer's law allows for the determination of the exact concentration of compounds that are of interest (Cervera *et al.*, 2009):

Different compounds absorb light at different optimum wavelengths, which are usually determined by measuring a compound at a wavelength range to investigate where the absorption peak is.

A paper by Oushiki *et al.*, (2012) showed an application to monitor enzymes by applying a Near-Infrared (NIR) fluorescence probe. A review by Gishen *et al.*, (2005) showed applications of spectroscopic sensors in the Australian wine industry. A lot of research is focused on correlating signal changes to off line measurements when using NIR to monitor processes. Literature describes an example of the application of a NIR-based control system. This system allowed the full automation of a small-scale pilot plant for lactic acid production using *Lactobacillus casei*. In this process the three critical control parameters were glucose, lactic acid and biomass, which were measured using a NIR control loop (Scarff *et al.*, 2006, Cervera *et al.*, 2009).

Similar work could be applied to monitor fungal fermentations, however no applied practical examples were found. As culture viscosity seems to inhibit mass transfer of oxygen, monitoring biomass seems extremely important. This means that first of all a reliable method has to be found to monitor fungal biomass growth inside bioreactors. The added difficulty of this is the

morphological change that occurs inside reactors, as fungal fermentations start out as pellets but convert to hyphae during fermentation.

Temperature

SOD and catalase play important roles in the heat shock response. Previous research at this university has studied the effects of elevated culture temperature on protein carbonylation and intracellular proteolytic activity in batch cultures (Li *et al.*, 2008c). The main outcome of this work was that higher temperature seemed to increase the respiration rate, resulting in a higher carbon source and nitrogen source uptake rate and ATP content, during the exponential phase (Li *et al.*, 2008c). A higher respiration rate also results in a higher generation of oxygen radicals, thereby increasing oxidative stress.

Medium

Paragraph 1.6.1 and 1.6.2 described that SOD and CAT activities during cultivation in a reactor exhibit peak activities during the lag phase and at the onset of the stationary phase in *Kluyveromyces marxianus* and *Blakeslea trispora* (Dellomonaco *et al.*, 2007, Nanou *et al.*, 2011). Both these papers attributed these peak activities of SOD and CAT to too much oxygen transfer at the start of the fermentation and culture age at the end of the fermentation, but not to the depletion of the carbon or nitrogen sources.

1.13 Summary and aims

1.13.1 Summary

ROS are normal by-products of respiration by aerobic microorganisms. All aerobic microorganisms have developed defence mechanisms to counteract these oxygen radicals and prevent damage to intracellular components as much as possible. These defence mechanisms have shown to be enzymatic and non-enzymatic.

Usually ROS generation and ROS defence mechanisms are in balance, however when an imbalance occurs cells can be severely damaged or die. In a bioreactor this results in a lower production of biomass or desired product, which is often a specific enzyme or protein. Literature also quite clearly shows that cells who survive this imbalance will have developed more adaptive responses to this imbalance and can therefore tolerate more oxidative stress than before. An example of oxidative stress is an oxygen radical burst associated with an immune response.

Literature also showed that NO is a highly versatile molecule involved in many cellular processes. In filamentous fungi it is generally accepted that NO is involved in the formation of NO₂ during the denitrification (removal of nitrates or nitrites) process of soil. Figure 1-6 shows that there should be a clear interaction between aerobic and anaerobic respiration. This has however not been shown yet in experiments.

In a bioreactor fungal fermentations clearly have a problem that is associated with oxygen transfer due to the high apparent viscosity of the fermentation broth. Literature clearly shows a few solutions such as oxygen enrichment, air flow increases and increasing the stirring rate to make sure the oxygen concentration inside the reactor doesn't become limiting. A downside to all these approaches is that the organism or the product could be damaged by shear rate and oxidative stress.

1.13.2 Aims

The aims of this work can be summarised as follows:

- Studying the effect of increasing amounts of polymyxin B on oxidative stress defence mechanisms during cultivation of *A. niger B1-D*.
- The aim of this study was to see whether *A. niger B1-D* can cope with increasing levels of oxidative stress during the lag phase of the

fermentation. This will be achieved by studying the levels of activity of the defensive enzymes against oxidative stress at different agitation speeds.

- The primary aim of this study was to observe the effects of increasing amounts of sodium nitroprusside (SNP) on SOD and CAT activities in a bioreactor and to see if they corresponded with other physiological parameters of *A. niger B1-D* commonly measured during cultivation in bioreactors.
- The aim of this chapter was to investigate, with an industry partner, whether a simple spectroscopic sensor, the buglab from Applikon could be used to monitor fungal fermentations utilising *Aspergillus niger B1-D*.

Chapter 2

Materials and Methods

2 Materials and methods

2.1 Stirred tank reactor (STR), control system and associated analytical reactor equipment

STR experiments were carried out using a control system called the Bioflo3000 (New Brunswick Scientific, Edison USA) and a bench-top fermenter with 3.3 l total volume and a work volume of 2.5 l. Air and water were supplied by the main laboratory lines. Filtered air was sparged into the reactor using a circular annular sparger with four holes for an even distribution of air bubbles inside the reactor.

The following parameters could be controlled with this experimental setup; dissolved oxygen tension (DOT), pH, stirring rate, air flow and temperature.

The reactor itself had an aspect ratio 2:1 and the diameter of the reactor was 13.5 cm. Custom made internal baffles (four) were used to increase oxygen transfer. Each baffle had a length of 17.5 cm and a width of 1.5 cm. Two adjustable six-bladed Rushton turbines were placed on the stirrer shaft with a diameter of 6.5 cm. The reactor needed to be sterilized using an autoclave, which was set at 121 °C for 20 minutes.

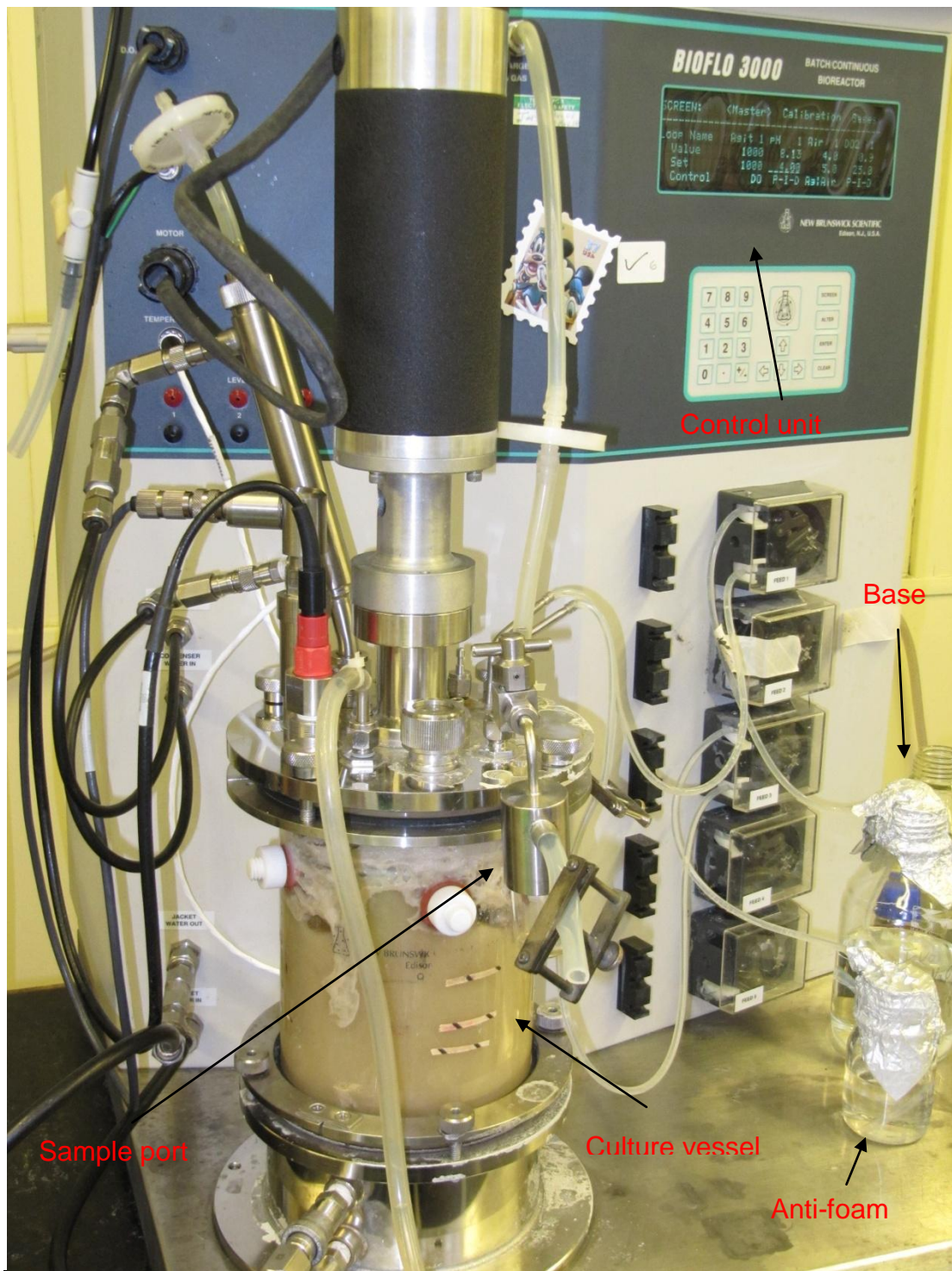


Figure 2-1: Operational setup of Bioflo3000 with reactor during *A. niger* B1-D fermentation.

Temperature

The temperature was controlled using the jacketed stainless steel bottom-dished head in which heated or cooled water was circulated depending on the control needs of the experiment. The temperature was measured by a resistance temperature detector (RTD) submerged in a thermo well which was mounted in the head plate of the reactor.

Oxygen

For the measurement of DOT a pO₂-electrode (Mettler Toledo, Leicester UK) was utilised. This electrode was sterilized together with the reactor before it was calibrated. Calibration was done using 500 rpm and sparging nitrogen and air vigorously for the zero and 100% point respectively at 25⁰C.

pH

To measure the pH a pH electrode (Mettler Toledo, Leicester UK) was used which was sterilized with the reactor. The calibration was performed before sterilization using a two-point calibration (pH 4 and 7).

Buglab

The buglab BE2100 (Aplikon, Schiedam, The Netherlands) was utilised as an online sensor for biomass measurements. This sensor is non invasive as it is strapped around the reactor with the sensor head on the glass or viewing port in larger reactors. The sensor utilises an array of infrared lasers and detectors and combines the signal changes (called spectral values) to linearize the responses over a very wide dynamic range (Aplikon). The sampling interval of the sensor was set to two minutes.

Gas analyzer

The exit gas from the reactor was analyzed using a digital gas analyser TANDEM PRO (Applikon Biotechnology Ltd, Tewkesbury, Gloucestershire, UK). The analyser was calibrated using 19% (v/v) oxygen and 1.75% (v/v) carbon dioxide (BOC Ltd., Glasgow The UK).

2.2 Culture conditions

2.2.1 Strain

The fungal strain that was used for this study was *Aspergillus niger* B1-D. This strain was kindly provided by Professor David Archer of the University of Nottingham. This fungal strain has the hen egg white lysozyme (HEWL) cDNA cloned into an integrating plasmid and is controlled by the *Aspergillus awamori* glucoamylase promoter (*glaA*) (Archer et al., 1990).

2.2.2 Medium

The culture medium for all growth experiments was based on (Li, 2008). The medium composition used in batch or shake flask cultivation was; 50g glucose, 10g NH₄Cl, 20ml salt solution, 10ml vitamin solution and water to 1l.

Salt solution: 26g KCl, 26g MgSO₄·7H₂O, 76g KH₂PO₄, 50 ml trace element solution and distilled water to 1l.

Trace element solution: 40mg Na₂B₄O₇·10H₂O, 400mg CuSO₄·5H₂O, 800mg FePO₄·2H₂O, 800mg MnSO₄·2H₂O, 800mg Na₂MoO₄·2H₂O, 8g ZnSO₄·7H₂O and distilled water to 1l.

Vitamin solution: 20mg p-aminobenzoic acid, 50mg thiamine hydrochloride, 10mg biotin, 100mg nicotinic acid, 200mg calcium D-pantothenic acid, 50mg pyridoxine monohydrochloride, 100mg riboflavin and water to 1l. After this the solution was filter sterilised through a syringe using 0.2 µm cellulose acetate filters.

All reagents were purchased from Sigma-Aldrich unless stated otherwise.

2.2.3 Inoculum preparation for batch fermentations

Spores of *A. niger* B1-D were harvested from a 7-day old potato dextrose agar plate with sterile distilled water containing 0.1 % (w/v) Tween 80. Using a haemocytometer, the spore concentration was counted. The shake flasks were inoculated to a final spore concentration of 1×10^5 per ml in a total work volume of 250 ml. The inoculum was grown for 48 hours prior to a reactor experiment in an incubator (New Brunswick Scientific, Edison USA), set at 25°C and 200 rpm.

2.2.4 Shake flask cultivation

The shake flask experiments in Chapter 5 were done using 500 ml Erlenmeyer's with a work volume of 200 ml. Inoculation of these shake flask experiments was done with spores and placed in an incubator, as described in 2.2.3.

2.2.5 Stirred tank reactor

Sterilization

The reactor itself was sterilized with 1.5 litre of distilled water in an autoclave. The following solutions were sterilized separately (under the same conditions); 500 ml of distilled water containing glucose, 225 ml of distilled water consisting of ammonium chloride and the salt solution, 200 ml of 2M NaOH and 200 ml of 2M H₂SO₄. The vitamin solution was filter sterilized and added aseptically prior to inoculation of the reactor (25 ml).

Reactor settings and experimental conditions

General reactor settings and experimental conditions that were kept constant for all experiments were; inoculum was 10% (v/v), pH was set to 4 using 2M

H₂SO₄ and 1M NaOH, the set temperature was 25⁰C, air flow was 2 l/min and the sample volume was 40 ml for each sample taken.

2.3 Analyses

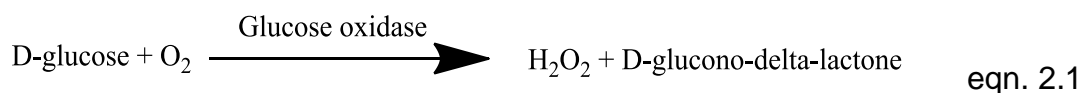
For the analyses of intracellular compounds cells had to be disrupted. This was done by using a high pressure cell disrupter (Model 4000, Constant System Ltd., Warwick, UK). After this the resulting cell debris had to be removed, which was done by using a centrifuge (Jouan BR4i, Thermo Electron Corporation, East Grinstead, West Sussex, UK) set at 14,000 rpm, 4 ⁰C and 30 minutes. Assays described below that utilised a spectroscopic measurement used the Biomate 5, Thermo scientific, Hemel Hempstead, Hertfordshire, The UK.

2.3.1 Biomass

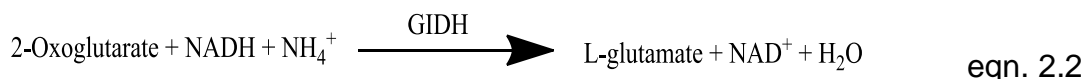
Biomass was determined using a method based on (Li, 2008). For each measurement a sample of 5 ml was taken from the reactor. This was subsequently filtered, using a Buchner funnel, washed twice with distilled water and put in an oven at 105⁰C for 20 minutes (determined experimentally) after which the filter was placed inside a desiccator for another hour before the weight was measured. All measurements were done in triplicate.

2.3.2 Glucose and ammonium

Glucose was measured in the medium, after separation of medium and biomass, with the YSI 2700 (YSI (UK) Limited). This was a direct reading of dextrose in solution at the enzyme sensor. The analysis is a measurement of hydrogen peroxide after conversion has taken place according to eqn 2.1:



Ammonium was analyzed using an enzymatic assay kit from RBiopharm Rhone Ltd. (ref. 11112732035). The principle of this kit is as followed; In the presence of glutamate dehydrogenase (GDH) and NADPH, ammonium reacts with 2-oxoglutarate to L-glutamate, whereby NADH is oxidized according to eqn 2-2:



The amount of NADH that is oxidized is stoichiometric to the amount of ammonium and can be measured at 340 nm. All measurements were done in triplicate.

2.3.3 Adenosine triphosphate (ATP)

Samples from the bioreactor were analyzed on ATP content using a commercial kit (Sigma ref. FL-AA), and results were obtained as relative light units (RLU) on a Spectramax plus 384 microplate reader. Prior to analyses ATP had to be extracted. The procedure for this was to boil 3 ml of biomass, from the bioreactor, in Tris-EDTA buffer, pH 7.4. This boiling procedure inhibits enzymes and allows ATP to exit the cell as it becomes porous. After boiling the sample for about 3-5 minutes the samples were placed on ice (about 15 minutes) and centrifuged as described previously prior to analyses.

2.3.4 Culture viability

Principle

The reaction that is analyzed in this assay is the conversion of 3-(4,5-Dimethyl-2-thiazolyl)-2,5-diphenyl-2H-tetrazolium bromide (MTT) to formazan

(Vistica *et al.*, 1991, Emri *et al.*, 2005). The formazan has its absorption peak at 570 nm and this can be measured and expressed as $A_{570\text{nm}}/\text{g DCW}$ (dry cell weight).

Solutions

Solution 1: 5 mg/ml solution of 3-(4,5-Dimethyl-2-thiazolyl)-2,5-diphenyl-2H-tetrazolium bromide (MTT, Sigma ref. M2128)

Solution 2: Dodecyl sulphate (SDS, Sigma ref. L4509) in 20 mM HCl

Procedure

To 2 ml of fungal culture, from the bioreactor, 50 μ l of solution 1 was added and was incubated for 24 hours at 30 $^{\circ}$ C, within these 24 hours the colour of the biomass will turn purple. After 24 hours 1 ml of solution 2 was added to the vials and then it was incubated for another 24 hours at 30 $^{\circ}$ C. After these last 24 hours the absorbance was measured at 570 nm with the previously described spectrometer. All results are expressed as $A_{570\text{nm}}/\text{g CDW}$ and all samples were analyzed in triplicate.

2.3.5 Lysozyme

Principle

Hen egg white lysozyme (HEWL) was determined based on methods used previously in this laboratory (Li, 2008). This assay measures the lysis of *Micrococcus lysodeikticus* (5 g/l) by lysozyme in samples that were obtained during STR experiments.

Solutions

Solution 1: 50 mM sodium phosphate buffer at pH 6.2

Solution 2: *Micrococcus lysodeikticus* (Sigma ref. M3770) at a concentration of 5 mg/ml dissolved in solution 1

Procedure

Biomass was separated from medium by filtration using the Buchner funnel as described in 2.3.1. After which 1 ml culture filtrate was mixed with 0.1 ml of solution 2. The absorption was measured at 600 nm for 5 minutes with intervals of 1 minute. Linearity of the samples was checked after the assay and results were compared to a standard calibration curve (0-5 mg/l, see **Figure 2-2**). All samples were analyzed in triplicate.

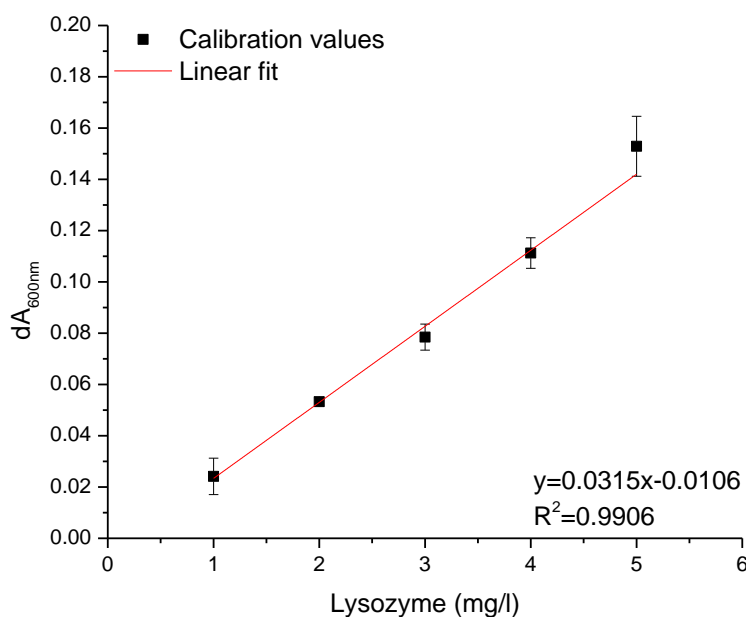


Figure 2-2: Calibration curve used for the estimation of lysozyme.

2.3.6 Nitrite assay

Principle

Nitric oxide release was measured indirectly, in the medium, by measuring the nitrite concentration in a sample, therefore the Griess reaction can be utilised to measure nitrite. Briefly the Griess reaction is a two-step diazotization where nitrite reacts with sulphanilic acid which results in the

diazonium ion. This ion is then coupled to N-(1-naphthyl)naphtylethylenediamine to form the azo chromophore derivative that is sensitive to a wavelength of 540 nm (Nagano, 1999, Bryan and Grisham, 2007); (Figure 2-3).

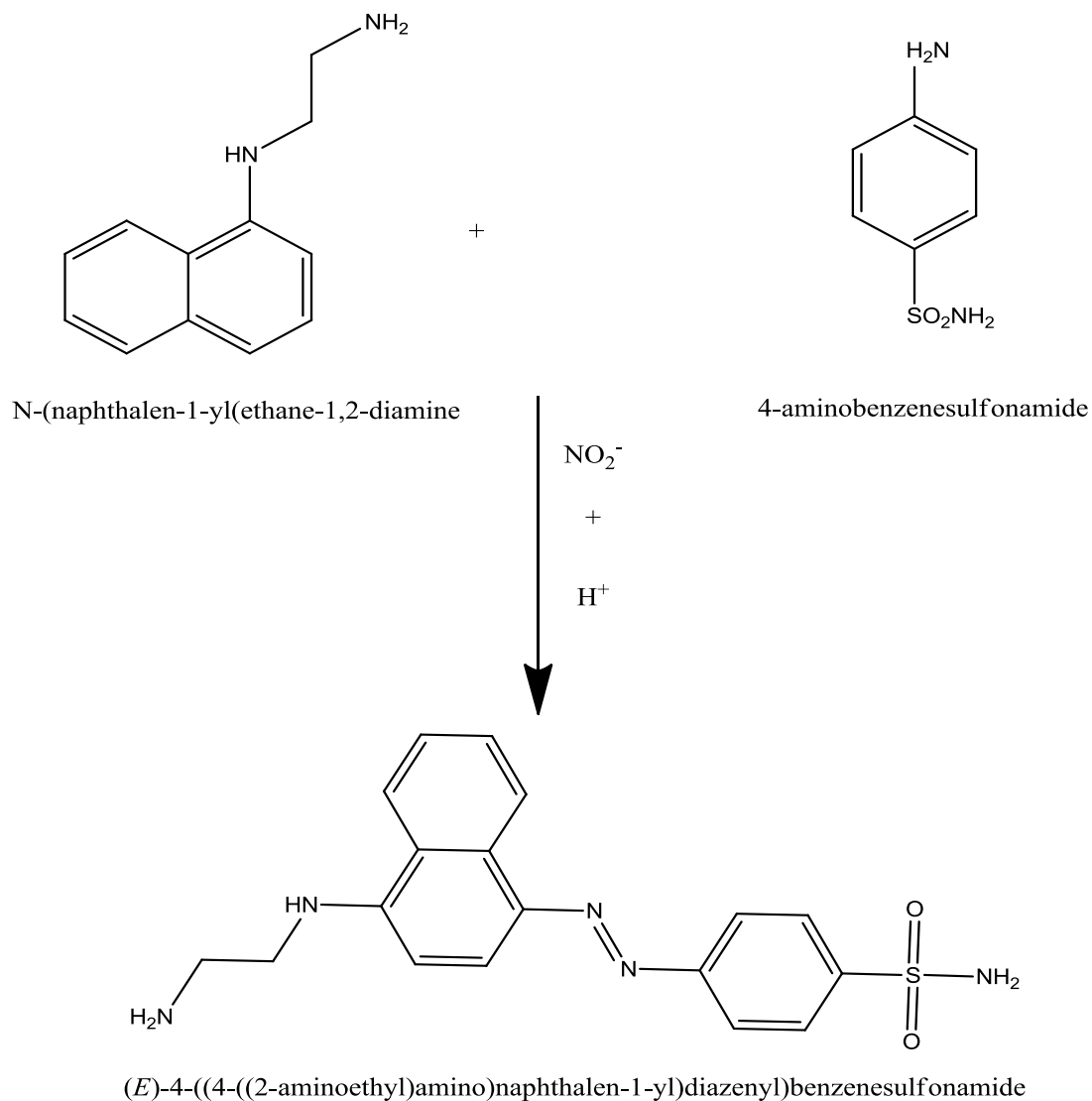


Figure 2-3: Griess reaction resulting in the azo chromophore, adapted from (Bryan and Grisham, 2007).

Solutions

Solution 1: 1% (w/v) sulphanilamide (Sigma ref. S9251) in 1M HCl

Solution 2: 0.2% (w/v) N-naphtylethylenediamine hydrochloride (Sigma ref. N9125)

Procedure

The previously described solutions and samples were mixed according to the following amounts: 0.9 ml of solution 1 with 0.1 ml of sample and 0.1 ml of solution 2. After 25 minutes the absorbance was measured at 540 nm at room temperature and the concentrations were determined based on a calibration curve (see **Figure 2-4**). All analyses were done in triplicate.

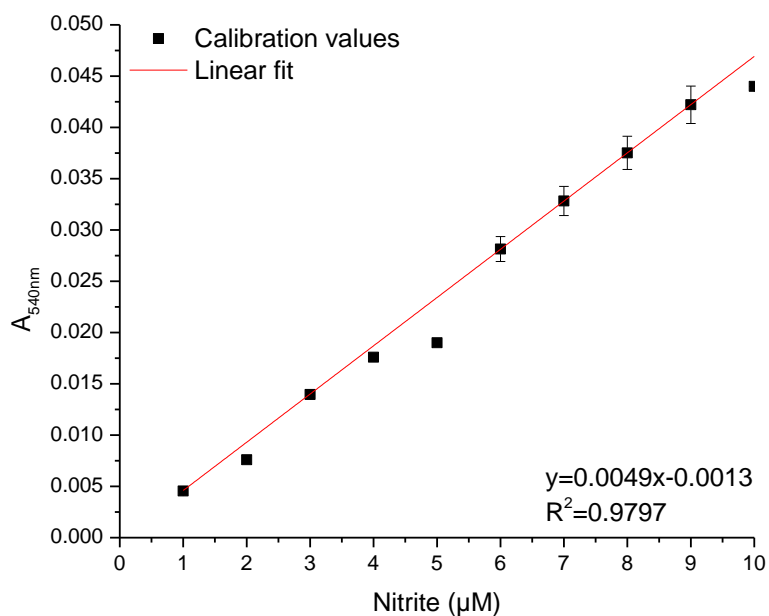


Figure 2-4: Calibration curve used for the estimation of nitrite.

2.3.7 Superoxide dismutase (SOD)

Principle

SOD is capable of inhibiting the reduction of cytochrome c with the superoxide radical, which is produced by the xanthine/xanthine oxidase system (Vistica et al., 1991, Crapo et al., 1978); (Figure 2-5).

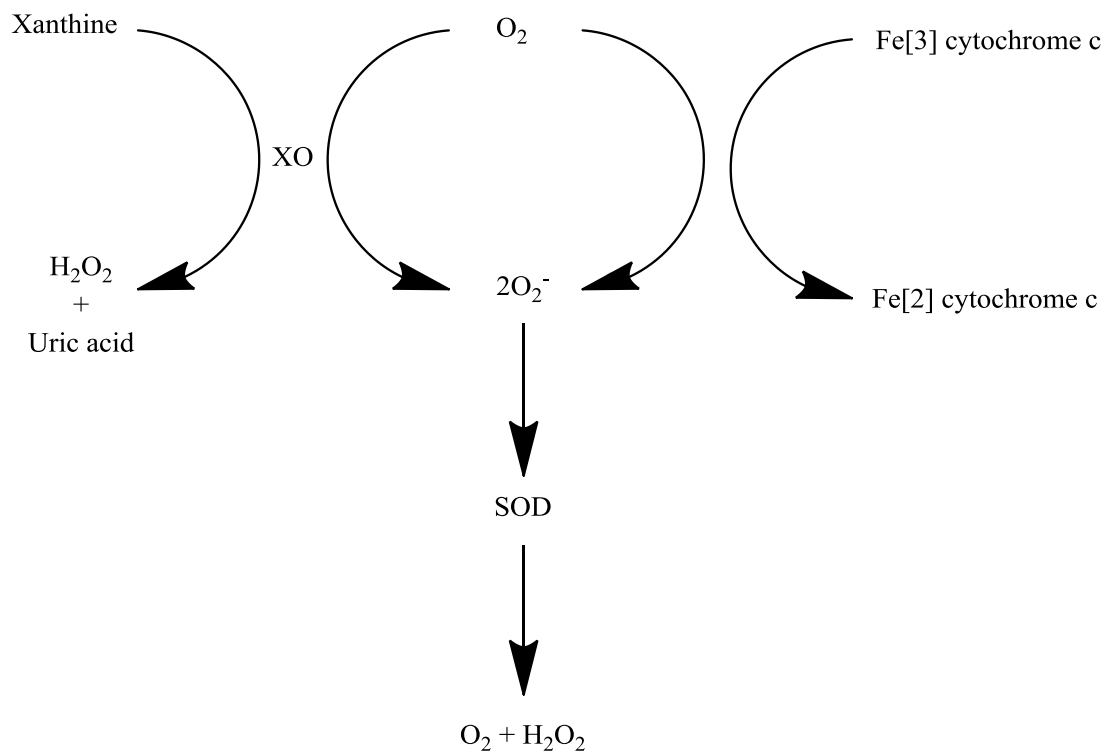


Figure 2-5: Reaction mechanism monitored during analyses of SOD, based on (Crapo et al., 1978, Vistica et al., 1991).

Solutions

Solution 1: 100 mM potassium phosphate buffer at pH 7.8 with 0.1 mM EDTA

Solution 2: 0.5 mM Xanthine (Sigma ref. X4002) in solution 1

Solution 3: 0.1 mM cytochrome c (Sigma ref. C2436) in solution 1

Solution 4: Xanthine oxidase (Sigma ref. X1875) diluted 20 times in solution 1

Procedure

Biomass was separated from medium as described in 2.3.1 and the medium was dissolved in solution 1 after which the sample was disrupted. . After this the sample was centrifuged for 30 minutes at 14,000 rpm using the centrifuge mentioned in 2.1.6 after which the samples were frozen (-20 °C) for analyses at a later time (within 10 days of freezing).

After thawing the samples were mixed in the following order:

0.8 ml of properly diluted sample (dilution depended on expected inhibition)

0.1 ml of solution 2

0.3 ml of solution 3

5 µl of solution 4

After mixing the reaction was measured for 15 minutes with 1 minute intervals. Figure 2-6 shows a typical trace of a sample (in this case a standard) and a blank (with no SOD).

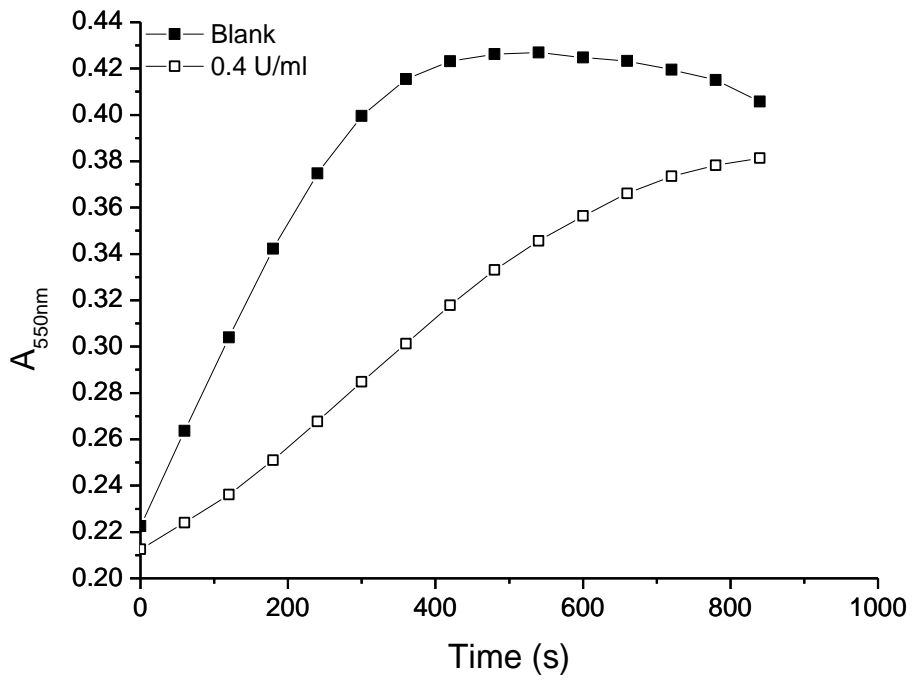


Figure 2-6: Optical density (OD) plotted against time for one of the standards that were used during this project.

The inhibition was calculated according to:

$$inhibition = \frac{slope\ of\ the\ blank - slope\ of\ the\ sample}{slope\ of\ the\ blank} \qquad eqn.\ 2.3$$

The calculated inhibition was compared to a standard curve (Sigma ref. S7446 for the standards and see Figure 2-7 for the standard curve).

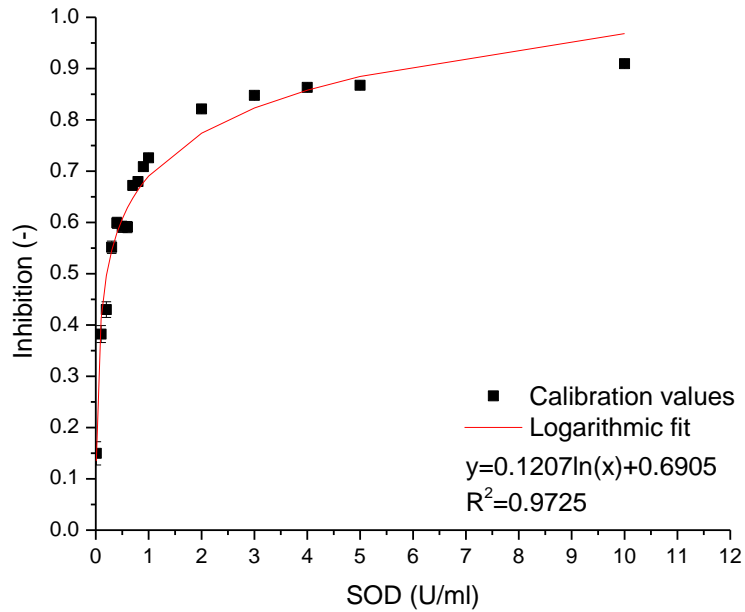


Figure 2-7: Calibration curve used for the estimation of SOD.

2.3.8 Catalase (CAT)

Principle

Catalase activity was measured by monitoring the conversion of hydrogen peroxide into water and oxygen (See Chapter 1 for a better description). The method was based on literature and was slightly modified to make it more precise (Aebi, 1984).

Solutions

Solution 1: 50 mM sodium phosphate buffer at pH 7

Solution 2: 30 mM of hydrogen peroxide diluted in solution 1

Procedure

The protocol is shortly as followed Biomass was separated from medium as described in 2.3.1 and the biomass was re-dissolved in solution 1 after which the cells were disrupted. After this the sample was centrifuged for 30 minutes at 14,000 rpm after which the samples were analyzed immediately to prevent loss of activity. In a 3 ml glass cuvette, 1.8 ml of solution 1 was pipetted together with 0.2ml of sample and 1ml of solution 2. After mixing the absorbance was measured at 240 nm for 2.5 minutes with a 30 seconds interval. Figure 2-8 shows a typical trace of a sample (in this case a standard).

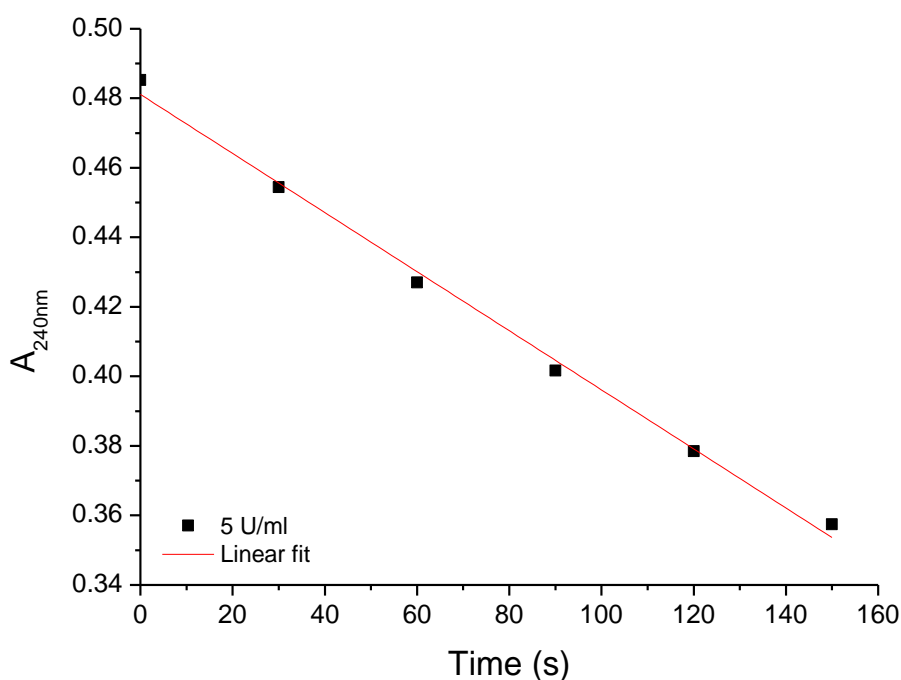


Figure 2-8: Optical density (OD) plotted against time for one of the standards that were used during this project.

The initial absorbance should be approximately 0.5 and all samples were analyzed in triplicate. After analyses slope values were calculated and compared with a standard curve (Merck ref. 219261 for the standards and see Figure 2-9 for the standard curve).

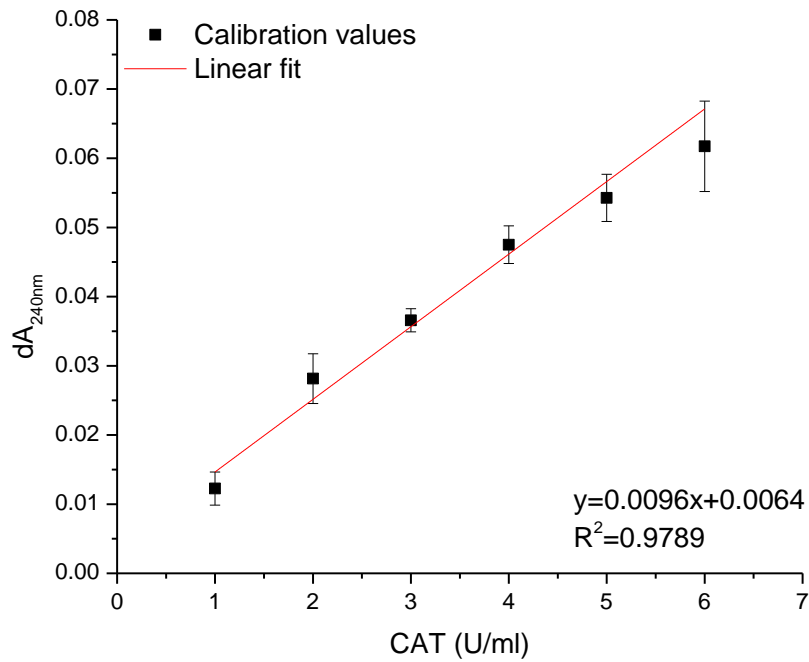


Figure 2-9: Calibration curve used for the estimation of CAT.

2.3.9 Intracellular protein content

Principle

To measure intracellular protein content the Bradford method (Bradford, 1976, Li, 2008) was used with a slight modification to the protocol. The principle of this assay is that Coomassie blue forms a protein-dye complex that has a strong absorbance at 595 nm.

Solutions

Solution 1: Bradford reagent (Sigma B6916).

Solution 2: 50 mM sodium phosphate buffer at pH 7

Procedure

Cell free extract was obtained as described in 2.3.1 and 33 μ l was added to 1 ml of Bradford reagent. After this the cuvette was mixed and after five minutes the absorbance was measured at 595 nm against a blank and compared to standard protein solutions (Bovine serum albumin, BSA, A2153 from Sigma, see Figure 2-10 for the standard curve).

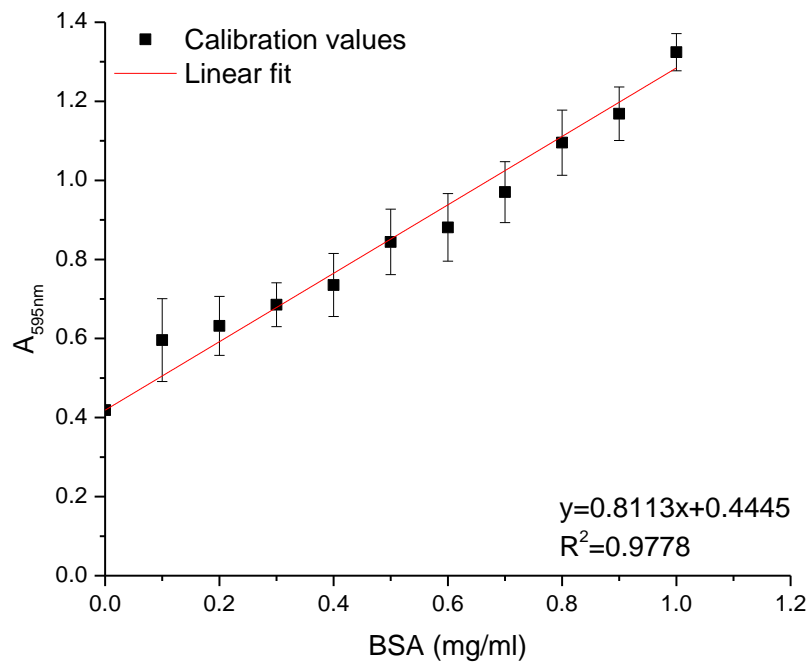


Figure 2-10: Calibration curve used for the estimation of intracellular protein content.

2.4 Data treatment

2.4.1 Statistics

All statistical analyses used in this thesis have been done utilising Origin 8.6, which is a statistical software package.

Error

All experimental results are expressed as mean \pm SD, for $n = 3$, which can be calculated according to equation 2.4.

$$s = \sqrt{\frac{1}{N-1} \sum_{i=1}^N (x_i - \bar{x})^2} \quad \text{eqn. 2.4}$$

In this thesis the assay results of SOD, CAT, OUR, CER, viability, ATP and intracellular protein content are expressed per gram of DCW. This meant that the standard deviation had to be combined with the DCW measurement standard deviation meaning in the case of this thesis the SOD, CAT, protein and viability values, which was done according to equation 2.5.

$$s = \sqrt{s_1^2 + s_2^2} \quad \text{eqn. 2.5}$$

One-way ANOVA

Specific growth rate (μ), glucose consumption rate (GCR) and ammonium consumption rate (ACR) were analyzed for significance using one-way ANOVA, with the Tukey test as the post hoc test for comparisons to see where significance was. A significance level of less than 5% was considered to be a significant difference between experiments.

Two-way ANOVA

All trend figures (variable plotted against time) have been analyzed using a two-way ANOVA. A two-way ANOVA has two defined factors and in the case of the research described here the two factors were time and treatment. The post-hoc test that was used after the two-way ANOVA was the Bonferoni test to see where significance was. A significance level of less than 5% was considered to be a significant difference between experiments.

2.4.2 Data representation

Chapter 3, 4 and 5 represent datasets of four experiments each, varying 1 factor per chapter. From these datasets two experiments were repeated, the control experiment to see how reproducible the process was and one of the factor changes to see if the effects that were observed could be repeated. The results that were obtained for these experiments are plotted with the corresponding original experiments in Appendix I, II and III.

Even though the repeat fermentations are not incorporated into the plots and tables that are in Chapter 3, 4 and 5 the statistical analyses did incorporate these duplicate results. This results; in unbalanced one- and two-way ANOVA's but as long as the imbalance is not more than 50% (for n) then this was considered to be acceptable.

2.4.3 Experimental data modifications

Specific growth rate, carbon consumption and nitrogen consumption

Specific growth rate was determined by taking the natural logarithm of the linear part of the growth curve, while carbon and nitrogen consumption rates were calculated by taking the slope of the linear parts of the glucose and ammonium curves respectively.

Off-gas analyses

From the off-gas analyzer the oxygen uptake rate (OUR) and carbon evolution rate (CER) can be calculated. The OUR was calculated according to the following equation (van 't Riet and Tramper, 1991, Garcia-Ochoa and Gomez, 2009):

$$OUR = \frac{F_g(C_{ogi} - C_{ogo})}{V_l C_x} \quad \text{eqn. 2.6}$$

In which:

- OUR is the oxygen uptake rate in mM/g/h
- F_g airflow into reactor in l/h
- C_{ogi} concentration of oxygen going into the reactor in mM/l
- C_{ogo} concentration of oxygen coming out of the reactor in mM/l
- V_l liquid volume present inside the reactor in l
- C_x concentration of biomass present inside the reactor in g/l

When the DOT values are still higher than zero, OUR values need to be compensated by the differences in DOT between two time points. For this thesis a solubility of oxygen in water of 0.26 mM was used to correct for these values (Carpente.Jh, 1966).

The CER can be calculated in a similar way:

$$CER = \frac{F_g(C_{C_{gi}} - C_{C_{go}})}{C_x} \quad \text{eqn. 2.7}$$

In which:

- CER is the carbon evolution rate in mM/g/h
- F_g airflow into reactor in l/h
- $C_{C_{gi}}$ concentration of carbon dioxide going into the reactor in mM/l
- $C_{C_{go}}$ concentration of carbon dioxide coming out of the reactor in mM/l
- V_l liquid volume present inside the reactor in l
- C_x concentration of biomass present inside the reactor in g/l

With CER and OUR values the R.Q. (respiration quotient) can be calculated:

$$R.Q. = \frac{CER}{OUR} \quad \text{eqn. 2.8}$$

In which:

- R.Q. is the respiration quotient (no units)

In Chapter 6 a logistic model (already pre-programmed in Origin 8.6) was used to obtain a working model to predict DCW values when utilising *A. niger* during fermentations.

$$y = \frac{A_1 - A_2}{1 + \left(\frac{x}{x_0}\right)^p} + A_2 \quad \text{eqn 2.9}$$

2.5 Experimental variations and assays used in each chapter

2.5.1 The effect of polymyxin B on oxidative stress defence mechanisms during cultivation of *Aspergillus niger* B1-D.

The concentrations of polymyxin B used were 5, 10 and 20 μM (final concentration inside the reactor), added during inoculation of the experiment and were compared to experimental data obtained during the control experiment to which no polymyxin B was added. The following assays were used to analyze the results obtained during this experimental series; dry cell weight (DCW), glucose, ammonium, off-gas analyses, SOD, CAT, intracellular protein content, lysozyme and viability. The control and the 20 μM polymyxin B processes were repeated to look at process- and effect reproducibility. Graphs showing these results can be found in Appendix I.

2.5.2 Oxygen transfer at the start of a fermentation can lead to oxidative stress in *Aspergillus niger* B1-D

In Chapter 5 agitation settings were varied to study oxygen transfer effects at the start of fermentations utilising *A. niger*. The agitation settings used were 100-400, 200-400, 300 and 400 rpm, where the 100-400 and 200-400 processes had DOT control set at 25% and were consequently increased in increments. The following assays were used to analyze the bioprocess: dry cell weight (DCW), glucose, ammonium, off-gas analyses, SOD, CAT, intracellular protein content, lysozyme and viability. The 200-400 rpm and 300 rpm processes were repeated to look at process- and effect reproducibility. Graphs showing these results can be found in Appendix II.

k_La values were not taken into account in the results described here as no comparisons between different reactors are done. Another reason for not measuring k_La values is that k_La values are determined using water only

inside a reactor and will only give a characteristic of the oxygen transfer capabilities of a reactor without biomass.

2.5.3 Nitric oxide and its interaction with oxidative stress defences in submerged cultures of *Aspergillus niger*

Growth experiments using sodium nitrite, hydroxy urea and sodium nitroprusside (SNP)

The three NO-donors that were tested were; sodium nitrite, hydroxy urea and SNP. The analyses used for this experimental series were for all NO-donors biomass (DCW). The concentrations used for all shake flask experiments were the same: 150, 250 and 350 μM . 150, 250 and 350 μM (final concentration inside shake flask) were single additions of each compound (at 24 hours) and 250 μM^* was an addition carried out every 24 hours until 120 hours into the experiment, for each compound.

Reactor experiments for studying the effect of sodium nitroprusside (SNP) on cultivation of *A. niger* B1-D

The concentrations of SNP used were 400, 700 and 1000 μM added at 24 hours of the experiment and were compared to experimental data obtained during the control experiment to which no SNP was added. The following assays were used to analyze the results obtained during this experimental series; nitrite, dry cell weight (DCW), glucose, ammonium, off-gas analyses, ATP, SOD, CAT, intracellular protein content, lysozyme and viability. The control and 1000 μM processes were repeated to look at process- and effect reproducibility. Graphs showing these results can be found in Appendix IV.

2.5.4 Infrared monitoring of hyphal growth during submerged culture of *Aspergillus niger*

Different agitation settings were employed; 100-400, 200-400, 300 and 400 rpm. The first two agitation settings were varied based on the control of dissolved oxygen tension (DOT) which had 25% as setpoint. The following measurements were done to analyze the results obtained during this experimental series; dry cell weight (DCW) and spectral values obtained from the sensor.

As the sensor only gives what is called a spectral value, three calibration runs had to be done to obtain a model. These processes were 100-400, 200-400 and 400 rpm. The validation process was the process with 300 rpm.

Chapter 3

The effect of polymyxin B on oxidative stress defence mechanisms during cultivation of *Aspergillus niger* B1-D.

3 The effect of polymyxin B on oxidative stress defence mechanisms during cultivation of *Aspergillus niger* B1-D.

3.1 Introduction and aims

Fungal fermentations are often characterized by high viscosity (Wongwicharn *et al.*, 1999, Bhargava *et al.*, 2003, Wang *et al.*, 2005) and therefore oxygen enrichment protocols have been developed to prevent oxygen limitation during these processes (O'Donnell *et al.*, 2011). Sparging enriched oxygen into the reactor leads to enhanced oxygen transfer, which in turn helps to maintain sufficient oxygen levels inside the reactor. Examples of this strategy being utilised in practice for filamentous fungi are; lovastatin production using *Aspergillus terreus* (Lopez *et al.*, 2005) and citric acid production by *Aspergillus niger* (Kubicek *et al.*, 1980). However, these oxygen enrichment measures may be responsible for increased oxidative stress in filamentous fungi, thereby potentially decreasing productivity such as growth rate and protein expression (Bai *et al.*, 2004).

Filamentous fungi have developed different defence mechanisms against oxidative stress of which one of these mechanisms is thought to be the alternative pathway, which in short bypasses the main respiratory pathway resulting in the production of heat (Joseph-Horne *et al.*, 2001) (see chapter 1.8). Briefly, the electron transport chain of filamentous fungi is a highly complex system with four complexes to generate ATP (Joseph-Horne *et al.*, 2001). There are also alternative enzymes that are responsible for bypassing this electron transport chain. These alternative enzymes include NADH: ubiquinone oxidoreductase (NADH dehydrogenase), which can bypass complex I (Videira and Duarte, 2001) and an alternative oxidase that has the ability to bypass complexes III and IV.

The big gap in knowledge of the alternative pathway is: how it is regulated at the physiological level and even if it is there to only counteract oxidative

stress. The heat generation from this pathway and the ability of fungi to grow at colder temperatures also point towards a pathway that exists to regulate temperature. O'Donnell *et al.*, (2011) showed, during reactor studies utilising *Aspergillus niger B1-D*, that up to 25% oxygen enrichment there was no substantial difference in carbon consumption compared to the control experiment (no oxygen enrichment) (O'Donnell *et al.*, 2011). This study did show a substantial inhibition in biomass formation of *A. niger B1-D*, indicating an increase in utilisation of the alternative pathway, when sparging oxygen enriched air into a bioreactor. This was also confirmed by a decrease in peak ATP values (O'Donnell *et al.*, 2011). Other researchers have shown that increasing the temperature resulted in a general enhancement of metabolism; however, temperatures higher than 30⁰C had the added effect of increased protein carbonylation (Li *et al.*, 2008c). The results presented by Li *et al.*, (2008c) do not discuss the cause of this metabolic enhancement, but might indicate a decrease in the use of the alternative pathway due to increased temperature, which consequently decreased the need to produce heat from the alternative pathway.

From a bioprocessing point of view the alternative pathway is wasteful, as heat from cells is not a product that would be commercially viable. This heat generation also decreases yields of various products as no ATP is generated when the main respiratory pathway is bypassed. This ATP is needed to produce these products. Therefore research into the manipulation of this pathway could potentially enhance protein or biomass production during fermentations, utilising fungal strains.

Decreasing NADH dehydrogenase activity could result in more cellular metabolism, thereby generating more ATP instead of heat. Previous approaches have been to block NADH dehydrogenase activity and measure various physiological parameters that would indicate blocking of this enzyme. A study by Voulgaris *et al.*, (2012) showed that 7-iodoacridone 4-carboxylic acid (IACA) might be capable of blocking NADH dehydrogenase activity, because adding this compound to a bioreactor resulted in increased biomass

and intracellular protein content (Voulgaris *et al.*, 2012). Other identified blocking compounds of NADH dehydrogenase (in vitro) are polymyxin B, scopafungin and staurosporine (Mogi *et al.*, 2009b, Mogi *et al.*, 2009a).

Previous research involving the use of IACA mainly focused on studying the concentration of the superoxide anion (O_2^-); it would therefore be interesting to understand how fungal defence mechanisms react to an identified NADH dehydrogenase blocking agent. Polymyxin B was selected for this study, as this compound is less expensive than IACA. Superoxide dismutase and catalase were selected, because these enzymes are directly involved in the defence against O_2^- and hydrogen peroxide (Kreiner *et al.*, 2003). These radicals are produced in larger quantities, when cellular metabolism is increased, which is indicative for increased oxidative stress levels.

3.1.1 Aims

The aim of this chapter was to study the effect of increasing amounts of polymyxin B on oxidative stress defence mechanisms during cultivation of *A. niger B1-D*. Other physiological process parameters such as biomass growth and lysozyme production were monitored as well to get an idea on the effect of polymyxin B on these parameters.

3.2 Results

The polymyxin B concentrations were chosen based on previous work done in shake flasks (Griffin, 2011).

3.2.1 Polymyxin B and its effect on biomass formation, carbon consumption and nitrogen consumption

Figure 3-1 shows the effect of polymyxin B on biomass growth during fermentation of *A. niger* B1-D.

The time at which the stationary phase was reached differs from the control process in the presented processes here. The control experiment reached its stationary phase at around 80 hours. This was also similar for the 20 μ M process. The 5 μ M process reaches its stationary phase at around 70 hours, while that was 90 hours in the 10 μ M process. The stationary biomass concentration for *A. niger* was in the range of 12-14 g/l in the control, 5 and 20 μ M processes, however for the 10 μ M polymyxin B process this was around 16 g/l.

The statistical analyses showed that results were significantly different (two-way ANOVA, $p < 0.05$) and the Bonferoni post-hoc test showed that this difference was significant for all processes compared to the control experiment. The largest mean difference was for the 10 μ M experiment (Table 3-2), indicating the largest effect on DCW.

Table 3-1 shows specific growth rates for each process. The effect of polymyxin B on specific growth rate was only significant, when looking at the 20 μ M process (one-way ANOVA with Tukey's post-hoc test, $p < 0.05$, Table 3-3).

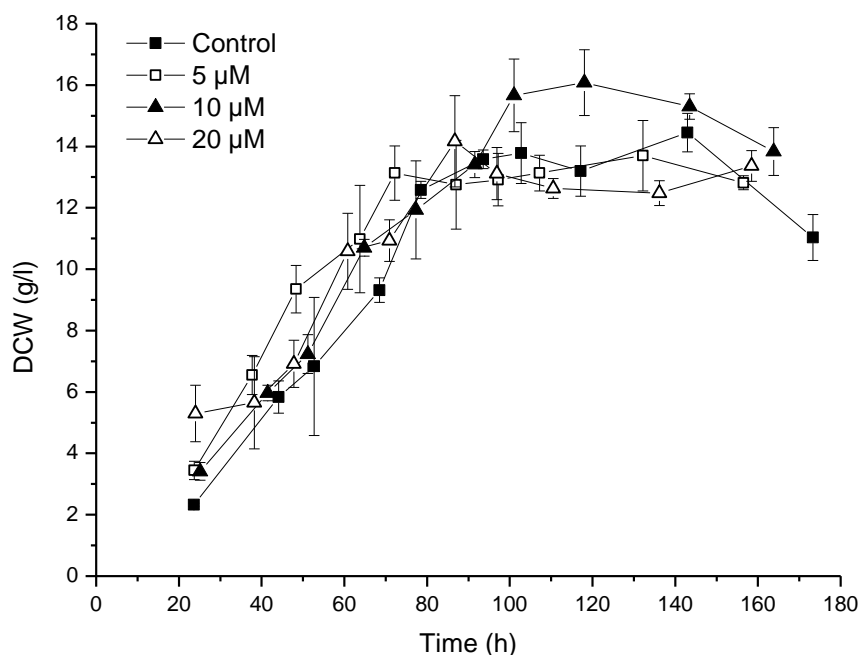


Figure 3-1: DCW (g/l) during batch cultivation in a STR of *A. niger B1-D*.

A range of concentrations (see graph) of polymyxin B were added at 1.5 hours. Cultivation conditions were: airflow 2 lpm, 200-400 rpm, pH 4, temperature 25 °C. Results are expressed as mean ± stdev.

Table 3-1: Effect of polymyxin B on specific growth rate during batch fermentations of *A. niger B1-D*.

Cultivation conditions were: airflow 2 lpm, 200-400 rpm, pH 4, temperature 25 °C. specific growth rate was determined from the linear part of the graph and is expressed as mean ± stdv.

Concentration polymyxin B (μM)	Specific growth rate (h ⁻¹)
Control	0.025 ± 0.0022
5	0.028 ± 0.0021
10	0.021 ± 0.0009
20	0.019 ± 0.0072

Table 3-2: Statistical analyses of DCW using the Bonferoni post-hoc test, with significant differences between treatment. In which; SEM is standard error of means, LCL is lower confidence limit and UCL is upper confidence limit.

	Mean Diff.	SEM	t-Value
5 µM polymyxin B vs Control	1.0375	0.23633	4.39008
10 µM polymyxin B vs Control	1.5125	0.23633	6.4
20 µM polymyxin B vs Control	0.66056	0.19296	3.42326
	P-Value	LCL	UCL
5 µM polymyxin B vs Control	1.33E-04	0.40502	1.66998
10 µM polymyxin B vs Control	1.31E-08	0.88002	2.14498
20 µM polymyxin B vs Control	0.00487	0.14414	1.17697

Table 3-3: Statistical analyses of specific growth rate using the Tukey post-hoc test. In which; SEM is standard error of means, LCL is lower confidence limit and UCL is upper confidence limit.

	Mean Diff.	SEM	t-Value
5 µM polymyxin B vs Control	0.00452	0.00313	2.04025
10 µM polymyxin B vs Control	-0.00247	0.00313	1.11573
20 µM polymyxin B vs Control	-0.00752	0.00256	4.15502
	P-Value	LCL	UCL
5 µM polymyxin B vs Control	0.49524	-0.00459	0.01363
10 µM polymyxin B vs Control	0.85826	-0.01159	0.00664
20 µM polymyxin B vs Control	0.04719	-0.01496	-8.06E-05

The effect of polymyxin B on glucose concentrations and Glucose Consumption Rate (GCR) are presented in Figure 3-2 and Table 3-4.

The addition of increasing amounts of polymyxin B results in a faster decrease of glucose concentrations inside the reactor. The statistical analyses of results from Figure 3-2 confirms this as each process was significantly different compared to the control experiment (two-way ANOVA with Bonferoni post-hoc test) and that the highest difference could be observed in the 5 μM polymyxin B process, based on the largest mean difference (Table 3-5).

The GCR results showed (Table 3-4) that only the 5 μM process was significantly different compared to the control experiment. Analyses was done using a one-way ANOVA with the Tukey post-hoc test ($p < 0.05$, Table 3-6).

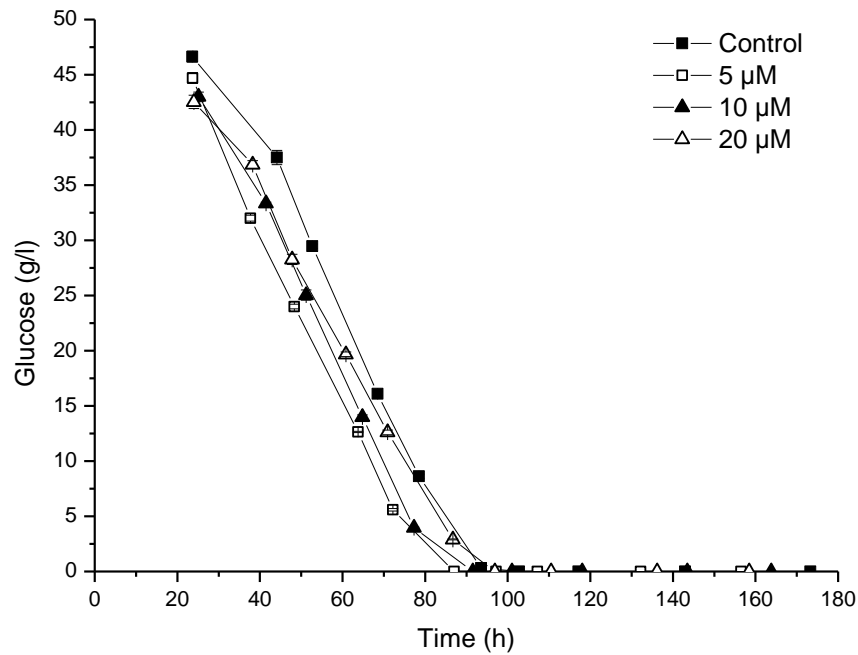


Figure 3-2: Residual glucose (g/l) during batch cultivation in a STR of *A. niger B1-D*.

A range of concentrations (see graph) of polymyxin B were added at 1.5 hours. Cultivation conditions were: airflow 2 lpm, 200-400 rpm, pH 4, temperature 25 °C. Results are expressed as mean ± stdev.

Table 3-4: Effect of polymyxin B on GCR during batch fermentations of *Aspergillus niger B1-D*.

Cultivation conditions were: airflow 2 lpm, 200-400 rpm, pH 4, temperature 25 °C. GCR was determined from the linear part of the graph and is expressed as mean ± stdv.

Concentration polymyxin B (μM)	GCR (g/l/h)
Control	0.69 ± 0.006
5	0.81 ± 0.010
10	0.65 ± 0.007
20	0.70 ± 0.007

Table 3-5: Statistical analyses of residual glucose using the Bonferoni post-hoc test, with significant differences between treatment. In which; SEM is standard error of means, LCL is lower confidence limit and UCL is upper confidence limit.

	Mean Diff.	SEM	t-Value
5 μ M polymyxin B vs Control	-1.75058	0.30624	-5.71636
10 μ M polymyxin B vs Control	-1.70992	0.30624	-5.58357
20 μ M polymyxin B vs Control	1.49208	0.25004	5.96727
	P-Value	LCL	UCL
5 μ M polymyxin B vs Control	3.79E-07	-2.57016	-0.931
10 μ M polymyxin B vs Control	7.10E-07	-2.5295	-0.89034
20 μ M polymyxin B vs Control	1.13E-07	0.8229	2.16127

Table 3-6: Statistical analyses of GCR using the Tukey post-hoc test. In which; SEM is standard error of means, LCL is lower confidence limit and UCL is upper confidence limit.

	Mean Diff.	SEM	t-Value
5 μ M polymyxin B vs Control	0.16449	0.02961	7.85573
10 μ M polymyxin B vs Control	0.00487	0.02961	0.23254
20 μ M polymyxin B vs Control	0.02011	0.02418	1.17631
	P-Value	LCL	UCL
5 μ M polymyxin B vs Control	3.66E-04	0.07842	0.25055
10 μ M polymyxin B vs Control	0.99834	-0.0812	0.09094
20 μ M polymyxin B vs Control	0.83856	-0.05016	0.09038

Figure 3-3 and Table 3-7 show ammonium concentrations and ammonium consumption rate (ACR) respectively. The concentration of ammonium in the medium at the time of inoculation was 5 g/l for each of the experiments (see chapter 2. 2).

Figure 3-3 shows that polymyxin B results in a faster utilisation of ammonium in the first 24 hours. The 5 μ M process has a sharp decrease in ammonium until around 60 hours into the process, after which residual ammonium concentrations stay stable for about 60 hours. The final concentrations for ammonium were comparable to the other processes. The 10 μ M process has a virtual linear decrease in ammonium concentrations until around 90 hours, which was also the time at which glucose was depleted. The 20 μ M process has a similar trend compared to the 5 μ M process with the difference that residual ammonium concentrations were stable from around 24 to 80 hours (at values of around 2.5 g/l), instead of 60 to 110 hours in the 5 μ M process. Statistical analyses of these trends showed that only the 10 μ M process was significantly different compared to the control experiment (two-way ANOVA with Bonferoni post-hoc test, $p < 0.05$, Table 3-8)

The effect of polymyxin B on ACR is shown in Table 3-7 and is only significantly different for the 5 μ M process (one-way ANOVA with Tukey post-hoc test, $p < 0.05$, see Table 3-9).

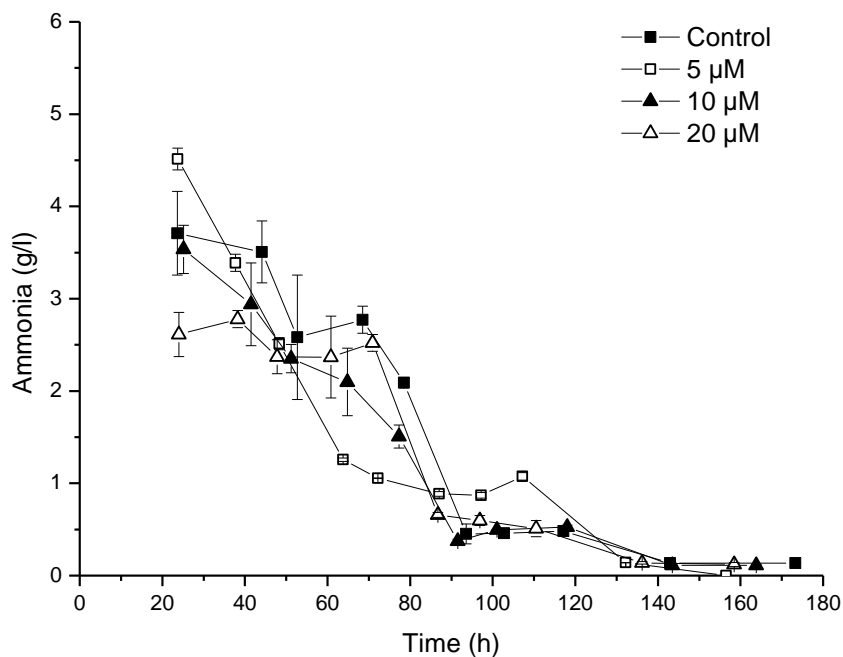


Figure 3-3: Residual Ammonium (g/l) during batch cultivation in a STR of *A. niger B1-D*.

A range of concentrations (see graph) of polymyxin B were added at 1.5 hours. Cultivation conditions were: airflow 2 lpm, 200-400 rpm, pH 4, temperature 25 °C. Results are expressed as mean ± stdev.

Table 3-7: Effect of polymyxin B on ACR during batch fermentations of *A. niger B1-D*.

Cultivation conditions were: airflow 2 lpm, 300 rpm, pH 4, temperature 25 °C. ACR was determined from the linear part of the graph and is expressed as mean ± stdv.

Concentration polymyxin B (μM)	ACR (g/l/h)
Control	0.030 ± 0.0092
5	0.071 ± 0.0024
10	0.048 ± 0.0041
20	0.044 ± 0.0015

Table 3-8: Statistical analyses of residual ammonium using the Bonferoni post-hoc test, with significant differences between treatment. In which; SEM is standard error of means, LCL is lower confidence limit and UCL is upper confidence limit.

	Mean Diff.	SEM	t-Value
5 µM polymyxin B vs Control	-0.30583	0.13379	-2.28588
10 µM polymyxin B vs Control	-0.47078	0.13379	-3.51882
20 µM polymyxin B vs Control	-0.15517	0.10924	-1.42043
	P-Value	LCL	UCL
5 µM polymyxin B vs Control	0.14258	-0.66389	0.05223
10 µM polymyxin B vs Control	0.00351	-0.82884	-0.11273
20 µM polymyxin B vs Control	0.94623	-0.44752	0.13719

Table 3-9: Statistical analyses of ACR using the Tukey post-hoc test. In which; SEM is standard error of means, LCL is lower confidence limit and UCL is upper confidence limit.

	Mean Diff.	SEM	t-Value
5 µM polymyxin B vs Control	0.03109	0.00627	7.01084
10 µM polymyxin B vs Control	0.00731	0.00627	1.64803
20 µM polymyxin B vs Control	0.00876	0.00512	2.421
	P-Value	LCL	UCL
5 µM polymyxin B vs Control	0.00107	0.01286	0.04931
10 µM polymyxin B vs Control	0.65719	-0.01092	0.02553
20 µM polymyxin B vs Control	0.35415	-0.00612	0.02365

3.2.2 Polymyxin B and its effect on respiration

The off-gas analyzer allows for the calculation of oxygen uptake rates and carbon evolution rates (for calculation see chapter 2.4). Figure 3-4 (A) and (B) shows results of oxygen uptake rate (OUR) and carbon evolution rate (CER) respectively. Figure 3-4 (A) and (B) are divided into two parts. The first part is highlighted using a grey box until around 50 hours into the process at which DOT becomes limiting.

In Figure 3-4 (A) the control process has a peak value of around 5.5 mM/g/h in the first part of this process, after which there is a sharp drop to around 0.5 mM/g/h, which remains stable until the end of the process. The processes where polymyxin B was added had more stable values during the entire process time. After 50 hours Figure 3-4 (A) clearly shows that all polymyxin B experiments have higher OUR values compared to the control process in which the 10 μ M process had the highest values, however statistical analyses showed no significance between the polymyxin B processes and the control process (two-way ANOVA with Benferoni post-hoc test, $p < 0.05$, Table 3-10).

Figure 3-4 (B) has the same initial peak value (4 mM/g/h) that can also be observed in Figure 3-4 (A). After 40 hours into the process CER values decreased for all processes. In the grey part of the graph, as well during the rest of the process time, CER values for the control process were higher compared to the polymyxin B processes. Statistical analyses showed that the 5 and 20 μ M polymyxin B process were significantly different compared to the control process (two-way ANOVA with Bonferoni post-hoc test, $p < 0.05$), where 20 μ M of polymyxin B had the largest effect on CER values compared to the control process (largest mean difference value, Table 3-11).

The respiratory quotient (RQ) can be determined using OUR and CER values and are shown in Figure 3-5. All processes had peak values in the grey highlighted part of the graph of which the control process had the highest peak at around 2.5. After 50 hours all processes with polymyxin B had lower

RQ values compared to the control experiment. The overall trend after glucose was depleted (ranging from 90 to 100 hours) was an increase in RQ with fluctuating values for 10 μ M polymyxin B. Statistical analyses showed a significant difference in this dataset (two-way ANOVA, $p < 0.05$) with 5 μ M of polymyxin B having the largest effect on RQ values (largest mean difference using the Bonferoni post-hoc test, Table 3-12)

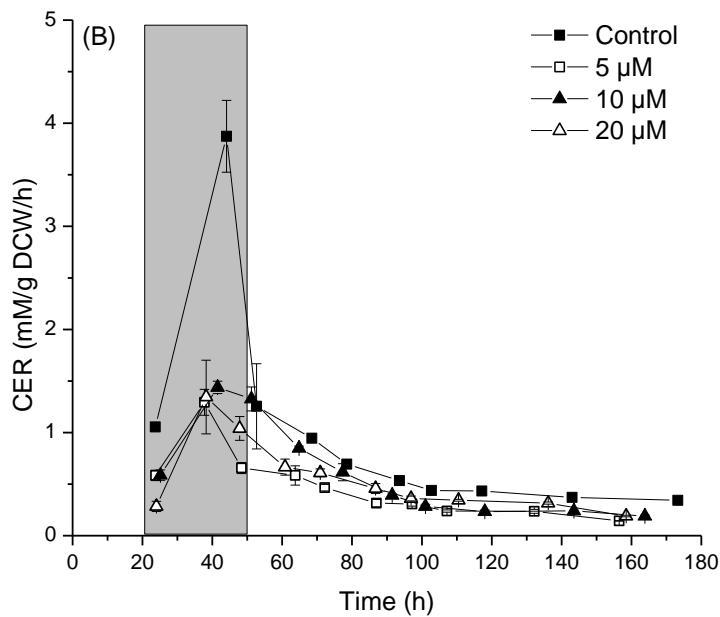
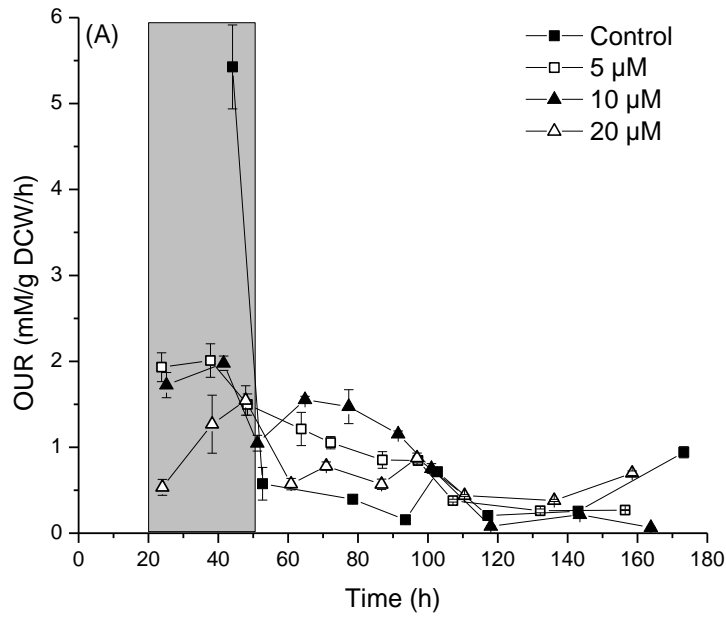


Figure 3-4: OUR (mM/g DCW/h) and (B) CER (mM/g DCW/h) during batch cultivation in a STR of *A. niger* B1-D.

A range of concentrations (see graph) of polymyxin B were added at 1.5 hours. Cultivation conditions were: airflow 2 lpm, 200-400 rpm, pH 4, temperature 25 °C. Results are expressed as mean ± stdev. At around 50 hours DOT becomes limiting (end of grey highlighted part).

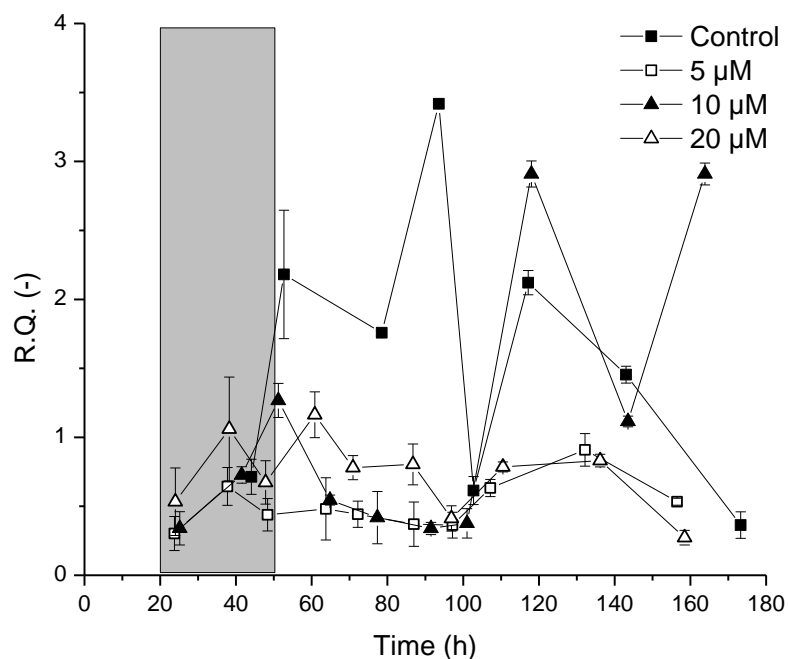


Figure 3-5: R.Q. during batch cultivation in a STR of *A. niger B1-D*.

A range of concentrations (see graph) of polymyxin B were added at 1.5 hours. Cultivation conditions were: airflow 2 lpm, 200-400 rpm, pH 4, temperature 25 °C. Results are expressed as mean \pm stdev. At around 50 hours DOT becomes limiting (end of grey highlighted part).

Table 3-10: Statistical analyses of OUR using the Bonferoni post-hoc test, with significant differences between treatment. In which; SEM is standard error of means, LCL is lower confidence limit and UCL is upper confidence limit.

	Mean Diff.	SEM	t-Value
5 μ M polymyxin B vs Control	0.13724	0.06922	1.98265
10 μ M polymyxin B vs Control	0.1416	0.06922	2.04569
20 μ M polymyxin B vs Control	0.09329	0.05702	1.63619
	P-Value	LCL	UCL
5 μ M polymyxin B vs Control	0.29671	-0.04813	0.3226
10 μ M polymyxin B vs Control	0.25646	-0.04377	0.32696
20 μ M polymyxin B vs Control	0.62488	-0.0594	0.24599

Table 3-11: Statistical analyses of CER using the Bonferoni post-hoc test, with significant differences between treatment. In which; SEM is standard error of means, LCL is lower confidence limit and UCL is upper confidence limit.

	Mean Diff.	SEM	t-Value
5 µM polymyxin B vs Control	-0.25833	0.07915	-3.26389
10 µM polymyxin B vs Control	-0.1257	0.07915	-1.58817
20 µM polymyxin B vs Control	-0.26119	0.0652	-4.00604
	P-Value	LCL	UCL
5 µM polymyxin B vs Control	0.00837	-0.47029	-0.04637
10 µM polymyxin B vs Control	0.68763	-0.33766	0.08626
20 µM polymyxin B vs Control	6.11E-04	-0.43579	-0.08659

Table 3-12: Statistical analyses of R.Q. using the Bonferoni post-hoc test, with significant differences between treatment. In which; SEM is standard error of means, LCL is lower confidence limit and UCL is upper confidence limit.

	Mean Diff.	SEM	t-Value
5 µM polymyxin B vs Control	-0.96884	0.08412	-11.51699
10 µM polymyxin B vs Control	-0.40387	0.08412	-4.80102
20 µM polymyxin B vs Control	-0.95725	0.0693	-13.81388
	P-Value	LCL	UCL
5 µM polymyxin B vs Control	5.53E-21	-1.19411	-0.74356
10 µM polymyxin B vs Control	2.49E-05	-0.62915	-0.17859
20 µM polymyxin B vs Control	9.22E-27	-1.14282	-0.77167

3.2.3 Polymyxin B and its effect on oxidative stress related biomarkers

Figure 3-6 and Figure 3-7 show the effect of polymyxin B on the oxidative stress related enzymes, SOD and CAT respectively (see Chapter 2.3 how to measure). Figure 3-6 shows that 24 hours after the addition of polymyxin B, the 5 and 10 μM processes had increased SOD activities compared to the control process. The 20 μM process showed, at 24 hours, a similar SOD value as the control process (around 110 U/g). After 24 hours the control process shows an increase in SOD activity, which levels off at around 3500-4000 U/g, until glucose is depleted at around 90 hours after which a drop in SOD activity occurs. Even though the 20 μM process shows a peak SOD value at 40 hours into the process, of around 1000 U/g all other values in the first 100 hours are lower than the control experiment. The 10 μM polymyxin B process shows consistently lower values compared to the control process and the 5 μM process had large fluctuating SOD activities during the entire process. In which these two peak values were at those timepoints higher than the control process (around 3000 and 4000 U/g respectively). The added comment that can be made here is that the second sharp decrease in SOD activity for the 5 μM process corresponds with the depletion of glucose inside the reactor.

The statistical analyses of Figure 3-6 showed significance within this dataset (two-way ANOVA, $p < 0.05$). The Bonferoni post-hoc test showed that all polymyxin processes were significantly different compared to the control process and that the 5 μM of polymyxin B had the largest effect on SOD activity (largest mean difference, Table 3-13).

The effect of polymyxin B on CAT activity during *A. niger* B1-D cultivation is shown in Figure 3-7. The 5 and 10 μM processes show increased CAT activities 24 hours after addition of polymyxin B, which was a similar trend compared to the SOD activities in Figure 3-6. After 40 hours into the processes the control, 5 and 10 μM processes start to show similar CAT activities of around 2500 U/g. This phase lasts until 70 hours, after which CAT activities start to diverge again. The control experiment starts to show a

decreasing CAT activity, while the 5 and 10 μM show increasing CAT activities. The 20 μM process shows CAT activities that are consistently lower than the control experiment; however values do start converging at around 90 hours, where these values remain the same until around 110 hours into the process.

The two-way ANOVA test of this dataset showed a significant difference ($p < 0.05$), where the 10 and 20 μM processes were significantly different compared to the control process (Bonferoni post-hoc test). According to the statistical analyses 20 μM of polymyxin B had the largest effect on CAT activity during cultivation of *A. niger B1-D* (Table 3-14).

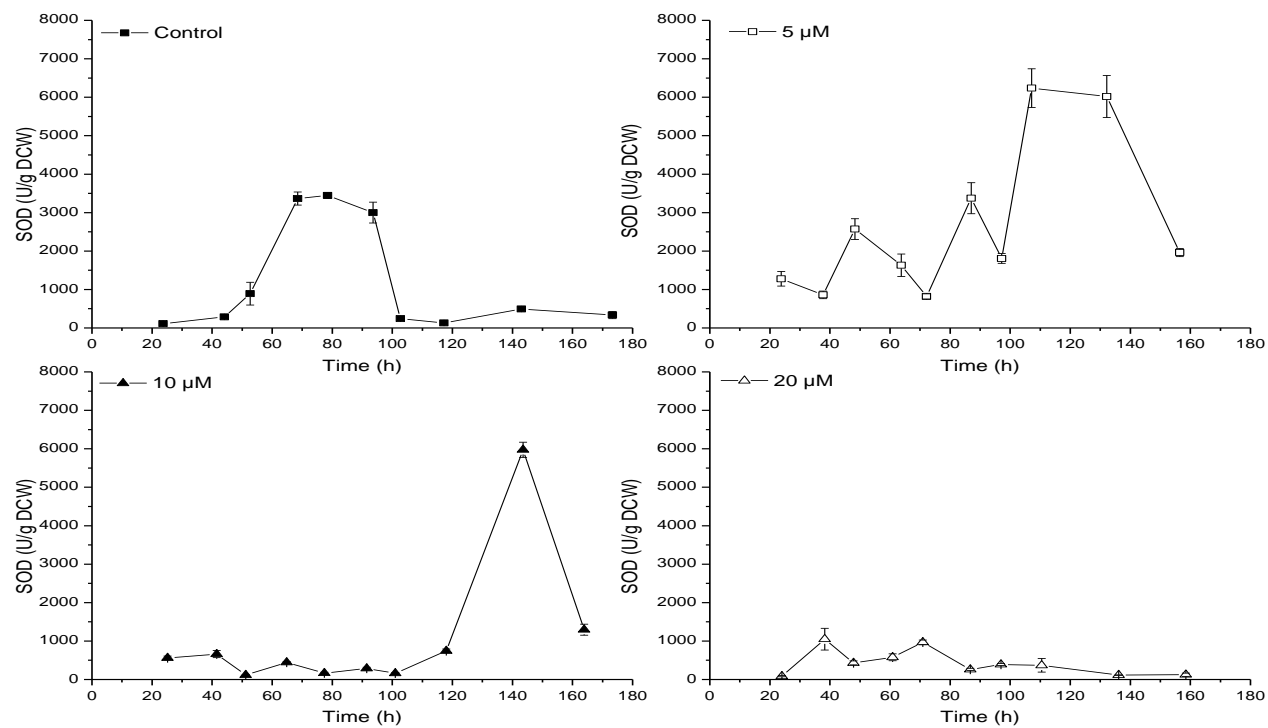


Figure 3-6: SOD (U/g DCW) during batch cultivation in a STR of *A. niger* B1-D.

A range of concentrations (see graph) of polymyxin B were added at 1.5 hours. Cultivation conditions were: airflow 2 lpm, 200-400 rpm, pH 4, temperature 25 °C. Results are expressed as mean ± stdev.

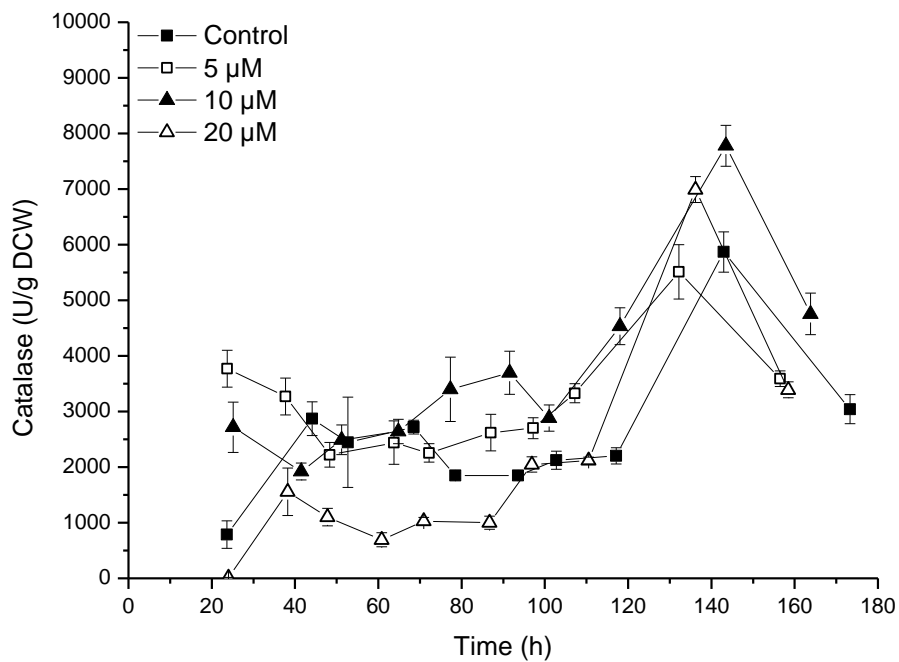


Figure 3-7: CAT (U/g DCW) during batch cultivation in a STR of *A. niger* B1-D.

A range of concentrations (see graph) of polymyxin B were added at 1.5 hours. Cultivation conditions were: airflow 2 lpm, 200-400 rpm, pH 4, temperature 25 °C. Results are expressed as mean ± stdev.

Table 3-13: Statistical analyses of SOD using the Bonferoni post-hoc test, with significant differences between treatment. In which; SEM is standard error of means, LCL is lower confidence limit and UCL is upper confidence limit.

	Mean Diff.	SEM	t-Value
5 μ M polymyxin B vs Control	1415.77315	67.62723	20.93496
10 μ M polymyxin B vs Control	-199.35079	67.62723	-2.94779
20 μ M polymyxin B vs Control	-861.04955	55.2174	-15.59381
	P-Value	LCL	UCL
5 μ M polymyxin B vs Control	3.51E-44	1234.78475	1596.76155
10 μ M polymyxin B vs Control	0.02251	-380.33918	-18.36239
20 μ M polymyxin B vs Control	1.24E-31	-1008.826	-713.27314

Table 3-14: Statistical analyses of CAT using the Bonferoni post-hoc test, with significant differences between treatment. In which; SEM is standard error of means, LCL is lower confidence limit and UCL is upper confidence limit.

	Mean Diff.	SEM	t-Value
5 μ M polymyxin B vs Control	153.17821	166.59687	0.91945
10 μ M polymyxin B vs Control	644.88171	166.59687	3.87091
20 μ M polymyxin B vs Control	-1040.2122	136.02578	-7.64717
	P-Value	LCL	UCL
5 μ M polymyxin B vs Control	1.00E+00	-292.67921	599.03563
10 μ M polymyxin B vs Control	9.94E-04	199.02428	1090.73913
20 μ M polymyxin B vs Control	1.79E-11	-1404.2533	-676.17114

3.2.4 Polymyxin B and its effect on intracellular protein content, lysozyme production and viability

In Figure 3-8 the effect of polymyxin B on intracellular protein content can be seen. The effect of polymyxin B on intracellular protein content shows similar results 24 hours into the process compared to the SOD and CAT values (Figure 3-6 and Figure 3-7). The 5 μM process had the highest intracellular protein content, while the 20 μM process had the lowest intracellular protein content. After 24 hours protein content showed converging values for each process after which for the control, 5 and 20 μM process the intracellular protein content remains at a similar levels during the entire process. The 10 μM shows consistent lower values compared to the control (and other) processes during the entire fermentation at around 120 mg/g DCW.

The statistical analyses showed that all polymyxin B processes were significantly different compared to the control process (two-way ANOVA, $p < 0.05$). The addition of 10 μM polymyxin B resulted in the largest effect on intracellular protein content during cultivation of *A. niger* (Bonferoni post-hoc test, largest mean difference, Table 3-15).

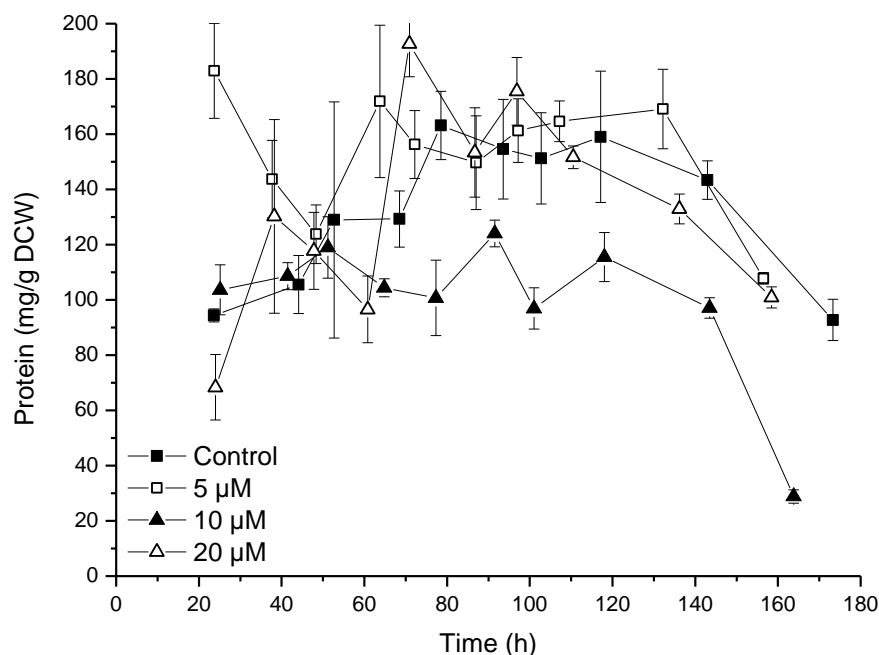


Figure 3-8: Intracellular protein content (mg/g DCW) during batch cultivation in a STR of *A. niger* B1-D.

A range of concentrations (see graph) of polymyxin B were added at 1.5 hours. Cultivation conditions were: airflow 2 lpm, 200-400 rpm, pH 4, temperature 25 °C. Results are expressed as mean ± stdev.

Table 3-15: Statistical analyses of intracellular protein using the Bonferoni post-hoc test, with significant differences between treatment. In which; SEM is standard error of means, LCL is lower confidence limit and UCL is upper confidence limit.

	Mean Diff.	SEM	t-Value
5 μM polymyxin B vs Control	13.29421	3.98578	3.33541
10 μM polymyxin B vs Control	-40.27309	3.98578	-10.10418
20 μM polymyxin B vs Control	-15.62394	3.25438	-4.8009
	P-Value	LCL	UCL
5 μM polymyxin B vs Control	0.00654	2.62719	23.96123
10 μM polymyxin B vs Control	1.38E-17	-50.94011	-29.60607
20 μM polymyxin B vs Control	2.40E-05	-24.33353	-6.91436

The addition of polymyxin B at the start of the process results in a large effect on lysozyme production (Figure 3-9). Every process where polymyxin B was added had a lower production of lysozyme. The control had the highest maximum lysozyme value at around 12 mg/l, whereby the polymyxin B processes had lysozyme values ranging from 2 mg/l (20 μ M) to 4 mg/l (10 μ M).

Statistical analyses showed a significant difference in this dataset (two-way ANOVA, $p < 0.05$). All processes with polymyxin B were significantly different compared to the control process (Bonferoni post-hoc test), where 20 μ M had the largest effect on lysozyme production according to mean difference values (Table 3-16).

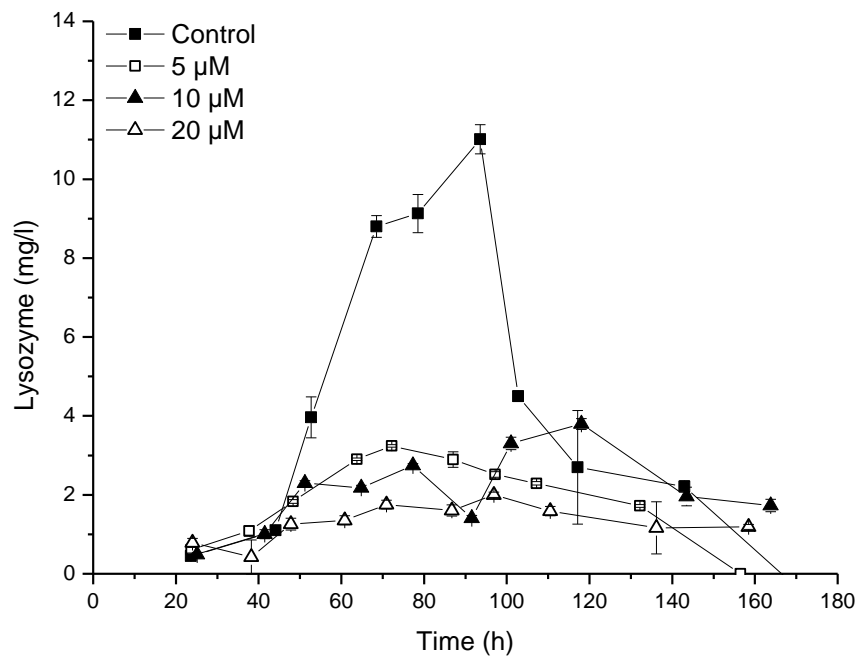


Figure 3-9: Lysozyme concentration (mg/l) during batch cultivation in a STR of *A. niger* B1-D.

A range of concentrations (see graph) of polymyxin B were added at 1.5 hours. Cultivation conditions were: airflow 2 lpm, 200-400 rpm, pH 4, temperature 25 $^{\circ}$ C. Results are expressed as mean \pm stdev.

Table 3-16: Statistical analyses of lysozyme using the Bonferoni post-hoc test, with significant differences between treatment. In which; SEM is standard error of means, LCL is lower confidence limit and UCL is upper confidence limit.

	Mean Diff.	SEM	t-Value
5 μ M polymyxin B vs Control	-2.28137	0.15984	-14.2728
10 μ M polymyxin B vs Control	-2.13244	0.15984	-13.34109
20 μ M polymyxin B vs Control	-3.35271	0.13051	-25.68951
	P-Value	LCL	UCL
5 μ M polymyxin B vs Control	2.59E-28	-2.70914	-1.85359
10 μ M polymyxin B vs Control	6.17E-26	-2.56022	-1.70467
20 μ M polymyxin B vs Control	4.59E-54	-3.70199	-3.00343

The addition of polymyxin B resulted in consistent lower viability values over the entire process (Figure 3-10) compared to the control process. With the exception of one point during the 10 μ M process.

The statistical analyses showed that all polymyxin B processes were significantly different compared to the control process (two-way ANOVA with Bonferoni post-hoc test, $p < 0.05$), where 20 μ M of polymyxin B had the largest effect on viability during cultivation of *A. niger B1-D* (largest mean difference in Table 3-17).

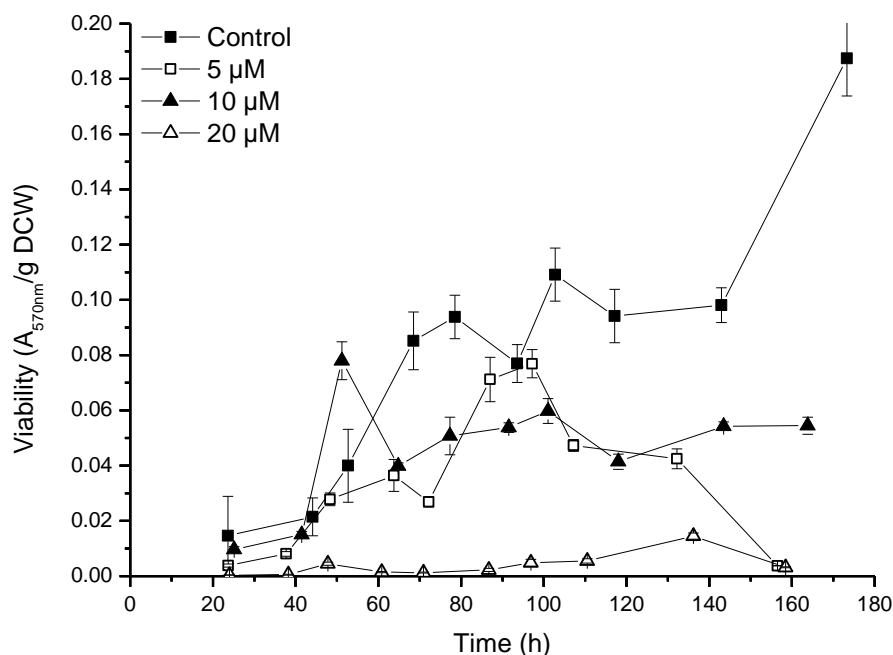


Figure 3-10: Viability (A_{570nm}/g DCW) values during batch cultivation in a STR of *A. niger* B1-D.

A range of concentrations (see graph) of polmyxin B were added at 1.5 hours. Cultivation conditions were: airflow 2 lpm, 200-400 rpm, pH 4, temperature 25 °C. Results are expressed as mean \pm stdev.

Table 3-17: Statistical analyses of Viability using the Bonferoni post-hoc test, with significant differences between treatment. In which; SEM is standard error of means, LCL is lower confidence limit and UCL is upper confidence limit.

	Mean Diff.	SEM	t-Value
5 μ M polmyxin B vs Control	-0.03302	0.00295	-11.19381
10 μ M polmyxin B vs Control	-0.02177	0.00295	-7.3785
20 μ M polmyxin B vs Control	-0.0575	0.00241	-23.87251
	P-Value	LCL	UCL
5 μ M polmyxin B vs Control	2.15E-20	-0.04092	-0.02513
10 μ M polmyxin B vs Control	7.74E-11	-0.02966	-0.01387
20 μ M polmyxin B vs Control	1.99E-50	-0.06395	-0.05106

3.2.5 Overview of statistics

As many processes inside cells are linked and related to each other, an overview table of all the statistical analyses was made to see if any of the measured physiological parameters corresponded with each. Results from this comparison are presented in Table 3-18. This comparison table has been repeated in Chapter 4 and 5.

Table 3-18: Statistical overview of all the tests done in this chapter.

Each result is a means comparison between the control experiment and an experiment where polymyxin B was added. Non-significant differences are represented with a 0 and significant differences are represented with 1. The Bonferroni also answers the question which experiment had the largest effect and that is presented as 1*. All tables with the specific data can be found in Appendix I.

Experiment	DCW	Glucose	Ammonium	OUR	CER	RQ	SOD	CAT	Protein	Lysozyme	Viability	
5 μ M Control	-	1	1*	0	0	1	1*	1*	0	1	1	1
10 μ M Control	-	1*	1	1	0	0	1	1	1	1*	1	1
20 μ M Control	-	1	1	0	0*	1*	1	1	1*	1	1*	1*

Experiment	Specific growth rate	GCR	ACR	
5 μ M Control	-	0	1	1
10 μ M Control	-	0	0	0
20 μ M Control	-	1	0	0

3.3 Discussion

3.3.1 Polymyxin B and its effect on biomass formation, carbon consumption and nitrogen consumption

The alternative pathway is in effect a bypass to avoid normal respiration, thereby avoiding the formation of oxygen radicals. As this bypass creates heat instead of ATP, it is logical to assume that, when this bypass is blocked, this will have a positive effect on biomass formation. If polymyxin B inhibits alternative NADH dehydrogenase as was described in the introduction, it should force the organism to utilise the core electron transport chain more extensively resulting in more ATP formation. This hopefully will result in more and/or faster biomass formation in a bioreactor, which has been shown in previous research using IACA (Voulgaris *et al.*, 2012). Results presented in this chapter show that there is an increase in maximum biomass concentration for the 10 μM process. This is a similar outcome compared to previous mentioned research. The 20 μM process had a significantly lower specific growth rate during this process, which wasn't recorded when IACA was used, however this chapter shows polymyxin B effects with increasing doses. Previous research has given evidence of lower specific growth rates when there is too much oxidative stress using *A.niger B1-D*, resulting in lower specific growth rates (O'Donnell *et al.*, 2011). Growth rates can be diminished by either the increase of oxidative stress defence mechanisms, which uses ATP, or oxidative damage to cells, which compromise the cells ability to divide.

Fungi use diffusion or an active transport system for glucose uptake. The active transport system is only activated when low concentrations of glucose are present (Carlile and Watkinson, 1997). Previous research, found no significant difference in glucose consumption when IACA was added (Voulgaris *et al.*, 2012), while results described here do show this. As glucose utilisation is mostly a diffusion process the most direct factor that has

the potential of influencing glucose utilisation is oxygen availability, which can influence the main and alternative respiratory pathway. The increased use of oxygen (Figure 3-4 (A)) can potentially increase the utilisation of glucose..

Ammonium uptake by fungal cells proceeds via an active transport mechanism to maintain the ionic balance of the cell by extrusion of hydrogen ions (Carlile and Watkinson, 1997). The trends observed in Figure 3-3 are very similar compared to work previously done in this lab using IACA, which can point towards inhibition of NADH dehydrogenase (Voulgaris *et al.*, 2012). A reason for this is that as ammonium uptake is an active process it therefore requires ATP and if more ATP can be produced by utilising the core electron transport chain then ammonium uptake will be faster. This has been confirmed by previous research into the alternative pathway that showed elevated ATP levels together with increased ammonium uptake using IACA to block NADH dehydrogenase (Voulgaris *et al.*, 2012), research shown here also shows a faster utilisation of ammonium.

The increase in maximum biomass concentration and the faster decreases in glucose and ammonium indicate more utilisation of the main respiratory pathway and less use of the alternative pathway, thereby pointing towards (partially) blocking NADH dehydrogenase in *A. niger B1-D* by polymyxin B.

3.3.2 Polymyxin B and its effect on respiration

As previously stated NADH dehydrogenase bypasses complex I (Joseph-Horne *et al.*, 2001). If polymyxin B is blocking this enzyme than this should result in increased OUR values as complex I is more utilised then before. Figure 3-4 (A) shows this from 60 hours onwards. The statistical analyses didn't show any significant differences, however Figure 3-4 (A) clearly shows relative stable differences between the polymyxin processes and the control process from 60 hours onwards. Therefore there was also a statistical analyses performed with the values obtained from 60 hours onwards, thereby

ignoring the OUR values from the first 60 hours. This analysis showed that all polymyxin B processes were significantly different compared to the control process and that the 10 μM process had the largest effect on OUR values during cultivation of *A. niger B1-D*. The 20 μM process had OUR values that were lower than the other polymyxin processes. This could mean that the main respiratory pathway has been over utilised and this has damaged the complexes, thereby inhibiting the capacity of *A. niger B1-D* to use oxygen. This was also confirmed by the lower specific growth rate during the 20 μM process mentioned previously. Research in literature also links damaged or dysfunctional mitochondria, due to oxidative stress, to a reduced capacity of oxygen uptake in fission yeast (Zuin *et al.*, 2008).

Previous research in this lab has shown two outcomes, when studying the effect of oxidative stress on CER values during cultivation of *A. niger B1-D*. Experiments done previously showed increased CER values when utilising oxygen enriched air concentrations of 25% and lower CER values when using 50% oxygen enriched air compared to the control process, this decrease in CER values was attributed to an increase in alternative respiration (O'Donnell *et al.*, 2011). The second result utilising IACA with the aim of blocking NADH dehydrogenase showed that per gram of biomass CER values were lower than the control experiment. This is a similar outcome compared to the 50% oxygen enriched air experiment. This negative effect on CER values can be the result of two processes; oxidative stress or a higher utilisation of alternative oxidase to bypass Complex III (Voulgaris *et al.*, 2012).

The increased OUR and decreased CER in the polymyxin B processes resulted in decreased respiration (R.Q., Figure 3-5) compared to the control process. Previous research done in this lab showed that imposed oxidative stress on *A. niger* resulted in lower R.Q. values (O'Donnell *et al.*, 2011), which is an outcome that is similar to results obtained here. The mitochondrial complexes are built up from various proteins and these proteins can also be sensitive to oxidative stress via oxidation of Fe-S groups

(Li, 2008), thereby potentially reducing respiration. Qin *et al.*, (2011) proved this by showing that most protein damage occurred in the mitochondria of *Penicillium expansum*, which would explain the lower R.Q. during the polymyxin B processes.

The higher OUR values clearly showed two things; first of all more oxygen is being used by *A. niger* in the polymyxin B processes and secondly the OUR values increased with increasing concentrations of polymyxin B, which shows a dose dependent effect. CER and R.Q. values clearly show that oxidative stress is occurring inside *A. niger* cells. All the off-gas analyses performed in this chapter clearly indicate (partial) blocking of NADH dehydrogenase in *A. niger*.

3.3.3 Polymyxin B and its effect on oxidative stress related biomarkers

SOD activity under oxidative stress conditions have been well characterized in the literature, where an increase in oxygen radicals has been associated with a increase in SOD activity in filamentous fungi (Angelova *et al.*, 2001, Krumova *et al.*, 2009). There is however also evidence of a limit to SOD's ability to cope with prolonged high oxidative stress which was shown in the organism *Fusarium equiseti*, where increasing concentrations of carbon source during cultivation resulted in higher SOD activities until a maximum was reached before SOD activities decreased again pointing towards oxidative damage to SOD (Ayar-Kayali and Tarhan, 2004). SOD activity in the first 50 hours of the 5 and 10 μM polymyxin B processes are clearly higher, which indicates more oxidative stress. The gradual increase in SOD activity, with increasing polymyxin B concentrations, in this time frame also indicates a dose effect of polymyxin B indicating that if NADH dehydrogenase is blocked that this effect is only partial for the lower concentrations of polymyxin B. The inhibition of SOD that seems to occur can be caused by excess hydrogen peroxide generation. SOD is known to be inactivated by exposure to hydrogen peroxide, which might explain the SOD

inhibition seen after the 50 hour mark for the polymyxin B processes (Pigeolet *et al.*, 1990, Jakubowski *et al.*, 2000).

The previous mentioned cause for increased SOD activity can also be repeated for CAT activity, meaning increased oxidative stress causes CAT activity to rise. The increased CAT activity for the polymyxin B processes immediately after adding polymyxin B show similar results compared to SOD activity which (from 24 to around 50 hours in Figure 3-7) point towards increased oxidative stress caused by higher intracellular H₂O₂ concentrations in *A. niger B1-D* (Kreiner *et al.*, 2002). The very low CAT activity values during the 20 µM process are likely due to oxidative damage to the enzyme, which is known to be caused by the superoxide anion (Pigeolet *et al.*, 1990, Jakubowski *et al.*, 2000). The converging CAT values in Figure 3-7 coincides with exponential growth. However DCW, glucose, ammonium, SOD and previous CAT values still indicate that there is less alternative respiration taking place. A potential explanation for these converging CAT values could be oxygen limitation. DOT values approach zero at around 50 hours which coincides with CAT values becoming similar for the control, 5 and 10 µM polymyxin processes. The diverging values after 70 hours might have been caused by anaerobic respiration (see Chapter 1.10), which has been shown in literature to be another source for ATP in fungi (Morozkina and Kurakov, 2007, Thomson *et al.*, 2012). This anaerobic ATP source could provide the necessary extra ATP to increase cellular defence mechanisms against oxidative stress resulting in higher CAT activity shown in Figure 3-7. These increased CAT values after 70 hours are together with the increased OUR values an indication that effect of polymyxin B on NADH dehydrogenase activity is permanent. All fungal fermentations presented in this thesis have high CAT activity values at the end of the processes. These high activities can mostly be linked with proteolytic activity in combination with autolysis (Li *et al.*, 2008d) shown by the decreases in DCW and intracellular protein.

SOD and CAT activities are clearly elevated at the start of the polymyxin B processes caused by the elevated OUR values, measured during the

polymyxin B processes. These results indicate (partial) blocking of NADH dehydrogenase.

3.3.4 Polymyxin B and its effect on intracellular protein content, lysozyme production and viability

The increased intracellular protein concentrations in the first 40 hours of the polymyxin B processes (5 μ M) point towards NADH dehydrogenase blocking, as this enzyme is blocked more ATP is generated resulting in higher protein levels. Research done by Voulgaris *et al.*, (2012) showed higher intracellular protein and ATP levels, when utilising IACA to inhibit NADH dehydrogenase. Results presented in this chapter show that only the 10 μ M polymyxin B process has a negative effect on intracellular protein content, while the other polymyxin B processes show similar levels over the whole process time, when comparing these to the control process. This decrease may be caused by protein oxidation by way of increased ROS generation in that process (Wongwicharn *et al.*, 1999), which would be caused by increased electron leakage from Complex I as NADH dehydrogenase might be blocked. Previous research done in this lab showed an increase in protein carbonylation when sparging enriched oxygen into the bioreactor, followed by an increase in proteolytic activity (Li *et al.*, 2008d) to deal with the accumulation of damaged proteins. The same paper also points towards a maximum in proteolytic activity, as proteolytic activity for 50% and 75% oxygen enrichment were similar to each other or even lower in case of the 75% process indicating impairment in this cellular process to deal with damaged proteins. This might explain why the 20 μ M polymyxin B process had similar values compared to the control process as the cells ability to deal with oxidated proteins might be compromised, as the assay to measure total intracellular protein content doesn't distinguish between oxidated proteins and non-oxidated proteins it is entirely possible that a large part of the intracellular protein content in the 20 μ M process consists of oxidated

proteins, which results in similar levels of intracellular protein content compared to the control process.

Lysozyme concentrations were lower in all polymyxin B processes than the control experiment, which is likely associated with the increased oxidative stress, pointing towards the alternative pathway being (partially) blocked. Bai *et al.*, (2004) showed a similar effect utilising the *A. niger* strain doing oxygen enrichment experiments.

Viability is an assay which measures reductase activity (Emri *et al.*, 2005). The mitochondrial complexes consist of reductase; therefore viability would be an interesting parameter to observe. The viability in all processes utilising polymyxin B were badly affected and resulted in lower viability for all processes. This result corresponds very well with the R.Q. values, which were lower in each polymyxin B process as well. Both viability and R.Q. values are an indication of mitochondrial activity and oxidative stress has been known to oxidize the complexes of the mitochondria (Qin *et al.*, 2011), which would explain the lower viability and R.Q. values.

The reduced viability, lower lysozyme yield, decreased intracellular protein content (10 μ M) point towards more oxidative stress. This would mean that polymyxin B is (partially) blocking the alternative pathway.

3.4 Conclusions

The aim of this work was to study the effect of polymyxin B on the oxidative stress response of *A. niger B-1D*. The effect of polymyxin B showed an increase in oxidative stress resulting in increased maximum DCW (10 μ M process), glucose uptake, ammonium uptake, OUR, SOD and CAT values and decreased R.Q., intracellular protein values (10 μ M), viability and lysozyme values. The decreased lysozyme production shows that an increase of oxidative stress can have a large negative effect on the production of enzymes inside bioreactors.

Chapter 4

Does oxidative stress in the lag phase of a fermentation cause adverse effects?

4 Does oxidative stress in the lag phase of a fermentation cause adverse effects?

4.1 Introduction and aims

Filamentous fungi have long been applied in the food industry e. g. cheese production (Chavez *et al.*, 2010) and also have become an important source of various enzymes and proteins (Archer *et al.*, 1994). As developments in genetic engineering and molecular biology now allow for heterologous protein production, research in process optimization has since consequently become important due to the often disappointing yields of these proteins due to the characteristically high viscosity of fungal fermentations resulting in poor oxygen transfer inside the reactor (Wang *et al.*, 2005). As described previously oxygen enrichment of the bioreactor will help against poor oxygen transfer inside the reactor however this can also result in lower yields due to oxidative damage of heterologous proteins.

The main process parameters that can affect heterologous protein production and oxidative stress levels in a bioreactor are: inoculum, pH, agitation, airflow, medium design, reactor modes of operation, bioreactor design (see Chapter 1) (Li *et al.*, 2002, Wang *et al.*, 2005, Tang *et al.*, 2009).

General accepted knowledge on oxygen transfer rate (OTR) is that the higher the total surface to transfer oxygen across, from the gas to the liquid phase the higher the oxygen transfer rate (van 't Riet and Tramper, 1991). Therefore transfer from gas to liquid can be manipulated by varying the agitation rate, airflow and the pressure inside the reactor thereby forcing more air from the gas to the liquid phase (Pinheiro *et al.*, 2000, Belo *et al.*, 2003).

A comprehensive comparison of batch and continuous fermentation modes, utilising the *Aspergillus niger* B1-D strain, to study the effect of oxygen

enrichment on lysozyme and protein production was carried out by Bai *et al.*, (2004). The main results of this study were that during batch cultivation there was a substantial negative effect of oxygen enrichment on production of intracellular protein content during batch cultivation of *Aspergillus niger B1-D*. During oxygen enrichment processes, processes where oxygen enriched air was sparged into the bioreactor, intracellular protein content was for each oxygen enrichment process lower. Negative effects on lysozyme production were less severe with only 75% (v/v) of oxygen enrichment having a severe negative effect on lysozyme production. Continuous fermentation of *Aspergillus niger B1-D* showed the opposite effect, where both lysozyme production and native protein content were higher during the oxygen enrichment experiments (Wongwicharn *et al.*, 1999, Bai *et al.*, 2004). Other studies have shown the same severe inhibition of intracellular protein content and lysozyme production during batch cultivation of *Aspergillus niger B1-D* when utilising oxygen enrichment (O'Donnell, 2008, O'Donnell *et al.*, 2011).

Thus a large negative effect of oxidative stress on production of lysozyme and intracellular protein content was not observed when utilising oxygen enrichment protocols during continuous fermentation modes. It may therefore be a valid assumption that *Aspergillus niger B1-D* shows the highest oxidative stress levels during the lag phase and beginning of the exponential phase, where potentially damaging effects could inhibit heterologous protein production and intracellular protein content. O'Donnell *et al.*, (2007) partially confirmed this by showing that inoculation of a bioreactor with *A. niger B1-D* results in an oxidative shock to which the organisms have to adapt first. Previous research utilising an industrial *Saccharomyces cerevisiae* strain, for beer production, suggests that the effect of oxidative stress in the lag phase of the fermentation can be of substantial importance to the final quality of the beer product (Higgins *et al.*, 2003).

Most research described here connected the previously described effects on lysozyme production and protein content to the increased concentration of the superoxide anion (Bai *et al.*, 2004, O'Donnell, 2008, O'Donnell *et al.*,

2011). While investigations have been done to determine how oxidative stress defence mechanisms respond to oxidative stress (Kreiner *et al.*, 2003), to this authors knowledge no definitive link has been established between heterologous protein production, native protein content and oxidative stress defence mechanisms in filamentous fungi during the lag phase of the bioprocess.

4.1.1 Aims

The aim of this study was to see whether *Aspergillus niger* B1-D can cope with increasing levels of oxidative stress during the lag phase of the fermentation. This will be achieved by studying the levels of activity of the defensive enzymes against oxidative stress at different agitation speeds. The selected enzymes were superoxide dismutase (SOD) and catalase (CAT) and the relationship between these enzymes, lysozyme production, intracellular protein content and various other physiological parameters will be determined.

4.2 Results

This work points towards an optimum agitation setting and as lysozyme is the main product of the strain utilised this optimum setting will be determined by the process which has the highest yield of this product. As described in Chapter 2.5; kLa values are not taken into account in the results described here. Figure 4-1 and Table 4-1 (Yield of product on substrate Y_{ps}) show the optimum process to be the 200-400 rpm process. The effect of increased agitation on the product yield on substrate (Y_{ps}) is at least threefold as shown in Table 4-1. The statistical analyses will therefore be a comparison between this optimum setting and the other processes.

All processes in Figure 4-1 were significantly different compared to the 200-400 rpm process (two-way ANOVA with Bonferoni post-hoc test $p < 0.05$), with the 100-400 rpm process having the largest effect on lysozyme production, when looking at mean difference values (Table 4-2).

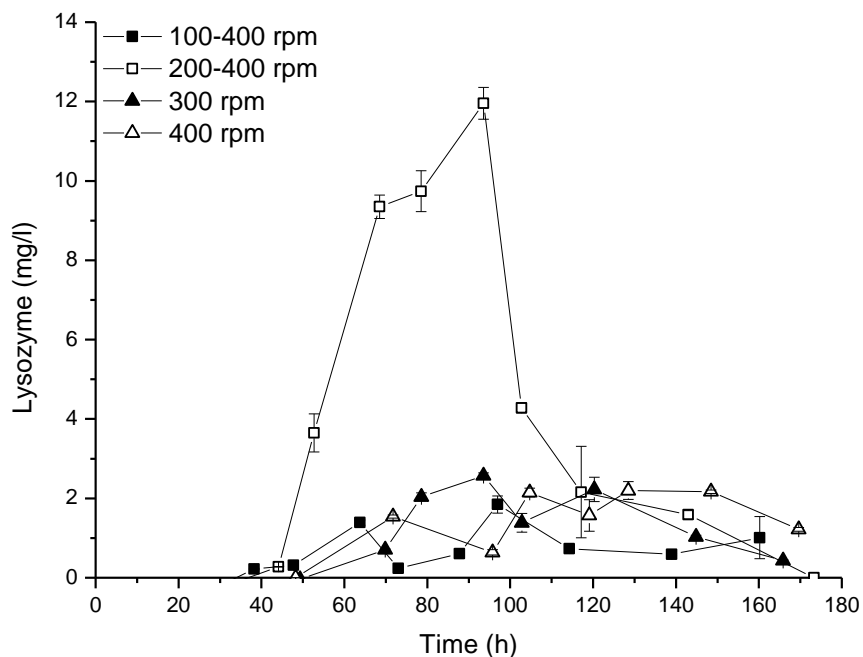


Figure 4-1: Lysozyme concentration (mg/l) during batch cultivation in a STR of *A. niger* B1-D.

Various agitation settings were used. Various agitation settings were used. Cultivation conditions were: airflow 2 lpm, pH 4, temperature 25 °C. Results are expressed as mean ± stdev.

Table 4-1: Effect of various agitation settings on Yps during batch fermentations of *A. niger* B1-D.

Cultivation conditions were: airflow 2 lpm, pH 4, temperature 25 °C. Specific growth rate was determined from the linear part of the graph and is expressed as mean ± stdv.

Agitation settings (rpm)	Yps (%)
100-400	0.005
200-400	0.230
300	0.007
400	0.006

Table 4-2: Statistical analyses of Lysozyme using the Bonferoni post-hoc test. In which; SEM is standard error of means, LCL is lower confidence limit and UCL is upper confidence limit.

	Mean Diff.	SEM	t-Value
200-400 rpm vs 100-400 rpm	2.90223	0.11427	25.39784
300 rpm vs 200-400 rpm	-2.48232	0.11427	-21.7232
400 rpm vs 200-400 rpm	-2.79517	0.13195	-21.18384
	P-Value	LCL	UCL
200-400 rpm vs 100-400 rpm	1.72E-53	2.59641	3.20804
300 rpm vs 200-400 rpm	6.66E-46	-2.78814	-2.1765
400 rpm vs 200-400 rpm	9.95E-45	-3.1483	-2.44204

Another general remark for this work is that the processes utilising DOT setpoints by controlling the agitation speed had the initial agitation speed for at least 24 hours before the increase in agitation started.

4.2.1 Agitation and its effect on biomass formation, carbon consumption and nitrogen consumption

Figure 4-2 shows the effect of different agitation settings on DCW during fermentation of *Aspergillus niger* B1-D.

The stationary phase was reached at different times for each process. The 100-400 rpm process reached its stationary phase at around 60 hours, while the 400 rpm process reached its stationary phase at around 90 hours. DCW values fluctuated between 12 to 15 g/l. Statistical analyses showed that the 100-400 rpm process was significantly different compared to the 200-400 rpm process (two-way ANOVA with Bonferoni post-hoc test, $p < 0.05$, see Table 4-4).

Table 4-3 shows the effect of different agitation settings on specific growth rate. The 200-400 rpm process had the highest specific growth rate (0.037 h^{-1}) resulting in significant differences when comparing the 100-400, 300 and 400 rpm processes to the 200-400 rpm process (one-way ANOVA with Tukey posthoc test, $p < 0.05$, Table 4-5), with the 100-400 rpm process having the largest effect on specific growth rate (based on largest mean difference).

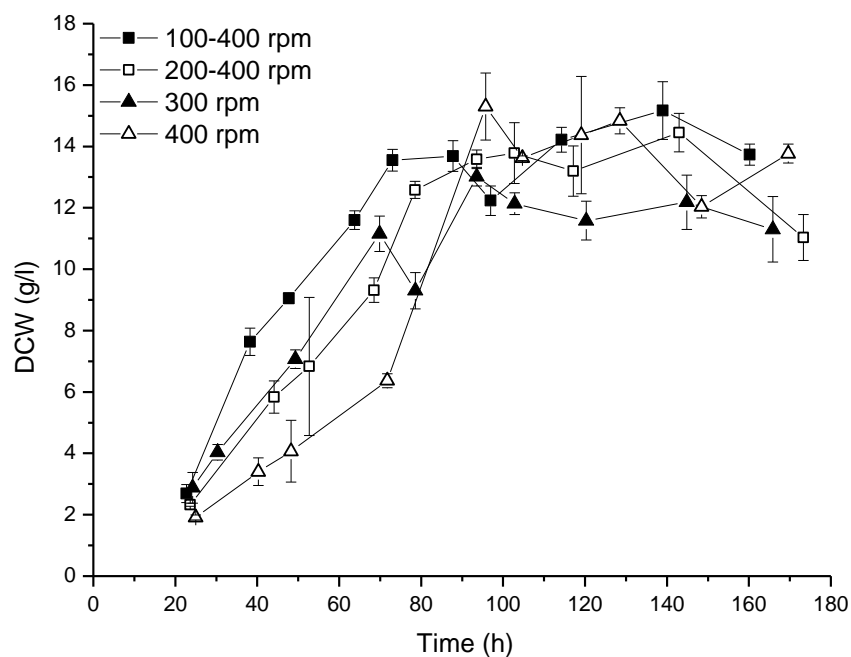


Figure 4-2: DCW (g/l) during batch cultivation in a STR of *A. niger B1-D*. Various agitation settings were used. Cultivation conditions were: airflow 2 lpm, pH 4, temperature 25 °C. Results are expressed as mean \pm stdev.

Table 4-3: Effect of various agitation settings on specific growth rate during batch fermentations of *A. niger B1-D*.

Cultivation conditions were: airflow 2 lpm, pH 4, temperature 25 °C. Specific growth rate was determined from the linear part of the graph and is expressed as mean \pm stdv.

Agitation settings (rpm)	Specific growth rate (h ⁻¹)
100-400	0.017 \pm 0.0009
200-400	0.037 \pm 0.0017
300	0.022 \pm 0.0030
400	0.022 \pm 0.0052

Table 4-4: Statistical analyses of DCW using the Bonferoni post-hoc test. In which; SEM is standard error of means, LCL is lower confidence limit and UCL is upper confidence limit.

	Mean Diff.	SEM	t-Value
200-400 rpm vs 100-400 rpm	-1.12778	0.19721	-5.7186
300 rpm vs 200-400 rpm	-0.16472	0.19721	-0.83525
400 rpm vs 200-400 rpm	0	0.22772	0
	P-Value	LCL	UCL
200-400 rpm vs 100-400 rpm	3.75E-07	-1.65557	-0.59999
300 rpm vs 200-400 rpm	1	-0.69251	0.36307
400 rpm vs 200-400 rpm	1	-0.60944	0.60944

Table 4-5: Statistical analyses of specific growth rate using the Tukey post-hoc test. In which; SEM is standard error of means, LCL is lower confidence limit and UCL is upper confidence limit.

	Mean Diff.	SEM	t-Value
200-400 rpm vs 100-400 rpm	0.01997	0.00195	14.44949
300 rpm vs 200-400 rpm	-0.01483	0.00195	10.73111
400 rpm vs 200-400 rpm	-0.01556	0.00226	9.74972
	P-Value	LCL	UCL
200-400 rpm vs 100-400 rpm	3.28E-07	0.01429	0.02565
300 rpm vs 200-400 rpm	1.34E-05	-0.02051	-0.00915
400 rpm vs 200-400 rpm	3.91E-05	-0.02212	-0.009

Figure 4-3 and Table 4-6 show the effect on glucose concentrations and glucose consumption rate (GCR) when using different agitation speeds (100-400, 200-400, 300 and 400 rpm) during cultivation of *A. niger* B1-D.

The initial 24 hours of each process had 100, 200, 300 and 400 rpm as its agitation speed respectively. This increasing agitation setting resulted in a delay in glucose uptake by *A. niger*. The glucose supply during the 100-400 rpm process was completely depleted at around 90 hours, while the 400 rpm process had no glucose left at around 105 hours. Statistical analyses (two-way ANOVA with Bonferoni post-hoc test, $p < 0.05$) showed that the 100-400 and 200-400 rpm processes weren't significantly different from each other, while the 300 and 400 rpm processes were significantly different compared to the 200-400 process. The mean differences showed that the 400 rpm process had the largest effect on residual glucose concentration (Table 4-7).

Analyses of GCR (Table 4-6) showed that varying agitation settings had a negative effect on GCR with all processes having lower GCR values compared to the 200-400 rpm process. The 300 and 400 rpm processes were significantly different compared to the 200-400 rpm process in which the 400 rpm process had the largest effect on GCR values based on the largest mean difference that was obtained (one-way ANOVA with Tukey post-hoc test, $p < 0.05$, Table 4-8).

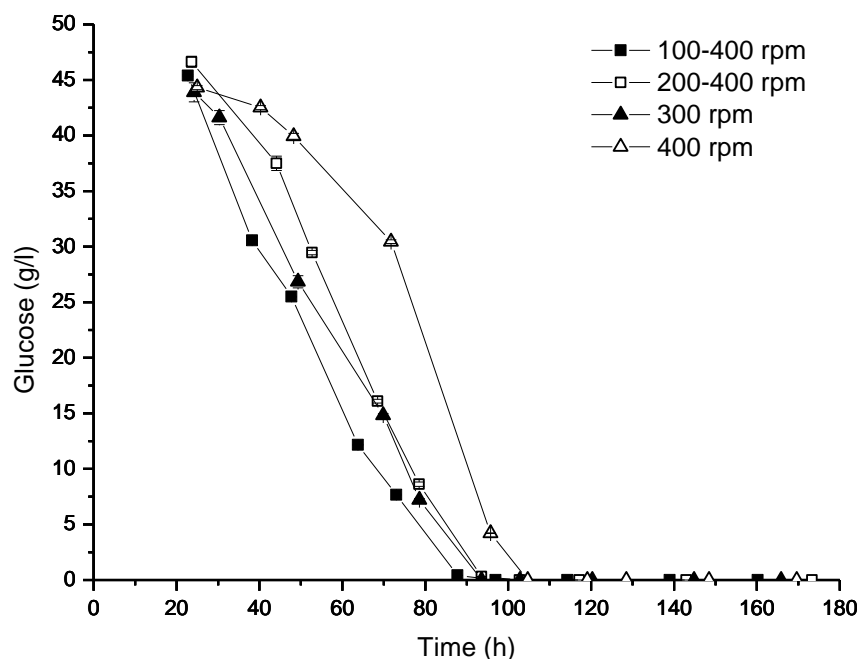


Figure 4-3: Residual glucose (g/l) during batch cultivation in a STR of *A. niger B1-D*.

Various agitation settings were used. Cultivation conditions were: airflow 2 lpm, pH 4, temperature 25 °C. Results are expressed as mean ± stdev.

Table 4-6: Effect of various agitation settings on GCR rate during batch fermentations of *A. niger B1-D*.

Cultivation conditions were: airflow 2 lpm, pH 4, temperature 25 °C. Specific growth rate was determined from the linear part of the graph and is expressed as mean ± stdv.

Agitation speed (rpm)	GCR (g/l/h)
100-400	0.65 ± 0.0086
200-400	0.69 ± 0.0062
300	0.63 ± 0.0123
400	0.22 ± 0.0025

Table 4-7: Statistical analyses of residual glucose using the Bonferoni post-hoc test. In which; SEM is standard error of means, LCL is lower confidence limit and UCL is upper confidence limit.

	Mean Diff.	SEM	t-Value
200-400 rpm vs 100-400 rpm	0.5455	0.59965	0.9097
300 rpm vs 200-400 rpm	1.89437	0.59965	3.15913
400 rpm vs 200-400 rpm	2.28004	0.69241	3.29288
	P-Value	LCL	UCL
200-400 rpm vs 100-400 rpm	1	-1.05932	2.15032
300 rpm vs 200-400 rpm	0.01163	0.28955	3.49919
400 rpm vs 200-400 rpm	0.00753	0.42695	4.13312

Table 4-8: Statistical analyses of GCR using the Tukey post-hoc test. In which; SEM is standard error of means, LCL is lower confidence limit and UCL is upper confidence limit.

	Mean Diff.	SEM	t-Value
200-400 rpm vs 100-400 rpm	-0.01278	0.0387	0.46682
300 rpm vs 200-400 rpm	-0.12555	0.0387	4.58727
400 rpm vs 200-400 rpm	-0.4749	0.04469	15.02744
	P-Value	LCL	UCL
200-400 rpm vs 100-400 rpm	0.98706	-0.12527	0.09972
300 rpm vs 200-400 rpm	0.02673	-0.23804	-0.01305
400 rpm vs 200-400 rpm	1.87E-07	-0.6048	-0.345

The effect of different agitation settings during cultivation of *A. niger* on ammonium levels and consumption rate are given in Figure 4-4 and Table 4-9 respectively.

The 100-400 process has a rapid decrease in ammonium concentration and reaches 1 g/l at around 50 hours, after which the uptake of ammonium slows down substantially. The 200-400 and 300 processes have a similar rate of ammonium uptake and reach 0.5 g/l at around 90 hours; the 100-400 rpm process has an ammonium concentration of around 0.6 g/l at that time. The 400 rpm process seems to have an extended lag phase, after which ammonium concentrations decrease from around 4.5 g/l to around 1 g/l. Statistical analyses showed a significant difference in this dataset (two-way ANOVA, $p < 0.05$). The Bonferoni post-hoc test showed that the 100-400 and 300 rpm processes were significantly different from the 200-400 rpm process (Table 4-10).

The effect of agitation settings on ACR values is significant when comparing the 100-400 and 300 rpm processes with the 200-400 process (one-way ANOVA and Tukey post-hoc test, $p < 0.05$). ACR values in both of these processes were significantly higher than the 200-400 process, with the 100-400 rpm process having the largest effect when looking at the mean difference values (Table 4-11).

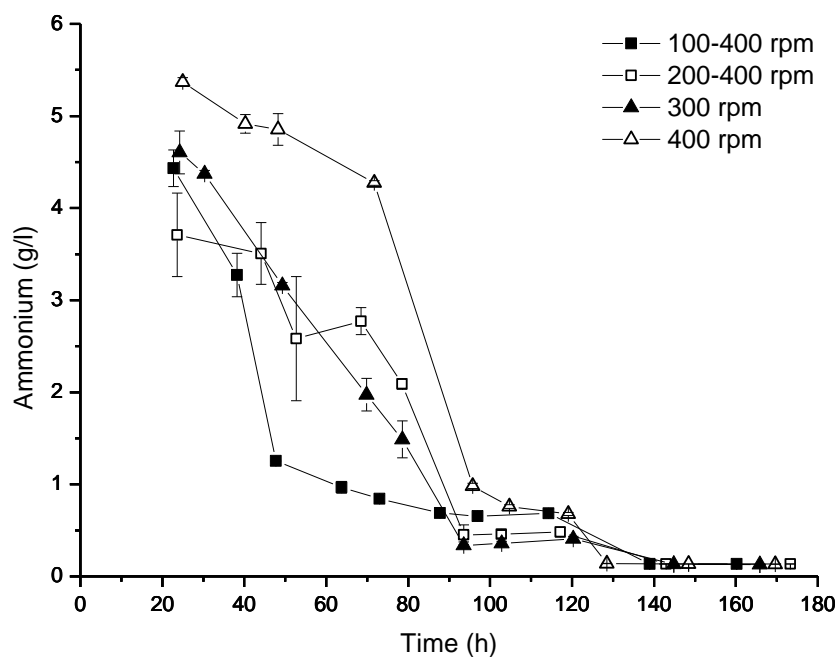


Figure 4-4: Residual ammonium (g/l) during batch cultivation in a STR of *A. niger B1-D*.

Various agitation settings were used. Cultivation conditions were: airflow 2 lpm, pH 4, temperature 25 °C. Results are expressed as mean ± stdev.

Table 4-9: Effect of various agitation settings on ACR rate during batch fermentations of *A. niger B1-D*.

Cultivation conditions were: airflow 2 lpm, pH 4, temperature 25 °C. Specific growth rate was determined from the linear part of the graph and is expressed as mean ± stdv.

Agitation settings (rpm)	ACR (g/l/h)
100-400	0.069 ± 0.0060
200-400	0.030 ± 0.0092
300	0.062 ± 0.0029
400	0.020 ± 0.0030

Table 4-10: Statistical analyses of residual ammonium using the Bonferoni post-hoc test. In which; SEM is standard error of means, LCL is lower confidence limit and UCL is upper confidence limit.

	Mean Diff.	SEM	t-Value
200-400 rpm vs 100-400 rpm	0.21441	0.05852	3.66362
300 rpm vs 200-400 rpm	0.14486	0.05852	2.47528
400 rpm vs 200-400 rpm	0.59174	0.06758	8.75653
	P-Value	LCL	UCL
200-400 rpm vs 100-400 rpm	0.00211	0.05778	0.37103
300 rpm vs 200-400 rpm	0.08704	-0.01176	0.30149
400 rpm vs 200-400 rpm	3.54E-14	0.41089	0.7726

Table 4-11: Statistical analyses of ACR using the Tukey post-hoc test. In which; SEM is standard error of means, LCL is lower confidence limit and UCL is upper confidence limit.

	Mean Diff.	SEM	t-Value
200-400 rpm vs 100-400 rpm	-0.04885	0.00533	12.96066
300 rpm vs 200-400 rpm	0.03166	0.00533	8.39971
400 rpm vs 200-400 rpm	-0.01154	0.00616	2.65205
	P-Value	LCL	UCL
200-400 rpm vs 100-400 rpm	2.32E-06	-0.06435	-0.03336
300 rpm vs 200-400 rpm	1.88E-04	0.01617	0.04715
400 rpm vs 200-400 rpm	0.28185	-0.02943	0.00635

4.2.2 Agitation and its effect on dissolved oxygen tension (DOT) and respiration

Figure 4-5 (A) and (B) show dissolved oxygen tension (DOT) and oxygen uptake rate (OUR). The OUR values can be calculated based on the off-gas analyses (for calculation see chapter 2.4).

The DOT (Figure 4-5 (A)) was measured during each of the processes presented in this chapter. Each process reaches a DOT value of 0%, but the time at which this value is reached is markedly different in each process. A value of 0% was reached at 40 hours for the 100-400 rpm process, while the 400 rpm process reached its zero value at around 100 hours.

The grey highlighted part of Figure 4-5 (B) shows that OUR values during the 100-400 rpm process are lower compared to the other processes. After 60 hours OUR values in the 200-400 rpm process have the lowest values at around 0.5 mM/g DCW/h (200-400 rpm) while the 400 rpm process has higher values compared to the other processes during the entire fermentation ranging from 10 to 2 mM/g DCW/h. The statistical analyses of this dataset showed a significant difference between the 400 and 200-400 rpm process (two-way ANOVA, $p < 0.05$, with a Bonferoni post-hoc test, Table 4-12).

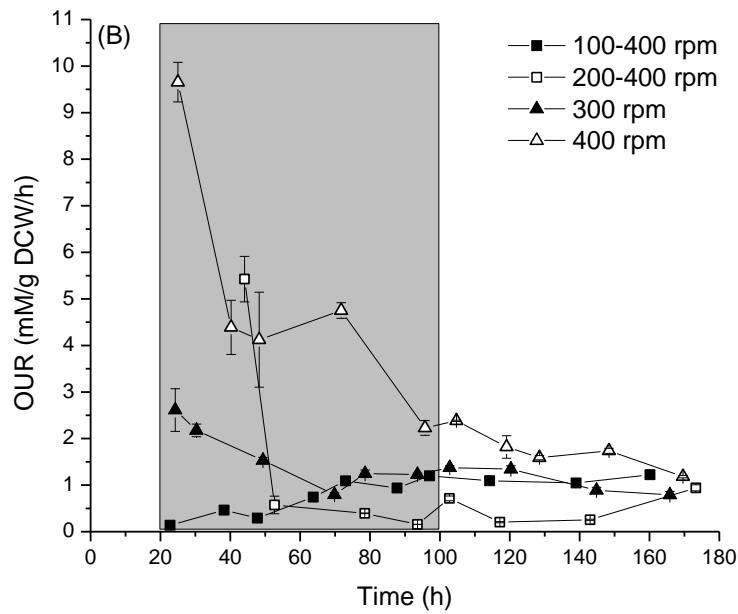
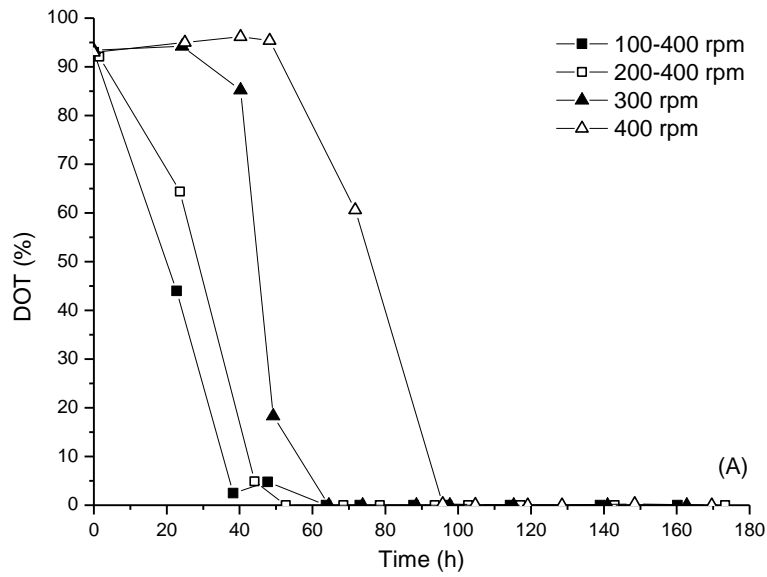


Figure 4-5: (A) DOT (%) and (B) OUR (mM/g DCW/h) during batch cultivation in a STR of *A. niger* B1-D.

Various agitation settings were used. Various agitation settings were used. Cultivation conditions were: airflow 2 lpm, pH 4, temperature 25 °C. Results are expressed as mean ± stdev. At around 100 hours DOT becomes limiting in each process (end of grey highlighted part)

Table 4-12: Statistical analyses of OUR using the Bonferoni post-hoc test. In which; SEM is standard error of means, LCL is lower confidence limit and UCL is upper confidence limit.

	Mean Diff.	SEM	t-Value
200-400 rpm vs 100-400 rpm	-0.20612	0.10066	-2.04781
300 rpm vs 200-400 rpm	0.14542	0.10147	1.43311
400 rpm vs 200-400 rpm	2.47005	0.11522	21.43765
	P-Value	LCL	UCL
200-400 rpm vs 100-400 rpm	0.25519	-0.47568	0.06343
300 rpm vs 200-400 rpm	0.92494	-0.12632	0.41717
400 rpm vs 200-400 rpm	2.31E-44	2.16149	2.77861

In Figure 4-6 (A) and (B) carbon evolution rate (CER) and respiration quotient (R.Q.) values can be observed respectively.

The highlighted grey area in Figure 4-6 (A), shows a peak value for the 200-400 rpm process of around 4 mM/g DCW/h process. After 60 hours all processes start to show converging CER values at around 0.3 mM/g DCW/h. The statistical analyses showed that all processes were significantly different compared to the 200-400 rpm process (two-way ANOVA with Bonferoni post-hoc test, $p < 0.05$) of which the 100-400 rpm process had the largest effect on CER values when looking at the mean difference values (Table 4-13).

From OUR and CER values the R.Q. of each process can be calculated (Figure 4-6 (B)). The highlighted grey part shows a peak value for the 100-400 rpm process of around 4.5, while the other processes show lower values. After 60 hours the 200-400 and 300 rpm processes show higher R.Q. values of which the 200-400 rpm process has high R.Q values during the remaining time of the process, with a maximum value of around 3.5. The statistical analyses showed a significant difference between the 100-400, 300 and 400 rpm processes and the 200-400 rpm process (two-way ANOVA with Bonferoni post-hoc test, $p < 0.05$, Table 4-14). The 400 rpm process had the largest effect on RQ values, based on the largest mean difference.

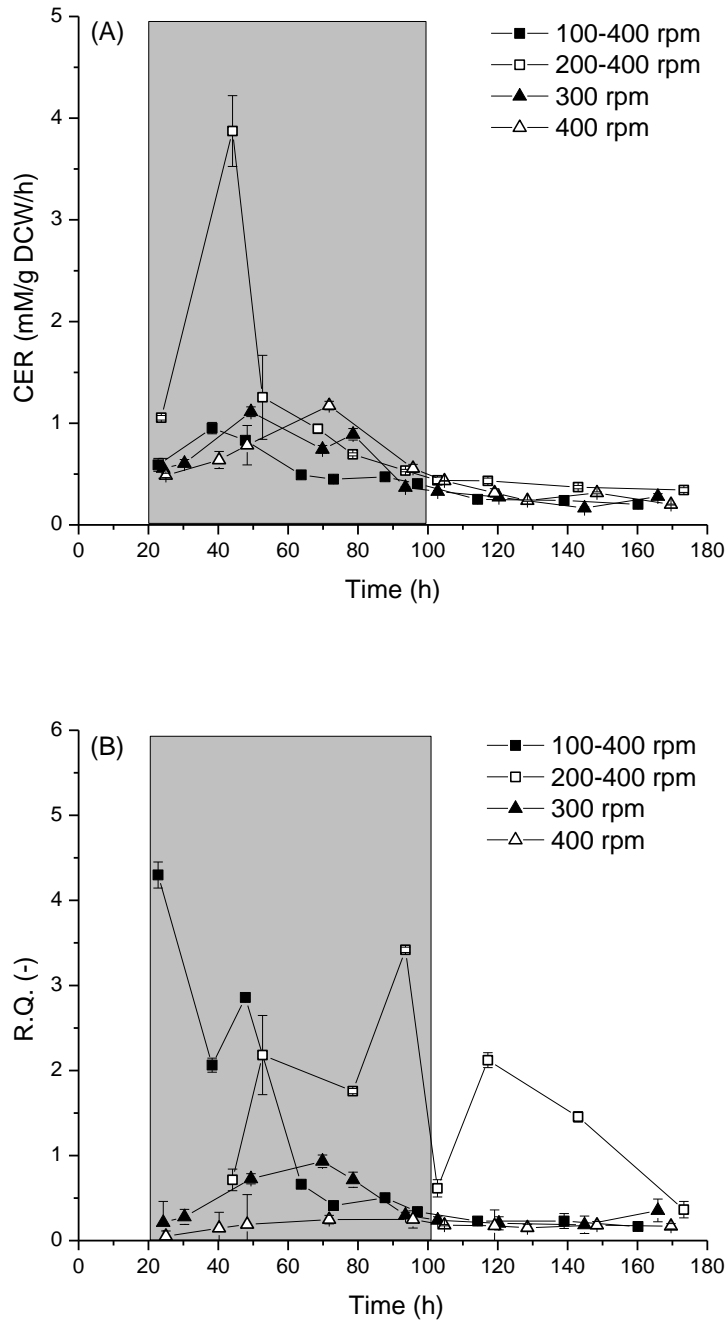


Figure 4-6: (A) CER (mM/g DCW/h) and (B) R.Q. during batch cultivation in a STR of *A. niger* B1-D.

Various agitation settings were used. Various agitation settings were used. Cultivation conditions were: airflow 2 lpm, pH 4, temperature 25 °C. Results are expressed as mean \pm stdev. At around 100 hours DOT becomes limiting in each process (end of grey highlighted part)

Table 4-13: Statistical analyses of CER using the Bonferoni post-hoc test. In which; SEM is standard error of means, LCL is lower confidence limit and UCL is upper confidence limit.

	Mean Diff.	SEM	t-Value
200-400 rpm vs 100-400 rpm	0.53587	0.03121	17.17225
300 rpm vs 200-400 rpm	-0.47141	0.03146	-14.98486
400 rpm vs 200-400 rpm	-0.47326	0.03572	-13.24876
	P-Value	LCL	UCL
200-400 rpm vs 100-400 rpm	6.99E-35	0.4523	0.61943
300 rpm vs 200-400 rpm	1.19E-29	-0.55566	-0.38716
400 rpm vs 200-400 rpm	2.37E-25	-0.56892	-0.3776

Table 4-14: Statistical analyses of R.Q. using the Bonferoni post-hoc test. In which; SEM is standard error of means, LCL is lower confidence limit and UCL is upper confidence limit.

	Mean Diff.	SEM	t-Value
200-400 rpm vs 100-400 rpm	0.3645	0.13211	2.75916
300 rpm vs 200-400 rpm	-0.48345	0.13318	-3.63005
400 rpm vs 200-400 rpm	-0.92722	0.15122	-6.1315
	P-Value	LCL	UCL
200-400 rpm vs 100-400 rpm	0.03964	0.01072	0.71828
300 rpm vs 200-400 rpm	0.00241	-0.8401	-0.12679
400 rpm vs 200-400 rpm	5.48E-08	-1.33219	-0.52225

4.2.3 Agitation and its effect on oxidative stress related biomarkers

Figure 4-7 (A) and (B) show the effect of different agitation speeds on the oxidative stress related enzymes, SOD and CAT respectively. Figure 4-7 (A) shows two distinct trend characteristics. The first trend was observed during the 100-400 rpm process with peak SOD activities in the first 50 hours and in the last 50 hours of around 1500 U/g DCW and 1250 U/g DCW respectively, while in the mid exponential phase SOD activities are very low. The other processes presented in this chapter have low initial SOD activities, while during mid exponential phase their maximum activities are reached. These activities are the highest for the 200-400 rpm (around 3600 U/g DCW) process and have the lowest values for the 400 rpm process (around 500 U/g DCW) respectively. Another interesting observation that can be made from this graph is that, when maximum SOD values are reached during the mid exponential phase (50 to 100 hours), the plateau of these values decrease when the initial agitation rate (first 24 hours) is increased, from 200 to 300 to 400 rpm.

The statistical analyses showed that all processes were significantly different from the 200-400 rpm process of which the 400 rpm process had the largest effect on SOD activity during cultivation of *A. niger B1-D* (two-way ANOVA with Bonferoni post-hoc test, $p < 0.05$, Table 4-15).

The variation of agitation settings, in the first 24 hours, results in higher CAT activities, with maximum values ranging from 2000 U/g DCW, for the 100-400 rpm process, to 5000 U/g DCW, for the 400 rpm process (Figure 4-7 (B)). All processes had peak values at the end of the fermentations.

The two way ANOVA showed that results were significantly different from each other ($p < 0.05$). The Bonferoni post-hoc test showed that all processes were significantly different compared to the 200-400 rpm process and that 400 rpm agitation setting had the largest effect on CAT values during cultivation of *A. niger B1-D* (largest mean difference, Table 4-16).

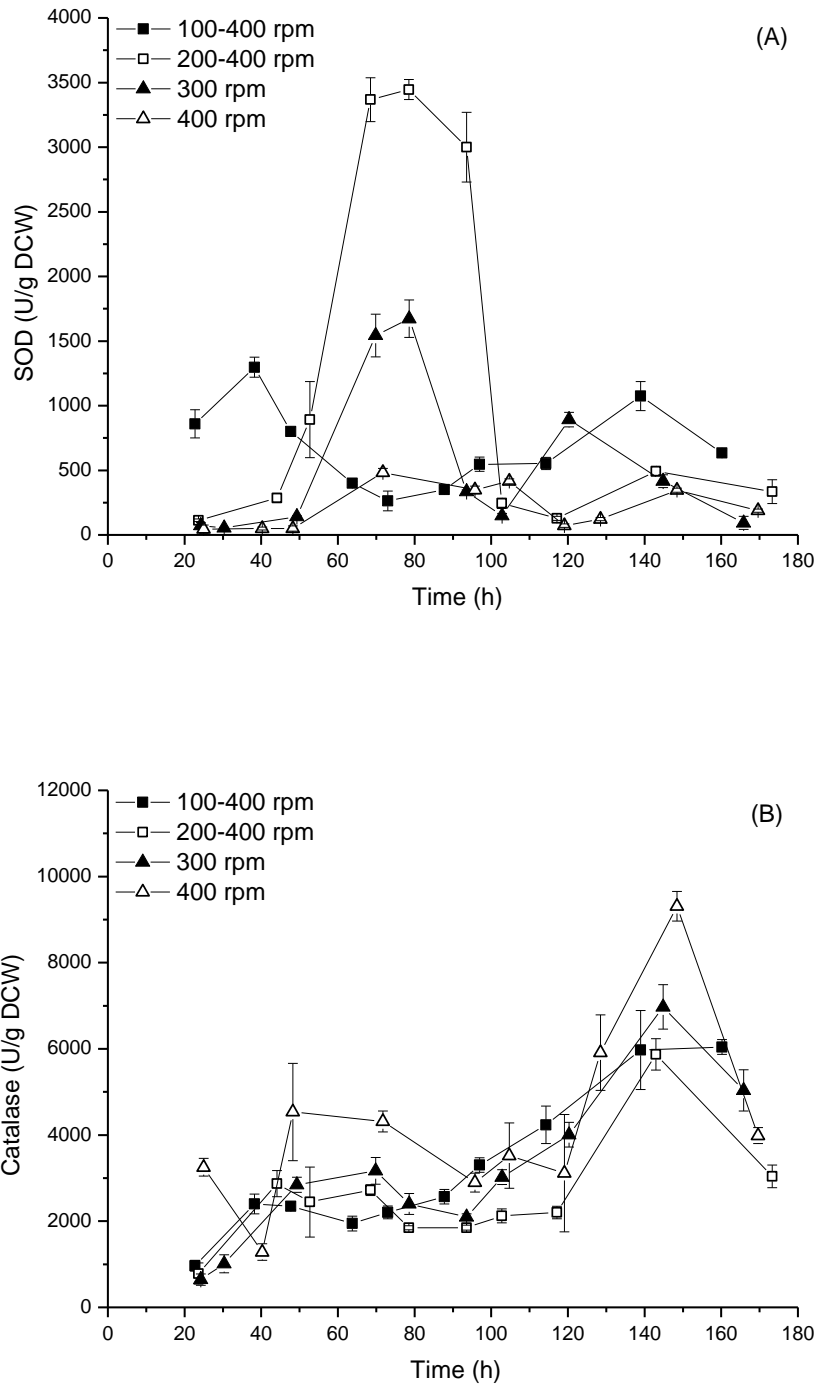


Figure 4-7: (A) SOD (U/g DCW) and (B) CAT (U/g DCW) during batch cultivation in a STR of *A. niger* B1-D.

Various agitation settings were used. Various agitation settings were used. Cultivation conditions were: airflow 2 lpm, pH 4, temperature 25 °C. Results are expressed as mean \pm stdev.

Table 4-15: Statistical analyses of SOD using the Bonferoni post-hoc test. In which; SEM is standard error of means, LCL is lower confidence limit and UCL is upper confidence limit.

	Mean Diff.	SEM	t-Value
200-400 rpm vs 100-400 rpm	611.71904	55.38648	11.04456
300 rpm vs 200-400 rpm	-623.58387	55.38648	-11.25877
400 rpm vs 200-400 rpm	-1018.6431	63.9548	-15.92755
	P-Value	LCL	UCL
200-400 rpm vs 100-400 rpm	5.23E-20	463.49014	759.94795
300 rpm vs 200-400 rpm	1.46E-20	-771.81277	-475.35496
400 rpm vs 200-400 rpm	1.86E-32	-1189.8031	-847.48309

Table 4-16: Statistical analyses of CAT using the Bonferoni post-hoc test. In which; SEM is standard error of means, LCL is lower confidence limit and UCL is upper confidence limit.

	Mean Diff.	SEM	t-Value
200-400 rpm vs 100-400 rpm	-384.73486	139.74179	-2.75318
300 rpm vs 200-400 rpm	504.25448	139.74179	3.60847
400 rpm vs 200-400 rpm	1529.11016	161.35992	9.47639
	P-Value	LCL	UCL
200-400 rpm vs 100-400 rpm	0.04011	-758.72097	-10.74876
300 rpm vs 200-400 rpm	0.00257	130.26837	878.24058
400 rpm vs 200-400 rpm	5.49E-16	1097.2682	1960.95211

4.2.4 Agitation and its effect on intracellular protein content and viability

Figure 4-8 shows the effect of different agitation speeds on intracellular protein content during cultivation of *A. niger B1-D*. Until around 60 hours all processes show an increase in intracellular protein content, after this time intracellular protein contents fluctuates between 110 and 130 mg/g DCW for the 100-400 rpm process, barring a sudden drop at around 90 hours, and decrease for the 300 and 400 rpm processes. The 300 and 400 rpm process had intracellular protein values from 90 hours onwards at around 50 mg/g DCW. The 200-400 has increasing intracellular protein content until around 80 hours, after which values remain stable, at around 160 mg/g DCW. All processes had big drops in intracellular protein content after 150 hours into the process.

Statistical analyses showed that results were significantly different (two-way ANOVA, $p < 0.05$). All processes were significantly different compared to the 200-400 rpm process (Bonferoni post-hoc test) of which 300 rpm had the largest effect on intracellular protein content (largest mean difference, Table 4-17).

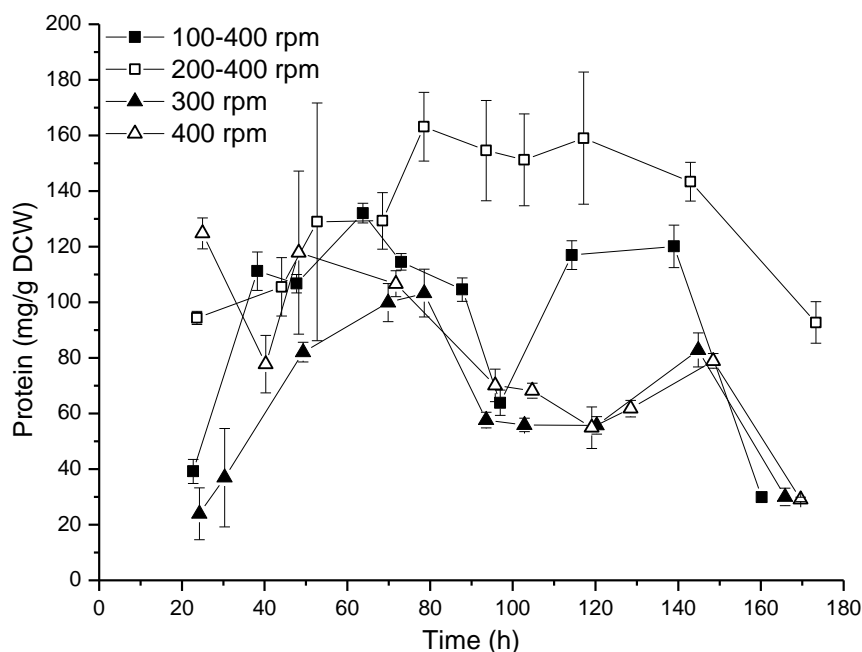


Figure 4-8: Intracellular protein content (mg/g DCW) during batch cultivation in a STR of *A. niger* B1-D.

Various agitation settings were used. Various agitation settings were used. Cultivation conditions were: airflow 2 lpm, pH 4, temperature 25 °C. Results are expressed as mean ± stdev.

Table 4-17: Statistical analyses of intracellular protein content using the Bonferoni post-hoc test. In which; SEM is standard error of means, LCL is lower confidence limit and UCL is upper confidence limit.

	Mean Diff.	SEM	t-Value
200-400 rpm vs 100-400 rpm	45.54572	3.55277	12.81978
300 rpm vs 200-400 rpm	-66.54719	3.55277	-18.73108
400 rpm vs 200-400 rpm	-54.56061	4.10238	-13.29973
	P-Value	LCL	UCL
200-400 rpm vs 100-400 rpm	1.35E-24	36.03756	55.05387
300 rpm vs 200-400 rpm	3.47E-39	-76.05534	-57.03904
400 rpm vs 200-400 rpm	7.88E-26	-65.53967	-43.58154

Figure 4-9 shows viability results during these processes. The first 90 hours the 200-400 rpm process has higher viability values compared to the rest of the processes. This continues after 90 hours as well with a certain overlap of viability values with the 400 rpm process. The 100-400 rpm process has overall lower viability values compared to the other processes during the entire process time.

A two-way ANOVA showed that varying agitation rates had a significant effect on viability values during cultivation of *A. niger B1-D* (two-way ANOVA, $p < 0.05$). The Bonferoni post-hoc test showed that all processes were significantly different compared to the 200-400 rpm process and that the 100-400 rpm process had the largest effect on viability in this dataset (largest mean difference, see Table 4-18).

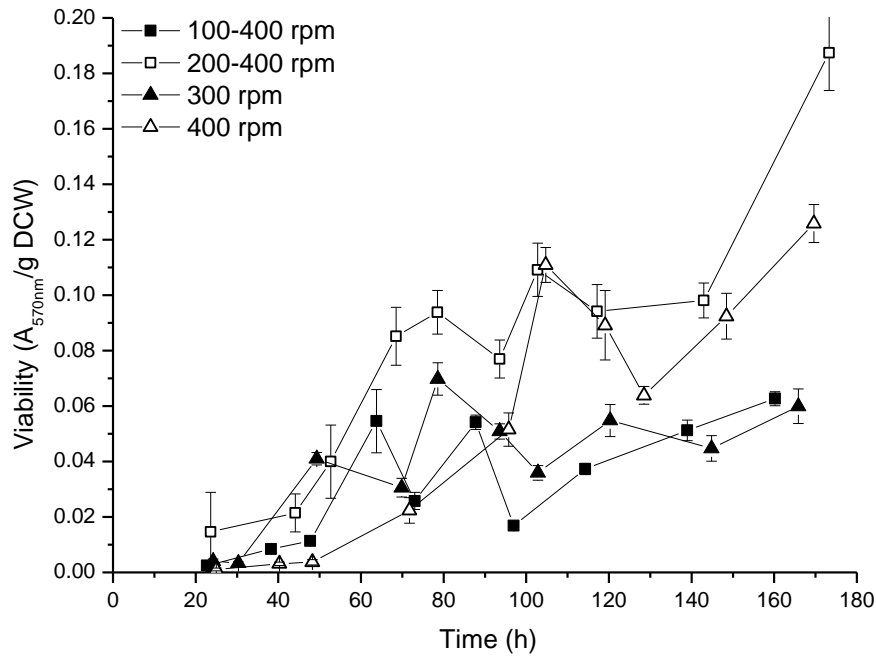


Figure 4-9: Viability (A_{570nm}/g DCW) during batch cultivation in a STR of *A. niger B1-D*.

Various agitation settings were used. Various agitation settings were used. Cultivation conditions were: airflow 2 lpm, pH 4, temperature 25 °C. Results are expressed as mean \pm stdev.

Table 4-18: Statistical analyses of Viability using the Bonferoni post-hoc test. In which; SEM is standard error of means, LCL is lower confidence limit and UCL is upper confidence limit.

Viability	Mean Diff.	SEM	t-Value
200-400 rpm vs 100-400 rpm	0.04577	0.00239	19.17401
300 rpm vs 200-400 rpm	-0.03693	0.00239	-15.47165
400 rpm vs 200-400 rpm	-0.02569	0.00276	-9.31977
	P-Value	LCL	UCL
200-400 rpm vs 100-400 rpm	3.27E-40	0.03938	0.05216
300 rpm vs 200-400 rpm	2.51E-31	-0.04332	-0.03054
400 rpm vs 200-400 rpm	1.37E-15	-0.03306	-0.01831

4.2.5 Overview of statistics

As many processes inside cells are linked and related to each other an overview table of all the statistical analyses was made to see if any of the measured physiological parameters corresponded with each. Results from this comparison are presented in Table 4-19.

Table 4-19: Statistical overview of all the tests done in this work.

Each result is a means comparison between the control experiment and an experiment where polymyxin B was added. Non-significant differences are represented with a 0 and significant differences are represented with 1. The Bonferroni also answers the question which experiment had the largest effect and that is presented as 1*. All tables with the specific data can be found in Appendix III.

Experiment	DCW	Glucose	Ammonium	OUR	CER	RQ	SOD	CAT	Protein	Lysozyme	Viability
200-400 rpm - 100-400 rpm	1	0	1	0	1*	1	1	1	1	1*	1*
300 rpm - 200-400 rpm	0	1	0	0	1	1	1	1	1*	1	1
400 rpm - 200-400 rpm	0	1*	1*	1	1	1*	1*	1*	1	1	1*

Experiment	Specific growth rate	GCR	ACR
200-400 rpm - 100-400 rpm	1*	0	1*
300 rpm - 200-400 rpm	1	1	1
400 rpm - 200-400 rpm	1	1*	0

4.3 Discussion

4.3.1 Agitation and its effect on biomass formation, carbon consumption and nitrogen consumption

Previous research showed that increased oxidative stress conditions can inhibit growth rate of biomass in reactors and also increase the lag phase during fungal fermentation (Li *et al.*, 2010b). Pinheiro *et al.*, (2000) used air pressure to try and improve the oxygen transfer, thereby hoping to improve biomass yield utilising two *Kluyveromyces* strains, which succeeded. The tested pressures were 2, 4 and 6 bar and while the 2 and 4 bar processes led to increased biomass growth, the 6 bar process led to a decrease in maximum biomass again (Pinheiro *et al.*, 2000). The same paper also points towards a *Pseudomonas fluorescens* strain in which growth was completely inhibited at elevated reactor pressures (Pinheiro *et al.*, 2000). Belo *et al.*, (2003) showed that an increase in reactor pressure already had an inhibiting effect on biomass growth, utilising *Saccharomyces cerevisiae*, at pressures of 3.2 to 5 bar. Shahrianiour *et al.*, (2011) used *Aspergillus terreus* in a bioreactor testing optimum growth conditions and found that elevated concentrations of DOT resulted in lower biomass formation (was set as a control DOT). All of these papers suggest that the response to extra oxygen inside the bioreactor can inhibit biomass growth, which is exactly what can be seen in Figure 4-2.

The statistical analyses presented here are not as expected. Figure 4-2 clearly shows very distinct differences when comparing the 100-400 and 400 rpm processes to the 200-400 rpm process. The statistical analysis only shows the 100-400 rpm process to be significantly different compared to the 200-400 rpm process. This result could be explained by the calculations itself. The Bonferoni post hoc test will reduce all values to a single mean difference value and then compare these mean difference values with each other for significance. As this happens differences between different

processes that only occur in a few points might not lead to a significant difference between datasets. In the 400 rpm process it can be clearly seen that the biomass concentrations are only different from 40 hours to around 80 hours. This might explain the results obtained for this post-hoc test.

As described previously (Chapter 3.3) fungi use diffusion for glucose uptake at high concentrations and need ATP for ammonium uptake (Carlile and Watkinson, 1997). When oxidative stress is increased, in this case by the increased stirring rate, more ATP is most likely spent on oxidative stress defence mechanisms to cope with the increased ROS generation, which can decrease ammonium uptake that also results in the same effect for glucose uptake. This is confirmed by increased CAT activity shown in Figure 4-7 (B). Previous research has also shown that oxidative stress can inhibit glucose-6-phosphate dehydrogenase which is a key enzyme in the pentose phosphate pathway thereby reducing glucose and ammonium uptake (Yu *et al.*, 2004, Li *et al.*, 2008a).

The effects of agitation setting, during the lag phase of the process, on biomass growth, glucose uptake and ammonium uptake are most likely caused by oxidative stress, which is confirmed by increased CAT activities and increased SOD activities.

4.3.2 Agitation and its effect on dissolved oxygen tension (DOT) and respiration

The slower decrease in DOT presented in Figure 4-5 (A) shows that the increased OTR, caused by the higher agitation setting at the start of the fermentation, replenishes the dissolved oxygen concentrations more quickly in bioreactor. This results in increased OUR values as shown in Figure 4-5 (B). A similar result was also obtained by Li *et al.*, (2002), by increasing rpm and monitoring DOT and OUR during fermentation of *Aspergillus oryzae*. The results obtained in this chapter show that increasing the agitation rate

resulted in a slower decrease of DOT during the fermentations. This is an effect that wasn't measured in the previously mentioned paper (Li *et al.*, 2002). The slower decrease is very likely a result of oxidative stress, as *A. niger* has to deal with more oxygen, oxidative stress defence mechanisms are in use thereby using a larger part of the ATP pool resulting in a slower growth rate and a slower decrease of DOT.

CER values show that the 200-400 rpm process has higher CER values during the first 60 hours. However this high peak wasn't reproduced when the process was repeated (see appendix II). The lower CER values, after 60 hours into the process, for the 100-400 rpm setting are most likely due to oxygen limitation (Li *et al.*, 2002, Wang *et al.*, 2005). This was also confirmed by the fast drop in DOT values Figure 4-5 (A), the very low OUR values (Figure 4-5 (B)) and the non significant GCR and glucose values (compared to the 200-400 rpm process). Another measurement that confirms oxygen limitation in the 100-400 rpm process is ammonium uptake which slows down as soon as DOT values become zero. According to literature ammonium uptake is an active process that requires ATP (Carlile and Watkinson, 1997). This also coincides with R.Q. values dropping very fast in the first 60 hours of the process Figure 4-6 (B).

The high R.Q. values, first 60 hours of the 100-400 rpm process, show that respiration of *A. niger* is likely more efficient than the other processes as similar amounts of CO₂, compared to the other processes is produced, with less oxygen (shown by the lower OUR values). The 200-400 rpm process has higher R.Q. values during the entire process, which also resulted in higher intracellular protein content and lysozyme production. This result seems to confirm that even though the 100-400 rpm process has lower oxidative stress levels, shown by SOD and CAT values (Figure 4-7); enough oxygen is still required to drive cellular processes that are needed to produce in this case lysozyme. The other processes seem to be affected by higher oxidative stress levels resulting in, less formation of lysozyme, which has

also been confirmed by previous research (Bai *et al.*, 2004, O'Donnell *et al.*, 2011).

4.3.3 Agitation and its effect on oxidative stress related biomarkers

As mentioned before the first 48 hours of the processes the OTR was varied by different agitation settings. The SOD results clearly show oxidative stress levels that are unfavorable during the lag phase of the fermentation, as there are very low levels of SOD activity for the 200-400, 300 and 400 rpm process. However the 100-400 rpm process has significantly higher levels of SOD activity during this phase of the process. This very clearly shows oxidative stress levels that inhibit SOD activities, most likely caused by oxidative stress levels that are too high, during the lag phase of the 200-400, 300 and 400 rpm processes, as explained previously (Chapter 3.3) Ayar-Kayali showed this as well using the organism *F. equiseti* (Ayar-Kayali and Tarhan, 2004). Previous research attributes higher SOD activity levels to oxidative stress, due to the higher concentration of oxygen radicals (in the case of this chapter caused by higher OTR values) (Bai *et al.*, 2003). The apparent sensitivity of SOD to higher OTR values makes SOD a very good indicator to study whether the process is running at an optimum level, however because of the sensitive nature of this enzyme it would be advisable to use CAT as an indicator as well as this enzyme seems to be more stable during all processes observed in this chapter. This apparent stability is likely a result of its sensitivity to the superoxide anion instead of H₂O₂ (Pigeolet *et al.*, 1990, Jakubowski *et al.*, 2000), as H₂O₂ is a more stable molecule oxidative stress should affect SOD more than CAT, which is more sensitive to the superoxide anion.

CAT levels increase with higher OTR levels at the beginning of the process; however no apparent inhibition was noticed in this dataset, which seemingly makes CAT a lot more stable to changes in OTR and therefore higher oxidative stress levels, however both enzymatic measurements confirm more oxidative stress when agitation rate is increased at the start (first 48 hours) of

the fermentation, which might contribute to the bad process outcomes in this dataset (a decrease in lysozyme production).

At a certain moment all processes, barring the 300 rpm process, reach the same agitation rate. It would seem logical that at this stage of the process SOD and CAT activity levels would converge again to levels that correspond with the same agitation setting (400 rpm). Literature indicates oxidative stress is able to damage cell components (see Chapter 1 for a background). The result of that is shown in Figure 4-7 (A) and (B), which indicates permanent damage to the organism. However the review by Wang indicates that even though biomass growth still takes place at higher agitation settings pellets are being destroyed by the high shear rate resulting in inactive biomass (Wang *et al.*, 2005). The review doesn't go into how this inactivity is defined, but results here clearly show biomass is still active it just seems occupied preventing more damage from oxidative stress.

Both SOD and CAT seem to cope with oxidative stress levels better at a lower rpm setting in which the 100-400 rpm process indicates on optimum from an oxidative stress point of view, which also would explain the faster growth rate during the first 48 hours of the process.

4.3.4 Agitation and its effect on intracellular protein content, lysozyme production and viability

The effect of oxidative stress on intracellular protein content in *A. niger B1-D* gives a mixed image. Adding polymyxin B with the aim of blocking NADH dehydrogenase resulted in higher or similar intracellular protein content (chapter 3 and (Voulgaris *et al.*, 2012)). While sparging enriched oxygen into the reactor resulted in lower intracellular protein content (O'Donnell *et al.*, 2011). Protein carbonylation has been shown to be a major damage mechanism in *A. niger* to a point where damaged proteins weren't removed by proteolysis anymore (Li *et al.*, 2008d). The results obtained in this chapter

do indicate that the increased OTR at the start of the fermentation results in oxidative stress; resulting in less intracellular protein content. This is also confirmed by the SOD and CAT values (Figure 4-7 (A and B)).

Lysozyme values follow a similar trend as the protein values, caused by most likely the same reasons as mentioned previously, when looking at the protein content values. Further evidence of the effect of agitation rate is mentioned in previous research; using an *Aspergillus oryzae* fungal strain (Li *et al.*, 2002) showed that varying agitation speed had a big effect on enzyme activity the older the culture became. The higher agitation setting could result in up to 20% lower enzyme yield. The paper however gives a different explanation as to why this is caused going more into heat dissipation at higher agitation settings and viscosity of the fermentation broth over the entire process instead of the evidence presented here that suggest agitation settings can also result in a severe oxidative shock at the initial phase of the process, which can affect process outcomes.

The viability results, shown in Figure 3-10, seem to indicate that increasing the agitation at the start of a fermentation results in mitochondrial inhibition that lasts the entire fermentation, compared to the 200-400 rpm process. This result corresponds very well with the R.Q. values, which were lower, compared to the 200-400 rpm process as well. Both viability and R.Q. values are an indication of mitochondrial activity and oxidative stress has been known to oxidize the complexes of the mitochondria (Qin *et al.*, 2011), which would explain the lower viability and R.Q. values.

4.4 Conclusions

Two conclusions can be drawn from the results presented here. The first one is that OTR, varied by agitation rate, can result in too much oxidative stress, thereby decreasing the production of lysozyme. This was confirmed by the slower increase in biomass, slower glucose and ammonium uptake,

increased CAT activity, decreased SOD activity for the 100-400, 300 and 400 rpm process, increased OUR, decreased CER, decreased R.Q. and decreased viability. The second conclusion is that for the system (Chapter 3) and strain utilised in this chapter an optimum rpm setting is 200-400, when looking at lysozyme production.

Chapter 5

Nitric oxide and its interaction with oxidative stress defences in submerged cultures of *Aspergillus niger*

5 Nitric oxide and its interaction with oxidative stress defences in submerged cultures of *Aspergillus niger*

5.1 Introduction and aims

The control of dissolved oxygen tension (DOT) inside bioreactors during fermentation has been shown to lead to oxidative stress which can lead to undesirable process outcomes such as; low growth rate and decreased secretion of proteins (O'Donnell *et al.*, 2011). In recent years extensive knowledge has been accrued on oxidative stress in filamentous fungi (see Chapter 2); (Li *et al.*, 2009, Lushchak, 2011). However recent publications have shown that catalase (CAT); (one of the main anti-oxidative enzymes) is also capable to scavenge for peroxynitrite (ONOO⁻) in a chemically defined system as well as in a biological system using *Saccharomyces cerevisiae* (Sahoo *et al.*, 2009, Gebicka and Didik, 2009).

Reactive oxygen species (ROS) are formed when oxygen is progressively reduced into water (for details see chapter 1.1). The reactivity of the superoxide anion (⁻O₂) with non-radical species is less when comparing it with the hydroxyl radical ([•]OH). ⁻O₂ does however react very rapidly with some other radicals such as nitric oxide (NO); (Wojtaszek, 1997, Chiang *et al.*, 2000).

Intracellular NO is considered to be a signalling molecule involved in processes such as smooth muscle relaxation, inhibition of platelet aggregation, neural communication and immune regulation in mammalian cells. In plant cells NO has been linked to disease resistance, a biotic stress, cell death, respiration, senescence, root development and seed germination (Crawford and Guo, 2005, Wendehenne *et al.*, 2001). In fungi it has been suggested that NO can be synthesized by nitric oxide synthase (NOS) type enzymes (Li *et al.*, 2010a), which is a two-step process that involves the

oxidation of the terminal guanidine nitrogen of L-arginine resulting in the formation of L-citrulline and NO (Zaki *et al.*, 2005). Another source of NO could be cytochrome c oxidase, because this enzyme reduces NO₂ to NO at low-oxygen concentrations (Li *et al.*, 2010a).

ONOO⁻ is one of the reactive nitrogen species (RNS) that can be formed along with ROS. ONOO⁻ is formed when O₂⁻ reacts with NO according to the reaction described in Chapter 2.2 (Brown *et al.*, 2009). Other RNS that can be formed are dinitrogen trioxide (N₂O₃), S-nitrosoglutathione (GSNO), nitrogen dioxide (NO₂) and the nitrosyl cation (NO⁺) (Poole, 2005, Valderrama *et al.*, 2007).

NO and RNS are capable of modifying proteins and other biological important molecules by nitration thereby altering their function, and this can irreversibly damage cells (Gebicka and Didik, 2009). Toxic effects may also arise from the inhibition of key enzymes including terminal oxidases and Fe-S centres in enzymes such as aconitase (Poole, 2005). All these effects arise when cells are exposed to a sustained higher concentration of NO, which is called nitrosative stress (see Chapter 1).

Most research focused on nitrosative stress has been carried out in the field of immunology to study the reaction of fungal pathogens to the host's immune armoury (Brown *et al.*, 2009, de Jesus-Berrios *et al.*, 2003), which consists of a burst of RNS and ROS to destroy pathogens. Because activated macrophages have the ability to produce NO and O₂⁻ it has been proposed that OONO⁻ is the most extreme RNS that can be generated by the immune response (Chiang *et al.*, 2000).

The majority of research use NO-donors as a research tool to expose cells to NO. Various NO-donors such as hydroxy urea (Huang *et al.*, 2004) and sodium nitrite (Lundberg and Weitzberg, 2005) have been identified in literature. Sodium nitroprusside (SNP) however seems to be the most generally accepted and widely used NO-donor in the field of nitrosative stress research (Li *et al.*, 2010a, Bhattacharjee *et al.*, 2010, Xu *et al.*, 2011). When

NO is released it can form nitrite under aerobic conditions, which can be easily measured utilising The Griess reaction (for the conversion of NO into nitrite Chapter 2.3) (Bryan and Grisham, 2007).

In filamentous fungi CAT and superoxide dismutase (SOD) are directly involved in the defence against $\cdot\text{O}_2^-$ and hydrogen peroxide (Kreiner *et al.*, 2003). These two enzymes are also one of the most studied anti oxidative stress enzymes in filamentous fungi (Abrashev *et al.*, 2005, Angelova *et al.*, 2000, Bai *et al.*, 2003, Buckova *et al.*, 2005, Kreiner *et al.*, 2003). $\cdot\text{O}_2^-$ can react with NO to form ONOO $^-$, which in *S. cerevisiae* has been shown to be scavenged by CAT (Sahoo *et al.*, 2009). However no studies have been found that show a dose-time response of these enzymes to NO in a fermentation system utilising a fungal strain.

Various organisms such as; *S. cerevisiae*, *Candida minitans*, *Escherichia coli*, *Apergillus niger*, *Monilinia fructicola*, *Penicillium italicum* have not only shown that there is a sensitivity to nitrosative stress but, also an interactive nature of oxidative and nitrosative stress however, most studies have been carried out on agar plates or in shake flasks (Bhattacharjee *et al.*, 2010, Brandes *et al.*, 2007, Lazar *et al.*, 2008, Li *et al.*, 2010a). Since a fermentation system provides for much better control of growth conditions a clearer quantitative assessment of the interaction between nitrosative stress and oxidative stress defences in fungi should arise. As currently the interactive nature between oxidative and nitrosative stress is not clear an added effect could be the potential of decreasing oxidative stress inside bioreactors thereby improving process outcomes. In case of the results presented here that would mean an improved yield of lysozyme as the organism of choice was *A. niger B1-D*.

5.1.1 Aims

As there is little published information on the effects of nitric oxide on the cultivation of *A. niger B1-D* this study had a three-fold aim.

In support of the reactor studies, performed in this chapter, a series of shake flask experiments were done to determine a proper concentration range and a suitable choice for an NO-donor. Selection criteria for the proper NO-donor were; effect on biomass growth and how common the NO-donor is used in literature as it would make comparison with available literature easier.

The primary aim of this study was to observe the effects of increasing amounts of the selected NO-donor on SOD and CAT activities in a bioreactor and to see if they corresponded with other physiological parameters of *A. niger B1-D* commonly measured during cultivation in bioreactors.

5.2 Results

5.2.1 Growth experiments using sodium nitrite, hydroxy urea and SNP

Figure 5-1 shows DCW values and how the addition of increasing amounts of sodium nitrite affects those values. The addition of sodium nitrite to a final concentration of 150, 250 and 350 μM clearly results in the inhibition of biomass growth during the lag phase of these experiments. While the 250 μM^* experiment (where additions of sodium nitrite were done every 24 hours until 120 hours into the experiment) showed a complete inhibition of biomass growth until 150 hours into the experiment after which growth started resulting in a final DCW value that was similar to the control experiment of around 13 g/l. Statistical analyses showed that all experiments were significantly different compared to the control with the 250 μM^* experiment having the largest effect based on mean difference (Two-way ANOVA with Bonferroni post-hoc test, $p < 0.05$, see Table 5-1).

Figure 5-2 shows the growth curves obtained using hydroxy urea. The addition of increasing amounts hydroxy urea results in differences, compared to the control experiment, at the start of that stationary phase at around 120 hours. The control experiment had a constant DCW of around 12 g/l and the experiments where hydroxy urea was added fluctuated substantially around this value. The experiment where hydroxy urea was added every day to a final concentration of 250 μM (250 μM^*) showed a substantial decrease in DCW as soon as the addition of hydroxy urea was halted, this was at 120 hours. Statistical analyses, using a two-way ANOVA, of DCW results showed that there were significant differences in this experimental series ($p < 0.05$). The Bonferroni post-hoc test showed that the 250 μM^* experiment was significantly different from the control experiment while the other experiments weren't (Table 5-2).

In Figure 5-3 the results of the study using SNP are shown. The DCW values using SNP show a similar trend compared to the hydroxy urea experiments, meaning fluctuations at the start of the stationary phase. The two-way ANOVA showed that results were significantly different after which the post-hoc test (Bonferroni) showed that the 250 μM^* experiment had the largest effect on DCW values of *A. niger B1-D* ($p < 0.05$, Table 5-3).

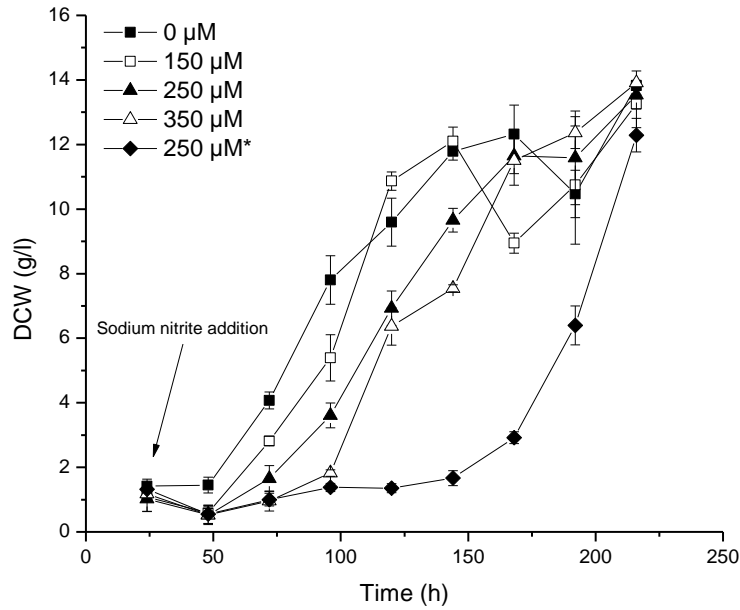


Figure 5-1: DCW (g/l) during shake flask cultivation of *A. niger* B1-D. Cultivation conditions were: 200 rpm, pH 4 and 25 °C. At 24 hours sodium nitrite was added to a final concentration of 150, 250 and 350 μM, whereby 250 μM* meant adding sodium nitrite every 24 hours until 120 hours. Results are expressed as mean ± standard deviation (stdev).

Table 5-1: Statistical analyses of DCW of the sodium nitrite series using the Bonferoni post-hoc test. In which; SEM is standard error of means, LCL is lower confidence limit and UCL is upper confidence limit.

	Mean Diff.	SEM	t-Value
150 μM vs. control	-0.72099	2.13E-01	-3.38625
250 μM vs. control	-1.3642	2.13E-01	-6.4072
350 μM vs. control	-1.61802	0.21292	-7.59935
250* μM vs. control	-3.15136	0.21292	-14.8009
	P-Value	LCL	UCL
150 μM vs. control	0.01052	-1.33374	-0.10824
250 μM vs. control	6.63E-08	-1.97695	-0.75145
350 μM vs. control	2.71E-10	-2.23077	-1.00528
250* μM vs. control	7.67E-25	-3.76411	-2.53861

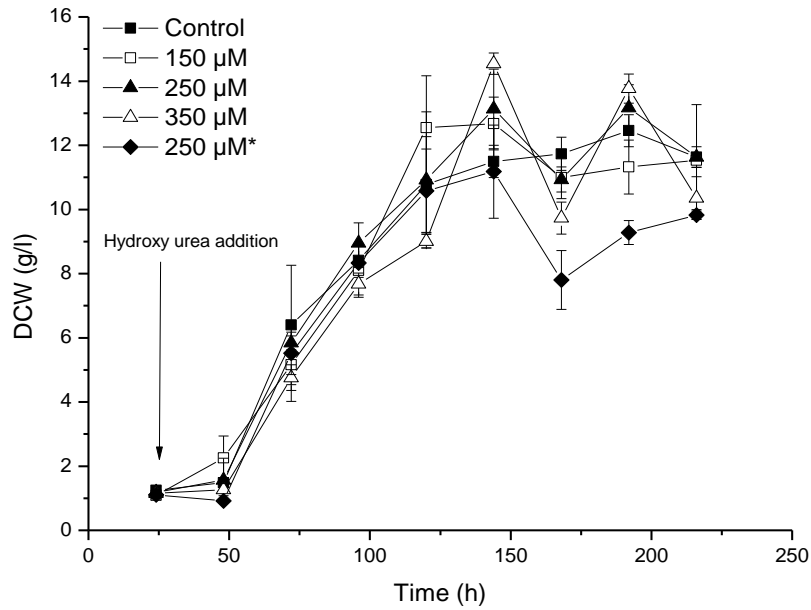


Figure 5-2: DCW (g/l) during shake flask cultivation of *A. niger* B1-D. Cultivation conditions were: 200 rpm, pH 4 and 25 °C. At 24 hours hydroxy urea was added to a final concentration of 150, 250 and 350 μM, whereby 250 μM* meant adding hydroxy urea every 24 hours until 120 hours. Results are expressed as mean ± standard deviation (stdev).

Table 5-2: Statistical analyses of DCW of the hydroxy urea series using the Bonferoni post-hoc test. In which; SEM is standard error of means, LCL is lower confidence limit and UCL is upper confidence limit.

	Mean Diff.	SEM	t-Value
150 μM vs. control	-0.28617	0.19696	-1.45294
250 μM vs. control	-0.3287	0.19696	-1.66888
350 μM vs. control	-0.3537	0.19696	-1.7958
250* μM vs. control	-1.03574	0.19696	-5.2586
	P-Value	LCL	UCL
150 μM vs. control	1	-0.853	0.28066
250 μM vs. control	0.98617	-0.89554	0.23813
350 μM vs. control	0.75881	-0.92054	0.21313
250* μM vs. control	9.72E-06	-1.60257	-0.46891

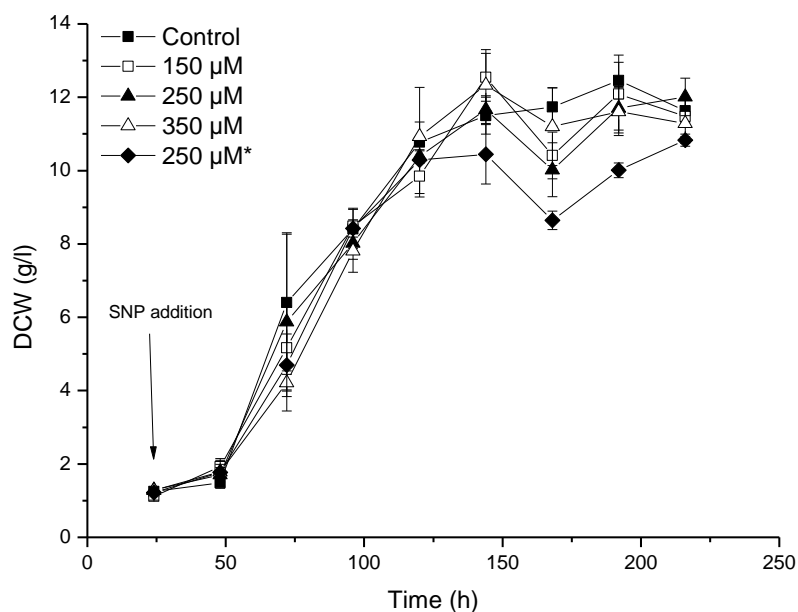


Figure 5-3: DCW (g/l) during shake flask cultivation of *A. niger* B1-D. Cultivation conditions were: 200 rpm, pH 4 and 25 °C. At 24 hours SNP was added to a final concentration of 150, 250 and 350 μM, whereby 250 μM* meant adding SNP every 24 hours until 120 hours. Results are expressed as mean ± standard deviation (stdev).

Table 5-3: Statistical analyses of DCW of the SNP series using the Bonferoni post-hoc test. In which; SEM is standard error of means, LCL is lower confidence limit and UCL is upper confidence limit.

	Mean Diff.	SEM	t-Value
150 μM vs. control	0.72	0.21241	3.3896
250 μM vs. control	1.04	0.21241	4.89608
350 μM vs. control	1.1	0.21241	5.17855
250* μM vs. control	0.96	0.21241	4.51946
	P-Value	LCL	UCL
150 μM vs. control	0.01003	0.11023	1.32977
250 μM vs. control	3.76E-05	0.43023	1.64977
350 μM vs. control	1.16E-05	0.49023	1.70977
250* μM vs. control	1.70E-04	0.35023	1.56977

5.2.2 Reactor experiments for studying the effect of SNP on cultivation of *A. niger* B1-D

After the initial shake flask experiments a series of fermentations were done where SNP was chosen as the NO-donor. The reasons for choosing this NO-donor were:

- To measure NO release the Griess reaction was used this made sodium nitrite unsuitable as an NO-donor, because nitrite is released into the medium.
- The reason for not using hydroxy urea was that there seemed to be more literature available on nitrosative stress using SNP so therefore it would be easier to compare results obtained in this chapter with experimental results already published. As all NO-donors had an effect on DCW results SNP was chosen to be utilised in the reactor experiments.

5.2.2.1 Analyses of NO release

Figure 5-4 shows nitrite concentrations during cultivation of *A. niger* B1-D. Adding SNP in increasing concentrations (400, 700 and 1000 μM) during the processes results in a significant increase in nitrite concentrations (two-way ANOVA, $p < 0.05$, with Bonferroni post-hoc test; see Table 5-4), this corresponds to an increase in NO inside the reactor (one molecule of NO is converted into one molecule of nitrite, with the help of oxygen).

Adding 1000 μM of SNP shows the highest concentration of NO at 32.6 μM followed by 400 and 700 μM , which had maximum values of 11.6 and 15.5 μM respectively. In all experiments that involved SNP the maximum concentration of NO was reached between 55 to 75 hours (grey highlighted box) after which NO concentrations decreased. The control experiment, to which no SNP was added to the reactor, had concentrations of NO of up to 2 μM .

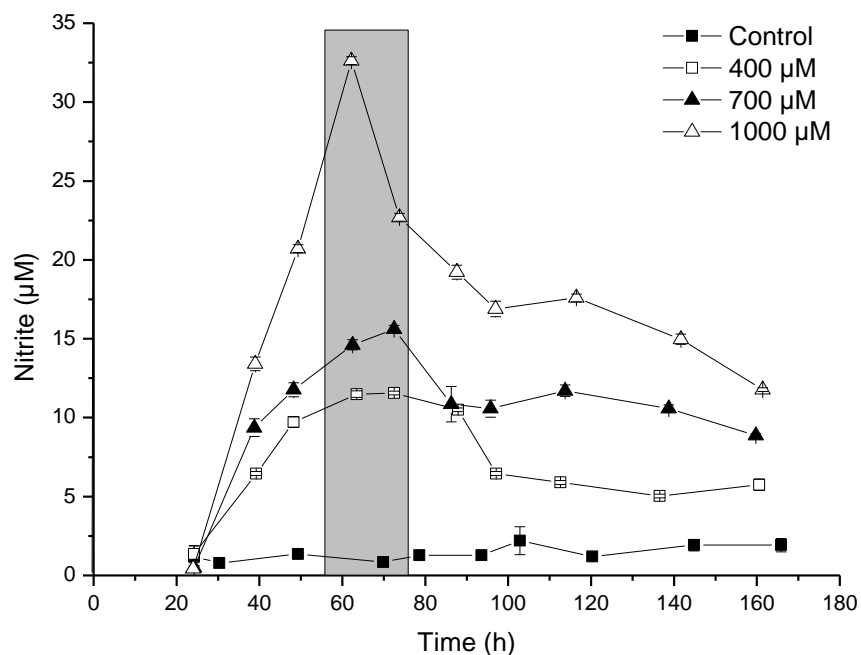


Figure 5-4: Nitrite concentration during batch cultivation in a stirred tank reactor of *A. niger* B1-D.

Various concentrations (see graph) of SNP were added at 24 hours. Cultivation conditions were: airflow 2 lpm, 300 rpm, pH 4, temperature 25 °C. The grey highlighted part represents maxima obtained. Results are expressed as mean ± stdev.

Table 5-4: Statistical analyses of nitrite using the Bonferoni post-hoc test. In which; SEM is standard error of means, LCL is lower confidence limit and UCL is upper confidence limit.

	Mean Diff.	SEM	t-Value
400 µM vs. Control	5.84058	0.19134	30.52453
700 µM vs. Control	8.78148	0.19134	45.8945
1000 µM vs. Control	15.07462	0.15623	96.49061
	P-Value	LCL	UCL
400 µM vs. Control	5.74E-63	5.3285	6.35266
700 µM vs. Control	1.76E-85	8.2694	9.29356
1000 µM vs. Control	3.60E-129	14.65651	15.49273

5.2.2.2 NO and its effect on biomass formation, carbon consumption and nitrogen consumption

Figure 5-5 shows the effect of SNP on DCW during fermentation of *A. niger* B1-D. The stationary phase for the control, 400 and 700 μM SNP experiments was reached at around 80 hours and at this point DCW values were around 12 g/l. The addition of 1000 μM SNP resulted in lower maximum DCW values. The stationary phase was reached later than the other batch cultures at around 100 hours, with a value of around 10 g/l of biomass. The statistical analyses showed that there was a significant difference in this dataset (two-way ANOVA, $p < 0.05$) and the Bonferroni post-hoc test showed that the 1000 μM SNP process was significantly different compared to the control experiment (Table 5-6).

Table 5-5 shows the effect of SNP on specific growth rate. The addition of SNP didn't result in a significant difference in growth rate for the whole experimental series. This was confirmed with a one-way ANOVA and Tukey's post-hoc test ($p > 0.05$) (Table 5-7).

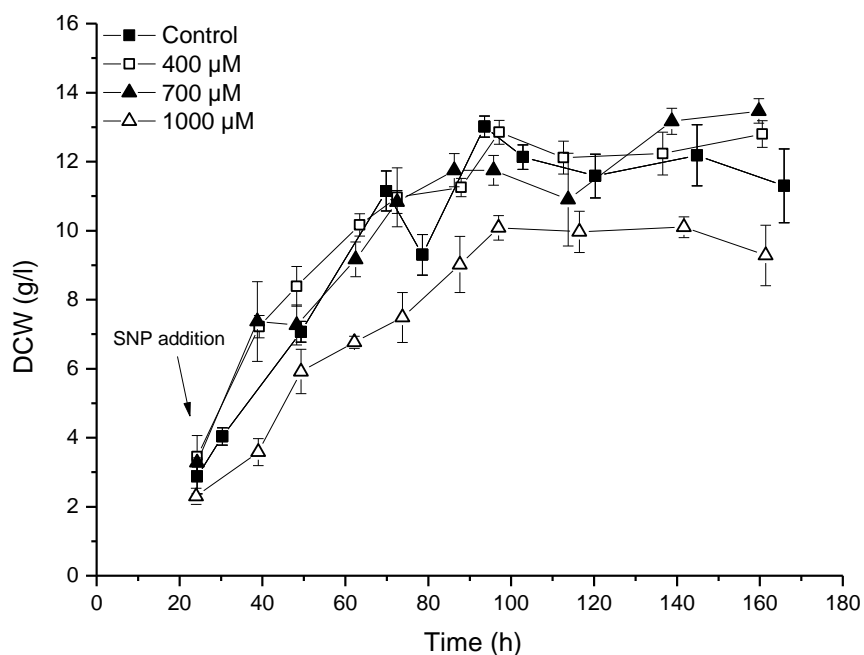


Figure 5-5: DCW (g/l) during batch cultivation in a STR of *A. niger B1-D*. Various concentrations (see graph) of SNP were added at 24 hours. Cultivation conditions were: airflow 2 lpm, 300 rpm, pH 4, temperature 25 °C. Results are expressed as mean ± stdev.

Table 5-5: Effect of SNP on specific growth rate during batch fermentations of *A. niger B1-D*. Cultivation conditions were: airflow 2 lpm, 300 rpm, pH 4, temperature 25 °C. Specific growth rate was determined from the linear part of the graph and is expressed as mean ± stdv.

Concentration SNP (μM)	Specific growth rate (h ⁻¹)
Control	0.022 ± 0.0030
400	0.019 ± 0.0032
700	0.021 ± 0.0007
1000	0.021 ± 0.0018

Table 5-6: Statistical analyses of DCW using the Bonferoni post-hoc test. In which; SEM is standard error of means, LCL is lower confidence limit and UCL is upper confidence limit.

	Mean Diff.	SEM	t-Value
400 μ M vs. Control	0.3425	0.17417	1.96647
700 μ M vs. Control	0.09306	0.17417	0.53428
1000 μ M vs. Control	-1.95222	0.14221	13.72782
	P-Value	LCL	UCL
400 μ M vs. Control	0.30733	-0.12363	0.80863
700 μ M vs. Control	1	-0.37307	0.55918
1000 μ M vs. Control	6.32E-27	-2.33281	-1.57163

Table 5-7: Statistical analyses of specific growth rate using the Tukey post-hoc test. In which; SEM is standard error of means, LCL is lower confidence limit and UCL is upper confidence limit.

	Mean Diff.	SEM	t-Value
400 μ M vs. Control	-0.00438	0.00151	4.0895
700 μ M vs. Control	-0.0025	0.00151	2.32921
1000 μ M vs. Control	-0.00328	0.00124	3.74855
	P-Value	LCL	UCL
400 μ M vs. Control	0.05138	-0.00878	2.24E-05
700 μ M vs. Control	0.38587	-0.0069	0.00191
1000 μ M vs. Control	0.07938	-0.00687	3.17E-04

Figure 5-6 and Table 5-8 show the effect of SNP on glucose concentrations and Glucose Consumption Rate (GCR) during fermentation of *A. niger B1-D*.

The addition of increasing amounts of SNP results in a slower decrease of glucose concentration, whereby the depletion of glucose in the control and 400 μM SNP experiment was around 90 hours. For the 700 and 1000 μM SNP experiment this point was reached at least 20 hours later. Analyses by two-way ANOVA showed a significant difference in results in Figure 5-6 ($p < 0.05$). The Bonferroni post-hoc test showed that addition of 700 and 1000 μM SNP resulted in significant differences when comparing these glucose concentrations with the control experiment. Looking at the mean differences showed that the 700 μM SNP experiment had the largest effect on residual glucose concentration (Table 5-9).

Analyses of GCR in Table 5-8 confirms results that have been shown in Figure 5-6 meaning that GCR values for the SNP processes were lower than the control experiment. Significance was tested by one-way ANOVA and using the Tukey post-hoc test to see where significance was. The one-way ANOVA showed a significant difference and the outcome of the Tukey test showed that only the 1000 μM SNP fermentation was significantly different ($p < 0.05$) compared to the control experiment (Table 5-10).

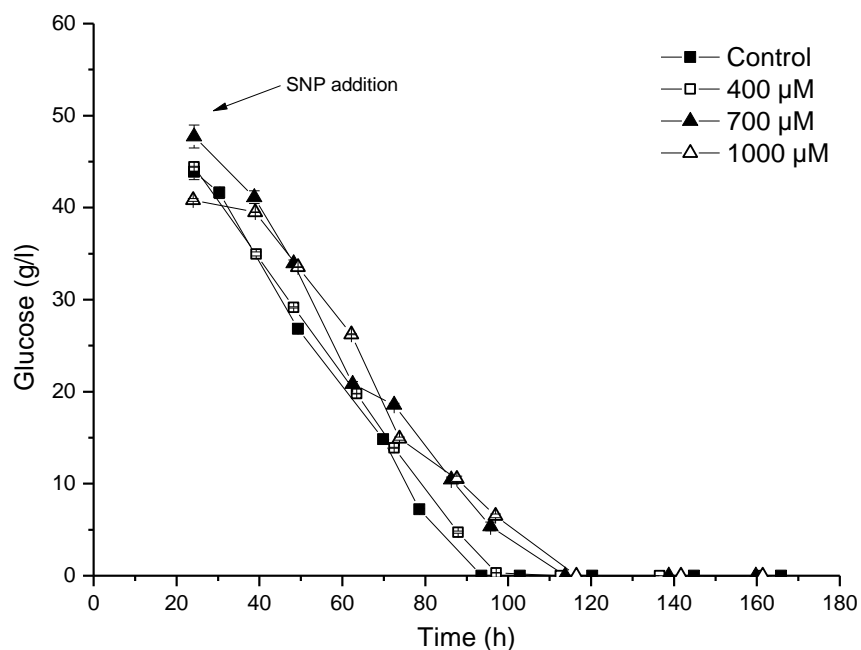


Figure 5-6: Residual glucose (g/l) during batch cultivation in a STR of *A. niger B1-D*.

Various concentrations (see graph) of SNP were added at 24 hours. Cultivation conditions were: airflow 2 lpm, 300 rpm, pH 4, temperature 25 °C. Results are expressed as mean ± stdev.

Table 5-8: Effect of SNP on GCR during batch fermentations of *A. niger B1-D*.

Cultivation conditions were: airflow 2 lpm, 300 rpm, pH 4, temperature 25 °C. GCR was determined from the linear part of the graph and is expressed as mean ± stdv.

Concentration SNP (μM)	GCR (g/l/h)
Control	0.63 ± 0.012
400	0.50 ± 0.003
700	0.53 ± 0.014
1000	0.44 ± 0.009

Table 5-9: Statistical analyses of residual glucose using the Bonferoni post-hoc test. In which; SEM is standard error of means, LCL is lower confidence limit and UCL is upper confidence limit.

	Mean Diff.	SEM	t-Value
400 μ M vs. Control	-1.02587	0.52554	-1.95201
700 μ M vs. Control	2.04254	0.52554	3.88652
1000 μ M vs. Control	1.7038	0.42911	3.97058
	P-Value	LCL	UCL
400 μ M vs. Control	0.3176	-2.43236	0.38063
700 μ M vs. Control	9.38E-04	0.63604	3.44904
1000 μ M vs. Control	6.85E-04	0.5554	2.8522

Table 5-10: Statistical analyses of GCR using the Bonferoni post-hoc test. In which; SEM is standard error of means, LCL is lower confidence limit and UCL is upper confidence limit.

	Mean Diff.	SEM	t-Value
400 μ M vs. Control	-0.06483	0.03179	2.88357
700 μ M vs. Control	-0.03437	0.03179	1.52897
1000 μ M vs. Control	-0.1129	0.02596	6.15046
	P-Value	LCL	UCL
400 μ M vs. Control	0.22063	-0.15724	0.02758
700 μ M vs. Control	0.70617	-0.12678	0.05804
1000 μ M vs. Control	0.0033	-0.18835	-0.03745

The effect of SNP on ammonium concentrations and ammonium consumption rate (ACR) are given in Figure 5-7 and Table 5-11 respectively.

SNP results in a slower utilisation of ammonium for each of the performed experiments where SNP was added. In Figure 5-7 the effect of SNP on residual ammonium concentrations only becomes apparent after 50 hours of fermentation. Whereby the 1000 μM experiment even still has 1 g/l left at 143 hours. Statistical significance was determined by using a two-way ANOVA ($p < 0.05$), whereby all experiments that had SNP added to the reactor were significantly different compared to the control when using the Bonferroni post-hoc test. The 1000 μM SNP fermentation had the largest effect on residual ammonium concentration as the mean difference was the highest (Table 5-12).

The effect of SNP on ACR is shown in Table 5-11 and is significantly lower (two-way ANOVA plus the Tukey post-hoc test) when adding 400, 700 and 1000 μM of SNP to the reactor. When looking at the mean differences it can be seen that 1000 μM SNP has the largest effect on ACR during fermentation of *A. niger B1-D* (Table 5-13).

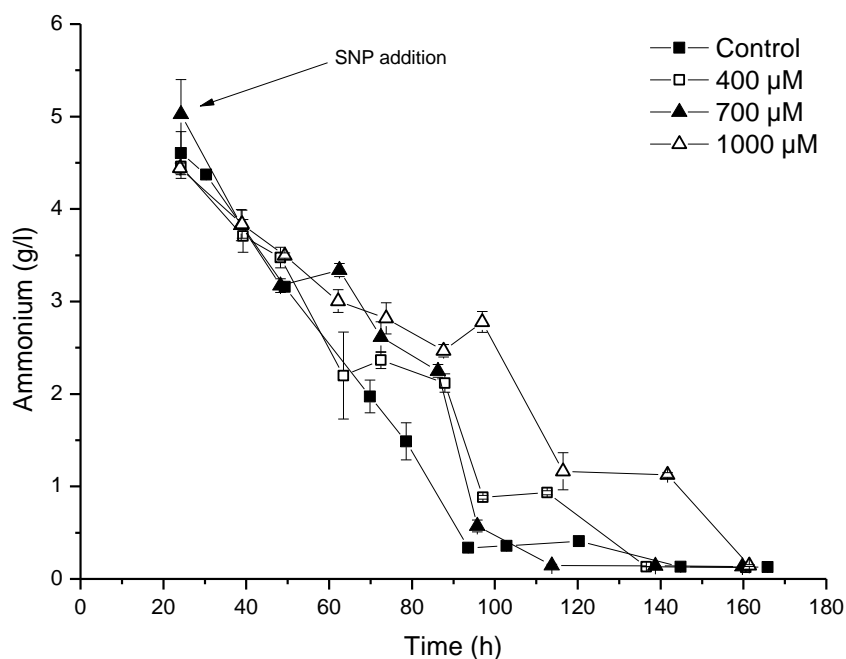


Figure 5-7: Residual Ammonium (g/l) during batch cultivation in a STR of *A. niger B1-D*.

Various concentrations (see graph) of SNP were added at 24 hours. Cultivation conditions were: airflow 2 lpm, 300 rpm, pH 4, temperature 25 °C. Results are expressed as mean ± stdev.

Table 5-11: Effect of SNP on ACR during batch fermentations of *A. niger B1-D*.

Cultivation conditions were: airflow 2 lpm, 300 rpm, pH 4, temperature 25 °C. ACR was determined from the linear part of the graph and is expressed as mean ± stdv.

Concentration SNP (μM)	ACR (g/l/h)
Control	0.062 ± 0.0029
400	0.049 ± 0.0021
700	0.055 ± 0.0043
1000	0.032 ± 0.0003

Table 5-12: Statistical analyses of residual ammonium using the Bonferoni post-hoc test. In which; SEM is standard error of means, LCL is lower confidence limit and UCL is upper confidence limit.

	Mean Diff.	SEM	t-Value
400 μ M vs. Control	0.26335	0.03941	6.68164
700 μ M vs. Control	0.34521	0.03941	8.75856
1000 μ M vs. Control	0.74384	0.03218	23.11362
	P-Value	LCL	UCL
400 μ M vs. Control	3.10E-09	0.15787	0.36884
700 μ M vs. Control	3.50E-14	0.23973	0.4507
1000 μ M vs. Control	7.38E-49	0.65771	0.82996

Table 5-13: Statistical analyses of ACR using the Bonferoni post-hoc test. In which; SEM is standard error of means, LCL is lower confidence limit and UCL is upper confidence limit.

	Mean Diff.	SEM	t-Value
400 μ M vs. Control	-0.01208	0.00162	10.55505
700 μ M vs. Control	-0.00666	0.00162	5.81886
1000 μ M vs. Control	-0.03075	0.00132	32.90137
	P-Value	LCL	UCL
400 μ M vs. Control	1.62E-05	-0.01679	-0.00738
700 μ M vs. Control	0.00513	-0.01137	-0.00196
1000 μ M vs. Control	0	-0.0346	-0.02691

5.2.2.3 NO and its effect on respiration and ATP generation

Based on the off-gas analyses specific oxygen uptake rates and carbon evolution rates can be calculated (see Chapter 2.4 for details). Figure 5-8 (A) and (B) show results for specific oxygen uptake rate (OUR) and specific carbon evolution rate (CER) respectively.

After addition of SNP two effects can be seen until around 60 hours (the highlighted grey box in the graph). During this part of the process the 400 μM experiment shows a drop in OUR, that is comparable to the control experiment. However the addition of 700 and 1000 μM SNP results in an increase in OUR, represented by the grey highlighted part of the graph. The increase in OUR, is faster for the 1000 μM experiment when comparing it to the 700 μM experiment.

After 60 hours OUR stabilizes for each experiment; for the control and 700 μM processes experimental values vary between 1-1.5 mM/g/h, whereas the 400 μM fermentation run stabilizes at around 0.5 mM/g/h. The 1000 μM process has stable OUR values of around 2.3 mM/g/h until 90 hours when OUR values start decreasing. A two-way ANOVA showed significant difference in this dataset ($p < 0.05$). The Bonferroni post-hoc test showed that there was a significant difference between the 1000 μM SNP process and the control fermentation ($p < 0.05$, Table 5-14).

In Figure 5-8 (B) the effect of SNP on CER values can be observed. While in the first 60 hours the control experiment has CER values that are increasing (until a maximum of 1.1 mM/g/h), the experiments adding SNP show either stable or increasing CER values. After 60 hours CER values decrease for all experiments and between 90-100 hours CER values converge and the decrease in all experiments is the same from that moment. Statistical significance was tested using a two-way ANOVA ($p < 0.05$). This and the Bonferroni post-hoc test showed no significant difference between the control and SNP processes (Table 5-15).

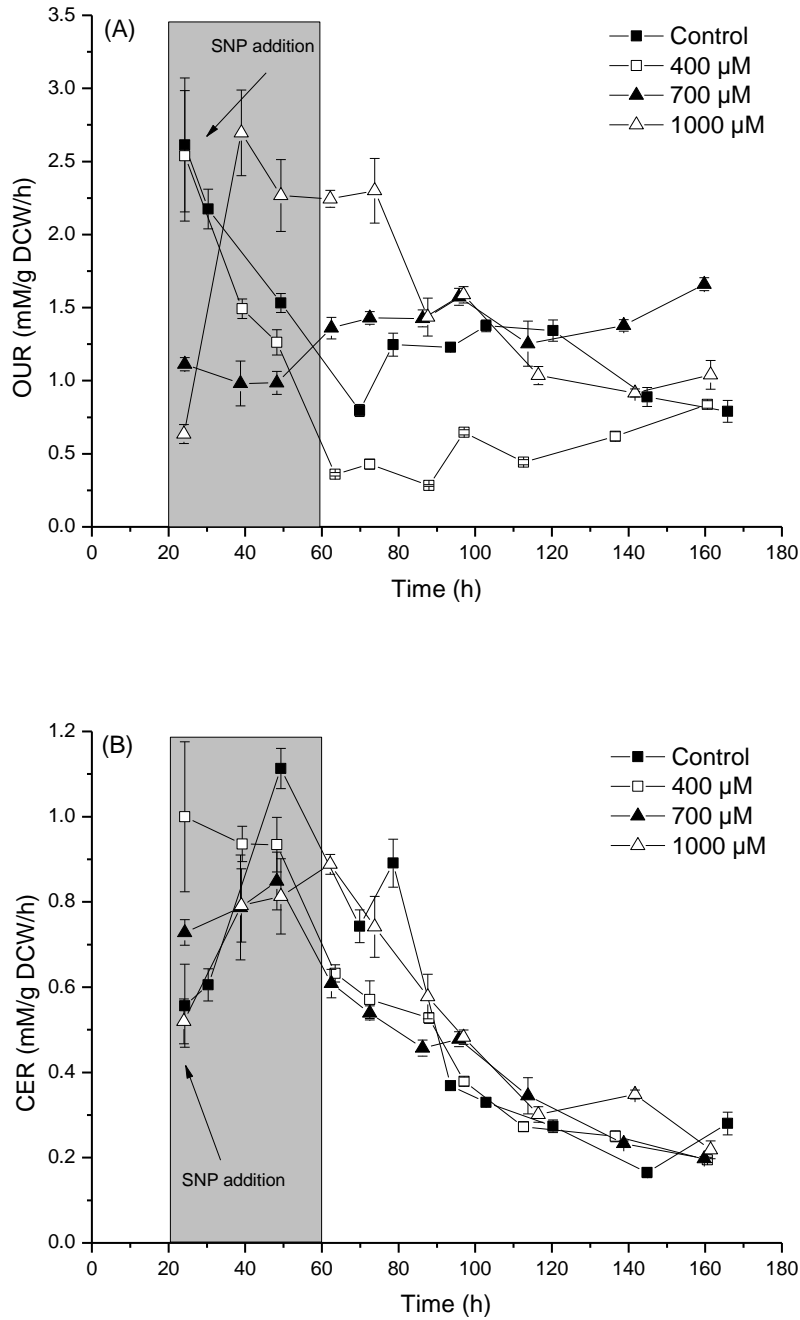


Figure 5-8: (A) OUR (mM/g DCW/h) and (B) CER (mM/g DCW/h) during batch cultivation in a STR of *A. niger* B1-D.

Various concentrations (see graph) of SNP were added at 24 hours. Cultivation conditions were: airflow 2 lpm, 300 rpm, pH 4, temperature 25 °C. Results are expressed as mean ± stdev. At around 60 hours DOT becomes limiting (end of grey highlighted part)

Table 5-14: Statistical analyses of OUR using the Bonferoni post-hoc test. In which; SEM is standard error of means, LCL is lower confidence limit and UCL is upper confidence limit.

	Mean Diff.	SEM	t-Value
400 μ M vs. Control	-0.17899	0.097	-1.84536
700 μ M vs. Control	0.24588	0.097	2.53499
1000 μ M vs. Control	0.65799	0.07954	8.27275
	P-Value	LCL	UCL
400 μ M vs. Control	0.40287	-0.43866	0.08068
700 μ M vs. Control	0.07421	-0.01379	0.50555
1000 μ M vs. Control	6.17E-13	0.44506	0.87092

Table 5-15: Statistical analyses of CER using the Bonferoni post-hoc test. In which; SEM is standard error of means, LCL is lower confidence limit and UCL is upper confidence limit.

	Mean Diff.	SEM	t-Value
400 μ M vs. Control	0.05366	0.02709	1.98068
700 μ M vs. Control	0.00621	0.02709	0.2293
1000 μ M vs. Control	0.00814	0.02221	0.36654
	P-Value	LCL	UCL
400 μ M vs. Control	0.29778	-0.01887	0.12618
700 μ M vs. Control	1	-0.06631	0.07873
1000 μ M vs. Control	1	-0.05133	0.06761

From OUR and CER values the respiratory quotient (RQ) can be determined (see Chapter 2.4, see Figure 5-9). The addition of SNP results for the 400 and 700 μM SNP processes in faster increases in RQ values compared to the control experiment. The addition of 1000 μM SNP results in an immediate decrease in RQ values.

After 60 hours the 400 μM experiment reaches its maximum RQ, which is around 1.8. This 400 μM process had higher RQ values until the last 20 hours of the fermentation compared to the other processes. The control experiment reaches its maximum RQ (around 1.1) between 50 and 70 hours. Statistical analyses, using two-way ANOVA ($p < 0.05$), showed that results were significantly different whereby the Bonferroni post-hoc test showed significant differences between the 400, 700 and 1000 μM SNP experiments compared to the control experiment (Table 5-16). An amount of 1000 μM SNP has the largest effect (looking at mean difference) on RQ values during fermentation of *A. niger B1-D*.

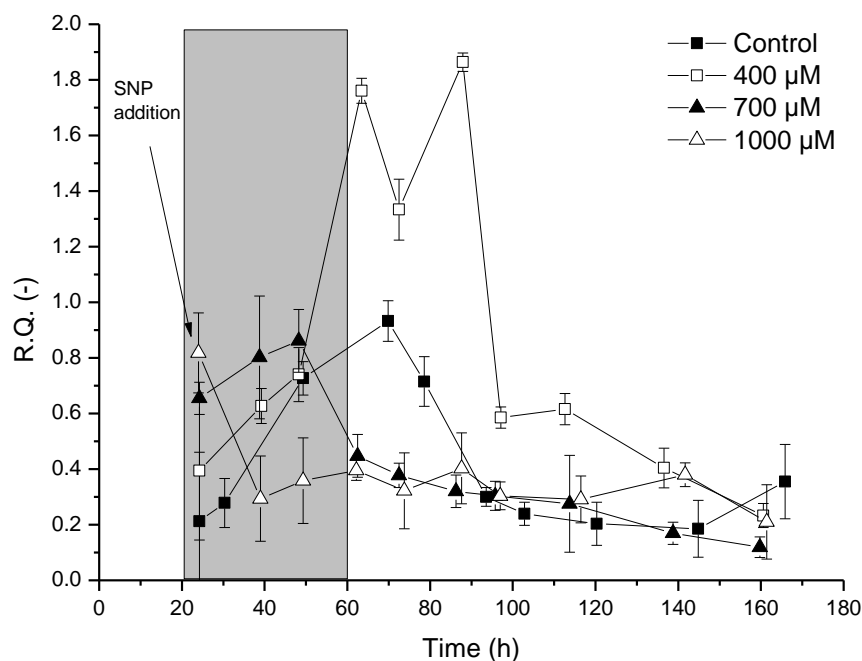


Figure 5-9: R.Q. during batch cultivation in a STR of *A. niger B1-D*.

Various concentrations (see graph) of SNP were added at 24 hours. Cultivation conditions were: airflow 2 lpm, 300 rpm, pH 4, temperature 25 °C. Results are expressed as mean \pm stdev. At around 60 hours DOT becomes limiting (end of grey highlighted part)

Table 5-16: Statistical analyses of R.Q. using the Bonferoni post-hoc test. In which; SEM is standard error of means, LCL is lower confidence limit and UCL is upper confidence limit.

	Mean Diff.	SEM	t-Value
400 μ M vs. Control	0.23944	0.05558	4.3077
700 μ M vs. Control	-0.18319	0.05558	-3.29573
1000 μ M vs. Control	-0.2908	0.04558	-6.38024
	P-Value	LCL	UCL
400 μ M vs. Control	1.88E-04	0.09063	0.38824
700 μ M vs. Control	0.0075	-0.33199	-0.03438
1000 μ M vs. Control	1.52E-08	-0.41282	-0.16878

In Figure 5-10 intracellular ATP concentrations obtained during these bioprocesses are plotted against time. Figure 5-10 shows two clear different trends. The control and 700 μM SNP experiment have two peak values whereas the addition of 400 and 1000 μM SNP results in only one peak value. Another characteristic of the 400 and 1000 μM SNP bioprocesses was that they lacked the drop in intracellular ATP content that the control and 700 μM experiments did have (between 70-90 hours)

The statistical difference was shown by using a two-way ANOVA ($p < 0.05$). The Bonferroni post-hoc test showed that the 400 and 1000 μM were significantly different compared to the control ($p < 0.05$). The largest mean difference compared to the control was in the bioprocess with 400 μM SNP, indicating that 400 μM of SNP has the largest effect on intracellular ATP content in *A. niger B1-D* (Table 5-17).

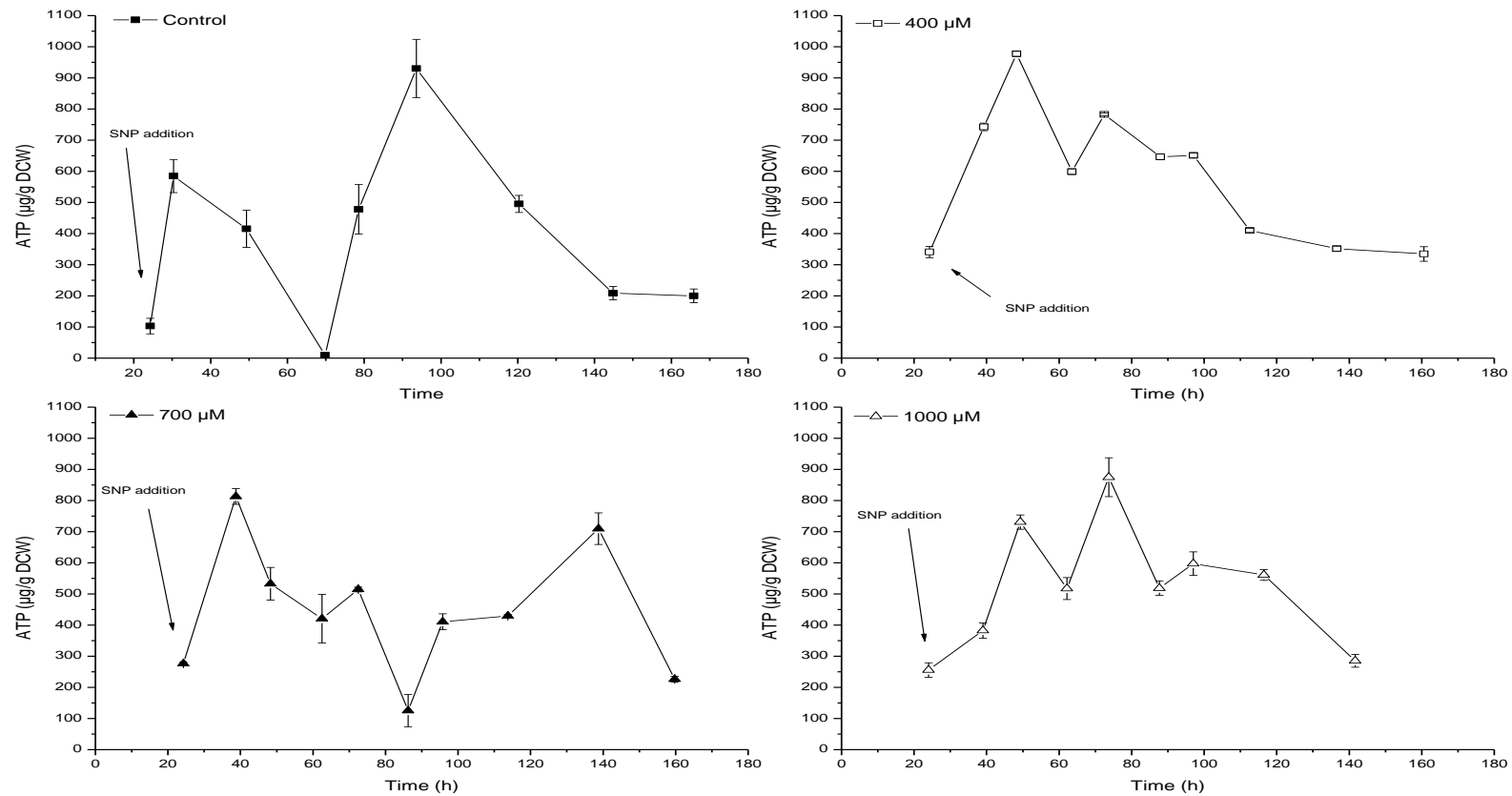


Figure 5-10: Intracellular ATP concentrations ($\mu\text{g/g DCW}$) during batch cultivation in a STR of *A. niger B1-D*.

Various concentrations (see graph) of SNP were added at 24 hours. Cultivation conditions were: airflow 2 lpm, 300 rpm, pH 4, temperature 25°C . Results are expressed as mean \pm stdev.

Table 5-17: Statistical analyses of ATP using the Bonferoni post-hoc test. In which; SEM is standard error of means, LCL is lower confidence limit and UCL is upper confidence limit.

	Mean Diff.	SEM	t-Value
400 μ M vs. Control	159.36175	25.99004	6.13165
700 μ M vs. Control	30.98051	25.99004	1.19201
1000 μ M vs. Control	85.94521	21.31205	4.03271
	P-Value	LCL	UCL
400 μ M vs. Control	5.24E-08	89.78359	228.93991
700 μ M vs. Control	1	-38.59765	100.55867
1000 μ M vs. Control	5.47E-04	28.89054	142.99989

5.2.2.4 NO and its effect on oxidative stress related biomarkers

Figure 5-11 (A) and (B) show the effect of SNP on oxidative stress related enzymes, SOD and CAT respectively. Figure 5-11 (A) shows that when adding SNP that in the first 30 hours after addition of SNP the SOD values of the 400 and 700 μM experiments were higher compared to the control experiment (up to around 700 U/g). After 60 hours of fermentation these two experiments had reduced SOD activity while the control experiment had values ranging between 1500-1800 U/g. The addition of 1000 μM of SNP resulted in lower SOD activities until 60 hours before SOD activity starts rising. All experiments with SNP addition large increases of SOD activities at the end of the fermentation, while the control experiment doesn't show this characteristic.

The statistical analysis that was performed on this dataset was a two-way ANOVA and showed that there was a significant difference between these experiments ($p < 0.05$). The Bonferroni post-hoc test showed that only the 700 μM was significantly different compared to the control experiment (Table 5-18).

The effect of SNP on CAT activity during batch cultures is shown in Figure 5-11 (B). The control experiment follows a trend which has rising CAT values until around 70 hours after which CAT activity decreases until it starts rising again after 100 hours. The addition of SNP at 24 hours resulted in consistently higher values, for all SNP processes, during most of the process, with the exception of the sample at 140 hours. The addition of 400 μM SNP resulted in a slow increase of CAT activity during the entire experiment, while the addition of 700 and 1000 μM SNP show a distinctive peak with maximum activity values of around 5600 and 6700 U/g respectively after these peaks CAT activity drops and stabilizes until around 100 hours before CAT activities start rising again.

The two-way ANOVA showed a significant difference ($p < 0.05$). The outcome of the Bonferroni post-hoc test was that the addition of 400, 700 and 1000

μM resulted in significant differences in CAT activity compared to the control experiment. The addition of 1000 μM of SNP had the largest effect on CAT activity as the mean difference between control and 1000 μM of SNP had the largest mean difference (Table 5-19).

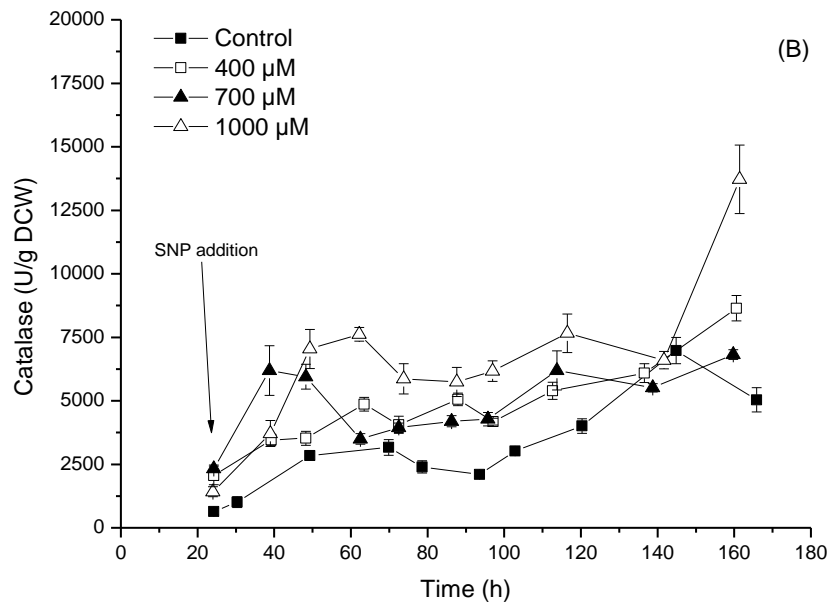
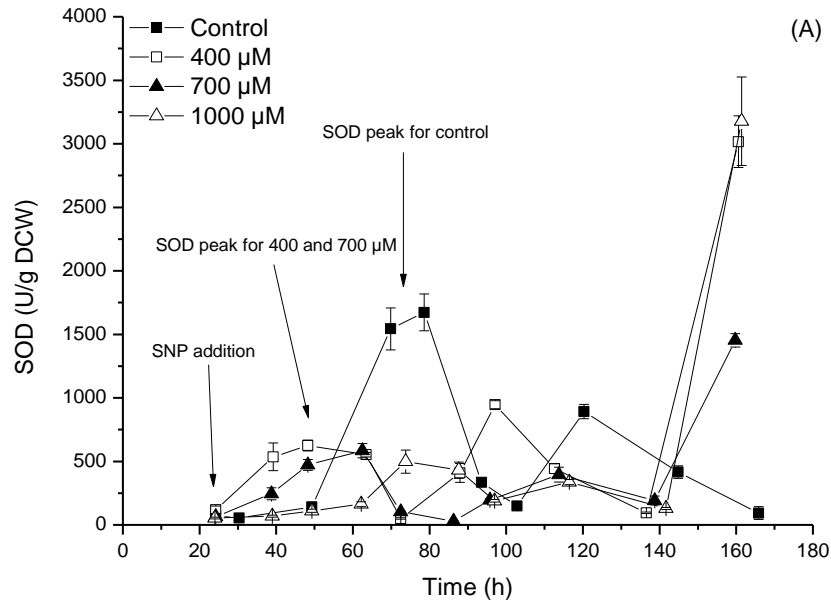


Figure 5-11: (A) SOD (U/g DCW) and (B) CAT (U/g DCW) during batch cultivation in a STR of *A. niger B1-D*.

Various concentrations (see graph) of SNP were added at 24 hours. Cultivation conditions were: airflow 2 lpm, 300 rpm, pH 4, temperature 25 °C. Results are expressed as mean ± stdev.

Table 5-18: Statistical analyses of SOD using the Bonferoni post-hoc test. In which; SEM is standard error of means, LCL is lower confidence limit and UCL is upper confidence limit.

	Mean Diff.	SEM	t-Value
400 μ M vs. Control	72.30388	53.14988	1.36038
700 μ M vs. Control	-233.4854	53.14988	-4.39296
1000 μ M vs. Control	-8.17864	43.39669	-0.18846
	P-Value	LCL	UCL
400 μ M vs. Control	1	-69.93929	214.54706
700 μ M vs. Control	1.31E-04	-375.72857	-91.24223
1000 μ M vs. Control	1	-124.31971	107.96242

Table 5-19: Statistical analyses of CAT using the Bonferoni post-hoc test. In which; SEM is standard error of means, LCL is lower confidence limit and UCL is upper confidence limit.

	Mean Diff.	SEM	t-Value
400 μ M vs. Control	1654.20999	153.6109	10.76883
700 μ M vs. Control	1819.80793	153.6109	11.84687
1000 μ M vs. Control	3491.20591	125.42278	27.8355
	P-Value	LCL	UCL
400 μ M vs. Control	2.69E-19	1243.10648	2065.31351
700 μ M vs. Control	4.40E-22	1408.70441	2230.91145
1000 μ M vs. Control	3.78E-58	3155.54129	3826.87053

5.2.2.5 NO and its effect on intracellular protein content, lysozyme production and viability

Figure 5-12 shows the effect of various concentrations of SNP on the intracellular protein content of *A. niger B1-D*. The dataset presented in Figure 5-12 show the same two trends that were described previously (see Figure 5-10). The control experiment and 700 μM SNP experiment show two distinct peak values in intracellular protein content. The first peak is during the exponential phase when there was still carbon source available. The other peak value was reached during the stationary phase when carbon source was depleted. The experiments with 400 and 1000 μM SNP have only one peak value which was reached at 90 and 100 hours respectively.

Statistical analyses shows that results were significantly different (Two-way ANOVA with a $p < 0.05$). The Bonferroni post-hoc test showed that all experiments were significantly different compared to the control whereby the mean difference for the 400 μM SNP experiment was the highest (Table 5-20). This indicates that 400 μM SNP had the largest effect on intracellular protein content.

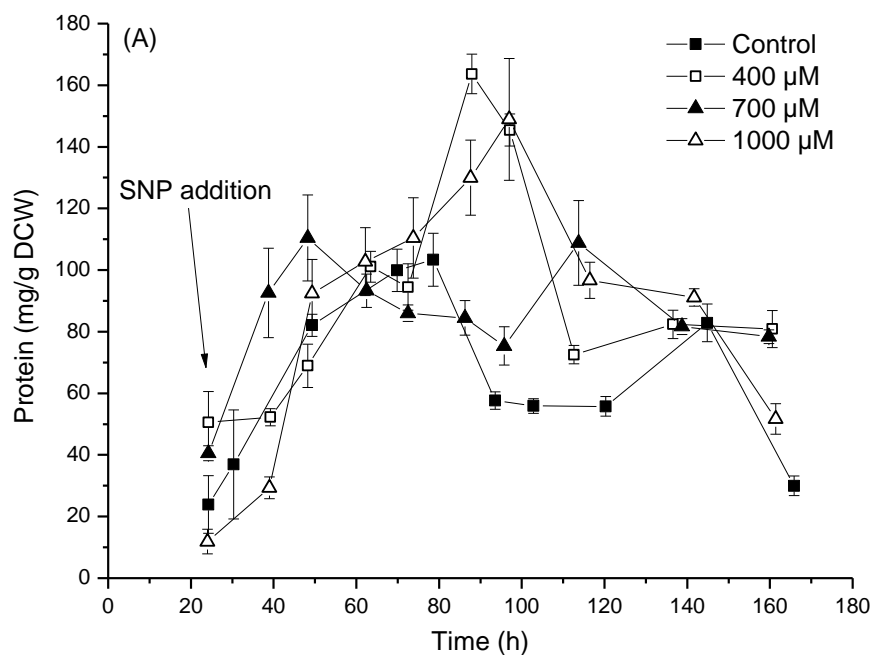


Figure 5-12: Intracellular protein content (mg/g DCW) during batch cultivation in a STR of *A. niger B1-D*.

Various concentrations (see graph) of SNP were added at 24 hours. Cultivation conditions were: airflow 2 lpm, 300 rpm, pH 4, temperature 25 °C. Results are expressed as mean ± stdev.

Table 5-20: Statistical analyses of intracellular protein using the Bonferoni post-hoc test. In which; SEM is standard error of means, LCL is lower confidence limit and UCL is upper confidence limit.

	Mean Diff.	SEM	t-Value
400 μM vs. Control	25.54129	2.62952	9.71327
700 μM vs. Control	18.88829	2.62952	7.18316
1000 μM vs. Control	24.85347	2.147	11.57592
	P-Value	LCL	UCL
400 μM vs. Control	1.37E-16	18.50398	32.57859
700 μM vs. Control	2.21E-10	11.85099	25.9256
1000 μM vs. Control	2.21E-21	19.10754	30.59941

Figure 5-13 shows the effect of SNP on lysozyme production of *A. niger B1-D*. Figure 5-13 shows that adding SNP had a surprising result on lysozyme concentrations. All experiments where SNP was injected had higher maximum lysozyme values, compared to the control process, whereby the 700 μM experiment had the highest value, which was around 6 mg/l. The 400 and 1000 μM SNP fermentations had maximum lysozyme concentrations around 4 mg/l.

Statistical analyses showed a significant difference (Two-way ANOVA, $p < 0.05$) that was the largest for the 700 μM , as the Bonferroni post-hoc test showed that this process had the largest mean difference therefore the largest effect on lysozyme concentration (Table 5-21).

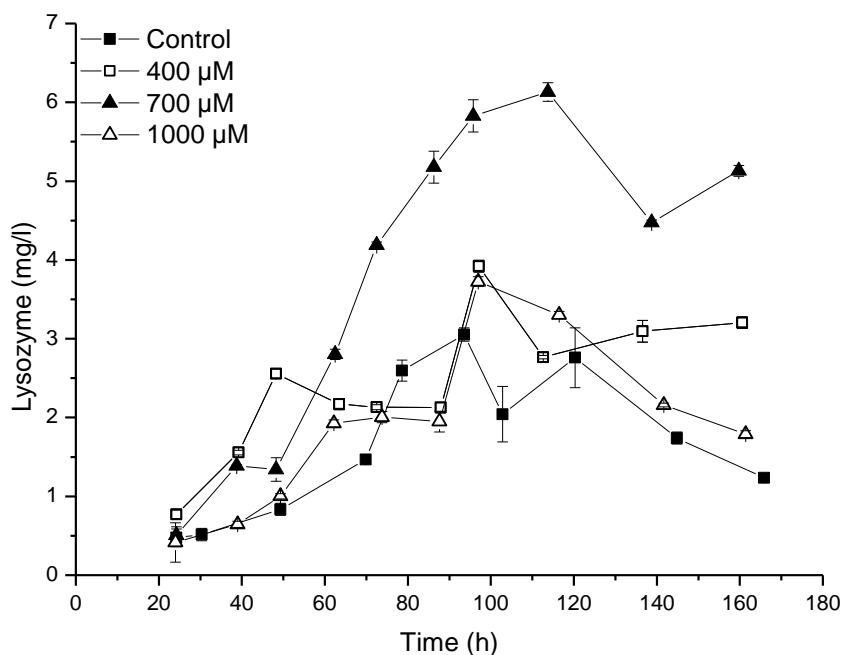


Figure 5-13: Lysozyme concentration (mg/l) during batch cultivation in a STR of *A. niger* B1-D.

Various concentrations (see graph) of SNP were added at 24 hours. Cultivation conditions were: airflow 2 lpm, 300 rpm, pH 4, temperature 25 °C. Results are expressed as mean ± stdev.

Table 5-21: Statistical analyses of lysozyme using the Bonferoni post-hoc test. In which; SEM is standard error of means, LCL is lower confidence limit and UCL is upper confidence limit.

	Mean Diff.	SEM	t-Value
400 μM vs. Control	0.36027	0.10005	3.60103
700 μM vs. Control	1.62775	0.10005	16.26998
1000 μM vs. Control	-0.31726	0.08169	-3.88381
	P-Value	LCL	UCL
400 μM vs. Control	0.00264	0.09252	0.62802
700 μM vs. Control	2.66E-33	1.36	1.8955
1000 μM vs. Control	9.48E-04	-0.53588	-0.09864

In Figure 5-14 viability results, during these fermentations, are plotted against time. Two observations can be made from this graph; the first observation is that all experiments where SNP was added have lower viability values over the entire fermentation; the second observation is that the addition of SNP results in an initial inhibition of viability which lasts until around 60 hours. As far as the effect of increasing the SNP concentration goes it looks as if there is no real decrease in viability when looking at the trends after 60 hours.

A two-way ANOVA showed that adding SNP results in significant changes in viability during fermentation of *A. niger* B1-D. The Bonferroni post-hoc test showed that all experiments where SNP was added were significantly different from the control experiment, whereby 400 μ M SNP had the largest effect on viability based on the highest mean difference value (Table 5-22).

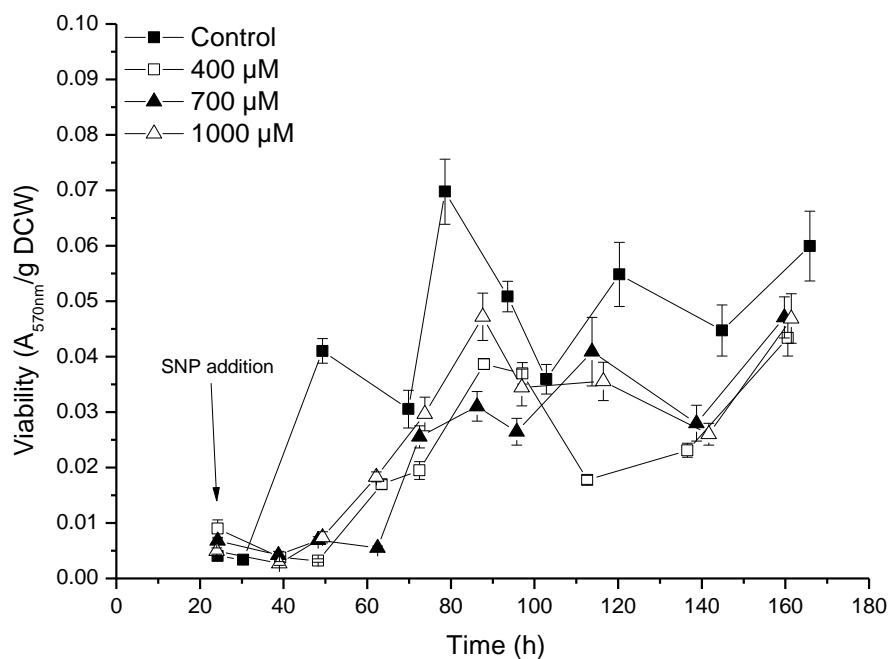


Figure 5-14: Viability (A_{570nm}/g DCW) during batch cultivation in a STR of *A. niger B1-D*.

Various concentrations (see graph) of SNP were added at 24 hours. Cultivation conditions were: airflow 2 lpm, 300 rpm, pH 4, temperature 25 °C. Results are expressed as mean \pm stdev.

Table 5-22: Statistical analyses of Viability using the Bonferoni post-hoc test. In which; SEM is standard error of means, LCL is lower confidence limit and UCL is upper confidence limit.

	Mean Diff.	SEM	t-Value
400 μ M vs. Control	-0.02392	0.00156	-15.32662
700 μ M vs. Control	-0.0229	0.00156	-14.67534
1000 μ M vs. Control	-0.0181	0.00127	-14.20804
	P-Value	LCL	UCL
400 μ M vs. Control	5.76E-31	-0.0281	-0.01974
700 μ M vs. Control	2.48E-29	-0.02708	-0.01873
1000 μ M vs. Control	3.78E-28	-0.02151	-0.01469

5.2.2.6 Overview of statistics

As many processes inside cells are linked and related to each other an overview table of all the statistical analyses was made to see if any of the measured physiological parameters corresponded with each. Results from this comparison are presented in Table 5-23.

Table 5-23: Statistical overview of all the tests carried out above.

Each result is a means comparison between the control experiment and an experiment where SNP was added. Non-significant differences are represented with a 0 and significant differences are represented with 1. The Bonferroni also answers the question which experiment had the largest effect and that is presented as 1*. All tables with the specific statistical data can be found in Appendix IV.

Experiment	Nitrite	DCW	Glucose	Ammonium	OUR	CER	RQ	ATP	SOD	CAT	Protein	Lysozyme	Viability
400 μ M - Control	1	0	0	1	0	0	1	1*	0	1	1*	1	1*
700 μ M - Control	1	0	1*	1	0	0	1	0	1	1	1	1*	1
1000 μ M - Control	1*	1*	1	1*	1*	0	1*	1	0	1*	1	1	1

Experiment	Specific growth rate	GCR	ACR
400 μ M - Control	0	0	1
700 μ M - Control	0	0	1
1000 μ M - Control	0	1*	1*

5.3 Discussion

The next paragraphs will explain all the data that was collected during these experiments. The previous description of results only showed the effect on the separate parameters that were measured, however all of these are closely linked together and the separate parts of the discussion described here will try and link these together with the help of figures at the end of this paragraph (Figure 5-15, Figure 5-16 and Figure 5-17).

5.3.1 Growth experiments using sodium nitrite, hydroxy urea and SNP

The shake flask experiments resulted for all NO-donors in significant effects in DCW of *A. niger B1-D*. The addition of sodium nitrite resulted in an inhibition of growth when increasing the concentration of sodium nitrite (Figure 5-1). This is a very clear indication of stress due to a too large amount of sodium nitrite being added to the shake flasks. Nitrite toxicity has been studied in *Aspergillus nidulans* and results presented here confirm this same sensitivity to nitrite (Pombeiro *et al.*, 1992).

The big fluctuations when the stationary phase starts, for the hydroxy urea and SNP processes (Figure 5-2 and Figure 5-3), are due to the effect of the compounds that were added into the shake flasks. The direct cause could be that NO induces a combination of autolysis and protease activity inside the shake flasks, whereby during extracellular protease activity the biomass increases (Li *et al.*, 2008b) and when autolysis (Emri *et al.*, 2008) starts the biomass decreases. Both these effects are linked to the depletion of carbon source however usually when the carbon source is depleted the nitrogen source is depleted as well, this might not be the case in these shake flask experiments, as nitrite contains nitrogen that can be utilised for biomass growth (Hwang *et al.*, 2004). The information available from literature is however very scarce and to this author's knowledge no studies have been

done to establish a direct link between biomass concentration and proteolysis and autolysis.

5.3.2 Reactor experiments for studying the effect of SNP on cultivation of *A. niger* B1-D

5.3.2.1 Analyses of NO release

The control experiment shows that *A. niger* B1-D also is capable of producing NO, indicating NO synthase activity, as nitrite concentrations vary from one to two μM . These concentrations are however very close to the lower limit of detection for the Griess method, which starts at one μM (Nagano, 1999, Bryan and Grisham, 2007).

The theoretical yield of NO from SNP is 15% (calculated based on molecular weight for SNP and NO respectively). Therefore maximum NO-release for the 400, 700 and 1000 μM SNP experiments can be 60, 105 and 150 μM respectively. Previous description of the reaction from NO to nitrite shows that the ratio for this reaction is 1:1 (see chapter 2.10). Adding all the nitrite values from Figure 5-4 together for each bioprocess separately results in total nitrite values of 14, 74, 104 and 170 μM nitrite corresponding to control, 400, 700 and 1000 μM SNP respectively. When subtracting the total nitrite value of the control experiment from the 400, 700, and 1000 μM SNP experiments results in values of 60, 90 and 156 μM respectively. These concentrations are close to the theoretical yield of NO from SNP. Literature confirms that NO in physiological fluids (in this case a bioreactor) is almost completely oxidized into nitrite, which will remain stable for hours (Bryan and Grisham, 2007).

The Griess reaction appears to be a very suitable method to monitor NO release from NO-donors this also explains the widespread use of this method

to monitor NO-release from NO-donors (Bryan and Grisham, 2007, Nagano, 1999). However the exposure time of the culture to NO from SNP directly seems to be extremely short this therefore can't explain the results obtained in this chapter. The exposure to nitrite is however prolonged and lasts the entire fermentation for each SNP experiment (including the control). Nitrite is also a well known NO-donor under acidic conditions (Lundberg and Weitzberg, 2005) (for mechanism see chapter 2.10). The reaction mechanism described in literature includes besides the formation of NO, also the formation of N_2O_3 and NO_2 , which are also known nitrosative stress causing molecules (Lundberg and Weitzberg, 2005, Weitzberg and Lundberg, 1998).

Even though NO release has been observed during cultivation of *A. niger B1-D* by using the Griess reaction the method itself seems unsuitable to monitor concentrations of NO in real time. This means different methods would have to be utilised to monitor NO in real time.

5.3.2.2 NO and its effect on biomass formation, carbon consumption and nitrogen consumption

Part of the SNP molecule consists of cyanide and can potentially be released into the medium when hydrogen is present (Nakamura *et al.*, 1977) as fermentations were done under low pH conditions it is likely that cyanide was released during the processes that were done in this chapter. Cyanide is able to inhibit complex IV in the main respiratory chain in *Aspergillus niger B1-D* (Joseph-Horne *et al.*, 2001) this could contribute to decreased respiration thereby reducing the uptake of glucose and ammonium which in turn can effect biomass growth. This is however not confirmed by DCW values (non significant for the 400 and 700 μ M SNP experiment compared to the control experiment, see Table 5-23) and specific growth rate (which is non significant in the whole dataset, see Table 5-23).

The impairment of carbon uptake of *A. niger B1-D* has been associated with an oxidative stress reaction to hydrogen peroxide in previous research done in this lab indicating impairment of the respiratory pathway (Li *et al.*, 2008a). Results described here show that the addition of a known NO-donor results in a similar impairment of the respiratory pathway for concentrations higher than 700 μM SNP and higher, pointing towards a stressful event, in this study, called nitrosative stress

Adding SNP in increasing amounts to the bioreactor has a severe inhibitory effect on the uptake of ammonium. The effect of NO-donors on the nitrogen metabolism of fungi has not been widely reported. Research done previously in this lab has confirmed inhibition of ammonium uptake when hydrogen peroxide was added. This effect however was mainly attributed to a decrease in intracellular amounts of ATP and NADPH by respiratory inhibition (Li *et al.*, 2008a), ATP results in this chapter however don't show this (see Figure 5-10).

Aspergillus niger has been shown to be able to utilise multiple nitrogen sources such as nitrite and ammonium (Hwang *et al.*, 2004). Fungi have highly complex nitrogen metabolic pathways in which literature links these pathways to ATP production via anaerobic respiration, utilising ethanol as a carbon source (Chapter 2.10) (Takaya, 2002, Takasaki *et al.*, 2004). This ATP generation coincides with the formation of ammonium which could explain the reduced ammonium uptake. Anaerobic respiration also explains why this effect can only be observed after 50 hours. At this time in the process dissolved oxygen (DO) becomes limiting inside the reactor during the control experiment, which could trigger anaerobic respiration thereby delaying ammonium uptake. Confirmation of DO values is difficult for the SNP experiments as the addition of SNP seemed to interfere with reliable measurement of DO inside the reactor; however as biomass growth was similar in most experiments (400 and 700 μM SNP) it is entirely possible oxygen depletion would occur around the same time inside the reactor compared to the control experiment. Literature shows that ammonium is the

preferred nitrogen source in fungi and represses the uptake of other nitrogen sources, therefore the most likely extra nitrogen comes from NO release from nitrite (Carlile and Watkinson, 1997). Preference for NO over ammonium is most likely the result of the fact that ammonium uptake is an active process (costing ATP) and NO can diffuse freely into the cell (Carlile and Watkinson, 1997). Ammonium fermentation using *Aspergillus nidulans* (Takasaki *et al.*, 2004) points towards NO dioxygenase activity that converts NO back into nitrate which is then converted back into ammonium. Ammonium fermentation has also previously been shown in this lab (Li *et al.*, 2008d) suggesting that *Aspergillus niger* has mechanisms in effect that can deal with nitrite, nitrate and NO. The described anaerobic respiration and NO donation from nitrite could contribute to the delay of ammonium utilisation during fermentation of *Aspergillus niger* when adding SNP to the reactor.

Results obtained for DCW, glucose and ammonium indicates that at lower concentrations for SNP (400 and 700) there are no significant effects on growth and carbon consumption. The NO released from SNP also seems to be utilised as an extra nitrogen source under anaerobic conditions, which would simultaneously explain the inhibition of ammonium uptake and the apparent non-significant effect of SNP on DCW and glucose during these processes.

5.3.2.3 NO and its effect on respiration and ATP generation

The differences in OUR (Figure 5-8 (A)) before the addition of SNP (time point relating to 24 hours) are most likely the result of the low amount of biomass which reduces the chance of a reliable off gas analyses. Oxygen enrichment processes using *A. niger* have shown that too much oxygen can have a profound negative effect on the respiration of this organism (O'Donnell *et al.*, 2011), which can result in bad process outcomes such as low yields in biomass and protein content due to oxidative stress. Practically this meant that the previous study done by O'Donnell showed increased

OUR values and decreased CER and R.Q. when enriched oxygen was sparged into the reactor. The increased OUR results in the increase of oxygen radical formation thereby having negative effects on the respiration of fungal cells. This study showed the opposite effect, a decrease in oxidative stress resulting in a higher R.Q. The lower maximum SOD values (Figure 5-11 (A)) and the apparent increase or lack of decrease in ATP values (Figure 5-10) for the 400 and 700 μM SNP processes seem to confirm this as well. The higher OUR values observed in Figure 5-8 (A) for the 1000 μM SNP process is most likely a result of a stress related reaction to the increased amounts of NO in the medium called nitrosative stress.

Previous research done in this lab showed that there is an extremely sensitive balance between oxidative stress and ATP generation, by looking at ATP and superoxide anion generation simultaneously, whereby high superoxide anion concentrations resulted in lower ATP values (Li *et al.*, 2008d, O'Donnell *et al.*, 2011, Voulgaris *et al.*, 2012). Oxidative stress seems to affect *A. niger* B1-D in such a way that ATP production can be compromised by inhibition/damage of the mitochondria caused by oxygen radicals (O'Donnell *et al.*, 2011, Li *et al.*, 2008a, Voulgaris *et al.*, 2012). Results presented in this chapter do not show this effect, as ATP values are the same or higher when adding SNP this indicates less oxidative stress as opposed to the research mentioned previously. The reaction between the superoxide anion radical and NO causes a decrease in the concentration of the superoxide anion radical, thereby decreasing mitochondrial inhibition/damage, which can be a likely cause for the decrease in oxidative stress when adding SNP to the bioreactor.

It should be noted that SNP has cyanide and cyanide can impair respiration by inhibiting complex IV (Joseph-Horne *et al.*, 2001). In literature this is associated with increased oxidative stress (Joseph-Horne *et al.*, 2001) and would therefore severely affect ATP content, which doesn't seem to be the case in this dataset. Therefore based on DCW values, RQ values and ATP values cyanide either isn't released from SNP or even if it is released is not

affecting *A. niger* B1-D in the measured parameters presented in this chapter.

5.3.2.4 NO and its effect on oxidative stress related biomarkers

SOD is of commercial interest for various reasons and for these reasons its production in bioreactors has been characterized in *Saccharomyces cerevisiae* showing two characteristic peaks in SOD activity during the entire process (Dellomonaco *et al.*, 2007). The first peak was at the lag phase and early exponential phase and the second peak occurred after the depletion of the carbon source. Causes for these two SOD peaks are associated with; oxidative stress in which the first peak in the lag phase is caused by the oxidative shock when a reactor is inoculated and the second SOD peak by oxidative stress associated with culture aging (O'Donnell *et al.*, 2007, Dellomonaco *et al.*, 2007). Chapter 5 showed that increasing the oxygen transfer rate resulted in a higher OUR (Figure 4-5 (B)). Previous research has also shown that higher OUR results in a higher generation of oxygen radicals (Bai *et al.*, 2004, Voulgaris *et al.*, 2012), which are followed by higher SOD and CAT values as a defensive response to the increased intracellular concentration of oxygen radicals (Kreiner *et al.*, 2003).

Results presented here show these same characteristic two peaks in which the SNP processes indicate less oxidative stress for *A. niger*, as SOD activity is lower during the exponential phase and higher during the lag phase for the 400 and 700 μM SNP processes (Figure 5-11(A)). The increase in SOD activities is usually associated with the increase in oxidative stress, as more oxygen radical formation leads to a higher utilisation of these oxidative stress defence mechanisms (SOD and CAT) (Li *et al.*, 2009, Kreiner *et al.*, 2002), however as respiration (until 60 hours), DCW, ATP content, protein content and lysozyme production weren't negatively affected the increase in SOD activity in the lag phase of the fermentation is unlikely to be associated with more oxidative stress. Less oxidative stress is likely caused by the reaction

between the superoxide anion with NO resulting in peroxynitrite formation, resulting in less intracellular superoxide anion (Brown *et al.*, 2009), which is a more likely explanation of the SOD activities obtained in this chapter as previously mentioned parameters were not adversely affected. The only known sensitivity of SOD to peroxynitrite is that it can react with its cysteine or Fe-S groups thereby inhibiting its activity this is however presented as protein sensitivity in general and is not referred to as SOD sensitivity to peroxynitrite specifically (Poole, 2005, Gebicka and Didik, 2009). The only experiment in this dataset that could be attributed to this is the 1000 μ M SNP experiment.

As described previously CAT has the potential to react with peroxynitrite, which is a reaction product of nitric oxide and the superoxide anion (Brown *et al.*, 2009). CAT activity during these experiments also confirms that there is an interaction between oxidative stress defences and nitric oxide release by SNP when observing the increased CAT activities in Figure 5-11(B). This interaction is likely caused by the reaction of the superoxide anion with NO, forming peroxynitrite. In plants the enzyme CAT has been extensively studied where this enzyme can exist in multiple molecular forms or isozymes encoded by multiple genes (Scandalios *et al.*, 1997). In *A. nidulans* catA and catB genes have been characterized (Kawasaki *et al.*, 1997). CatA seems to be active during the spore phase and catB is active in growing mycelia. Literature has identified two more genes for CAT, catC and catD which are active in *A. nidulans* (Kawasaki and Aguirre, 2001) and in *N. crassa* a third (Peraza and Hansberg, 2002) and a fourth gene (Schliebs *et al.*, 2006) were also reported. A study also reported three isoforms of CAT when *A. niger* was exposed to waste water polluted with arsenic (Buckova *et al.*, 2005). The findings described here and the studied literature point towards a complex regulation of the enzyme CAT in *A. niger* B1-D when it is confronted with nitric oxide. Figure 5-11(B) shows a very clear dose dependent response to increasing concentrations of SNP, meaning more SNP resulted in higher CAT activities, with clear peak trends when looking at 700 and 1000 μ M of SNP.

Previous research indicates that high ATP generation coincides with high superoxide anion generation (O'Donnell *et al.*, 2011, Voulgaris *et al.*, 2012). Oxidative stress has been defined in literature as an imbalance between oxygen radical formation and the cells ability to deal with these oxygen radicals resulting in oxidative stress (Angelova *et al.*, 2005). This suggests that during fermentation SOD and CAT activities should closely follow ATP levels to achieve an optimum result during bioprocesses in a reactor (optimum yield of product). Figure 5-15 plots SOD, ATP and protein content together in one graph. This figure clearly shows that the SOD trend starts overlapping ATP content in the 400 and 700 μM SNP experiments. CAT seems to correspond more with nitrite peak values in the 400 and 1000 μM SNP experiments (see Figure 5-16), indicating a direct response to the addition of SNP to the reactor instead of a response to oxygen radicals, but overlaps completely with ATP and SOD peaks in the 700 μM SNP experiment. The overlap of ATP, SOD and CAT for 700 μM SNP indicates an optimum concentration of NO inside the reactor thereby reducing oxidative stress in *A. niger B1-D*, which is why this process had the highest yield of lysozyme.

5.3.2.5 NO and its effect on intracellular protein content, lysozyme production and viability

Proteins can be damaged by oxidative stress (O'Donnell *et al.*, 2011). The main three mechanisms of damage are protein carbonylation, S-thiolation and oxidation of [4Fe-4S] groups (Chapter 2.5). There is however little known how protein content is affected in filamentous fungi when subjected to nitric oxide. The decrease of protein content after the depletion of glucose is indicative for proteolysis (Li *et al.*, 2008d, Emri *et al.*, 2008), SOD and CAT peaks at the end of fermentation seem to correspond with this, as proteolysis releases carbon source to use for intracellular processes (Figure 5-15). Protein content was added to Figure 5-15 to see how changes compared with SOD and ATP content. Protein content seems to overlap with

SOD activity mostly during the control and 700 μM experiment. This overlap indicates that a higher portion of intracellular protein content is influenced by oxidative stress defence mechanisms (specifically SOD and CAT). As this method only determines total protein content by using the Bradford reagent then from this graph the 400 and 1000 μM SNP experiment indicate the expression of other proteins or enzymes when looking at the 400 and 1000 μM SNP processes.

Viability is a method that measures mitochondrial activity by determining reductase activity (Emri *et al.*, 2005). The four complexes of the respiratory chain consists of reductases (Joseph-Horne *et al.*, 2001), therefore this assay should be able to indicate very well how mitochondrial activity is influenced by NO release from SNP. Previous oxygen enrichment processes showed an increase in viability when sparging oxygen enriched air into the reactor, meaning an increase in mitochondrial activity (O'Donnell *et al.*, 2011). The results obtained here indicate mitochondrial inhibition (see Chapter 2.10 as to how this is possible) as viability values are lower when adding SNP to the reactor (Figure 5-14), which can be an indication of less oxidative stress. The lower mitochondrial activity also results in less oxygen radical formation thereby decreasing oxidative stress. The RQ gives a measure of respiration based on the off gas analyses. Previous research shows that oxygen enrichment leads to lower respiration in *A. niger* indicating oxidative stress by mitochondrial damage or increased use of alternative respiration generating heat (O'Donnell *et al.*, 2011). Combining these two measurements, which to this authors knowledge hasn't been studied extensively yet, should give an indication of how efficiently mitochondria are working. The 700 μM SNP process very clearly shows that similar RQ values can be reached with lower mitochondrial activity, which is also a strong indication of less oxidative stress, as with less viability similar values for RQ can be reached. This results in spending less ATP on oxidative stress defence mechanisms resulting, in the case of the 700 μM SNP process, in higher lysozyme concentrations (Figure 5-17).

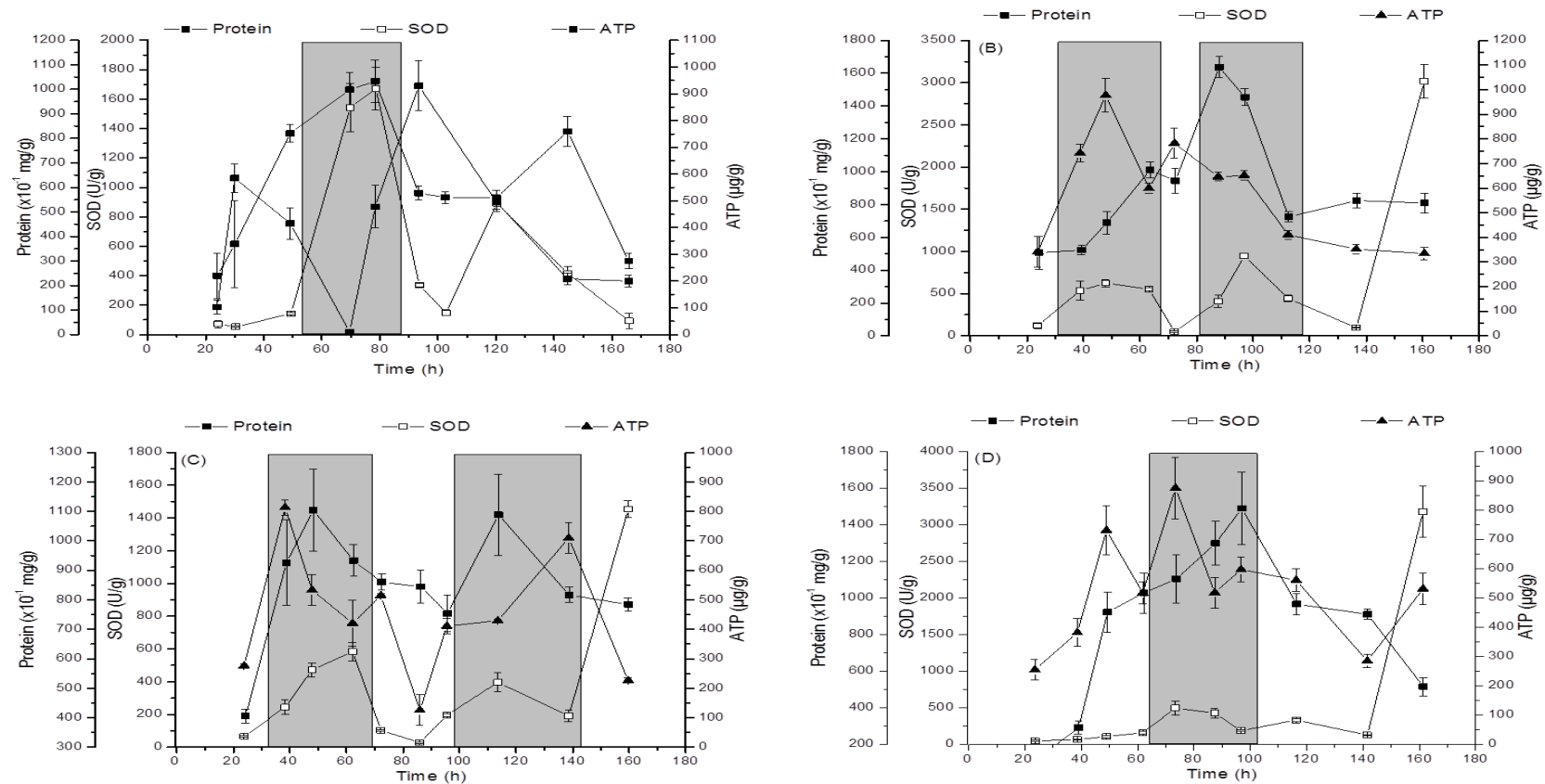


Figure 5-15: Intracellular protein, SOD and ATP concentrations during batch cultivation in a STR of *A. niger* B1-D.

With concentrations of (A) 0, (B) 400, (C) 700 and (D) 1000 μ M of SNP added at 24 hours. The grey areas highlight overlapping periods in the observed parameters. Cultivation conditions were: airflow 2 lpm, 300 rpm, pH 4, temperature 25 $^{\circ}$ C.

Results are expressed as mean \pm stdev.

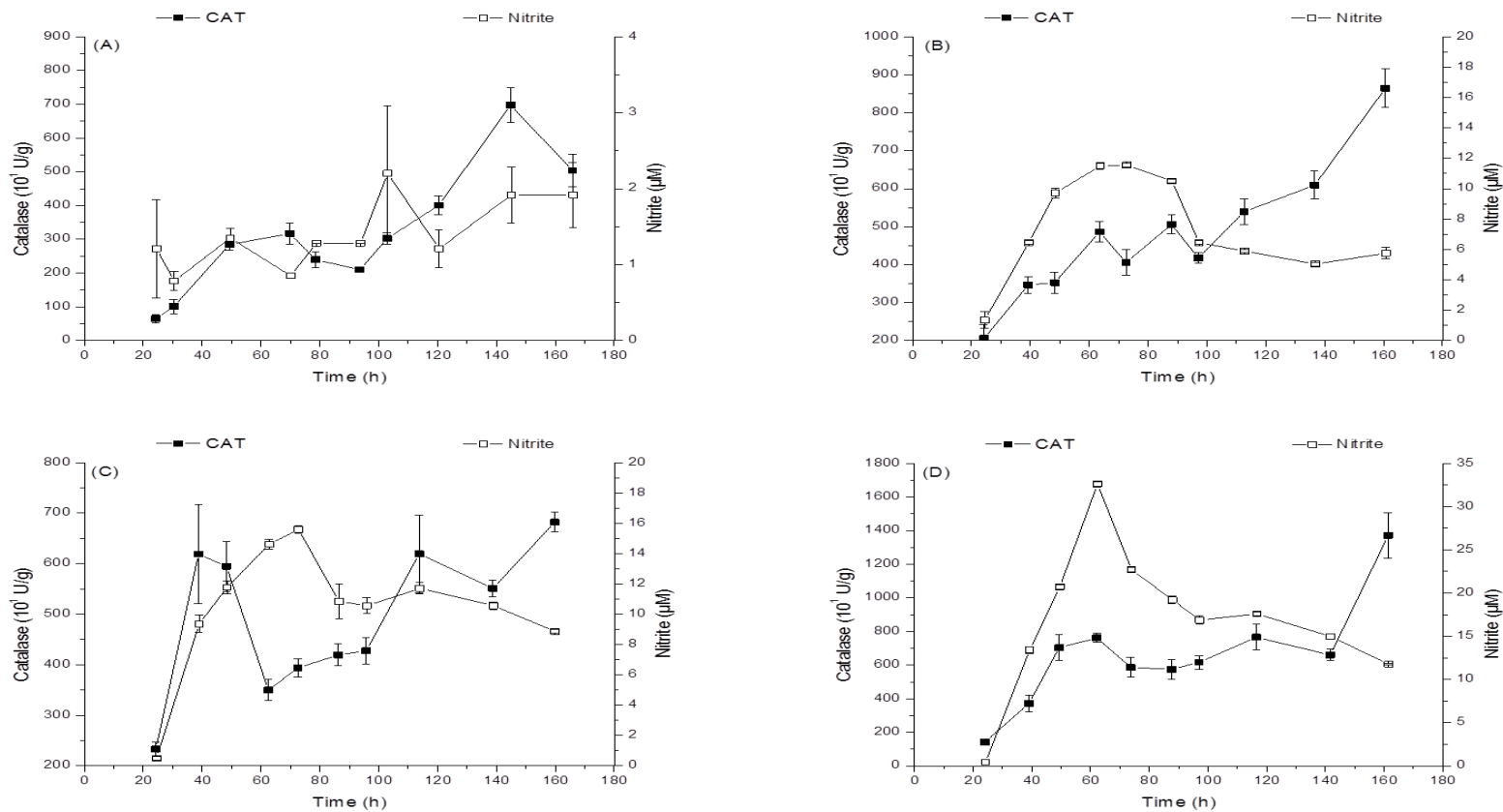


Figure 5-16: CAT and nitrite concentrations during batch cultivation in a STR of *A. niger* B1-D.

With concentrations of (A) 0, (B) 400, (C) 700 and (D) 1000 μ M of SNP added at 24 hours. Cultivation conditions were: airflow 2 lpm, 300 rpm, pH 4, temperature 25 $^{\circ}$ C. Results are expressed as mean \pm stdev.

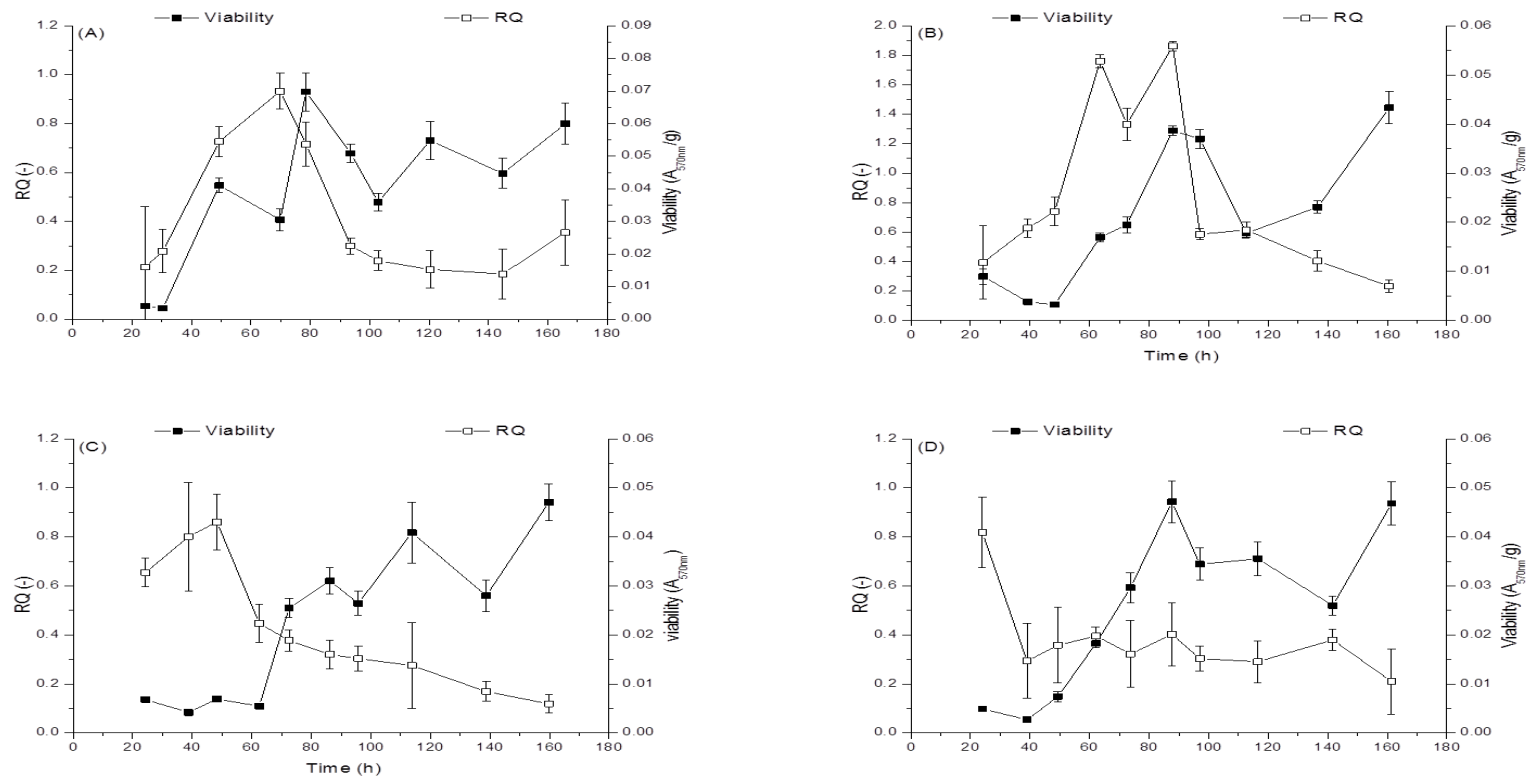


Figure 5-17: Viability and RQ during batch cultivation in a STR of *A. niger* B1-D.

With concentrations of (A) 0, (B) 400, (C) 700 and (D) 1000 μ M of SNP added at 24 hours. Cultivation conditions were: airflow 2 lpm, 300 rpm, pH 4, temperature 25 $^{\circ}$ C. Results are expressed as mean \pm stdev.

5.4 Conclusions

This chapter demonstrates the interaction between SNP and oxidative stress defences. The increased CAT values and SOD values in the first 48 hours of the process confirm this. The Results clearly show that NO reduces oxidative stress levels and increases lysozyme yield. Especially the multi functionality of CAT is clearly linked to nitric oxide release from SNP.

This chapter also shows that at sufficiently low concentrations of SNP there is the possibility of preventing oxidative stress inside reactors when looking at oxidative stress defences, respiration, ATP production, viability, intracellular protein content and lysozyme production, where for lysozyme 700 μM SNP seems to be the optimum concentration for lysozyme production.

Chapter 6

Infrared monitoring of hyphal growth during submerged culture of *Aspergillus niger*

6 Infrared monitoring of hyphal growth during submerged culture of *Aspergillus niger*

6.1 Introduction and aim

Fungal bioprocessing is widely used for the production of biochemicals such as anti-infectives and antibiotics (Vaidyanathan *et al.*, 2003). Submerged culturing of filamentous fungi is characterized by two morphological forms of growth, pelleted and dispersed, usually dependent on culture conditions (McIntyre *et al.*, 2001, Teng *et al.*, 2009). The commercial potential of fungal bioprocessing is considerable, however process control during fermentation of fungal strains is still sub-optimal (Vaidyanathan *et al.*, 2003). The off-line monitoring of process parameters results in a limitation for process control, as it is more time consuming to get the analyses results. This delay limits the ability to interfere with the process when it is not going as expected; for instance faster growth in a fed-batch process would mean starting the feeding earlier however this is mostly limited by the sample interval. Real-time monitoring could increase the accuracy of the starting time of this feeding and potentially increase product yield, thereby increasing profits.

Biomass measurements during fungal cultivation is a key bioprocess parameter, which provides important information on how the bioprocess is progressing. The standard method for fungal biomass analysis is performed off line by filtering a known volume of fermentation broth after which the filters are dried and measured to get a dry cell weight (DCW) (Wongwicharn *et al.*, 1999). Two major drawbacks exist of this method; the first one being morphology and the second one viscosity (see Chapter 2). Online measurement of this parameter would be advantageous, so several spectroscopic techniques such as; dielectric spectroscopy (Kiviharju *et al.*, 2008) and near infrared (NIR) (Nordon *et al.*, 2008, Vaidyanathan *et al.*, 2001b, Vaidyanathan *et al.*, 1999, Vaidyanathan *et al.*, 2001a, Vaidyanathan *et al.*, 2003, Arnold *et al.*, 2001), have been studied in recent years to

develop sensors to monitor biomass growth *in situ*. The challenge with many of these techniques is that it remains difficult to extract the relevant information from complex spectral datasets also the errors associated with the offline measurements are still of the same magnitude as the approach often is to correlate off and online measurements with each other (Arnold *et al.*, 2001).

6.1.1 Aim

The aim of this chapter was to investigate, with an industry partner, whether a simple spectroscopic sensor, the buglab from Applikon (Chapter 2.1), developed with the sole aim of monitoring cell mass, as an indicator of growth could be used to monitor fungal fermentations utilising *Aspergillus niger* B1-D.

6.2 Results

6.2.1 Biomass growth during stirred tank reactor experiments

Figure 6-1 shows all DCW values obtained using different stirrer settings. The inoculum of these processes consists of pellets, which changes to hyphae, as the process proceeds. The stationary phase of each process was reached at approximately 80 hours in each case. The amount of biomass in the stationary phase varied from 12 g/l to 16 g/l.

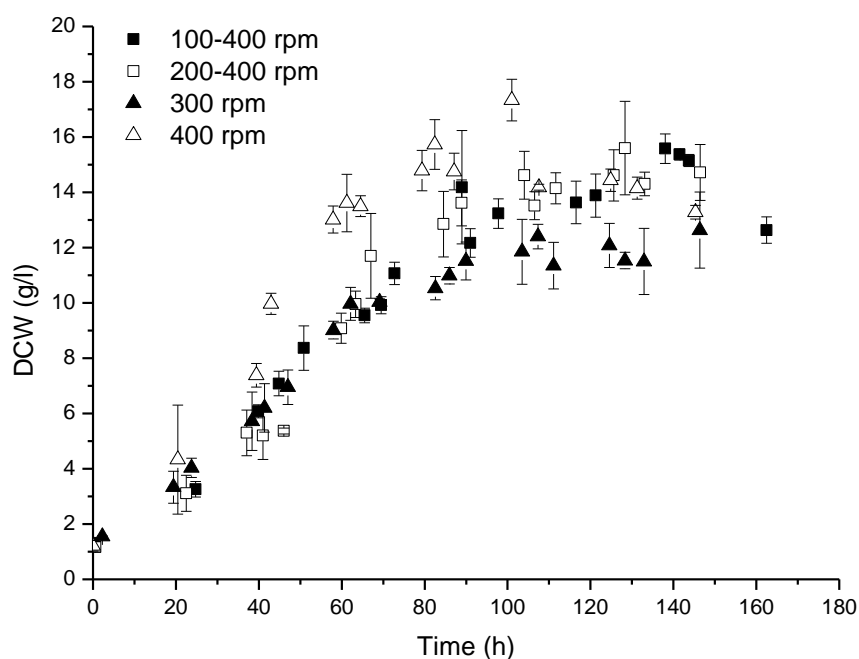


Figure 6-1: DCW values during batch cultivation in a STR of *A. niger* B1-D. Various agitation settings were used, non constant agitation was used to try and maintain a DOT of 25%. Cultivation conditions were: airflow 2 lpm, pH 4, temperature 25 °C. Results are expressed as mean \pm stdev.

6.2.2 Model based on raw data

Figure 6-2 (A) shows that low agitation settings at the start of the process (100 and 200 rpm) result in a constant signal from the buglab, which ranged from 9-12 spectral values (see Chapter 3.1 for an explanation on spectral values) respectively. These constant values did not correspond to the off-line biomass measurements (Figure 6-1). While the experiments with 300 and 400 rpm had signal changes that corresponded more to the off-line measurements of biomass (see Figure 6-1). The processes reached maximum agitation rates at 40 hours (100-400) and 50 hours (200-400) respectively, to maintain a DOT of 25%, at which time signal changes started to occur. These spectral value changes corresponded more closely to the offline measurements done for biomass.

The obtained DCW values were plotted against the spectral values (Figure 6-2 (B)) from the sensor after which a logistic model (with Origin 8.6) was fitted through the results. A logistic fit equation is commonly used for modeling biomass growth during fermentation (see Chapter 3.4 for the equation) (Lopez *et al.*, 2004). The R^2 of the model to the calibration values is 0.96 suggesting a good fit of the model to the plotted data.

After the model was developed, a validation run was performed to see how well the model predicted and fitted to the DCW values obtained during cultivation of *A. niger B1-D* utilising different agitation settings compared to the other processes. Figure 6-3 (A) shows these results. The DCW values and the predicted model values start to converge at around 50 hours which corresponds with a DCW value of around 7 g/l.

As the sensor response should be linear with changes in biomass DCW off-line measurements of biomass were plotted against the predicted DVW values calculated using the model equation determined, previously. Figure 6-3 (B) shows that by using linear regression the predicted and practical values are linear with an R^2 of 0.98.

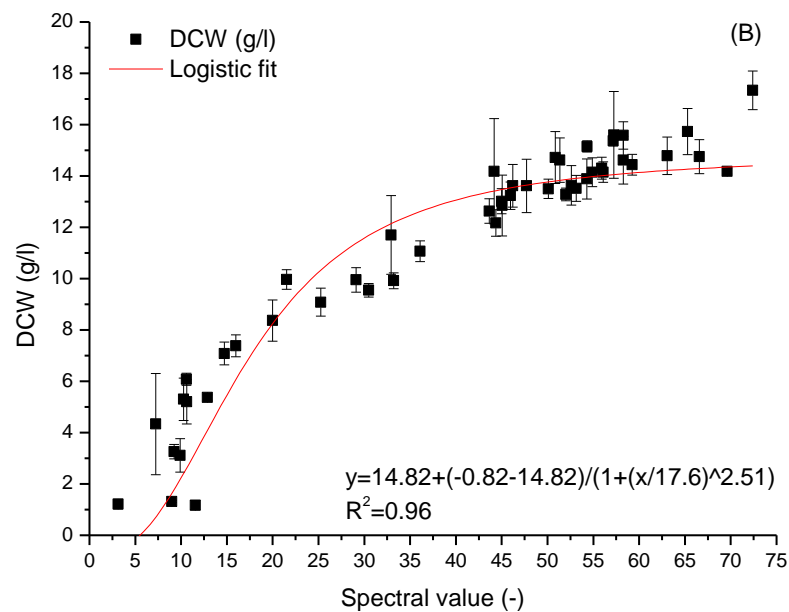
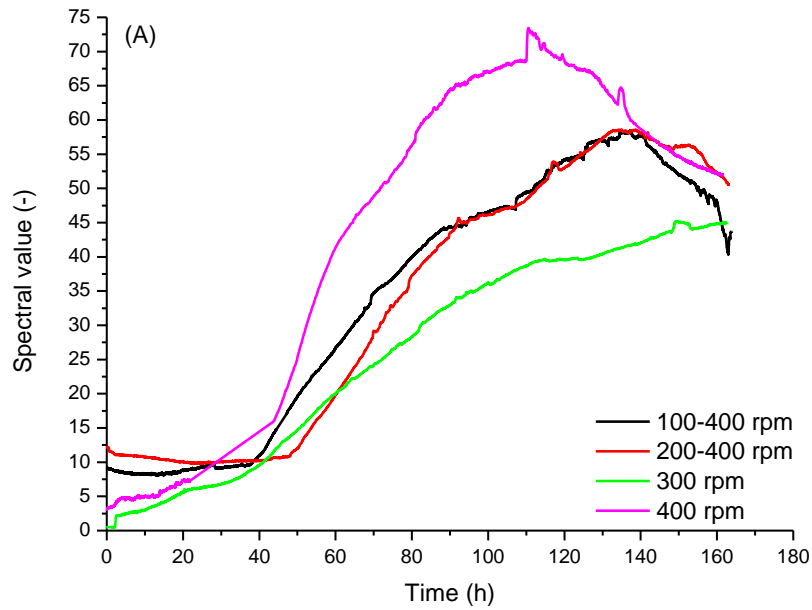


Figure 6-2: Spectral values against time (A) and DCW plotted against corresponding spectral values (B) during batch cultivation of *A. niger* B1-D in an STR.

Various agitation settings were used, non constant agitation was used to try and maintain a DOT of 25%. Cultivation conditions were: airflow 2 lpm, pH 4, temperature 25 °C. Results are expressed as mean ± stdev.

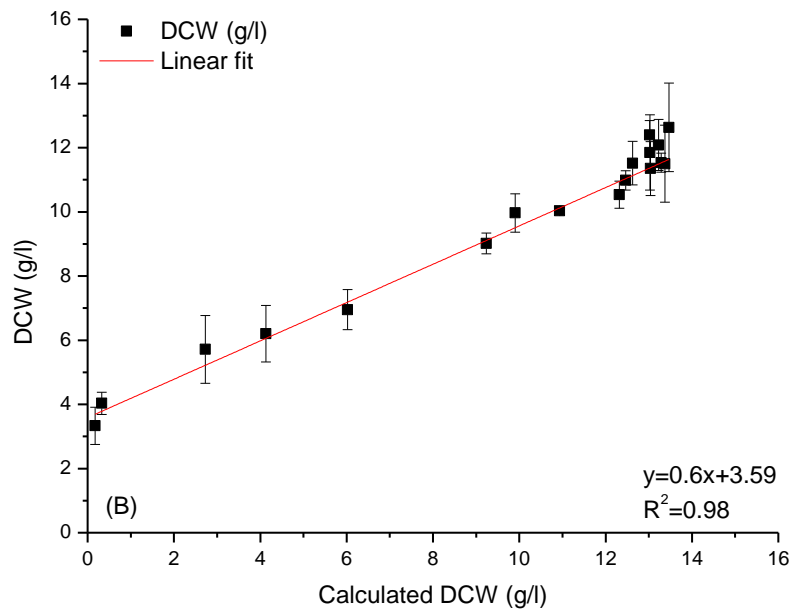
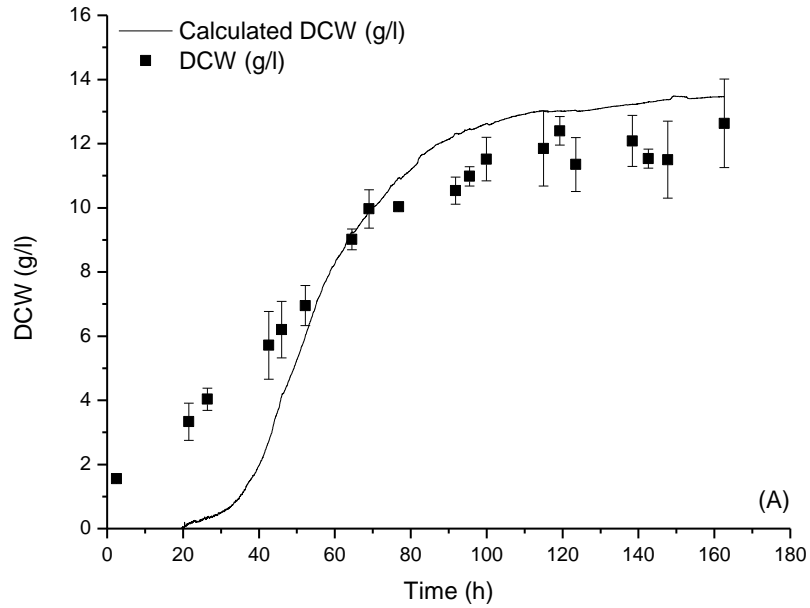


Figure 6-3: Measured DCW and predicted model values against time (A) and measured DCW values plotted against calculated DCW values (B) during batch cultivation *A. niger* B1-D in a STR.

Various agitation settings were used, non constant agitation was used to try and maintain a DOT of 25%. Cultivation conditions were: airflow 2 lpm, pH 4, temperature 25 °C. Results are expressed as mean \pm stdev.

6.3 Discussion

The high baseline spectral values of the 100-400 and 200-400 rpm processes (Figure 6-2 (A)) are most likely caused by the passing of pellets over the sensor, which can be influenced by the agitation rate inside the reactor. The spectral values in these experiments start increasing as the agitation rate reaches its maximum value as opposed to the 300 and 400 rpm processes that show a gradual increase in spectral values. Two reasons can be thought of that might cause this. According to the manual the sensor is slightly sensitive to bubble interference and as bubbles are larger at lower stirring settings this might have caused the increased signal, however some small tests were done with just water to see if signal changes did occur and no large signal changes were observed when agitations speeds were varied (settings that were used varies from 100 to 400 rpm). Another reason for these high baseline values can be; the residence time of pellets in front of the buglab sensor. The buglab sensor measures the absorbance of laser light over a surface using multiple laser sources. When the process starts the reactor is filled with pellets so the residence time in front of the sensor is higher for lower agitation rates compared to higher agitation settings. This might have resulted in a higher average signal, processing times of these types of sensors are in the millisecond range, which is likely faster than the residence time of the pellets in front of the sensor, and could therefore explain the high baseline values that were recorded during the 100-400 and 200-400 rpm processes.

According to the manufacturer of this sensor it should start giving correct biomass values at around 10 g/l for standard microbial fermentations such as *Escherichia coli* and *Saccharomyces cerevisiae*. The results obtained here clearly show accurate predictions of *A. niger B1-D* fermentations to start from 7 g/l.

6.4 Conclusions

This chapter shows that, based on the linearity between offline DCW values and calculated DCW values ($R^2=0.98$), the Buglab can be used to accurately predict fungal biomass growth of *Aspergillus niger* B1-D from 7 g/l onwards.

Chapter 7

Discussion, Conclusions and Future work

7 Discussion, Conclusions and Future Work

7.1 Discussion

The described studies here focus on physiological effects on *A. niger B1-D* of addition of polymyxin B, variation of stirring rate, addition of sodium nitroprusside and a study on using a new online monitor system to study hyphal growth online. Previous work has indicated a highly complex physiological response to oxidative stress in bioreactors and this work continues to study oxidative stress response further.

The addition of polymyxin B clearly results in higher oxidative stress conditions for *A. niger B1-D*. This was shown by the increased activity of oxidative stress enzymes, catalase and superoxide dismutase. An increased oxygen uptake, shown by increased OUR values, of the biomass also indicates this. This might be a result of (partial) blocking of NADH dehydrogenase resulting in more oxidative stress by a higher utilisation of the main respiratory pathway.

Varying process parameters such as stirring has a big impact on product yields, in the case of *A. niger B1-D* and its main product lysozyme. The increased agitation rate at the start of the fermentation resulted in too much oxidative stress, as was shown by the increased CAT and decreased SOD activity. This was a direct result of the higher OTR caused by the increased agitation rate. The interesting result in this part of the presented studies is that a lower agitation setting doesn't necessary result in an optimum yield of lysozyme. Therefore the main respiratory pathway has to be utilised sufficiently to reach an optimum process outcome.

The addition of a known nitric oxide donor to a fermentation of *A. niger B1-D* results in a decrease of oxidative stress, caused by the reaction between the superoxide anion and nitric oxide that can result in peroxynitrite, shown by the increased CAT activity. The decrease in oxidative stress results in an

increase in lysozyme production. The addition of sodium nitroprusside also results in what is most likely anaerobic respiration caused by the diffusion of nitric oxide into the fungal cells. The result is a decrease in ammonium uptake, showing a potential interaction between aerobic and anaerobic respiration (see Figure 1-6).

The use of an online sensor to monitor biomass results in proper online monitoring from 7 g/l onwards. The most likely reason for the incorrect spectral values at the start of a fermentation are caused by fungal morphology as a larger part of the sensor area is covered by these fungal pellets. This can disturb the signal processing because the frequency at which the signal is read might be lower than the residence time of the pellet in front of the sensor.

7.2 Conclusions

The described studies in this thesis have led to a number of conclusions and new insights that can be used to formulate new ideas:

- Polymyxin B increases oxidative stress in *A. niger* B1-D.
- Process control settings controlling the oxygen transfer rate during the lag phase of the fermentation are essential to get desirable process outcomes and the undesirable process outcomes are linked to oxidative stress levels.
- The optimum agitation setting for the system used for this system was 200-400 rpm.
- Catalase has clearly been shown to be multi functional, as is shown by the increases in activities that directly corresponded to the increasing amounts of sodium nitroprusside.
- At low concentrations sodium nitroprusside can be used to increase lysozyme production and a final reactor concentration of 700 μ M

seems to be the optimum concentration in the case presented in this thesis.

- The Buglab is capable of monitoring biomass growth of *A. niger* B1-D from 7 g/l onwards.

7.3 Future Work

Alternative pathway

A few examples from literature suggest that fungi are able to reduce metals into nanoparticle. Examples have been found where the fungus *Verticillium* was able to reduce Ag⁺ ions into nanoparticles (Mukherjee et al., 2001a, Mukherjee et al., 2001b). This formation was done below the cell surface. Literature suggest that the same thing is possible for AuCl₄⁻ ions (Mukherjee et al., 2001b). A thesis report also mentioned the ability of *Aspergillus niger* to reduce gold chloride into gold nanoparticles and store them in the cell wall (Samuel, 2005).

Various spectroscopic measurements can measure these particles. The optical properties of these nanoparticles changes with temperature (increases or decreases) that cause changes that can be measured. This might clarify how much heat is generated when the alternative pathway is being utilised.

Chapter 3

To conclusively show that polymyxin B (partially) blocks NADH dehydrogenase, this enzyme needs to be measured directly during. Repeating the same experiments shown in Chapter 3.

Chapter 4

At the moment most results relating to oxidative stress; in literature, from predecessors and in this thesis have been obtained in relative small scale

experiments, including these set of experiments. It would be highly interesting to see how results; obtained here and from previous studies, translate into larger scale experiments. A volume that is usually utilised before production scale is a 100 liter.

Chapter 5

This set of experiments had SNP as a nitric oxide donor, while the chapter clearly showed that nitrite was the cause for the results obtained here. A way forward would be to look at the effect of increasing amounts of nitrite during fungal cultivation, while monitoring nitric oxide using a more direct method if there is one available.

Chapter 6

This series could be expanded by applying a fed-batch control, based on the amount of biomass present inside the reactor. This would reduce, or keep constant, fluid viscosity thereby enhancing oxygen transfer properties inside the reactor. This could decrease oxidative stress by oxidative shocks when fungal biomass goes from oxygen depleted parts of the reactor to oxygen rich part of the reactor.

Chapter 8

References

8 References

- ABRASHEV, R., DOLASHKA, P., CHRISTOVA, R., STEFANOVA, L. & ANGELOVA, M. (2005) Role of antioxidant enzymes in survival of conidiospores of *Aspergillus niger* 26 under conditions of temperature stress. *Journal of Applied Microbiology*, 99, 902-909.
- AEBI, H. (1984) Catalase invitro. *Methods in Enzymology*, 105, 121-126.
- ALMEIDA, B., BUTTNER, S., OHLMEIER, S., SILVA, A., MESQUITA, A., SAMPAIO-MARQUES, B., OSORIO, N. S., KOLLAU, A., MAYER, B., LEO, C., LARANJINHA, J., RODRIGUES, F., MADEO, F. & LUDOVICO, P. (2007) NO-mediated apoptosis in yeast. *Journal of Cell Science*, 120, 3279-3288.
- ALVAREZ-VASQUEZ, F., GONZALEZ-ALCON, C. & TORRES, N. V. (2000) Metabolism of citric acid production by *Aspergillus niger*: Model definition, steady-state analysis and constrained optimization of citric acid production rate. *Biotechnology and Bioengineering*, 70, 82-108.
- AMANULLAH, A., CHRISTENSEN, L. H., HANSEN, K., NIENOW, A. W. & THOMAS, C. R. (2002) Dependence of morphology on agitation intensity in fed-batch cultures of *Aspergillus oryzae* and its implications for recombinant protein production. *Biotechnology and Bioengineering*, 77, 815-826.
- ANGELOVA, M., DOLASHKA-ANGELOVA, P., IVANOVA, E., SERKEDJIEVA, J., SLOKOSKA, L., PASHOVA, S., TOSHKOVA, R., VASSILEV, S., SIMEONOV, I., HARTMANN, H. J., STOEVA, S., WESER, U. & VOELTER, W. (2001) A novel glycosylated Cu/Zn-containing superoxide dismutase: production and potential therapeutic effect. *Microbiology-Sgm*, 147, 1641-1650.
- ANGELOVA, M. B., PASHOVA, S. B. & SLOKOSKA, L. S. (2000) Comparison of antioxidant enzyme biosynthesis by free and

immobilized *Aspergillus niger* cells. *Enzyme and Microbial Technology*, 26, 544-549.

ANGELOVA, M. B., PASHOVA, S. B., SPASOVA, B. K., VASSILEV, S. V. & SLOKOSKA, L. S. (2005) Oxidative stress response of filamentous fungi induced by hydrogen peroxide and paraquat. *Mycological Research*, 109, 150-158.

APLIKON BE2100 Noninvasive Biomass Monitor. Aplikon.

ARCHER, D. B., JEENES, D. J. & MACKENZIE, D. A. (1994) Strategies for improving heterologous protein-production from filamentous fungi. *Antonie Van Leeuwenhoek International Journal of General and Molecular Microbiology*, 65, 245-250.

ARCHER, D. B., JEENES, D. J., MACKENZIE, D. A., BRIGHTWELL, G., LAMBERT, N., LOWE, G., RADFORD, S. E. & DOBSON, C. M. (1990) Hen egg-white lysozyme expressed in, and secreted from *Aspergillus-niger* is correctly processed and folded. *Bio-Technology*, 8, 741-745.

ARGUELLES, J. C. (2000) Physiological roles of trehalose in bacteria and yeasts: a comparative analysis. *Archives of Microbiology*, 174, 217-224.

ARNOLD, S. A., MATHESON, L., HARVEY, L. M. & MCNEIL, B. (2001) Temporally segmented modelling: a route to improved bioprocess monitoring using near infrared spectroscopy? *Biotechnology Letters*, 23, 143-147.

AYAR-KAYALI, H. & TARHAN, L. (2004) The effect of cultural conditions on the variations of SOD, CAT and GSH-Px activities and LPO levels in the filamentous fungus *Fusarium equiseti*. *Turkish Journal of Chemistry*, 28, 213-222.

- BAI, Z. H., HARVEY, L. M. & MCNEIL, B. (2003) Physiological responses of chemostat cultures of *Aspergillus niger* (B1-D) to simulated and actual oxidative stress. *Biotechnology and Bioengineering*, 82, 691-701.
- BAI, Z. H., HARVEY, L. M., WHITE, S. & MCNEIL, B. (2004) Effects of oxidative stress on production of heterologous and native protein, and culture morphology in batch and chemostat cultures of *Aspergillus niger* (B1-D). *Enzyme and Microbial Technology*, 34, 10-21.
- BELO, I., PINHEIRO, R. & MOTA, M. (2003) Fed-batch cultivation of *Saccharomyces cerevisiae* in a hyperbaric bioreactor. *Biotechnology Progress*, 19, 665-671.
- BHARGAVA, S., NANDAKUMAR, M. P., ROY, A., WENGER, K. S. & MARTEN, M. R. (2003) Pulsed feeding during fed-batch fungal fermentation leads to reduced viscosity without detrimentally affecting protein expression. *Biotechnology and Bioengineering*, 81, 341-347.
- BHATTACHARJEE, A., MAJUMDAR, U., MAITY, D., SARKAR, T. S., GOSWAMI, A. M., SAHOO, R. & GHOSH, S. (2010) Characterizing the effect of nitrosative stress in *Saccharomyces cerevisiae*. *Archives of Biochemistry and Biophysics*, 496, 109-116.
- BLOKHINA, O. & FAGERSTEDT, K. V. (2010) Reactive oxygen species and nitric oxide in plant mitochondria: origin and redundant regulatory systems. *Physiologia Plantarum*, 138, 447-462.
- BLOKHINA, O., VIROLAINEN, E. & FAGERSTEDT, K. V. (2003) Antioxidants, oxidative damage and oxygen deprivation stress: a review. *Annals of Botany*, 91, 179-194.
- BRADFORD, M. M. (1976) Rapid and sensitive method for quantitation of microgram quantities of protein utilizing principle of protein-dye binding. *Analytical Biochemistry*, 72, 248-254.

- BRANDES, N., RINCK, A., LEICHERT, L. I. & JAKOB, U. (2007) Nitrosative stress treatment of *E-coli* targets distinct set of thiol-containing proteins. *Molecular Microbiology*, 66, 901-914.
- BROWN, A. J. P., HAYNES, K. & QUINN, J. (2009) Nitrosative and oxidative stress responses in fungal pathogenicity. *Current Opinion in Microbiology*, 12, 384-391.
- BROWN, G. C. (2001) Regulation of mitochondrial respiration by nitric oxide inhibition of cytochrome c oxidase. *Biochimica Et Biophysica Acta-Bioenergetics*, 1504, 46-57.
- BRYAN, N. S. & GRISHAM, M. B. (2007) Methods to detect nitric oxide and its metabolites in biological samples. *Free Radical Biology and Medicine*, 43, 645-657.
- BUCKOVA, M., GODOCIKOVA, J., SIMONOVICOVA, A. & POLEK, B. (2005) Production of catalases by *Aspergillus niger* isolates as a response to pollutant stress by heavy metals. *Current Microbiology*, 50, 175-179.
- CADENAS, E. & DAVIES, K. J. A. (2000) Mitochondrial free radical generation, oxidative stress, and aging. *Free Radical Biology and Medicine*, 29, 222-230.
- CARLILE, M. J. & WATKINSON, S. C. (Eds.) (1997) *The Fungi*, London, Academic Press Limited.
- CARPENTE.JH (1966) New measurements of oxygen solubility in pure and natural water. *Limnology and Oceanography*, 11, 264-&.
- CERVERA, A. E., PETERSEN, N., LANTZ, A. E., LARSEN, A. & GERNAEY, K. V. (2009) Application of Near-Infrared Spectroscopy for Monitoring and Control of Cell Culture and Fermentation. *Biotechnology Progress*, 25, 1561-1581.

- CHAVEZ, R., ROA, A., NAVARRETE, K., TREBOTICH, J., ESPINOSA, Y. & VACA, I. (2010) Evaluation of properties of several cheese-ripening fungi for potential biotechnological applications. *Mycoscience*, 51, 84-87.
- CHENG, J.-S., QIAO, B. & YUAN, Y.-J. (2008) Comparative proteome analysis of robust *Saccharomyces cerevisiae* insights into industrial continuous and batch fermentation. *Applied Microbiology and Biotechnology*, 81, 327-338.
- CHIANG, K. T., SWITZER, C. H., AKALI, K. O. & FUKUTO, J. M. (2000) The role of oxygen and reduced oxygen species in nitric oxide-mediated cytotoxicity: Studies in the yeast *Saccharomyces cerevisiae* model system. *Toxicology and Applied Pharmacology*, 167, 30-36.
- COSTA, V. & MORADAS-FERREIRA, P. (2001) Oxidative stress and signal transduction in *Saccharomyces cerevisiae*: Insights into ageing, apoptosis and diseases. *Molecular Aspects of Medicine*, 22, 217-246.
- CRAPO, J. D., MCCORD, J. M. & FRIDOVICH, I. (1978) Preparation and assay of superoxide dismutases. *Methods Enzymol*, 53, 382-93.
- CRAWFORD, N. M. & GUO, F. (2005) New insights into nitric oxide metabolism and regulatory functions. *Trends in Plant Science*, 10, 195-200.
- DALLE-DONNE, I., ROSSI, R., GIUSTARINI, D., MILZANI, A. & COLOMBO, R. (2003) Protein carbonyl groups as biomarkers of oxidative stress. *Clinica Chimica Acta*, 329, 23-38.
- DE JESUS-BERRIOS, M., LIU, L. M., NUSSBAUM, J. C., COX, G. M., STAMLER, J. S. & HEITMAN, J. (2003) Enzymes that counteract nitrosative stress promote fungal virulence. *Current Biology*, 13, 1963-1968.

- DELLOMONACO, C., AMARETTI, A., ZANONI, S., POMPEI, A., MATTEUZZI, D. & ROSSI, M. (2007) Fermentative production of superoxide dismutase with *Kluyveromyces marxianus*. *Journal of Industrial Microbiology & Biotechnology*, 34, 27-34.
- DOUKI, T. & CADET, J. (1996) Peroxynitrite mediated oxidation of purine bases of nucleosides and isolated DNA. *Free Radical Research*, 24, 369-380.
- DUARTE, M., PETERS, M., SCHULTE, U. & VIDEIRA, A. (2003) The internal alternative NADH dehydrogenase of *Neurospora crassa* mitochondria. *Biochemical Journal*, 371, 1005-1011.
- EISERICH, J. P., PATEL, R. P. & O'DONNELL, V. B. (1998) Pathophysiology of nitric oxide and related species: Free radical reactions and modification of biomolecules. *Molecular Aspects of Medicine*, 19, 221-357.
- EL-ENSHASY, H., KLEINE, J. & RINAS, U. (2006) Agitation effects on morphology and protein productive fractions of filamentous and pelleted growth forms of recombinant *Aspergillus niger*. *Process Biochemistry*, 41, 2103-2112.
- EMRI, T., MOLNAR, Z. & POCSI, I. (2005) The appearances of autolytic and apoptotic markers are concomitant but differently regulated in carbon-starving *Aspergillus nidulans* cultures. *FEMS Microbiology Letters*, 251, 297-303.
- EMRI, T., MOLNAR, Z., SZILAGYI, M. & POCSI, I. (2008) Regulation of Autolysis in *Aspergillus nidulans*. *Applied Biochemistry and Biotechnology*, 151, 211-220.
- FILLINGER, S., CHAVEROCHE, M. K., VAN DIJCK, P., DE VRIES, R., RUIJTER, G., THEVELEIN, J. & D'ENFERT, C. (2001) Trehalose is required for the acquisition of tolerance to a variety of stresses in the

- filamentous fungus *Aspergillus nidulans*. *Microbiology-Sgm*, 147, 1851-1862.
- FINKELSTEIN, D. B. (1987) Improvement of enzyme-production in *Aspergillus*. *Antonie Van Leeuwenhoek Journal of Microbiology*, 53, 349-352.
- GARCIA-OCHOA, F. & GOMEZ, E. (2009) Bioreactor scale-up and oxygen transfer rate in microbial processes: An overview. *Biotechnology Advances*, 27, 153-176.
- GASTON, B. (1999) Nitric oxide and thiol groups. *Biochimica Et Biophysica Acta-Bioenergetics*, 1411, 323-333.
- GEBICKA, L. & DIDIK, J. (2009) Catalytic scavenging of peroxynitrite by catalase. *Journal of Inorganic Biochemistry*, 103, 1375-1379.
- GISHEN, M., DAMBERGS, R. G. & COZZOLINO, D. (2005) Grape and wine analysis - enhancing the power of spectroscopy with chemometrics. A review of some applications in the Australian wine industry. *Australian Journal of Grape and Wine Research*, 11, 296-305.
- GIULIVI, C., BOVERIS, A. & CADENAS, E. (1995) Hydroxyl radical generation during mitochondrial electron-transfer and the formation of 8-hydroxydesoxyguanosine in mitochondrial-DNA. *Archives of Biochemistry and Biophysics*, 316, 909-916.
- GONG, X., FU, Y., JIANG, D., LI, G., YI, X. & PENG, Y. (2007) L-arginine is essential for conidiation in the filamentous fungus *Coniothyrium minitans*. *Fungal Genetics and Biology*, 44, 1368-1379.
- GRIFFIN, B. (2011) Stress in Filamentous Fungi. *BSc thesis, Strathclyde Institute of Pharmacy and Biomedical Sciences*. Glasgow, University of Strathclyde.

- HALLIWELL, B. & GUTTERIDGE, J. M. C. (Eds.) (1985) *Free radicals in biology and medicine*, Oxford, Oxford University Press Inc. .
- HAUPTMANN, N., GRIMSBY, J., SHIH, J. C. & CADENAS, E. (1996) The metabolism of tyramine by monoamine oxidase A/B causes oxidative damage to mitochondrial DNA. *Archives of Biochemistry and Biophysics*, 335, 295-304.
- HAUSLADEN, A., GOW, A. J. & STAMLER, J. S. (1998) Nitrosative stress: Metabolic pathway involving the flavohemoglobin. *Proceedings of the National Academy of Sciences of the United States of America*, 95, 14100-14105.
- HIGGINS, V. J., BECKHOUSE, A. G., OLIVER, A. D., ROGERS, P. J. & DAWES, I. W. (2003) Yeast genome-wide expression analysis identifies a strong ergosterol and oxidative stress response during the initial stages of an industrial lager fermentation. *Applied and Environmental Microbiology*, 69, 4777-4787.
- HOFRICHTER, M., ULLRICH, R., PECYNA, M. J., LIERS, C. & LUNDELL, T. (2010) New and classic families of secreted fungal heme peroxidases. *Applied Microbiology and Biotechnology*, 87, 871-897.
- HUANG, J. M., KIM-SHAPIRO, D. B. & KING, S. B. (2004) Catalase-mediated nitric oxide formation from hydroxyurea. *Journal of Medicinal Chemistry*, 47, 3495-3501.
- HWANG, S. C., LIN, C. S., CHEN, I. M., CHEN, J. M., LIU, L. Y. & DODDS, W. K. (2004) Removal of multiple nitrogenous wastes by *Aspergillus niger* in a continuous fixed-slab reactor. *Bioresource Technology*, 93, 131-138.
- IMLAY, J. A. (1995) A metabolic enzyme that rapidly produces superoxide, fumarate reductase of *Escherichia coli*. *Journal of Biological Chemistry*, 270, 19767-19777.

- IMLAY, J. A. & LINN, S. (1988) DNA damage and oxygen radical toxicity. *Science*, 240, 1302-1309.
- INOUE, Y., MATSUDA, T., SUGIYAMA, K., IZAWA, S. & KIMURA, A. (1999) Genetic analysis of glutathione peroxidase in oxidative stress response of *Saccharomyces cerevisiae*. *Journal of Biological Chemistry*, 274, 27002-27009.
- IZAWA, S., INOUE, Y. & KIMURA, A. (1996) Importance of catalase in the adaptive response to hydrogen peroxide: Analysis of acatalasaemic *Saccharomyces cerevisiae*. *Biochemical Journal*, 320, 61-67.
- IZAWA, S., MAEDA, K., MIKI, T., MANO, J., INOUE, Y. & KIMURA, A. (1998) Importance of glucose-6-phosphate dehydrogenase in the adaptive response to hydrogen peroxide in *Saccharomyces cerevisiae*. *Biochemical Journal*, 330, 811-817.
- JAKUBOWSKI, W., BILINSKI, T. & BARTOSZ, G. (2000) Oxidative stress during aging of stationary cultures of the yeast *Saccharomyces cerevisiae*. *Free Radical Biology and Medicine*, 28, 659-664.
- JOSEPH-HORNE, T., HOLLOMON, D. W. & WOOD, P. M. (2001) Fungal respiration: a fusion of standard and alternative components. *Biochimica Et Biophysica Acta-Bioenergetics*, 1504, 179-195.
- KAWASAKI, L. & AGUIRRE, J. (2001) Multiple catalase genes are differentially regulated in *Aspergillus nidulans*. *Journal of Bacteriology*, 183, 1434-1440.
- KAWASAKI, L., WYSONG, D., DIAMOND, R. & AGUIRRE, J. (1997) Two divergent catalase genes are differentially regulated during *Aspergillus nidulans* development and oxidative stress. *Journal of Bacteriology*, 179, 3284-3292.

- KAYALI, H. A. & TARHAN, L. (2005) Variations in metal uptake, antioxidant enzyme response and membrane lipid peroxidation level in *Fusarium equiseti* and *F-acuminatum*. *Process Biochemistry*, 40, 1783-1790.
- KIVIHARJU, K., SALONEN, K., MOILANEN, U. & EERIKAINEN, T. (2008) Biomass measurement online: the performance of in situ measurements and software sensors. *Journal of Industrial Microbiology & Biotechnology*, 35, 657-665.
- KREINER, M., HARVEY, L. M. & MCNEIL, B. (2002) Oxidative stress response of a recombinant *Aspergillus niger* to exogenous menadione and H₂O₂ addition. *Enzyme and Microbial Technology*, 30, 346-353.
- KREINER, M., HARVEY, L. M. & MCNEIL, B. (2003) Morphological and enzymatic responses of a recombinant *Aspergillus niger* to oxidative stressors in chemostat cultures. *Journal of Biotechnology*, 100, 251-260.
- KREINER, M., MCNEIL, B. & HARVEY, L. M. (2000) "Oxidative stress" response in submerged cultures of a recombinant *Aspergillus niger* (B1-D). *Biotechnology and Bioengineering*, 70, 662-669.
- KRUMOVA, E. Z., PASHOVA, S. B., DOLASHKA-ANGELOVA, P. A., STEFANOVA, T. & ANGELOVA, M. B. (2009) Biomarkers of oxidative stress in the fungal strain *Humicola lutea* under copper exposure. *Process Biochemistry*, 44, 288-295.
- KUBICEK, C. P., ZEHENTGRUBER, O., ELKALAK, H. & ROHR, M. (1980) Regulation of citric-acid production by oxygen-effect of dissolved-oxygen tension on adenylate levels and respiration in *Aspergillus-niger*. *European Journal of Applied Microbiology and Biotechnology*, 9, 101-115.

- KUO, W. N., KREHLING, J. M., SHANBHAG, V. P., SHANBHAG, P. P. & MEWAR, M. (2000) Protein nitration. *Molecular and Cellular Biochemistry*, 214, 121-129.
- LAZAR, E. E., WILLS, R. B. H., HO, B. T., HARRIS, A. M. & SPOHR, L. J. (2008) Antifungal effect of gaseous nitric oxide on mycelium growth, sporulation and spore germination of the postharvest horticulture pathogens, *Aspergillus niger*, *Monilinia fructicola* and *Penicillium italicum*. *Letters in Applied Microbiology*, 46, 688-692.
- LE ROES-HILL, M., KHAN, N. & BURTON, S. G. (2010) Actinobacterial Peroxidases: an Unexplored Resource for Biocatalysis. *Applied Biochemistry and Biotechnology*, 164, 681-713.
- LI, B., FU, Y. P., JIANG, D. H., XIE, J. T., CHENG, J. S., LI, G. Q., HAMID, M. I. & YI, X. H. (2010a) Cyclic GMP as a Second Messenger in the Nitric Oxide-Mediated Conidiation of the Mycoparasite *Coniothyrium minitans*. *Applied and Environmental Microbiology*, 76, 2830-2836.
- LI, Q. (2008) Oxidative stress in recombinant *Aspergillus niger* B1-D. *PhD thesis, Strathclyde Institute of Pharmacy and Biomedical Sciences*. Glasgow, University of Strathclyde.
- LI, Q., ABRASHEV, R., HARVEY, L. M. & MCNEIL, B. (2008a) Oxidative stress-associated impairment of glucose and ammonia metabolism in the filamentous fungus, *Aspergillus niger* B1-D. *Mycological Research*, 112, 1049-1055.
- LI, Q., BAI, Z., O'DONNELL, A., HARVEY, L. M., HOSKISSON, P. A. & MCNEIL, B. (2010b) Oxidative stress in fungal fermentation processes: the roles of alternative respiration. *Biotechnology Letters*, 33, 457-467.

- LI, Q., HARVEY, L. M. & MCNEIL, B. (2008b) The effects of bioprocess parameters on extracellular proteases in a recombinant *Aspergillus niger* B1-D. *Applied Microbiology and Biotechnology*, 78, 333-341.
- LI, Q., HARVEY, L. M. & MCNEIL, B. (2008c) The effects of elevated process temperature on the protein carbonyls in the filamentous fungus, *Aspergillus niger* B1-D. *Process Biochemistry*, 43, 877-881.
- LI, Q., HARVEY, L. M. & MCNEIL, B. (2008d) Oxygen enrichment effects on protein oxidation, proteolytic activity and the energy status of submerged batch cultures of *Aspergillus niger* B1-D. *Process Biochemistry*, 43, 238-243.
- LI, Q., HARVEY, L. M. & MCNEIL, B. (2009) Oxidative stress in industrial fungi. *Critical Reviews in Biotechnology*, 29, 199-213.
- LI, Q., MCNEIL, B. & HARVEY, L. M. (2008e) Adaptive response to oxidative stress in the filamentous fungus *Aspergillus niger* B1-D. *Free Radical Biology and Medicine*, 44, 394-402.
- LI, Z. J., SHUKLA, V., WENGER, K. S., FORDYCE, A. P., PEDERSEN, A. G. & MARTEN, M. R. (2002) Effects of increased impeller power in a production-scale *Aspergillus oryzae* fermentation. *Biotechnology Progress*, 18, 437-444.
- LOPEZ, J. L. C., PEREZ, J. A. S., SEVILLA, J. M. F., PORCEL, E. M. R. & CHISTI, Y. (2005) Pellet morphology, culture rheology and lovastatin production in cultures of *Aspergillus terreus*. *Journal of Biotechnology*, 116, 61-77.
- LOPEZ, S., PRIETO, M., DIJKSTRA, J., DHANOA, M. S. & FRANCE, J. (2004) Statistical evaluation of mathematical models for microbial growth. *International Journal of Food Microbiology*, 96, 289-300.

- LUNDBERG, J. O. & WEITZBERG, E. (2005) NO generation from nitrite and its role in vascular control. *Arteriosclerosis Thrombosis and Vascular Biology*, 25, 915-922.
- LUSHCHAK, V. I. (2011) Adaptive response to oxidative stress: Bacteria, fungi, plants and animals. *Comparative Biochemistry and Physiology C-Toxicology & Pharmacology*, 153, 175-190.
- MARNETT, L. J. (2000) Oxyradicals and DNA damage. *Carcinogenesis*, 21, 361-370.
- MARTINEZCAYUELA, M. (1995) Oxygen-free radicals and human-disease. *Biochimie*, 77, 147-161.
- MCINTYRE, M., DYNESEN, J. & NIELSEN, J. (2001) Morphological characterization of *Aspergillus nidulans*: growth, septation and fragmentation. *Microbiology-Uk*, 147, 239-246.
- MHAMDI, A., NOCTOR, G. & BAKER, A. (2012) Plant catalases: Peroxisomal redox guardians. *Archives of Biochemistry and Biophysics*, 525, 181-194.
- MINARD, K. L. & MCALISTER-HENN, L. (2001) Antioxidant function of cytosolic sources of NADPH in yeast. *Free Radical Biology and Medicine*, 31, 832-843.
- MOGI, T., MATSUSHITA, K., MURASE, Y., KAWAHARA, K., MIYOSHI, H., UI, H., SHIOMI, K., OMURA, S. & KITA, K. (2009a) Identification of new inhibitors for alternative NADH dehydrogenase (NDH-II). *Fems Microbiology Letters*, 291, 157-161.
- MOGI, T., MURASE, Y., MORI, M., SHIOMI, K., OMURA, S., PARANAGAMA, M. P. & KITA, K. (2009b) Polymyxin B Identified as an Inhibitor of Alternative NADH Dehydrogenase and Malate: Quinone Oxidoreductase from the Gram-positive Bacterium *Mycobacterium smegmatis*. *Journal of Biochemistry*, 146, 491-499.

- MOREL, Y. & BAROUKI, R. (1999) Repression of gene expression by oxidative stress. *Biochemical Journal*, 342, 481-496.
- MOROZKINA, E. V. & KURAKOV, A. V. (2007) Dissimilatory nitrate reduction in fungi under conditions of hypoxia and anoxia: A review. *Applied Biochemistry and Microbiology*, 43, 544-549.
- MORRIS, S. M. (2004) Enzymes of arginine metabolism. *Paper presented at Symposium on Arginine, Bermuda, April 5-6.*
- MUKHERJEE, P., AHMAD, A., MANDAL, D., SENAPATI, S., SAINKAR, S. R., KHAN, M. I., PARISHCHA, R., AJAYKUMAR, P. V., ALAM, M., KUMAR, R. & SASTRY, M. (2001a) Fungus-mediated synthesis of silver nanoparticles and their immobilization in the mycelial matrix: A novel biological approach to nanoparticle synthesis. *Nano Letters*, 1, 515-519.
- MUKHERJEE, P., AHMAD, A., MANDAL, D., SENAPATI, S., SAINKAR, S. R., KHAN, M. I., RAMANI, R., PARISCHA, R., AJAYAKUMAR, P. V., ALAM, M., SASTRY, M. & KUMAR, R. (2001b) Bioreduction of AuCl₄⁻ ions by the fungus, *Verticillium sp.* and surface trapping of the gold nanoparticles formed. *Angewandte Chemie-International Edition*, 40, 3585-+.
- MUTOH, N., KAWABATA, M. & KITAJIMA, S. (2005) Effects of four oxidants, menadione, 1-chloro-2,4-dinitrobenzene, hydrogen peroxide and cumene hydroperoxide, on fission yeast *Schizosaccharomyces pombe*. *Journal of Biochemistry*, 138, 797-804.
- NAGANO, T. (1999) Practical methods for detection of nitric oxide. *Luminescence*, 14, 283-290.
- NAKAMURA, S., SHIN, T., HIROKATA, Y. & SHIGEMATSU, A. (1977) INHIBITION OF MITOCHONDRIAL RESPIRATION BY SODIUM

NITROPRUSSIDE AND MECHANISM OF CYANIDE LIBERATION.

British Journal of Anaesthesia, 49, 1239-1244.

NANO, K., ROUKAS, T. & PAPADAKIS, E. (2011) Oxidative stress and morphological changes in *Blakeslea trispora* induced by enhanced aeration during carotene production in a bubble column reactor. *Biochemical Engineering Journal*, 54, 172-177.

NISHIKAWA, M., NAGATOMI, H., NISHIJIMA, M., OHIRA, G., CHANG, B. J., SATO, E. & INOUE, M. (2001) Targeting superoxide dismutase to renal proximal tubule cells inhibits nephrotoxicity of cisplatin and increases the survival of cancer-bearing mice. *Cancer Letters*, 171, 133-138.

NORDON, A., LITTLEJOHN, D., DANN, A. S., JEFFKINS, P. A., RICHARDSON, M. D. & STIMPSON, S. L. (2008) In situ monitoring of the seed stage of a fermentation process using non-invasive NIR spectrometry. *Analyst*, 133, 660-666.

O'DONNELL, A. (2008) Physiological responses to oxidative environments in submerged cultures of a filamentous fungus, *Aspergillus niger B1-D*. *PhD thesis, Strathclyde Institute of Pharmacy and Bioscience*. Glasgow, University of Strathclyde

O'DONNELL, A., BAI, Y. T., BAI, Z. H., MCNEIL, B. & HARVEY, L. M. (2007) Introduction to bioreactors of shake-flask inocula leads to development of oxidative stress in *Aspergillus niger*. *Biotechnology Letters*, 29, 895-900.

O'DONNELL, A., HARVEY, L. M. & MCNEIL, B. (2011) The roles of the alternative NADH dehydrogenases during oxidative stress in cultures of the filamentous fungus *Aspergillus niger*. *Fungal Biol*, 115, 359-69.

OUSHIKI, D., KOJIMA, H., TAKAHASHI, Y., KOMATSU, T., TERAJ, T., HANAOKA, K., NISHIKAWA, M., TAKAKURA, Y. & NAGANO, T.

- (2012) Near-Infrared Fluorescence Probes for Enzymes Based on Binding Affinity Modulation of Squarylium Dye Scaffold. *Analytical Chemistry*, 84, 4404-4410.
- PEARCE, L. L., EPPERLY, M. W., GREENBERGER, J. S., PITT, B. R. & PETERSON, J. (2001) Identification of respiratory complexes I and III as mitochondrial sites of damage following exposure to ionizing radiation and nitric oxide. *Nitric Oxide-Biology and Chemistry*, 5, 128-136.
- PERAZA, L. & HANSBERG, W. (2002) *Neurospora crassa* catalases, singlet oxygen and cell differentiation. *Biological Chemistry*, 383, 569-575.
- PERRONE, G. G., TAN, S. X. & DAWES, I. W. (2008) Reactive oxygen species and yeast apoptosis. *Biochimica Et Biophysica Acta-Molecular Cell Research*, 1783, 1354-1368.
- PIGEOLET, E., CORBISIER, P., HOUBION, A., LAMBERT, D., MICHIELS, C., RAES, M., ZACHARY, M. D. & REMACLE, J. (1990) Glutathione-peroxidase, superoxide dismutase and catalase inactivation by peroxides and oxygen derived free-radicals. *Mechanisms of Ageing and Development*, 51, 283-297.
- PINHEIRO, R., BELO, I. & MOTA, M. (2000) Air pressure effects on biomass yield of two different *Kluyveromyces* strains. *Enzyme and Microbial Technology*, 26, 756-762.
- POMBEIRO, S. R. C., ROSSI, A. & MARTINEZROSSI, N. M. (1992) Nitrite toxicity in *Aspergillus-nidulans* - effect of mutation at the NIHB gene. *World Journal of Microbiology & Biotechnology*, 8, 477-479.
- POOLE, R. K. (2005) Nitric oxide and nitrosative stress tolerance in bacteria. *Biochemical Society Transactions*, 33, 176-180.

- QIN, G., LIU, J., CAO, B., LI, B. & TIAN, S. (2011) Hydrogen Peroxide Acts on Sensitive Mitochondrial Proteins to Induce Death of a Fungal Pathogen Revealed by Proteomic Analysis. *Plos One*, 6.
- RADI, R., CASSINA, A. & HODARA, R. (2002) Nitric oxide and peroxynitrite interactions with mitochondria. *Biological Chemistry*, 383, 401-409.
- SAHOO, R., BHATTACHARJEE, A., MAJUMDAR, U., RAY, S. S., DUTTA, T. & GHOSH, S. (2009) A novel role of catalase in detoxification of peroxynitrite in *S. cerevisiae*. *Biochemical and Biophysical Research Communications*, 385, 507-511.
- SAMUEL, J., S. (2005) Biogenesis of Metal Nanoparticles. *Department of Biotechnology & Environmental Sciences*. Patiala, Thapar Institute of Engineering & Technology.
- SCANDALIOS, J. G., GUAN, L. & POLIDOROS, A. N. (1997) Catalases in plants: Gene structure, properties, regulation, and expression. *Cold Spring Harbor Monograph Series; Oxidative stress and the molecular biology of antioxidant defenses*. New York, Cold Spring Harbor laboratory.
- SCARFF, M., ARNOLD, S. A., HARVEY, L. M. & MCNEIL, B. (2006) Near Infrared Spectroscopy for bioprocess monitoring and control: Current status and future trends. *Critical Reviews in Biotechnology*, 26, 17-39.
- SCHLIEBS, W., WUERTZ, C., KUNAU, W.-H., VEENHUIS, M. & ROTTENSTEINER, H. (2006) A eukaryote without catalase-containing microbodies: *Neurospora crassa* exhibits a unique cellular distribution of its four catalases. *Eukaryotic Cell*, 5, 1490-1502.
- SCHOPFER, F., RIOBO, N., CARRERAS, M. C., ALVAREZ, B., RADI, R., BOVERIS, A., CADENAS, E. & PODEROSO, J. J. (2000) Oxidation of ubiquinol by peroxynitrite: implications for protection of mitochondria against nitrosative damage. *Biochemical Journal*, 349, 35-42.

- SHAHRIARINOUR, M., RAMANAN, R. N., WAHAB, M. N. A., MOHAMAD, R., MUSTAFA, S. & ARIFF, A. B. (2011) Improved cellulase production by *Aspergillus terreus* using oil palm empty fruit bunch fiber as substrate in a stirred tank bioreactor through optimization of the fermentation conditions. *Bioresources*, 6, 2663-2675.
- SHENTON, D. & GRANT, C. M. (2003) Protein S-thiolation targets glycolysis and protein synthesis in response to oxidative stress in the yeast *Saccharomyces cerevisiae*. *Biochemical Journal*, 374, 513-519.
- SIEDOW, J. N. & UMBACH, A. L. (1995) Plant mitochondrial electron-transfer and molecular-biology. *Plant Cell*, 7, 821-831.
- SIGLER, K., CHALOUPKA, J., BROZMANOVA, J., STADLER, N. & HOFER, M. (1999) Oxidative stress in microorganisms - I - Microbial vs. higher cells - Damage and defenses in relation to cell aging and death. *Folia Microbiologica*, 44, 587-624.
- SILVERMAN, P. M. & EPSTEIN, P. M. (1975) Cyclic nucleotide-metabolism coupled to cytodifferentiation of *Blastocladiella-emersonii*. *Proceedings of the National Academy of Sciences of the United States of America*, 72, 442-446.
- STRYER, L. (Ed.) (1995) *Biochemistry Fourth Edition*, New York, W. H. Freeman and Company.
- TAKASAKI, K., SHOUN, H., YAMAGUCHI, M., TAKEO, K., NAKAMURA, A., HOSHINO, T. & TAKAYA, N. (2004) Fungal ammonia fermentation, a novel metabolic mechanism that couples the dissimilatory and assimilatory pathways of both nitrate and ethanol - Role of acetyl CoA synthetase in anaerobic ATP synthesis. *Journal of Biological Chemistry*, 279, 12414-12420.

- TAKAYA, N. (2002) Dissimilatory nitrate reduction metabolisms and their control in fungi. *Journal of Bioscience and Bioengineering*, 94, 506-510.
- TANG, Y.-J., LI, H.-M. & HAMEL, J.-F. P. (2009) Effects of dissolved oxygen tension and agitation rate on the production of heat-shock protein glycoprotein 96 by MethA tumor cell suspension culture in stirred-tank bioreactors. *Bioprocess and Biosystems Engineering*, 32, 475-484.
- TENG, Y., XU, Y. & WANG, D. (2009) Changes in morphology of *Rhizopus chinensis* in submerged fermentation and their effect on production of mycelium-bound lipase. *Bioprocess and Biosystems Engineering*, 32, 397-405.
- THOMSON, A. J., GIANNOPOULOS, G., PRETTY, J., BAGGS, E. M. & RICHARDSON, D. J. (2012) Biological sources and sinks of nitrous oxide and strategies to mitigate emissions. *Philosophical Transactions of the Royal Society B-Biological Sciences*, 367, 1157-1168.
- TURRENS, J. F. (2003) Mitochondrial formation of reactive oxygen species. *Journal of Physiology-London*, 552, 335-344.
- VAIDYANATHAN, S., HARVEY, L. M. & MCNEIL, B. (2001a) Deconvolution of near-infrared spectral information for monitoring mycelial biomass and other key analytes in a submerged fungal bioprocess. *Analytica Chimica Acta*, 428, 41-59.
- VAIDYANATHAN, S., MACALONEY, G., HARVEY, L. M. & MCNEIL, B. (2001b) Assessment of the structure and predictive ability of models developed for monitoring key analytes in a submerged fungal bioprocess using near-infrared spectroscopy. *Applied Spectroscopy*, 55, 444-453.

- VAIDYANATHAN, S., MACALONEY, G. & MCNEIL, B. (1999) Fundamental investigations on the near-infrared spectra of microbial biomass as applicable to bioprocess monitoring. *Analyst*, 124, 157-162.
- VAIDYANATHAN, S., WHITE, S., HARVEY, L. M. & MCNEIL, B. (2003) Influence of morphology on the near-infrared spectra of mycelial biomass and its implications in bioprocess monitoring. *Biotechnology and Bioengineering*, 82, 715-724.
- VALDERRAMA, R., CORPAS, F. J., CARRERAS, A., FERNANDEZ-OCANA, A., CHAKI, M., LUQUE, F., GOMEZ-RODRIGUEZ, M. V., COLMENERO-VAREA, P., DEL RIO, L. A. & BARROSO, J. B. (2007) Nitrosative stress in plants. *Febs Letters*, 581, 453-461.
- VAN 'T RIET, K. & TRAMPER, J. (1991) *Basic Bioreactor Design*, New York, Marcel Dekker, inc.
- VIDEIRA, A. & DUARTE, M. (2001) On complex I and other NADH : Ubiquinone reductases of *Neurospora crassa* mitochondria. *Journal of Bioenergetics and Biomembranes*, 33, 197-203.
- VIEIRA, A. L. G., LINARES, E., AUGUSTO, O. & GOMES, S. L. (2009) Evidence of a Ca²⁺-(NO)-N-center dot-cGMP signaling pathway controlling zoospore biogenesis in the aquatic fungus *Blastocladiella emersonii*. *Fungal Genetics and Biology*, 46, 575-584.
- VISTICA, D. T., SKEHAN, P., SCUDIERO, D., MONKS, A., PITTMAN, A. & BOYD, M. R. (1991) Tetrazolium-based assays for cellular viability - A critical - examination of selected parameters affecting formazan production. *Cancer Research*, 51, 2515-2520.
- VORAUER-UHL, K., FURNSCHLIEF, E., WAGNER, A., FERKO, B. & KATINGER, H. (2001) Topically applied liposome encapsulated superoxide dismutase reduces postburn wound size and edema formation. *European Journal of Pharmaceutical Sciences*, 14, 63-67.

- VOULGARIS, I., O'DONNELL, A., HARVEY, L. M. & MCNEIL, B. (2012) Inactivating alternative NADH dehydrogenases: enhancing fungal bioprocesses by improving growth and biomass yield? *Scientific Reports*, 2.
- WANG, L., RIDGWAY, D., GU, T. & MOO-YOUNG, M. (2005) Bioprocessing strategies to improve heterologous protein production in filamentous fungal fermentations. *Biotechnology Advances*, 23, 115-129.
- WEITZBERG, E. & LUNDBERG, J. O. N. (1998) Nonenzymatic nitric oxide production in humans. *Nitric Oxide-Biology and Chemistry*, 2, 1-7.
- WENDEHENNE, D., PUGIN, A., KLESSIG, D. F. & DURNER, J. (2001) Nitric oxide: comparative synthesis and signaling in animal and plant cells. *Trends in Plant Science*, 6, 177-183.
- WIEBE, M. G. (2002) Myco-protein from *Fusarium venenatum*: a well-established product for human consumption. *Applied Microbiology and Biotechnology*, 58, 421-427.
- WOJTASZEK, P. (1997) Oxidative burst: An early plant response to pathogen infection. *Biochemical Journal*, 322, 681-692.
- WONGWICHARN, A., MCNEIL, B. & HARVEY, L. M. (1999) Effect of oxygen enrichment on morphology, growth, and heterologous protein production in chemostat cultures of *Aspergillus niger* B1-D. *Biotechnology and Bioengineering*, 65, 416-424.
- XU, L. L., LAI, Y. L., WANG, L. & LIU, X. Z. (2011) Effects of abscisic acid and nitric oxide on trap formation and trapping of nematodes by the fungus *Drechlerella stenobrocha* AS6.1. *Fungal Biology*, 115, 97-101.
- YABE, Y., KOBAYASHI, N., NISHIHASHI, T., TAKAHASHI, R., NISHIKAWA, M., TAKAKURA, Y. & HASHIDA, M. (2001) Prevention of neutrophil-mediated hepatic ischemia/reperfusion injury by superoxide dismutase

and catalase derivatives. *Journal of Pharmacology and Experimental Therapeutics*, 298, 894-899.

YERMILOV, V., RUBIO, J. & OHSHIMA, H. (1995) Formation of 8-nitroguanine in DNA treated with peroxynitrite in-vitro and its rapid removal from DNA by depurination. *Febs Letters*, 376, 207-210.

YU, L. J., LAN, W. Z., CHEN, C. & YANG, Y. (2004) Glutathione levels control glucose-6-phosphate dehydrogenase activity during elicitor-induced oxidative stress in cell suspension cultures of *Taxus chinensis*. *Plant Science*, 167, 329-335.

ZAKI, M. H., AKUTA, T. & AKAIKE, T. (2005) Nitric oxide-induced nitrate stress involved in microbial pathogenesis. *Journal of Pharmacological Sciences*, 98, 117-129.

ZUIN, A., GABRIELLI, N., CALVO, I. A., GARCIA-SANTAMARINA, S., HOE, K.-L., KIM, D. U., PARK, H.-O., HAYLES, J., AYTE, J. & HIDALGO, E. (2008) Mitochondrial Dysfunction Increases Oxidative Stress and Decreases Chronological Life Span in Fission Yeast. *Plos One*, 3.

Appendix I

Graphs repeat experiments for
Chapter 3

I Graphs repeat experiments for Chapter 3

I.1 Graphs of repeat experiments

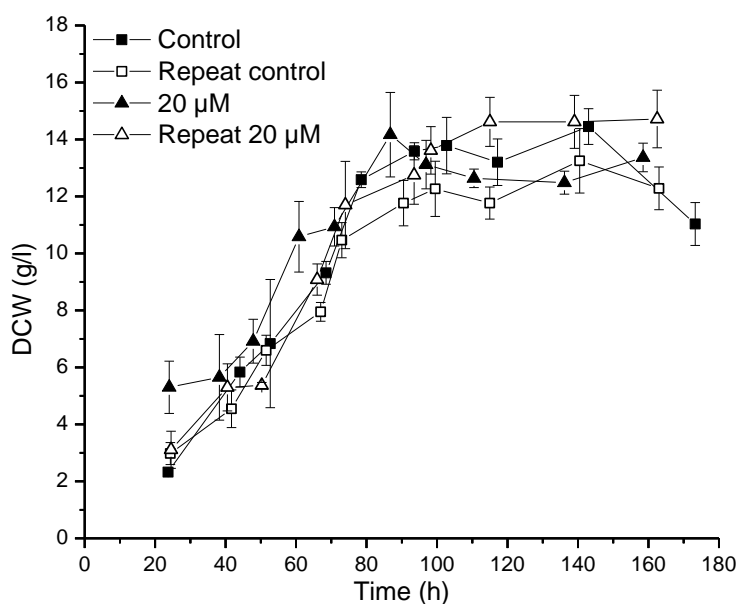


Figure I-1: DCW (g/l) during batch cultivation in a STR of *A. niger B1-D*.

Various concentrations (see graph) of polymyxin B were added at 1.5 hours. Cultivation conditions were: airflow 2 lpm, 200-400 rpm, pH 4, temperature 25 °C. Results are expressed as mean ± stdev.

Table I-1: Effect of polymyxin B on specific growth rate during batch fermentations of *A. niger B1-D*.

Cultivation conditions were: airflow 2 lpm, 200-400 rpm, pH 4, temperature 25 °C. Specific growth rate was determined from the linear part of the graph and is expressed as mean ± stdv.

Concentration polymyxin B (μM)	Specific growth rate (h ⁻¹)
Control	0.025 ± 0.0022
Repeat control	0.021 ± 0.0028
20	0.019 ± 0.0072
Repeat 20	0.012 ± 0.0032

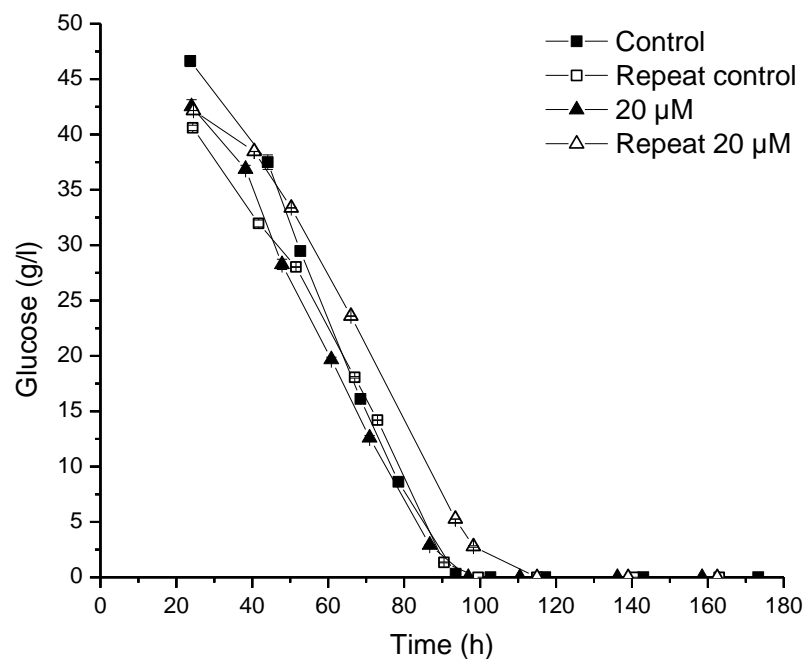


Figure I-2: Residual glucose (g/l) during batch cultivation in a STR of *A. niger* B1-D.

Various concentrations of polymyxin B were added at 1.5 hours. Cultivation conditions were: airflow 2 lpm, 200-400 rpm, pH 4, temperature 25 °C. Results are expressed as mean ± stdev.

Table I-2: Effect of polymyxin B on GCR during batch fermentations of *A. niger* B1-D.

Cultivation conditions were: airflow 2 lpm, 200-400 rpm, pH 4, temperature 25 °C. GCR was determined from the linear part of the graph and is expressed as mean ± stdv.

Concentration Polymyxin B (μM)	GCR (g/l/h)
Control	0.69 ± 0.0062
Repeat control	0.59 ± 0.0203
20	0.70 ± 0.0072
Repeat 20	0.63 ± 0.0009

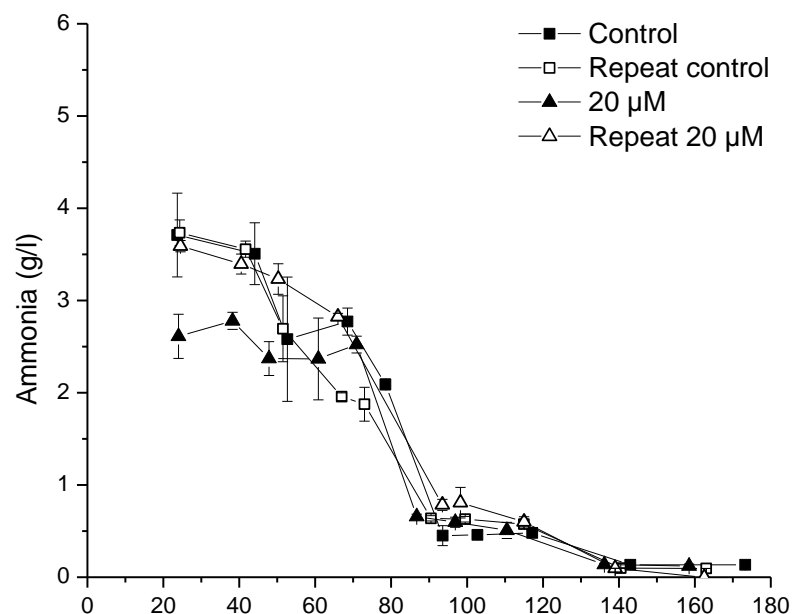


Figure I-3: Residual Ammonium (g/l) during batch cultivation in a STR of *A. niger B1-D*.

Various concentrations of polymyxin B were added at 1.5 hours. Cultivation conditions were: airflow 2 lpm, 200-400 rpm, pH 4, temperature 25 °C. Results are expressed as mean ± stdev.

Table I-3: Effect of polymyxin B on ACR during batch fermentations of *A. niger B1-D*.

Cultivation conditions were: airflow 2 lpm, 200-400 rpm, pH 4, temperature 25 °C. ACR was determined from the linear part of the graph and is expressed as mean ± stdv.

Concentration polymyxin B (μM)	ACR (g/l/h)
Control	0.029 ± 0.0092
Repeat control	0.052 ± 0.0022
20	0.044 ± 0.0041
Repeat 20	0.054 ± 0.0001

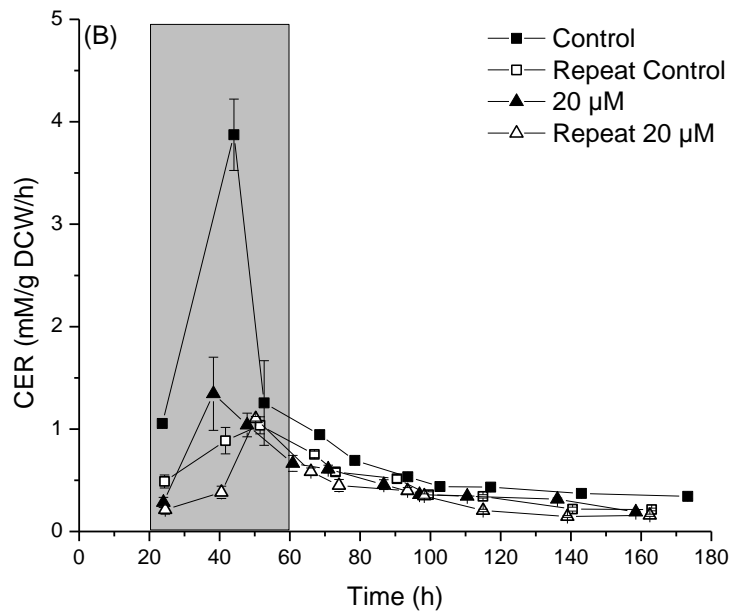
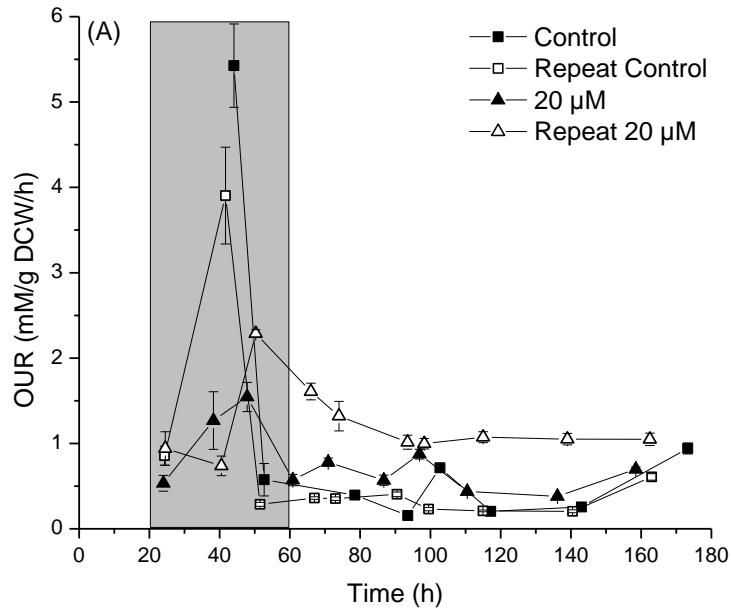


Figure I-4: (A) OUR (mM/g DCW/h) and (B) CER (mM/g DCW/h) during batch cultivation in a STR of *A. niger* B1-D.

Various concentrations of polymyxin B was added at 1.5 hours. Cultivation conditions were: airflow 2 lpm, 200-400 rpm, pH 4, temperature 25 °C. The grey highlighted part represents a less stable part of the process. Results are expressed as mean ± stdev.

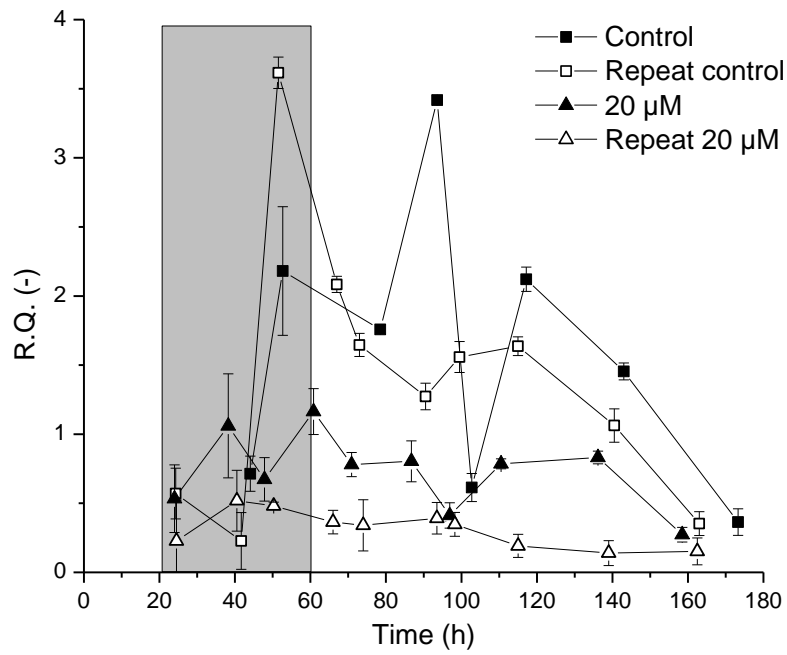


Figure I-5: R.Q. during batch cultivation in a STR of *A. niger B1-D*.

Various concentrations of polymyxin B were added at 1.5 hours. Cultivation conditions were: airflow 2 lpm, 200-400 rpm, pH 4, temperature 25 °C. The grey highlighted part represents a less stable part of the process. Results are expressed as mean \pm stdev.

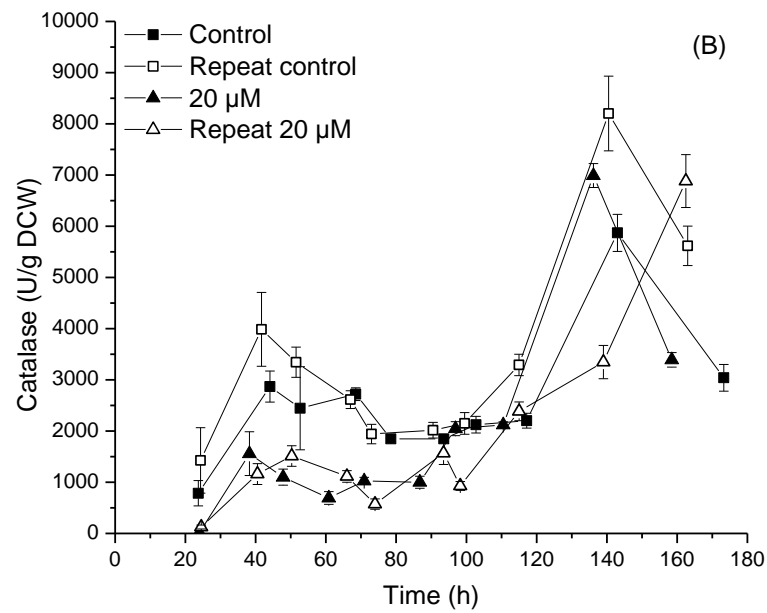
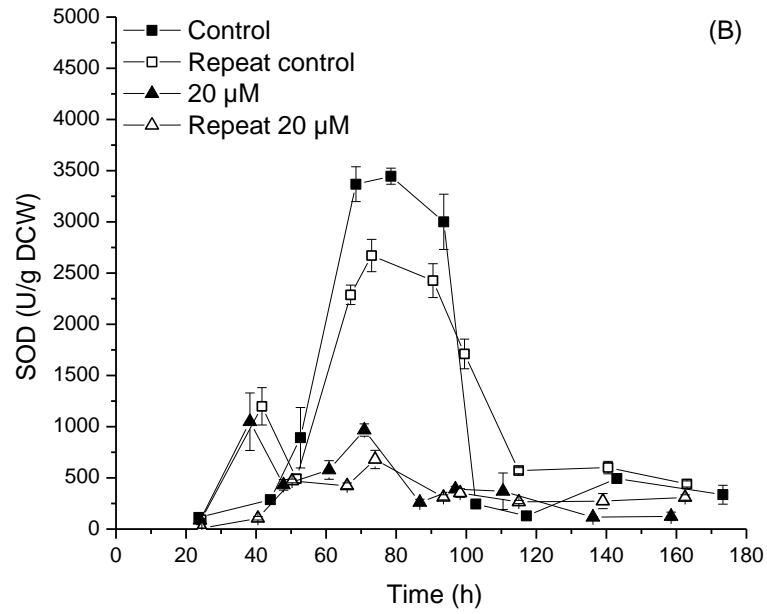


Figure I-6: (A) SOD (U/g DCW) and (B) CAT (U/g DCW) during batch cultivation in a STR of *A. niger* B1-D.

Various concentrations of polymyxin B were added at 1.5 hours. Cultivation conditions were: airflow 2 lpm, 200-400 rpm, pH 4, temperature 25 °C. Results are expressed as mean ± stdev.

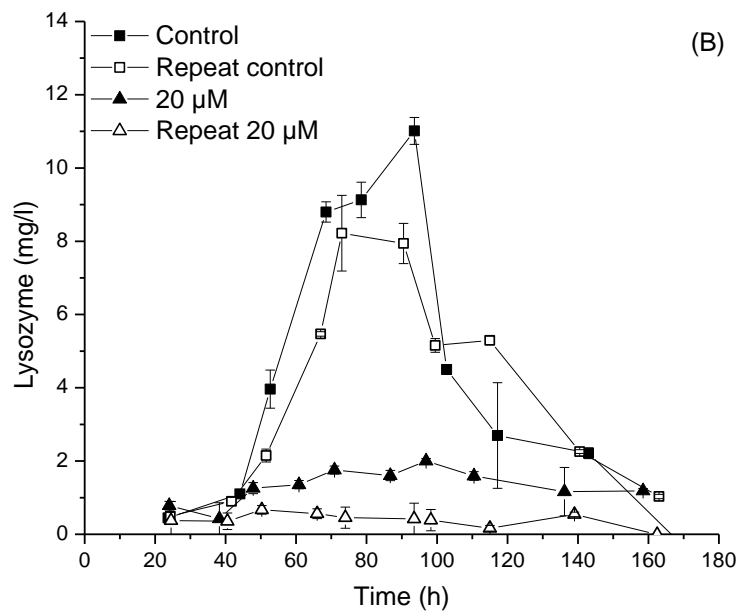
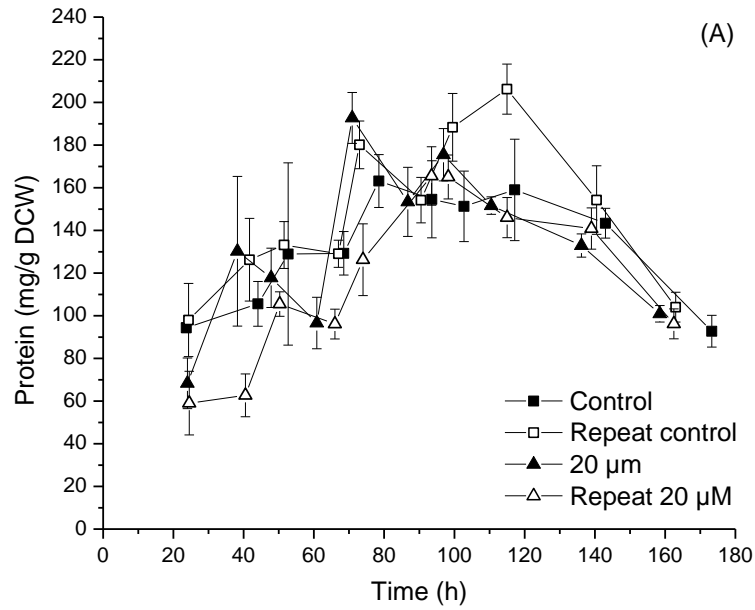


Figure I-7: (A) Intracellular protein content (mg/g DCW) and (B) Lysozyme concentration (mg/l) during batch cultivation in a STR of *A. niger* B1-D. Various concentrations of polymyxin B were added at 1.5 hours. Cultivation conditions were: airflow 2 lpm, 200-400 rpm, pH 4, temperature 25 °C. Results are expressed as mean \pm stdev.

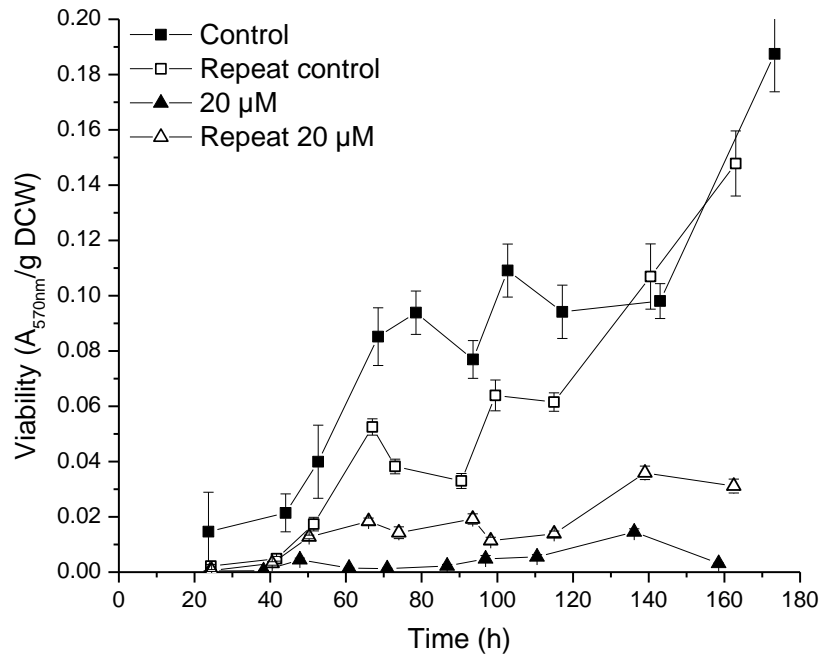


Figure I-8: Viability ($A_{570\text{nm}}/\text{g DCW}$) during batch cultivation in a stirred tank reactor of *A. niger* B1-D.

Various concentrations of polymyxin B were added at 1.5 hours. Cultivation conditions were: 2 lpm, 200-400 rpm, pH 4 at 25 °C. Results are expressed as mean \pm stdev.

Appendix II

Graphs repeat experiments for
Chapter 4

II Graphs repeat experiments for Chapter 4

II.1 Graphs of repeat experiments

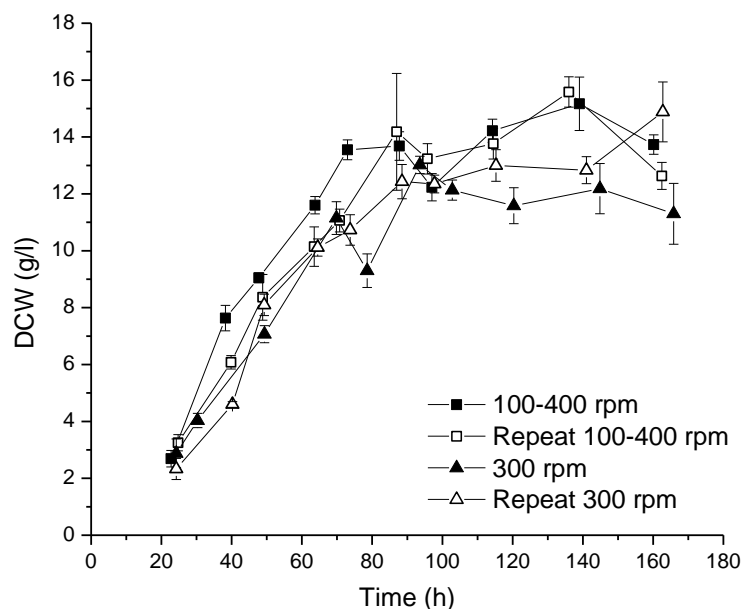


Figure II-1: DCW (g/l) during batch cultivation in a STR of *A. niger B1-D*.

Various agitation settings were used. Other Cultivation conditions were: airflow 2 lpm, pH 4, temperature 25 °C. Results are expressed as mean ± stdev.

Table II-1: Effect of various agitation settings on specific growth rate during batch fermentations of *A. niger B1-D*.

Other cultivation conditions were: airflow 2 lpm, pH 4, temperature 25 °C. Specific growth rate was determined from the linear part of the graph and is expressed as mean ± stdv.

Concentration SNP (μM)	Specific growth rate (h ⁻¹)
100-400	0.017 ± 0.0009
Repeat 100-400	0.019 ± 0.0005
300	0.022 ± 0.0030
Repeat 300	0.024 ± 0.0019

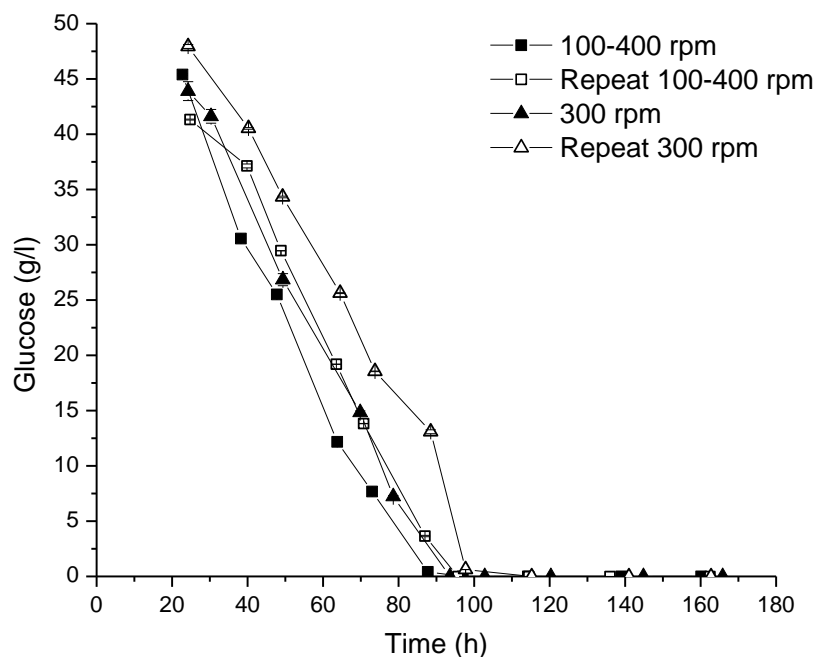


Figure II-2: Residual glucose (g/l) during batch cultivation in a STR of *A. niger B1-D*.

Various agitation settings were used. Other cultivation conditions were: airflow 2 lpm, pH 4, temperature 25 °C. Results are expressed as mean ± stdev.

Table II-2: Effect of various agitation settings on GCR rate during batch fermentations of *A. niger B1-D*.

Other cultivation conditions were: airflow 2 lpm, pH 4, temperature 25 °C. GCR rate was determined from the linear part of the graph and is expressed as mean ± stdv.

Agitation settings (rpm)	GCR (g/l/h)
100-400	0.65 ± 0.0086
Repeat 100-400	0.75 ± 0.0309
300	0.63 ± 0.0123
Repeat 300	0.50 ± 0.0134

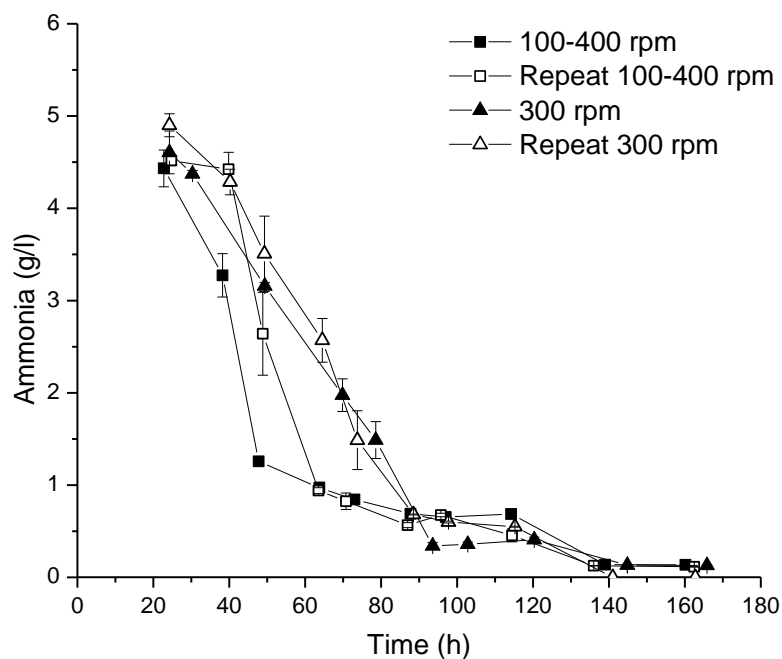


Figure II-3: Residual ammonium (g/l) during batch cultivation in a STR of *A. niger B1-D*.

Various agitation settings were used. Other cultivation conditions were: airflow 2 lpm, pH 4, temperature 25 °C. Results are expressed as mean ± stdev.

Table II-3: Effect of various agitation settings on ACR rate during batch fermentations of *A. niger B1-D*.

Other cultivation conditions were: airflow 2 lpm, pH 4, temperature 25 °C. ACR rate was determined from the linear part of the graph and is expressed as mean ± stdv.

Agitation settings (rpm)	ACR (g/l/h)
100-400	0.069 ± 0.0060
Repeat 100-400	0.087 ± 0.0065
300	0.062 ± 0.0029
Repeat 300	0.061 ± 0.0017

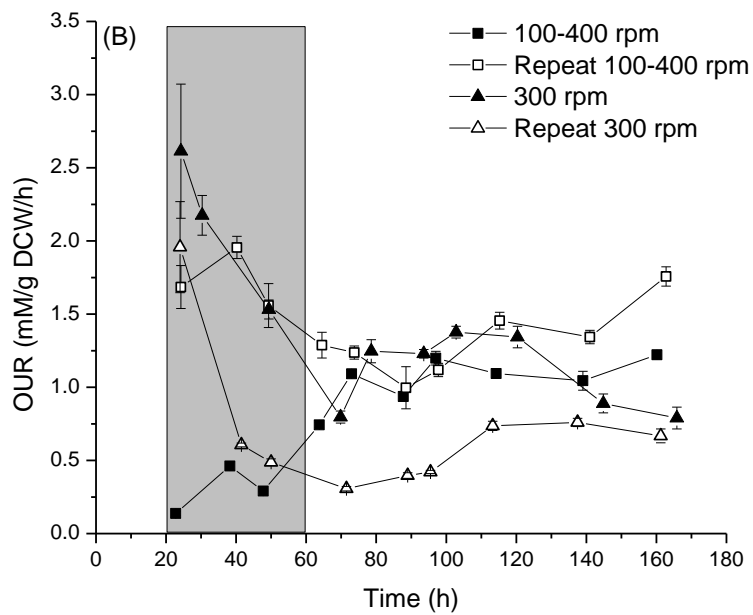
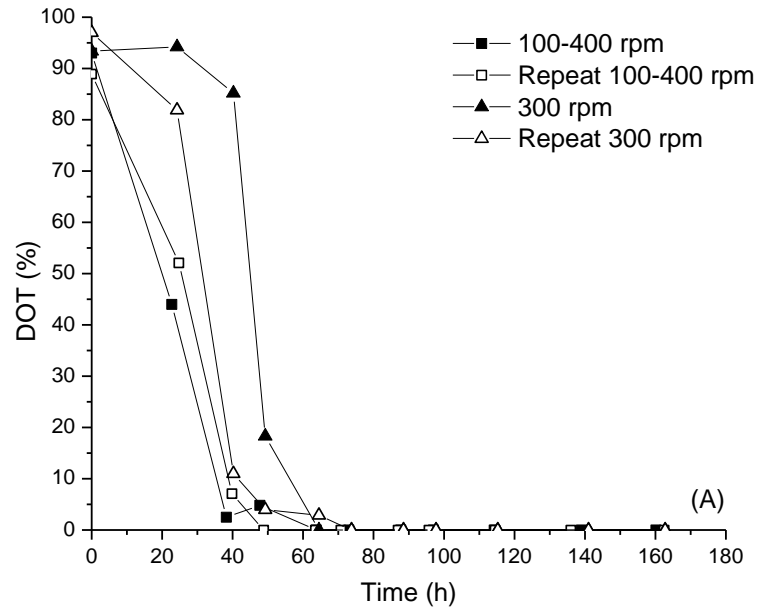


Figure II-4: (A) DOT (%) and (B) OUR (mM/g DCW/h) during batch cultivation in a STR of *A. niger* B1-D.

Various agitation settings were used. Other cultivation conditions were: airflow 2 lpm, pH 4, temperature 25 °C. The grey highlighted part represents a less stable part of the process. Results are expressed as mean \pm stdev.

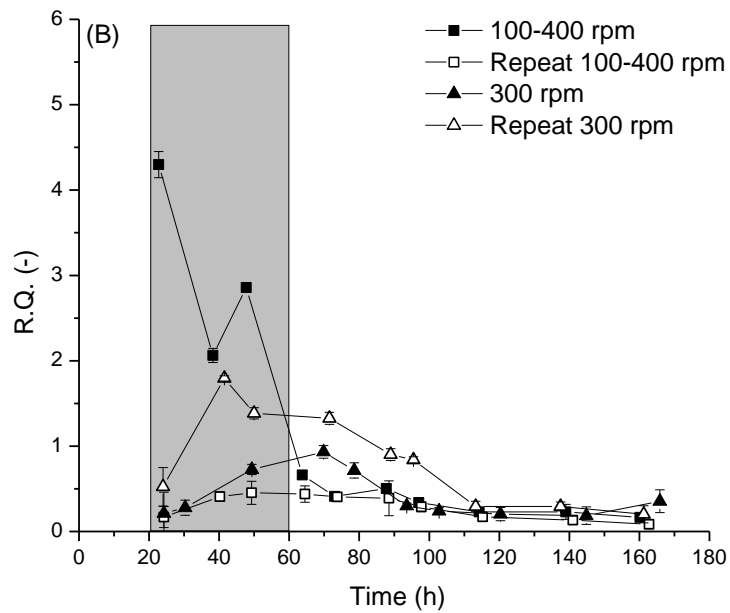
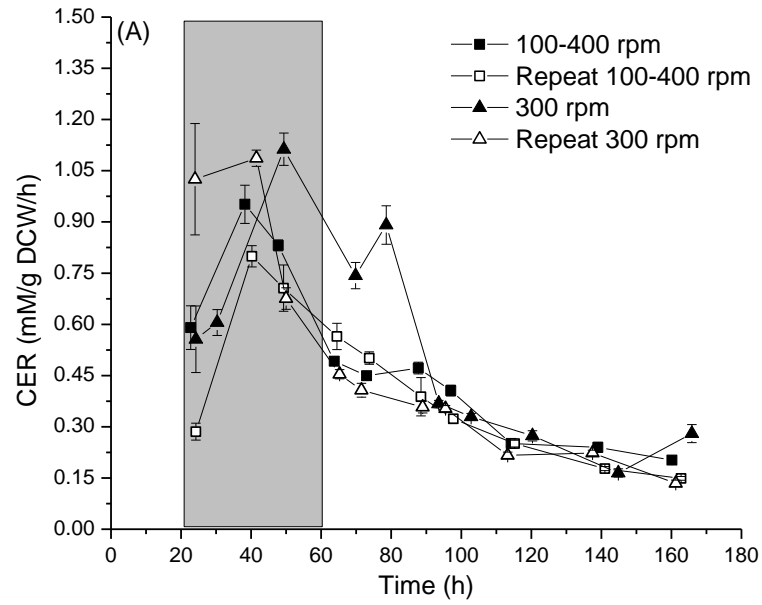


Figure II-5: (A) CER (mM/g DCW/h) and (B) R.Q. during batch cultivation in a STR of *A. niger* B1-D.

Various agitation settings were used. Other cultivation conditions were: airflow 2 lpm, pH 4, temperature 25 °C. The grey highlighted part represents a less stable part of the process. Results are expressed as mean \pm stdev.

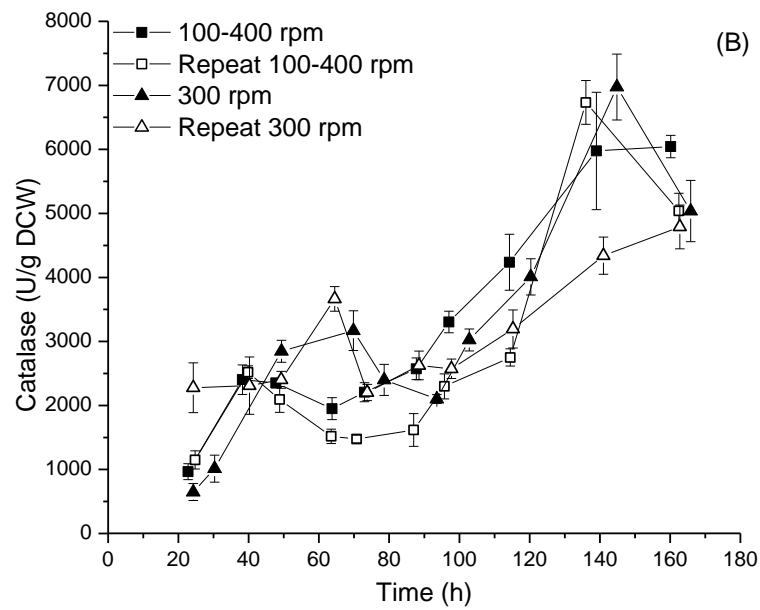
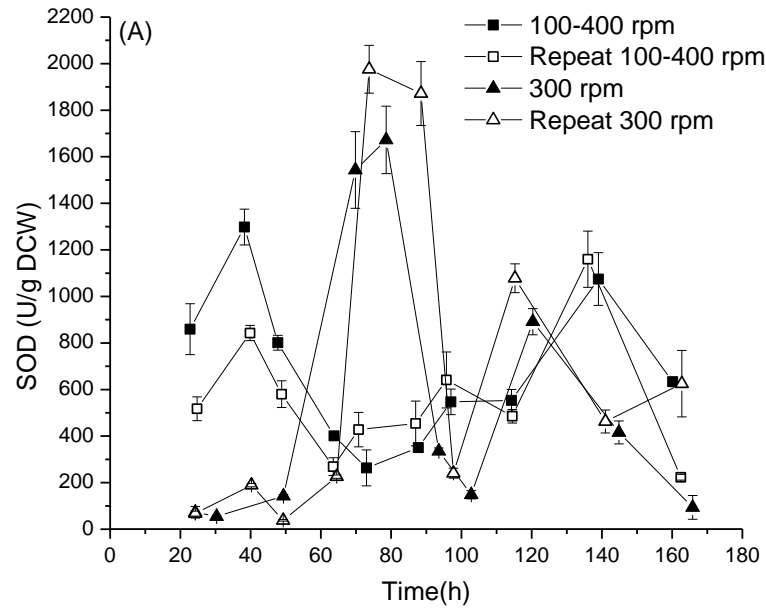


Figure II-6: (A) SOD (U/g DCW) and (B) CAT (U/g DCW) during batch cultivation in a STR of *A. niger* B1-D.

Various agitation settings were used. Other cultivation conditions were: airflow 2 lpm, pH 4, temperature 25 °C. Results are expressed as mean ± stdev.

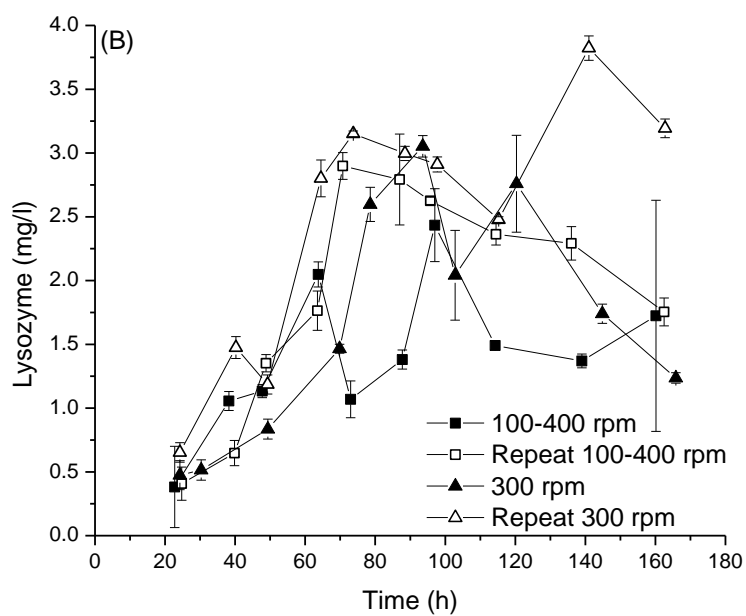
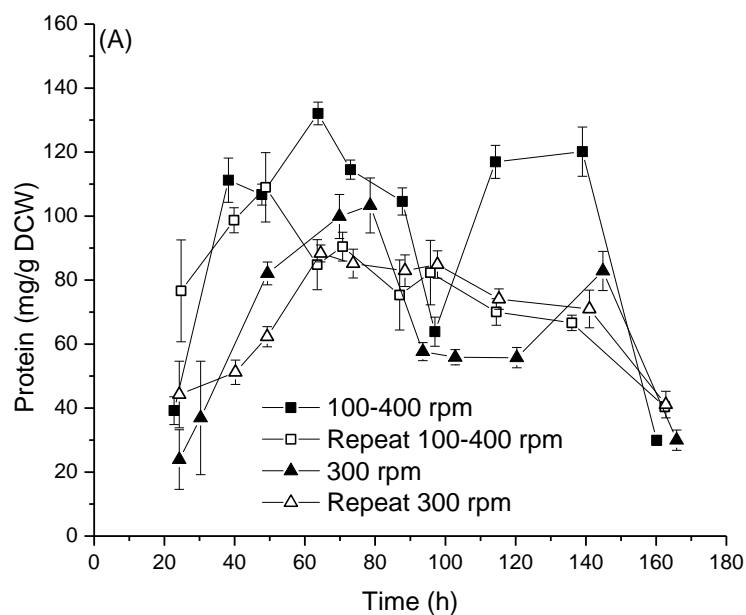


Figure II-7: (A) Intracellular protein content (mg/g DCW) and (B) Lysozyme concentration (mg/l) during batch cultivation in a STR of *A. niger* B1-D. Various agitation settings were used. Other cultivation conditions were: airflow 2 lpm, pH 4, temperature 25 °C. Results are expressed as mean ± stdev.

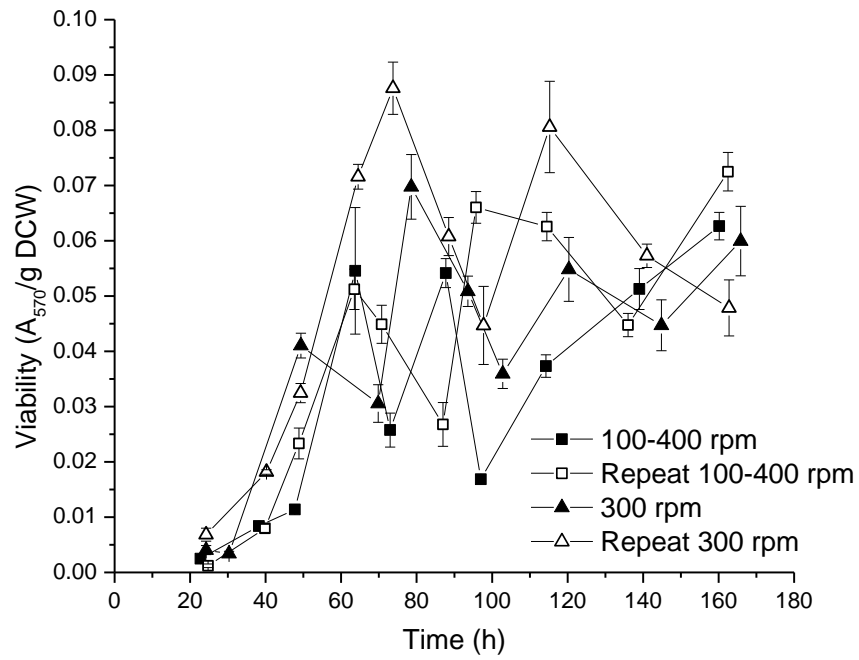


Figure II-8: Viability ($A_{570\text{nm}}/\text{g DCW}$) during batch cultivation in a stirred tank reactor of *A. niger* B1-D.

Various agitation settings were used. Other cultivation conditions were: airflow 2 lpm, pH 4, temperature 25 °C. Results are expressed as mean \pm stdev.

Appendix III

Graphs repeat experiments

Chapter 5

III Graphs repeat experiments for Chapter 5

III.1 Graphs of repeat experiments

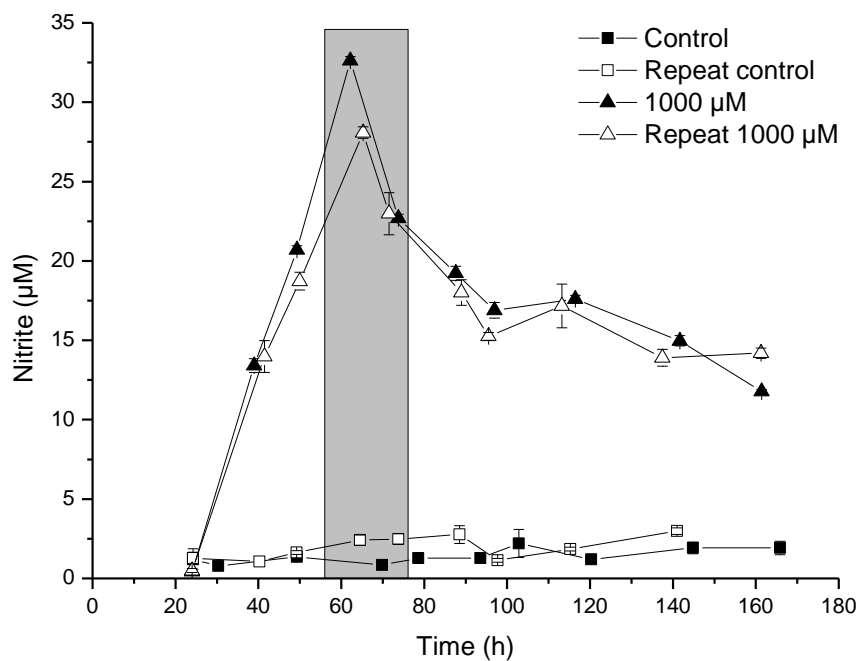


Figure III-1: Nitrite concentration during batch cultivation in a stirred tank reactor of *A. niger* B1-D.

Various concentrations (see graph) of sodium nitroprusside (SNP) were added at 24 hours. Cultivation conditions were: airflow 2 lpm, 300 rpm, pH 4, temperature 25 °C. Results are expressed as mean \pm stdev.

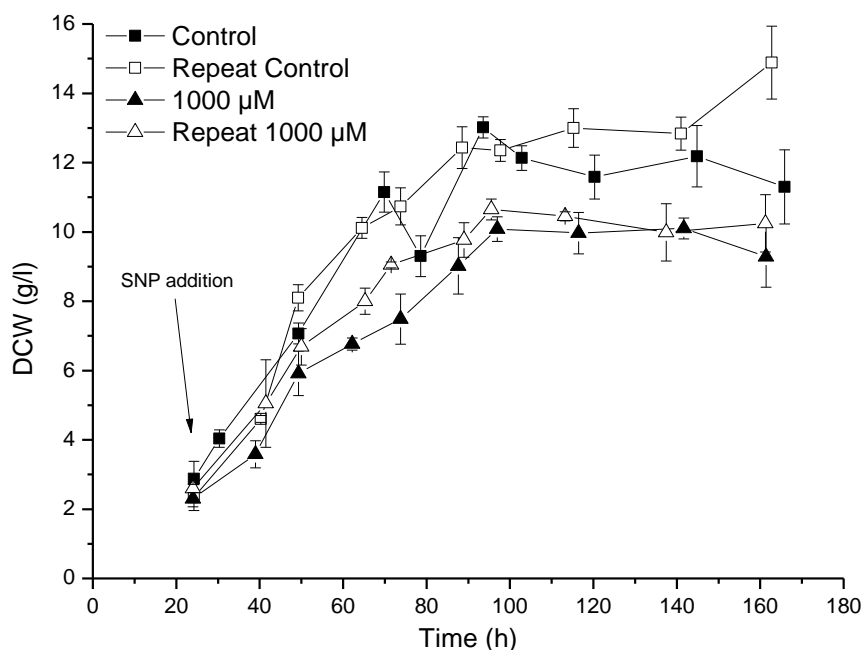


Figure III-2: DCW (g/l) during batch cultivation in a STR of *A. niger B1-D*.

Various concentrations (see graph) of sodium nitroprusside (SNP) were added at 24 hours. Cultivation conditions were: airflow 2 lpm, 300 rpm, pH 4, temperature 25 °C. Results are expressed as mean ± stdev.

Table III-1: Effect of SNP on specific growth rate of batch fermentations of *A. niger B1-D*.

Cultivation conditions were: airflow 2 lpm, 300 rpm, pH 4, temperature 25 °C. Specific growth rate was determined from the linear part of the graph and is expressed as mean ± stdv.

Concentration SNP (μM)	Specific growth rate (h ⁻¹)
Control	0.022 ± 0.003
Repeat control	0.024 ± 0.002
1000	0.021 ± 0.002
Repeat 1000	0.019 ± 0.001

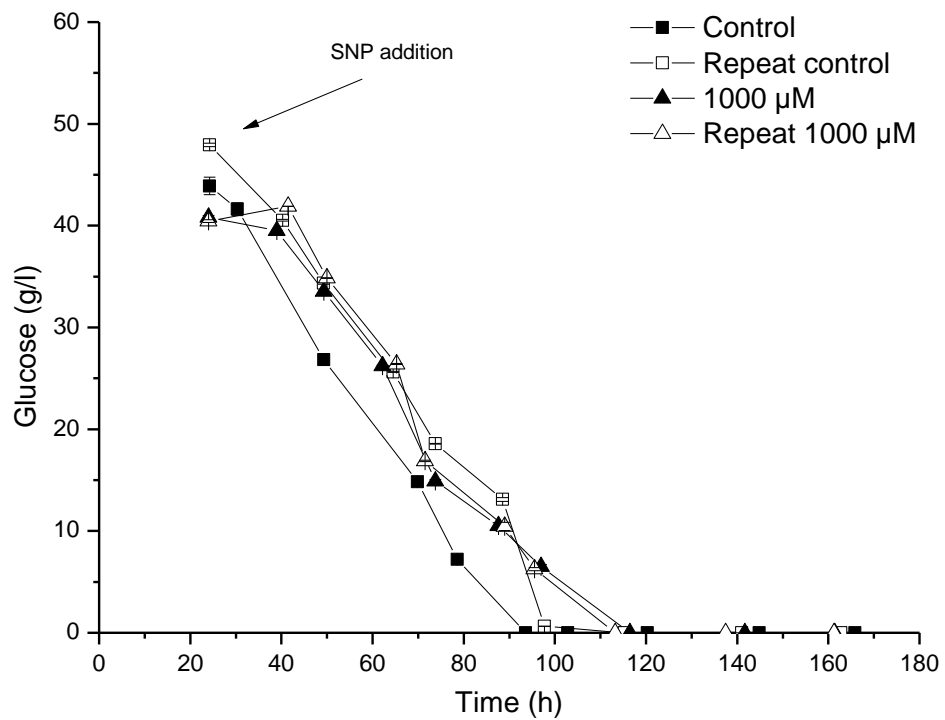


Figure III-3: Residual glucose (g/l) during batch cultivation in a STR of *A. niger B1-D*.

Various concentrations of sodium nitroprusside (SNP) were added at 24 hours. Cultivation conditions were: airflow 2 lpm, 300 rpm, pH 4, temperature 25 °C. Results are expressed as mean ± stdev.

Table III-2: Effect of SNP on GCR during batch fermentations of *A. niger B1-D*.

Cultivation conditions were: airflow 2 lpm, 300 rpm, pH 4, temperature 25 °C. GCR was determined from the linear part of the graph and is expressed as mean ± stdv.

Concentration SNP (μM)	GCR (g/l/h)
Control	0.63 ± 0.012
Repeat control	0.50 ± 0.013
1000	0.44 ± 0.009
Repeat 1000	0.47 ± 0.013

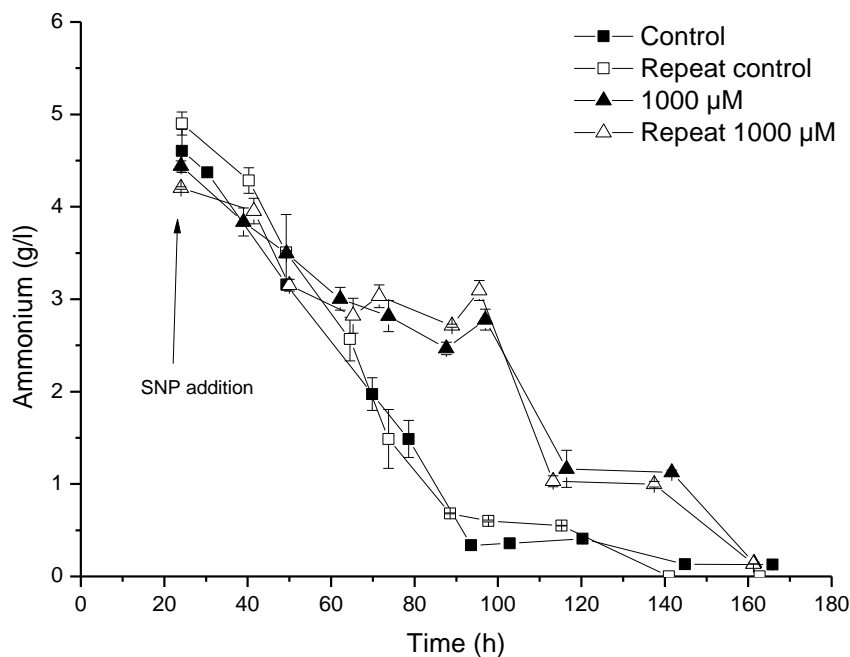


Figure III-4: Residual Ammonium (g/l) during batch cultivation in a STR of *A. niger B1-D*.

Various concentrations of sodium nitroprusside (SNP) were added at 24 hours. Cultivation conditions were: airflow 2 lpm, 300 rpm, pH 4, temperature 25 °C. Results are expressed as mean ± stdev.

Table III-3: Effect of SNP on ACR batch fermentations of *A. niger B1-D*.

Cultivation conditions were: airflow 2 lpm, 300 rpm, pH 4, temperature 25 °C. ACR was determined from the linear part of the graph and is expressed as mean ± stdv.

Concentration SNP (μM)	ACR (g/l/h)
Control	0.062 ± 0.0029
Repeat control	0.061 ± 0.0017
1000	0.032 ± 0.0003
Repeat 1000	0.030 ± 0.0001

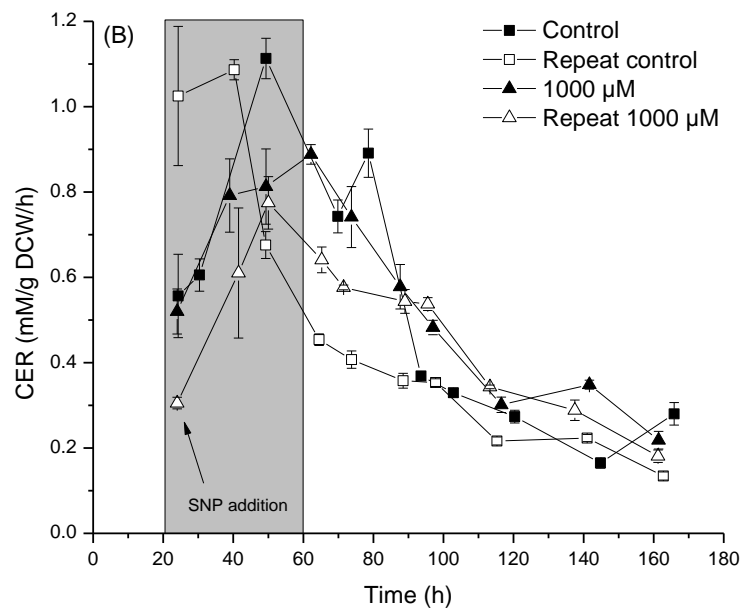
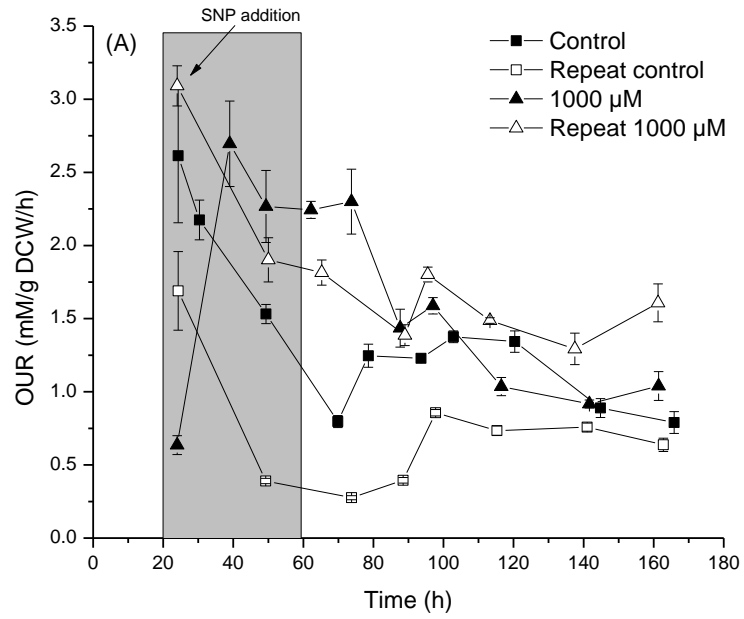


Figure III-5: (A) OUR (mM/g DCW/h) and (B) CER (mM/g DCW/h) during batch cultivation in a STR of *A. niger B1-D*.

Various concentrations of sodium nitroprusside (SNP) were added at 24 hours. Cultivation conditions were: airflow 2 lpm, 300 rpm, pH 4, temperature 25 °C. Results are expressed as mean \pm stdev.

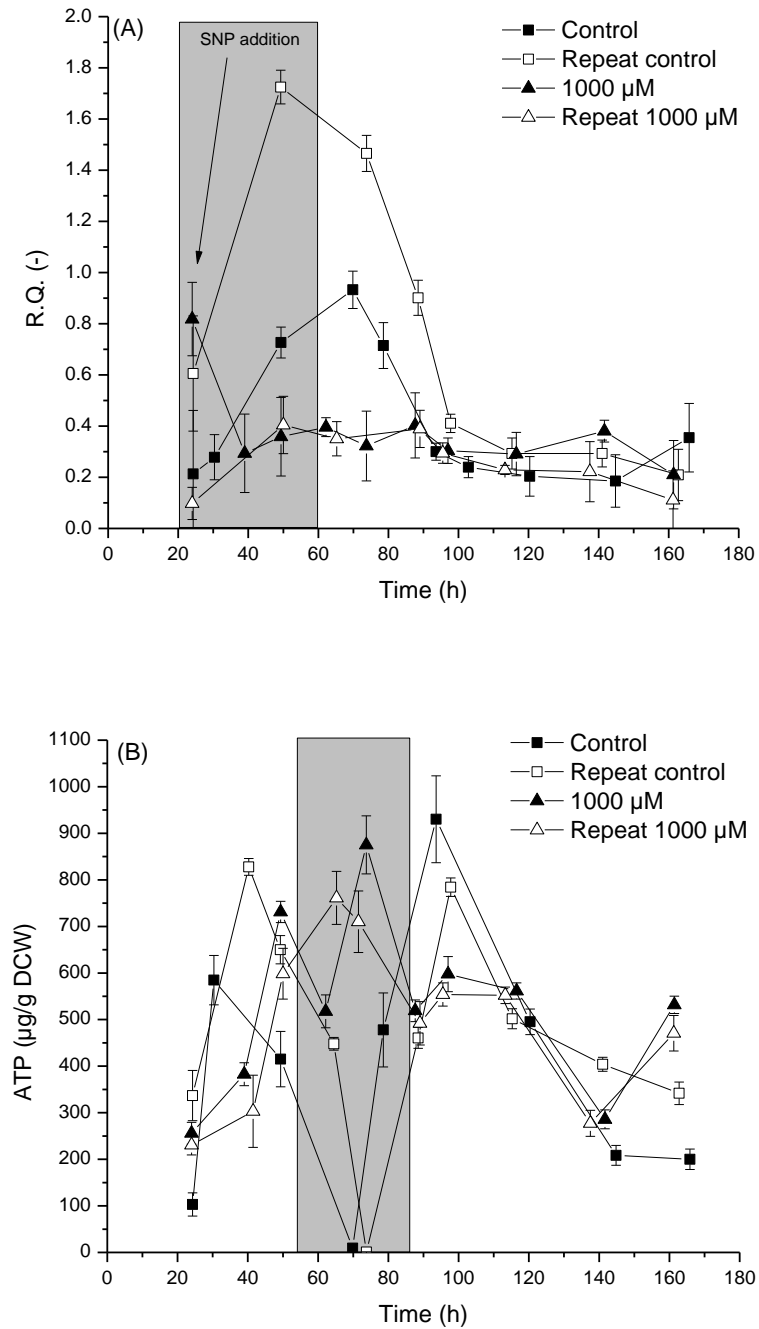


Figure III-6: R.Q. (A) and ATP ($\mu\text{g/g DCW}$); (B) during batch cultivation in a STR of *A. niger B1-D*.

Various concentrations of sodium nitroprusside (SNP) were added at 24 hours. Cultivation conditions were: airflow 2 lpm, 300 rpm, pH 4, temperature 25°C . Results are expressed as mean \pm stdev.

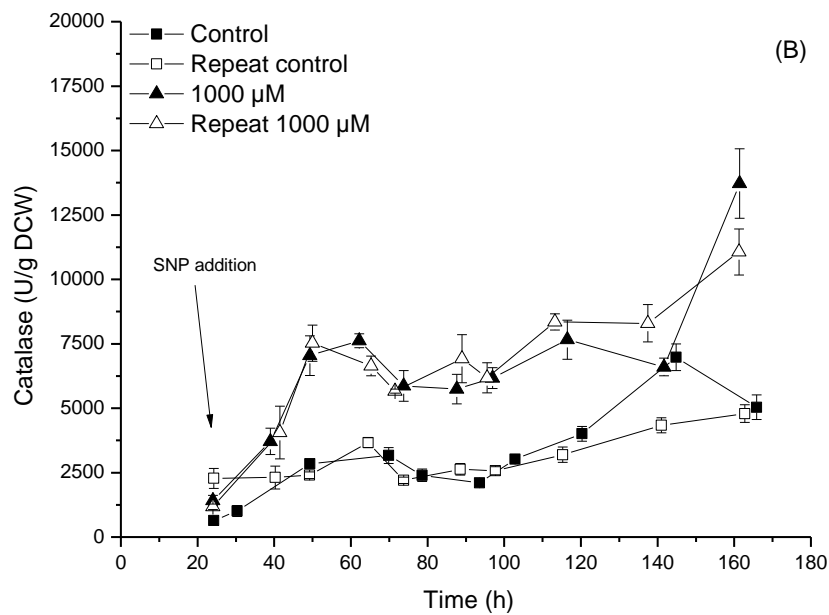
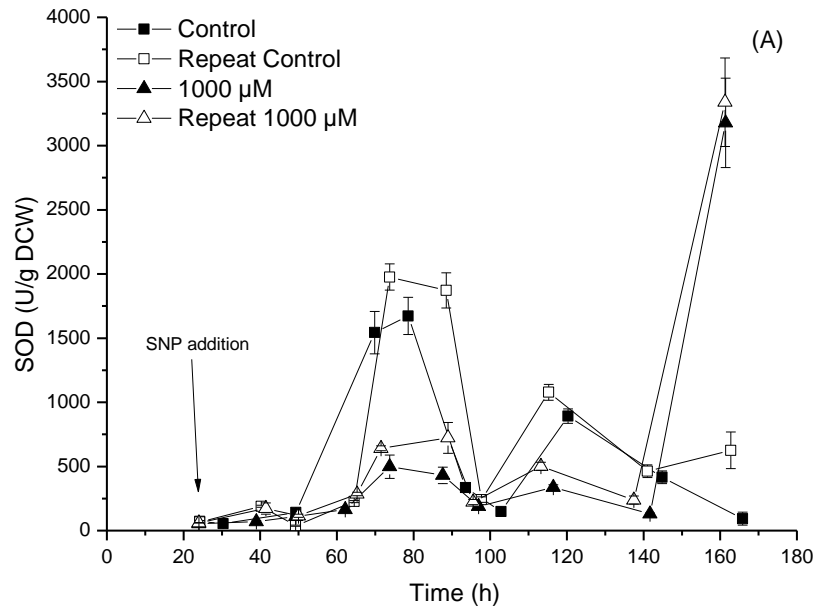


Figure III-7: (A) SOD (U/g DCW) and (B) CAT (U/g DCW) during batch cultivation in a STR of *A. niger B1-D*.

Various concentrations of sodium nitroprusside (SNP) were added at 24 hours. Cultivation conditions were: airflow 2 lpm, 300 rpm, pH 4, temperature 25 °C. Results are expressed as mean ± stdev.

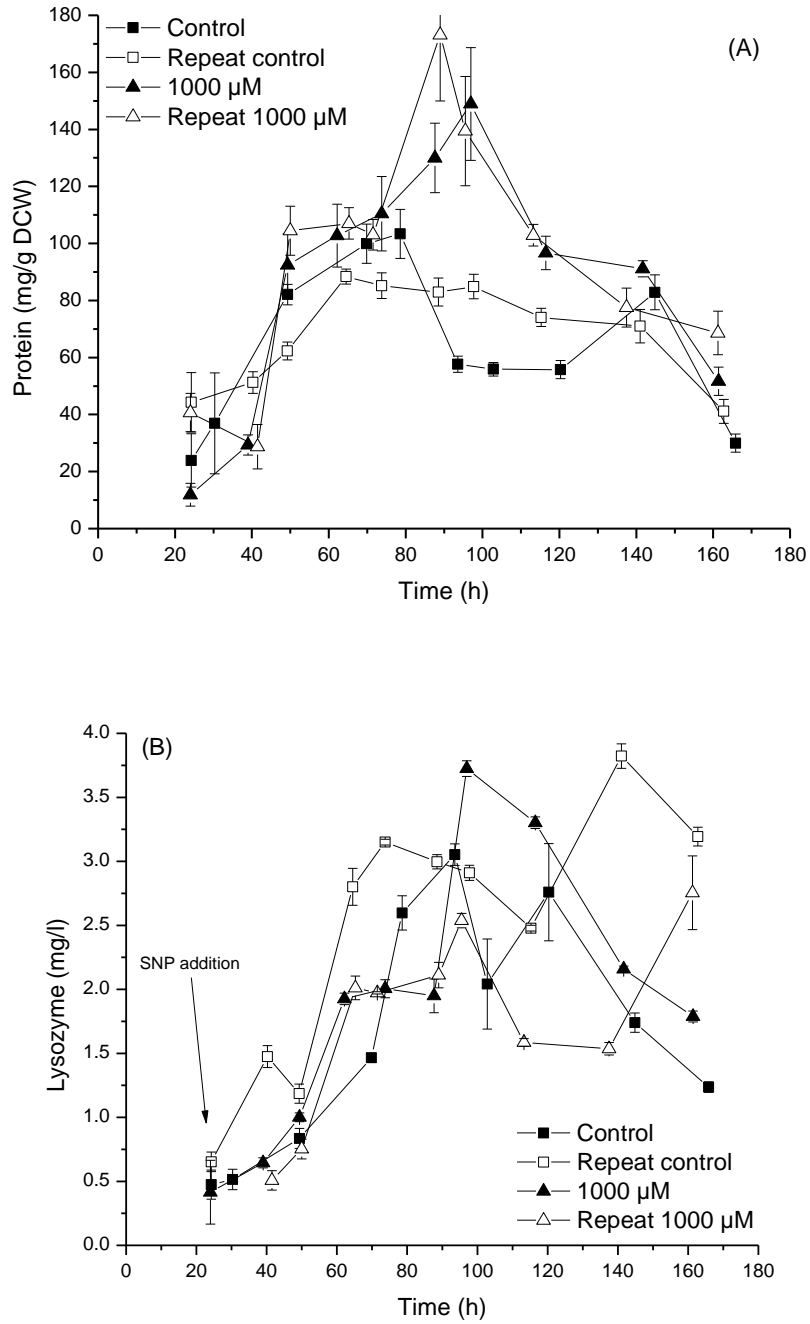


Figure III-8: (A) Intracellular protein content (mg/g DCW) and (B) Lysozyme concentration (mg/l) during batch cultivation in a STR of *A. niger B1-D*. Various concentrations of sodium nitroprusside (SNP) (see graph) were added at 24 hours. Cultivation conditions were: airflow 2 lpm, 300 rpm, pH 4, temperature 25 °C. Results are expressed as mean \pm stdev.

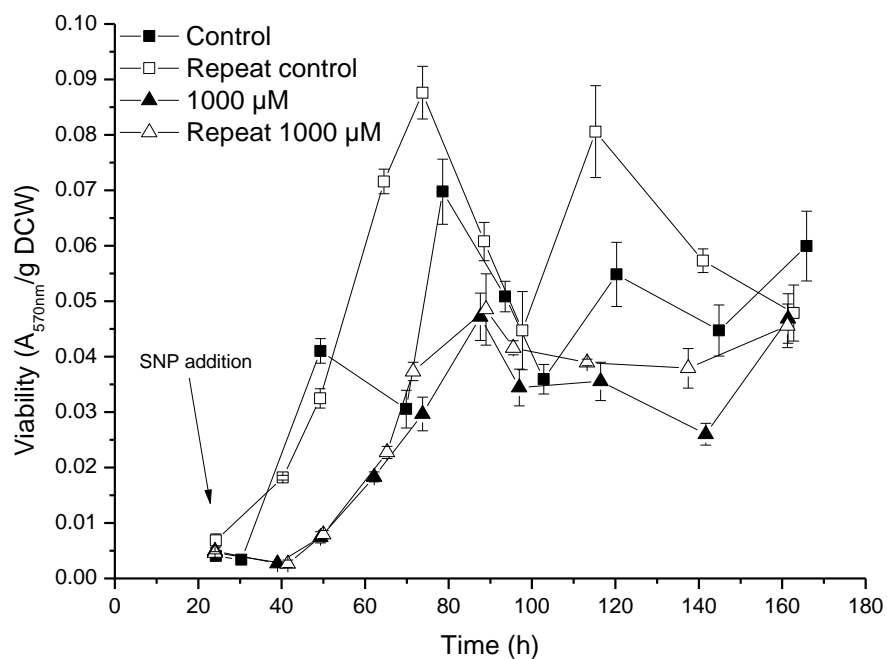


Figure III-9: Effect of various concentrations of SNP on viability ($A_{570\text{nm}}/\text{g DCW}$) during batch cultivation in a stirred tank reactor of *A. niger B1-D*. Various concentrations of sodium nitroprusside (SNP) were added at 24 hours. Cultivation conditions were: 2 lpm, 300 rpm, pH 4 at 25 °C. Results are expressed as mean \pm stdev.